The Development of PAM Enzyme Inhibitors and Cleavable Amino Acids for the Control of Peptide Hormone Levels

A thesis submitted in fulfilment of the

requirements for admission to the degree

of

Doctor of Philosophy (Organic Chemistry)

By

Brendon Jeffrey William Barratt

THE AUSTRALIAN NATIONAL UNIVERSITY

RESEARCH SCHOOL OF CHEMISTRY

INSTITUTE OF ADVANCED STUDIES

December 2004

"Science... never solves a problem without creating ten more"

George Bernhard Shaw

"The need to be right all the time is the biggest bar to new ideas. It is better to have enough ideas for some of them to be wrong than to be always right by having no ideas at all."

Edward de Bono

"Every truth passes through three stages before it is recognised. In the first it is ridiculed, in the second it is opposed, in the third it is regarded as self-evident"

Arthur Schopenhauer

Contents

Acknowledgements

I would like to acknowledge a number of people for their support during the preparation of this thesis.

Firstly, thank you to my supervisor Professor Chris Easton for all his help, guidance, encouragement and patience with me throughout the course of my PhD. Professor Eastons incredible diligence with respect to my training as a scientist over the past few years, in spite of so many other commitments and his capacity to balance this with being a great friend is something that I will never forget and will always be grateful for.

I would also like to thank Dr. Jamie Simpson for his help, guidance and encouragement over the course of my PhD. and for always having the office door open whenever I had a question to ask. Without the many hours spent debating chemistry on the white board in his office much of this thesis and many of the ideas described within would never have been produced.

I would like to thank all the technical staff for their help and in particular Tony Herlt for his assistance and for always making his great wealth of chemical knowledge available. Thanks must also go to the many members of the Easton group and Research School of Chemistry, past and present, whose support and friendship helped to make my PhD. such a wonderful experience. Their great friendship and the many laughs shared over the years will always be fondly remembered. Extra special thanks must however go to Dr. Adam Wright and Dr. Lorna Barr for proof reading sections of this thesis.

To those people who have been my friends both in and out of the lab over the last few years I must also say thanks for your support, in no particular order; Paul Dumanski, Dr. Adam Wright, Dr. Lorna Barr, Amy Philbrook, Dr. Magne Sydnes and Dr. Jamie Simpson.

Thanks must also go to my mother and father for their amazing support, not only over the course of the last few years, but also throughout my schooling life without which many of my dreams and aspirations and especially my PhD. would never have been made a reality.

I would like to thank Carmen and Vasanth for their help, love and support over the last few years and for providing me with the computer and desk on which much of this thesis was written.

Finally I must thank Nisha Bajpe, my beautiful wife who is always there for me and has been such a wonderful and understanding friend throughout the course of my PhD. Without her encouragement and support, this thesis would certainly never have been written.

Declaration

This is to declare that the work presented herein represents original work that I carried out during my Ph.D candidature from February 2001 – November 2004 except for the following experiments.

Presented in Results and Discussion Chapter 1: The synthesis of the diastereomers of *N*-acetylphenylalanyl-βββ-trifluoroalanine was performed by Dr. Jamie Simpson. The synthesis of 3-(*N*-acetylleucyl)propionic acid and its testing against PAM was performed by Ms. Iris Li. The synthesis of methyl 3-benzoylpropionate and the determination of its relative rate of bromination was performed by Ms. Iris Li.

Presented in Results and Discussion Chapter 2: The synthesis of *N*-benzoyl-α-hydroxyglycine was performed by Ms. Yi-Chin Tsai. The synthesis of *N*-benzoyl-α-hydroxyglycine methyl ester was performed by Dr. Adam Wright.

Presented in Future Work and Conclusions: The testing of the glycolate systems in cell based assays was organised by Dr. Adam Wright. Testing of the glycolate systems against human lung cancer cell line A549 were performed by MDS Pharma. Testing of the affect of glycolate systems on substance P levels in rat dorsal root ganglian cells were performed by Atsuko Inoue of Hiroshima University. Testing of the affect of glycolate systems on adrenomedullin levels in a U87 cell line were performed by L'Houcine Ouafik of the University of the Mediteranean.

To the best of my knowledge, this thesis does not contain material that has been previously published or accepted for the award of any other degree or diploma in any university or other tertiary institution. Published or written work by another person has been acknowledged through citation throughout the text.

I give consent for a copy of my thesis to be deposited in the University library and for it to be made available for loan and photocopying.

Brendon Barratt

December 2004

Publications

Some of the work in this thesis has been reported in the following publications:

"Inhibition of Peptidylglycine α-Amidating Monooxygenase by Exploitation of Factors Affecting the Stability and Ease of Formation of Glycyl Radicals" B. J. W. Barratt, C. J. Easton, D. J. Henry; I. H. W. Li, L. Radom, J. S. Simpson, *Journal of the American Chemical Society,* 2004, **126**, 13306-13311

B. J. W. Barratt, C. J. Easton, J. S. Simpson, 'Enzyme Inhibitors' Australian Provisional Patent Application No. 950185 **(2002)**.

B. J. W. Barratt, C. J. Easton, J. S. Simpson, 'Preparation of peptide glycolates and methylene analogues as enzyme inhibitors', International Patent Application No. PCT/AU2003/000905 **(2004)**.

Abstract

Peptidylglycine α-amidating monooxygenase catalyses the biosynthesis of peptide hormones through radical cleavage of the *C*-terminal glycine residues of the corresponding prohormones. The over-production of hormones by PAM has been implicated in disease states such as cancer, diabetes and inflammation. Correlations between ab initio calculations of radical stabilisation energies (RSE) and rates of free radical brominations with the extent of catalysis displayed by peptidylglycine α-amidating monoxygenase were used to identify classes of inhibitors of the enzyme.

The substitution of the nitrogen of glycine with electron-withdrawing groups was found to decrease rates of free radical brominations by up to a factor of 24 and the RSEs of α-carbon centred radicals by up to 9.2 kJ mol^{-1}. This was correlated with a 4.5 fold decrease in the rate of turnover by PAM of *N*-trifluoroacetylglycine in comparison to that of *N*-acetylglycine.

The substitution of glycine for βββ-trifluoroalanine was found to prevent free radical bromination and decrease the RSE of an α-carbon centred radical by 39.2 kJ mol^{-1} in comparison to the corresponding glycyl radical. This substitution was found to prevent catalysis by PAM, although it was found to have a detrimental effect on binding affinity.

The substitution of an acylglycine NH with O to give an acylglyolate was found to prevent free radical bromination and decrease the RSE of an α-carbon centred radical by 34.7 kJ mol^{-1} in comparison to the corresponding glycyl radical. The substitution of

glycine with glycolate was also found to prevent catalysis by PAM whilst not reducing binding affinity with the enzyme. Glycolates were therefore identified as a general class of PAM inhibitors.

The substitution of an acylglycine NH for a γ-keto acid CH_2 was found to prevent free radical bromination. Further, in comparison to an α-carbon centred glycyl radical, it decreased the RSE of the equivalent carbon centred radical by 44.2 kJ mol^{-1}. This substitution was also found to prevent catalysis by PAM, however it resulted in a large decrease in binding affinity with the enzyme.

The glycolates O^{α}-(decanoyl)glycolic acid, benzyl O^{α}-(decanoyl)glycolate, *N*-acetyl-O^{α}-(phenylalanylphenylalanyl)glycolic acid and benzyl *N*-acetyl-O^{α}-(phenylalanylphenylalanyl)glycolate were tested for their effects in cell based assays. It was found that these systems inhibit the proliferation of the A549 human lung cancer cell line, decrease levels of substance P produced in rat dorsal root ganglian cells and affect adrenomedullin hormone levels assays with a U87 cell line. In particular, the benzyl esters were found to have the highest efficacy presumably due to enhanced transport across cell membrances in comparison to the free acids.

The hydrolysis of α-substituted glycines at pH 4.0, 7.5 and 10.0 was investigated for their potential use as amide masking groups or to transiently link molecules. The rates of the hydrolysis reactions of *N*-benzoyl-α-hydroxyglycine and *N*-benzoyl-α-hydroxyglycine methyl ester to release benzamide were found to be similar at pH 7.5 and 10.0. The substitution of *N*-benzoylglycine methyl ester at the α-position with methoxy and ethoxy groups was found to prevent hydrolysis to release α-hydroxyglycines at pH 4.0, 7.5 and 10.0 due to the poor leaving abilities of methoxide

and ethoxide. The substitution of *N*-benzoylglycine methyl ester at the α-position with an acetoxy group was found to result in rapid hydrolysis to *N*-benzoyl-α-hydroxyglycine methyl ester at basic pH whilst being inert at pH 4.0. The substitution of *N*-benzoylglycine methyl ester with a phenoxy group at the α-position provided for the controlled hydrolytic release of α-hydroxyglycines at basic pH with a half-life of 0.40 hours at pH 7.5.

2-Nitrophenylalanine was identified as a new photocleavable amino acid for the release of amides under biological conditions. The peptides, *N*-benzoylvalyl-2-nitrophenylalanine methyl ester, *N*-benzoyl-2-nitrophenylalanylalanine methyl ester, *N*-benzoylvalyl-2-nitrophenylalanylalanine methyl ester and *N*-benzoylvalyl-2-nitro-4,5-dimethoxyphenylalanine methyl ester were found to photolyse at 254, 300 and 350 nm to release their respective amides, *N*-benzoylvalinamide, benzamide, *N*-benzoylvalinamide and *N*-benzoylvalinamide. Alteration of the carboxyl group of 2-nitrophenylalanine was found to have a profound effect on the efficiency of the photolysis reaction and the yield of amide released. It was found that if the carboxyl group of 2-nitrophenylalanine was protected as a methyl ester rather than an amide, the yield and rate of release of amide was increased and the half-life of the *aci*-nitro intermediate decreased. The photolysis of *N*-benzoylvalyl-2-nitrophenylalanine methyl ester was found to be the most efficient and high yielding.

Introduction

C-Terminal amidation is a required post translational modification of many bioactive peptides. The amides are synthesised *via* glycine-extended precursors and are transformed by peptidylglycine α-amidating monooxygenase (PAM) through the oxidative cleavage of the glycine N-C^{α} bond (Figure 1).[1]

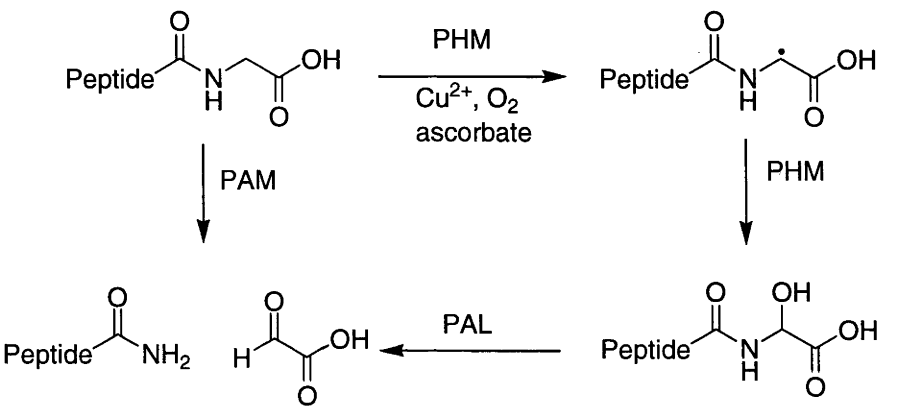

Figure 1. Mechanism of Catalysis by Peptidylglycine α-Amidating Monooxygenase.

The amidation reaction is catalysed by the two active sites of PAM: peptidylglycine α-hydroxylating monooxygenase (PHM) and peptidylamidoglycolate lyase (PAL).[1] The PHM step of the PAM mechanism is copper, molecular oxygen and ascorbate dependent.[1] The initial step involves the reduction of the resting oxidised form of the enzyme converting the two bound copper ions from Cu^{2+} to Cu^{+} by two one electron transfers from two ascorbates. The two ascorbates in turn are oxidised to the semihydroascorbates which disproportionate to yield ascorbate and dehydroascorbate. In the presence of substrate, molecular oxygen then binds to Copper B (CuB, Figure 3)

to give Cu^{I}-peroxide. The copper-peroxy radical then abstracts a hydrogen atom from the terminal glycine's α-carbon of the bound substrate forming an α-carbon centred glycyl radical intermediate (Figure 2). Homolysis of the copper bound hydroperoxide then forms the α-hydroxyglycine derivative.[1]

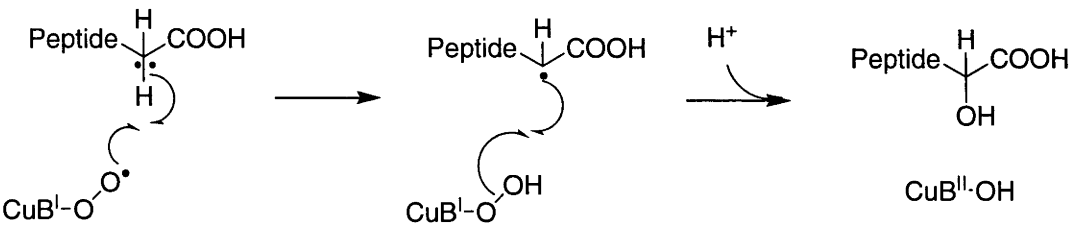

Figure 2. Mechanism for Abstraction of a Hydrogen Atom from the α-Carbon of a Glycine Substrate by PHM.[1]

The crystal structure of the active site of PHM in its oxidised, substrate bound form is illustrated (Figure 3). Included in the crystal structure are a number of features, which provide insight into how the enzyme binds substrates. Of particular note is the arginine residue R240 that acts like a claw in binding the terminal free carboxylate of the substrate. The importance of this interaction is observed in the fact that peptidic systems which do not possess the free carboxylate are known not to bind to PHM.[2] Further interactions involve an asparagine (N316), the side chain oxygen of which is hydrogen bonded with the substrate glycine NH. This interaction comes about through a large structural change upon substrate binding, which involves the breaking of a hydrogen bond with the neighbouring tyrosine (Y318) through a 30° rotation of the asparagine side chain. Also of interest is the substrates 3,5-diiodotyrosine residue which appears to be occupying a large hydrophobic pocket big enough to accommodate any proteinogenic amino acid side chain.[1]

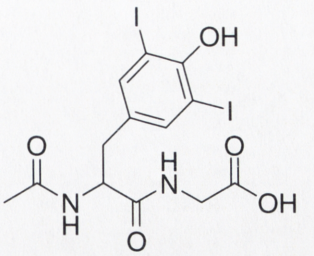

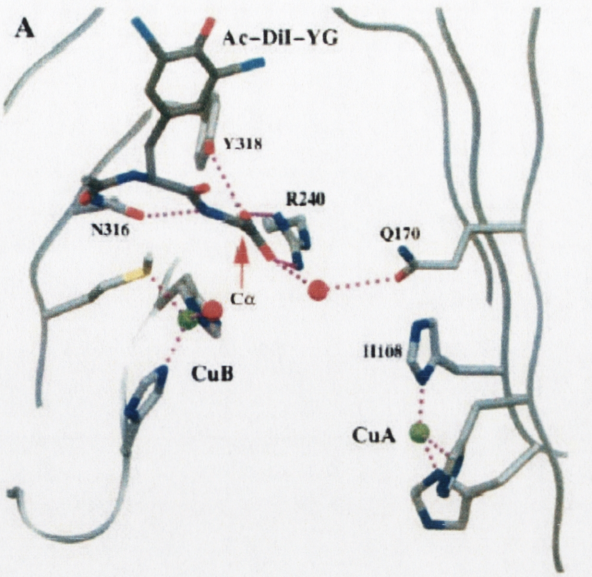

Figure 3. Crystal Structure of the Oxidised and Substrate Bound PHM Active Site.[1] Peptide substrate and protein side chains are shown coloured by atom type (carbon is grey, nitrogen is blue, oxygen is red, sulfur is yellow and iodine is turquoise). The copper atoms are green and the water molecules are red spheres.

The α-hydroxyglycine modified substrate is then processed by the second active site, PAL, where it undergoes zinc dependent cleavage to give glyoxylic acid and the *C*-terminal amidated product (Figure 4).[1]

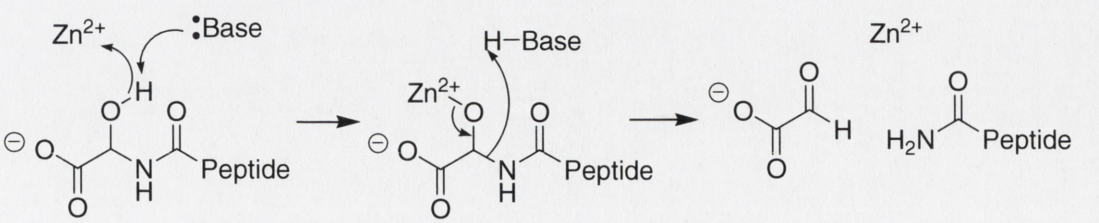

Figure 4. Proposed Mechanism of Catalysis by PAL.[1]

The expression of PAM is widespread through the body with high concentrations in many neurons, endocrine cells (especially the pituitary), ependymal cells, atrial myocytes and all major brain areas except the cerebellum.[3] To achieve its function in the amidation of peptides, PAM must be co-localised with its hormone precursor substrates. Resulting from this, regions known to contain high levels of peptide hormones also express high levels of PAM mRNA.

In addition to the bioactivation of a large number of peptides, PAM has also been implicated in the biosynthetic pathway of the production of fatty acid primary amides known as bioactive lipids.[4] As a result of the diversity of compounds that PAM is responsible for processing and their wide ranging biological roles, the enzyme has been implicated in a number of related disease states. The neuropeptides bombesin and calcitonin are bioactivated by PAM[5] and are known to stimulate the growth of prostate cancer cell lines through the inhibition of apoptosis.[6] Substance P is a neuropeptide which is known to be a modulator of nociception, involved in the signalling intensity of noxious or aversive stimuli.[7] Tachykinin peptides, substance P and neurokinin A are released from sensory nerves upon exposure to irritant chemicals and endogenous agents including bradykinin, prostaglandins and histamines as part of an inflammation response and are linked to bronchioconstriction (asthma).[8] Pancreastatin has been found to have a counter regulatory effect on insulin levels and therefore has been implicated in insulin-resistance.[9] The concentrations of the peptide hormones somatostatin and neuropeptide Y are known to be deficient in the cerebrospinal fluid of Alzheimer's patients, though galanin levels are increased.[10] The fatty acid primary amide, oleamide, is known to be involved in the control of sleep and potentiates the antiproliferative effects of arachidonoylethanolamide in breast cancer cells.[4]

Resulting from the large number of disease states associated with the over production of bioactive peptides by PAM such as asthma,[8] cancer,[6] and neuropathic pain,[11] PAM has become a target for drug development.[3] A variety of potential drug candidates have been developed such as *trans*-4-phenyl-3-butenoic acid (PBA) which is an enzyme-activated, mechanism based inhibitior.[12] PBA is one of the most potent PHM inhibitors with an apparent K_I in the range of 1 μM.[13] The inactivation of PHM by PBA is time, copper and ascorbic acid dependent. PBA is believed to form a reactive intermediate which binds covalently to an electron rich amino acid residue in the catalytic core of PHM.[3] The administration of PBA in rat assays has been shown to reduce carrageenan-induced inflammation through the inhibition of substance P production by PAM.[14] This identifies PAM as an excellent pharmacological target for the reduction of acute inflammatory responses.

Other mechanism based inhibitors of PAM include α,β-unsaturated acids such as *trans*-3-benzoylpropenoic acid, *trans*-3-(*N*-acetylphenylalanyl)propenoic acid and *trans*-5-acetamido-4-oxo-6-(2-thienyl)-hex-2-enoic acid with K_Is of 0.16, 0.095 and 0.026 mM, respectively.[13,15] Diastereomers of phenylalanylphenyalanyl-α-styrylglycine have also been studied and found to possess IC_{50} values against PAM in the millimolar range, as low as 0.1 mM.[16]

Other types of reported PAM inhibitors are inorganic sulfite, which appears to give irreversible inhibition through the Cu^{II} oxidation of sulfite (SO^{2-}_3) to sulfite radical anion ($SO^{\bullet-}_3$) in the active site. The sulfite radical then reacts with an amino acid residue in the PHM active site rendering the enzyme inactive.[17] Benzylhydrazine has also been identified as a PAM inhibitor. This occurs through the oxidation of the

hydrazine moiety by Cu^{II} to give a benzylic radical, which then binds covalently to a residue in the active site of PHM, blocking the enzyme.[18]

Chapter 1 of the Results and Discussion section of this thesis outlines a new approach to the development of PAM inhibitors. This approach involves the development of methods to decrease the stability of α-carbon centred glycyl radicals such as those formed by PAM. Therefore, a short review covering the nature of α-carbon centred amino acid radicals and methods with which they can be studied now follows.

α-Carbon centred amino acid radicals are peculiar in that their stability is much greater than that for typical carbon radicals.[19] This enhanced stability is the result of a phenomenon termed the 'captodative effect' which was first theorised by Dewar.[20] The captodative effect involves the extensive and synergistic delocalisation of the unpaired spin density, through the action of the electron-donating (dative) amino or amido substituent and the electron-withdrawing (capto) carboxy group.[19] Figure 5 illustrates how resonance forms contribute to the stability of α-carbon centred glycyl radicals formed on substrates by PAM.

α-Carbon centred amino acid radicals have been studied by measuring radical stabilisation energies (RSEs) and rates of bromination.[21] RSEs are calculated energies, which reflect the stability of radicals whilst rates of bromination reflect the ease of formation of the radicals. A short overview of these studies and how they will be applied to the development of inhibitors of PAM in Chapter 1 of the Results and Discussion section of this thesis is now presented.

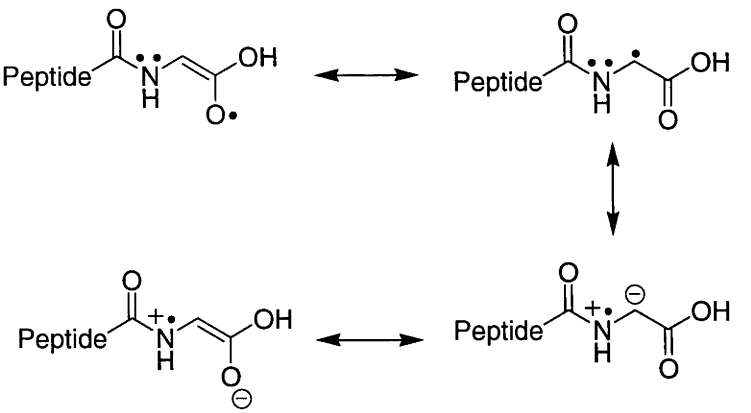

Figure 5. Resonance Contributors of α-Carbon Centred Glycyl Radicals.

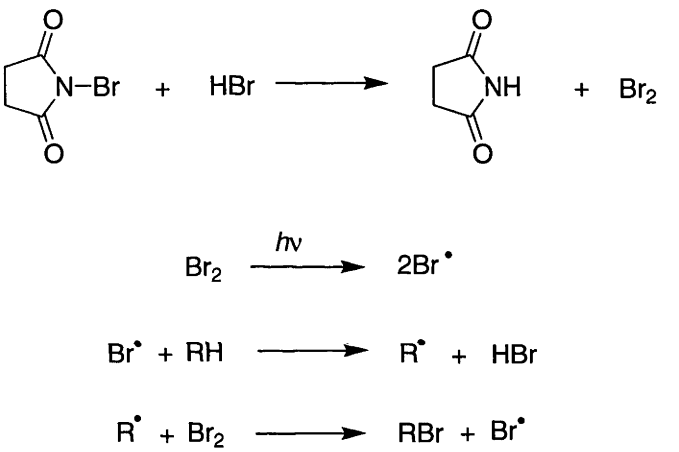

Figure 6. The Mechanism of Radical Bromination as Described by Goldfinger *et al.*[22]

The mechanism of radical bromination using NBS, illustrated in Figure 6, involves NBS as a provider of a small steady-state concentration of molecular bromine.[23] Photolysis of molecular bromine then releases a smaller steady-state amount of bromine atom which acts as the hydrogen abstracting species. This is followed by halogen abstraction from molecular bromine by the substrate radical forming the product bromide and a bromine atom, which continues the chain reaction.

Rates of reaction often give information about the steric, polar and resonance effects involved in free radical processes and provide information that can be utilised, for example, in the design of oxidation resistant peptides, enzyme inhibitors and synthetic schemes.[21] This is true of rates of bromination with NBS of α-amino acids which have been extensively used to investigate the effect that their substituents have on the ease of formation of their α-carbon centred radicals.[24] In the transition state of the reaction there exists a substantial degree of bond homolysis and therefore the transition state possesses substantial radical character. As a consequence the relative rates of radical formation tend to reflect the relative stabilities of the radicals being formed *i.e.* a substituent which stabilises a radical product can be assumed to have a similar effect on the stability of the 'radical-like' transition state.

RSEs can also be used to determine the effect that different substituents have on α-carbon centred glycyl radical stability.[21] In this dissertation, RSEs are reported as the energy changes in the isodesmic reactions represented in Figure 7. The RSEs correspond to the differences between the C-H bond dissociation energies of methane and RH,[25,26] and reflect the stability of $R^{\bullet}$ compared to $CH_3^{\bullet}$ (relative to the corresponding closed shell molecules). Therefore the larger the value of the RSE the more stable the radical.

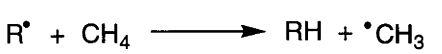

Figure 7. Isodesmic Reactions used to obtain RSEs.

The ability of different substituents to affect the rate of bromination of glycine derivatives with NBS and the RSEs of their α-carbon centred radicals has been

investigated.[21,27] It was established that rates of bromination and RSEs could be influenced through both steric and electronic effects induced by *N*-substituents and α-substituents.

The contribution of the amido or amino nitrogen of glycine derivatives, as part of the resonance forms involved in captodative stabilisation of α-carbon centred glycyl radicals, is electron donating.[19] The addition of electron withdrawing groups on the nitrogen of glycine has been shown to decrease rates of bromination with NBS and RSEs of α-carbon centred glycyl radicals.[21] The rate of radical bromination of *N*-trifluoroacetylglycine methyl ester **4** is 24 times slower than for *N*-acetylglycine methyl ester **1** (Figure 8). Further the RSE of the α-carbon centred glycyl radical of *N*-trifluoroacetylglycine methyl ester **5** is 9.8 kJ mol^{-1} less stable than for the *N*-acetylglycine methyl ester radical **2** (Figure 8).

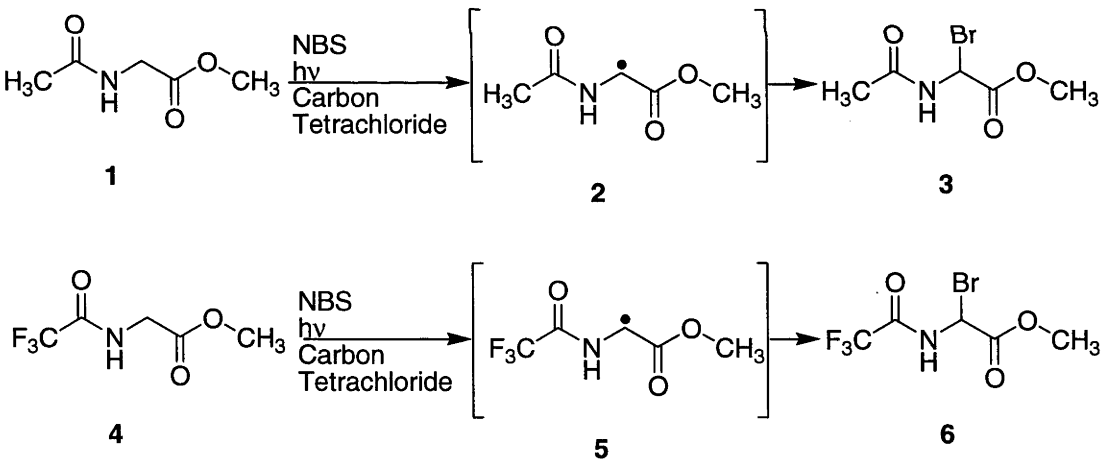

Figure 8. Bromination Reactions of **1** and **4** to give their α-Carbon Centred Radicals **2** and **5** and Brominated Products **3** and **6**, Respectively.[27]

Substitution at the α-carbon of *N*-acylglycines also affects the stability of the α-carbon centred amino acid radicals.[21] The favoured conformation adopted by the α-carbon of a glycine derivative upon radical formation is sp^2 trigonal planar. The addition of bulky groups at the α-position of *N*-acylglycines can affect the adoption of the trigonal planar geometry. The substitution of *N*-acetylglycine with a *tert*-butyl group results in a decrease in the RSE of 28.6 kJ mol^{-1} for the α-carbon centred radical. This is a consequence of the buttressing of the *tert*-butyl group with the amido carbonyl oxygen. This interaction inhibits the adoption of a trigonal planar geometry at the α-carbon during the formation of the α-carbon centred radical.

The intention of the studies described in Chapter 1 of the Results and Discussion section of this thesis was to determine whether the effect that different substituents on glycine have on rates of bromination and the RSEs of α-carbon centred radicals translates to differences in PAM activity towards analogous substrates. It was the further intention to determine whether glycine substituents which decrease the RSEs of α-carbon centred glycyl radicals and their ease of formation in radical brominations could be used in the development of PAM inhibitors. In order to achieve this, assays of various compounds with PAM were required. Therefore an overview of enzyme kinetics with respect to the parameters which describe enzyme-inhibitor and enzyme-substrate interactions now follows.

Enzymes accelerate reactions by factors of up to at least a million.[28] Indeed many enzymes such as superoxide dismutase, fumarase and triosephosphate isomerase are known to process their substrates such that the rate determining step is diffusion.[29] Enzymes are highly specific both in the reaction catalysed and in their choice of

reactants.[28] For example, PAM is known to be highly specific for glycine extended substrates over substrates terminating in more bulky amino acids such as alanine.[30] Much of the catalytic power of enzymes comes from their bringing substrates together in favourable orientations in enzyme-substrate complexes (ES). The following diagram (Figure 9) describes the simplest case of the reactions that take place between enzymes and substrates.

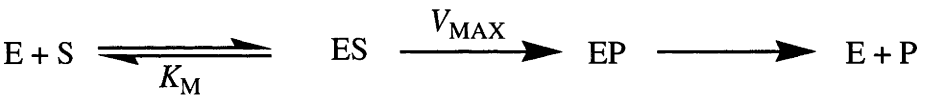

Figure 9. Reaction of an Enzyme (E) and Substrate (S) to give an Enzyme-Substrate Complex (ES) Followed by the Conversion to an Enzyme-Product Complex (EP) and Release of Product (P).

The K_M is the Michaelis constant which is equal to the substrate concentration at which the reaction rate v is half its maximal rate (V_{max}).[28] The K_M can also be defined as the substrate concentration at which the position of equilibrium between free enzyme and bound enzyme is such that half the enzyme active sites are occupied. Double reciprocal (Lineweaver-Burk) plots of $1/v$ versus 1/[S] (where [S] is substrate concentration) are used in this thesis to obtain K_M values (Figure 10). In order to obtain a K_M the reciprocal of the rate of turnover of substrate at different substrate concentrations is plotted and a trendline fitted. The K_M is then obtained from the value of $-x$ where the trendline intersects with the x-axis.

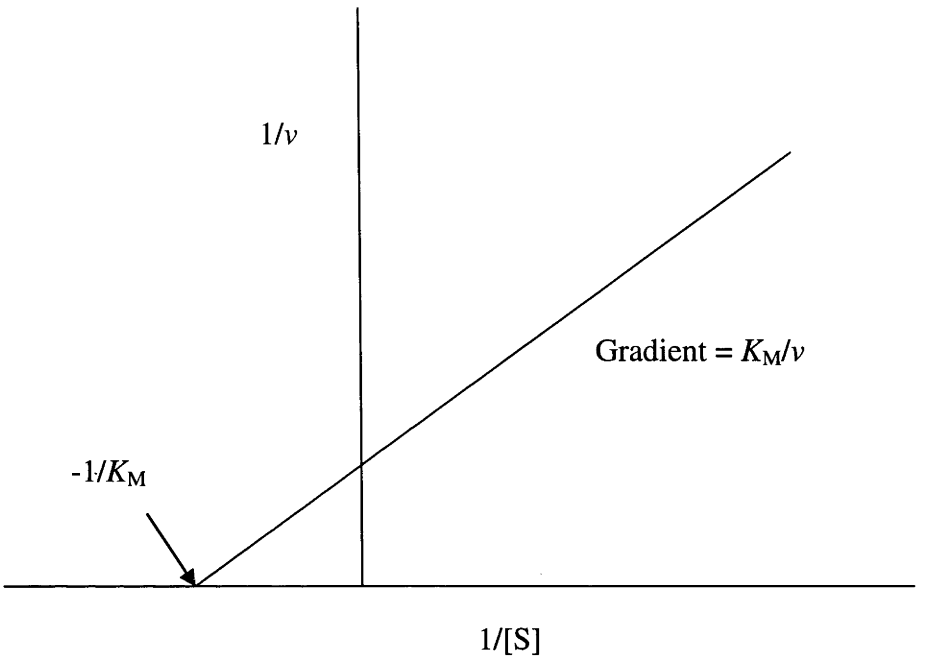

Figure 10. Double Reciprocal Plot Used to determine K_M Values.[31]

The inhibition of enzymatic activity by specific small molecules and ions is important because it serves as a major control mechanism in biological systems.[28] Also many drugs and toxic agents act by inhibiting enzymes. Furthermore, inhibition can be a source of insight into the mechanism of enzyme action. Different types of inhibitors include those that are competitive and non-competitive. The latter can act in a reversible or irreversible manner. In the majority of cases, inhibitors bind reversibly and can be released or displaced from the enzyme.[31] However, some inhibitors can bind so strongly that they cannot be detached. These include suicide substrates, which initially follow the catalytic process but subsequently form a covalent bond with a functional group of the enzyme active site and block the enzyme. The studies outlined in Chapter 1 of the Results and Discussion section of this thesis are assumed to involve

the development of competitive reversible inhibitors of PAM. A scheme describing enzyme and inhibitor interactions for simple competitive reversible inhibition is provided in Figure 11.

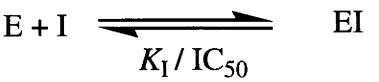

Figure 11. Reaction of Enzyme (E) and Inhibitor (I) to give an Enzyme-Inhibitor (EI) Complex.

In this thesis, the activity of inhibitors is described using either a K_I or an IC_{50} value. However, it is important to understand the extent to which the two numbers can be compared. The differences between an IC_{50} and a K_I are illustrated by the way in which the values are determined. To find a K_I value for an inhibitor, one must determine rates of enzyme-catalysed reactions while independently varying the concentration of substrate, [S], and the concentration of inhibitor, [I].[32] Specifically, the rate of an enzyme-catalysed reaction is measured for a range of substrate concentrations against one concentration of inhibitor. This experiment is then repeated, typically five or six times, for different concentrations of inhibitor. These data, usually requiring 75-100 individual rate measurements if the experiment is done in triplicate, are then used to determine a K_I. By comparison, IC_{50} values do not require as extensive experimentation. The IC_{50} value is determined at only one concentration of substrate over a range of inhibitor concentrations. Since determination of this value requires only about 15-20% as many data points and PAM enzyme solutions are highly expensive, IC_{50} values were obtained for the potential inhibitors reported in this thesis. While K_I is a constant value for a given compound with an enzyme, an IC_{50} is a relative value, the

magnitude of which is dependent on the concentration of substrate used in the assay. The relationship of an IC_{50} to a K_I is described mathematically in the Cheng-Prusoff relationship (Figure 12). From this equation it can be seen that the IC_{50} value of a given competitive inhibitor is related to the K_I value of the inhibitor as a function of the substrate concentration, [S], used in the assay, and the Michaelis constant, K_M, of the substrate. It is important to note that this relationship is specific for competitive inhibition and not for other modes such as uncompetitive inhibition. Therefore, IC_{50} values and K_I values can only be compared whilst considering the mode of inhibition and the concentration of substrate used in the assay. In the case of competitive inhibition, IC_{50} values approximate K_I when the [S] used in the assay is much lower than K_M. Therefore, in the case of competitive inhibition, IC_{50} values are always higher than K_Is.

$$IC_{50} = K_I \left(1 + \frac{[S]}{K_M}\right)$$

Figure 12. Cheng-Prusoff Relationship.[33]

The IC_{50} values of the potential inhibitors evaluated in this thesis were obtained using the Dixon plot method of $1/v$ versus [I] (where the initial concentration of substrate is constant over each assay and where [I] is different in each assay). The method used to determine a K_I for an inhibitor from a Dixon plot is illustrated in Figure 13 to clearly show how it relates to the compounds IC_{50} values. Inhibition data for a range of [I] at a constant [S] can be plotted as a Dixon plot to give the IC_{50} value at that [S] as the opposite value of the x-intercept. As the value of [S] decreases so does the opposite

value of the x-intercept, illustrating how an IC_{50} value approximates K_I as the value of $[S]/K_M$ becomes smaller in the Cheng-Prusoff relationship (Figure 12).

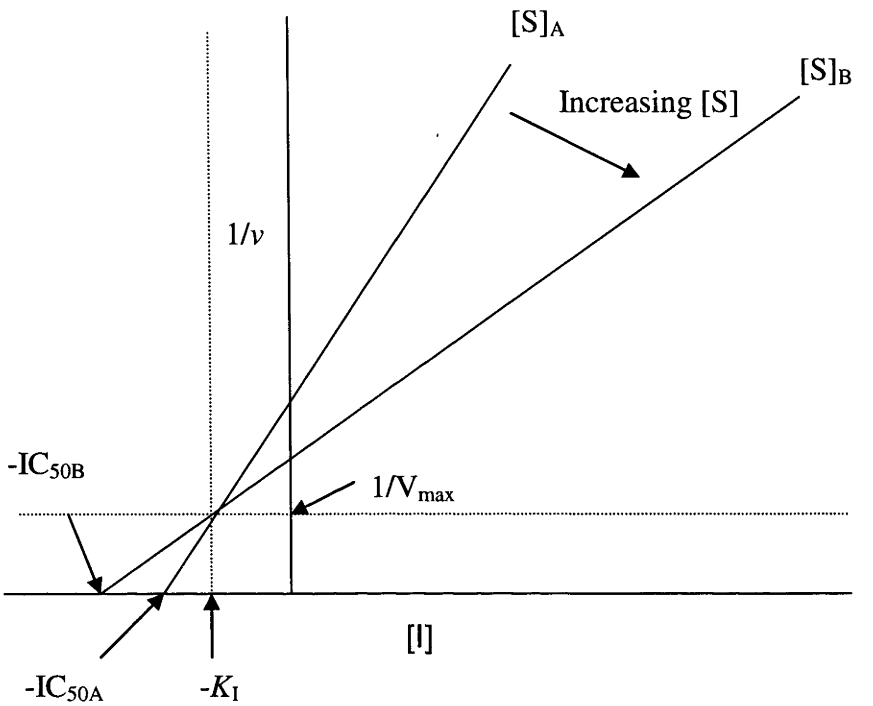

Figure 13. Dixon Plot as used to determine IC_{50} and K_I Values.

In this thesis IC_{50}s, K_Is and K_Ms are used to interpret the structural features of compounds, which are necessary for binding. Although only a K_I for an inhibitor is a constant which represents the concentration at which half the enzyme active sites are occupied, IC_{50}s are used as a general guide and can be considered to represent an upper limit estimation of K_I.

Chapter 1 of the Results and Discussion section of this thesis will outline research towards the development of PAM inhibitors for the treatment of disease states that arise from an over-production of peptide hormones. Conversely, Chapter 2 will cover

research into the controlled release of peptide hormones for the treatment of disease states resultant from their deficiency in the body.

Disease states associated with peptide hormone concentrations are not restricted to being due to their overproduction. Indeed, many disease states are treated through the direct administration of peptide hormones and suitable analogues.[34] Growth hormone and insulin-like growth factor are administered to patients with cardiac failure, sepsis, burns, cancer cachexia, end-stage renal failure, trauma and AIDS.[35] The administration of pancreastatin may constitute a method of treatment for insulin resistance.[9] Glucogen-like peptide 1 is a physiological incretin hormone from the lower gastrointestinal tract and it has been identified for possible use in the treatment of diabetes and Alzheimer's disease.[36,37] The somatostatin analogues octreotide, lanreotide and vapreotide are used clinically to treat pituitary and gastrointestinal cancers.[38] Vasopressin is used to treat enuresis.[34] Salmon, human and eel calcitonin are commonly used in the treatment of osteoporosis.

The use of peptides as therapeutic agents is hampered by their rapid elimination from circulation through renal filtration, enzymatic degradation, uptake by the reticuloendothelial system and accumulation in non-targeted organs and tissues.[38] In spite of the drawbacks of disease treatment with peptides, the worldwide market in peptide and protein drugs was worth USD 28 billion in 2000.[34] Therefore methods of administering peptide hormones as prodrugs which are initially inactive and are then rendered active once in contact with a selected stimulus warrants development.

It has been suggested that the administration of peptides in conjugation with molecules that can improve their lifetimes in the body and their selectivity for disease sites may allow the drawbacks of their use in disease treatment to be overcome.[38] Possible systems which could be used to this end include large polymers which improve the delivery of anti-cancer drugs through exploiting the enhanced permeability and retention of solid tumours towards macromolecules.[39] Further, antibodies which can recognise specific antigens produced in tumours, and immunotoxins which can select for specific cancer cells could also be used.[38] However, in order for hormones to be attached to such polymers, antibodies and immunotoxins, suitable linkers which allow for the liberation of the hormone must be developed.

As discussed above, the *C*-terminal amide of peptide hormones is essential to their bioactivity.[1] Therefore one approach towards the development of prodrugs of hormones is through the masking of the amide with a suitable protecting group which can be removed *in vivo*.[40] It seemed likely that functional amino acids which, upon exposure to specific stimuli, cleaved to release amides would constitute suitable protecting groups for the *C*-terminal amide of peptide hormones. Furthermore, such amino acids could potentially be utilised as cleavable linkers between hormones and the polymers, antibodies and immunotoxins anticipated to improve the selectivity of peptide hormone drug delivery. In this dissertation, the development of amino acids, which can be cleaved to release amides through hydrolysis will be outlined in Chapter 2 of the Results and Discussion section.

On the basis of the mechanism by which PAM catalyses the production of hormones, the administration of the α-hydroxyglycine extended precursors of *C*-terminal amidated

peptides may seem a suitable method by which to control the rate of hormone release. A number of α-hydroxyglycine extended peptides such as *N*-acetylphenylalanyl-α-hydroxyglycine, *N*-benzoylphenylalanyl-α-hydroxyglycine and *N*-acetylphenylalanyltyrosyl-α-hydroxyglycine have been studied to determine their rates of hydrolysis in aqueous buffered solutions and in 80% blood plasma at 37 °C.[40,41] It was found that their rates of hydrolysis were accelerated in 80% blood plasma with half-lives decreasing from 5.8-13.3 to 1.3-3.9 hours, apparently due to enzyme catalysed dealkylation.[40] It seemed likely that PAM was the enzyme responsible for the catalysed dealkylation as it is known to be present in human blood plasma.[42] Therefore the administration of α-hydroxyglycine extended peptides may not be suitable as they would be processed as soon as they entered the blood stream. It seemed likely that α-substituted glycines, which would not be expected to be PAM substrates, but would still hydrolyse at biological pH, may be suitable alternatives to α-hydroxyglycines. Therefore, a short review covering the chemistry of α-substituted glycines will now be outlined.

The hydrolysis of *N*-benzoyl-α-hydroxyglycine **7**, *N*-benzoyl-α-hydroxyglycine methyl ester **8** and *N*-benzoyl-α-hydroxyglycine benzyl ester **9** to release benzamide **10** and the glycolate derivatives **11-13** has been studied.[41] A mechanism for the non-enzyme catalysed hydrolysis of **7**, **8** and **9** to release **10** and **11-13** based on that proposed by Bundgaard *et al.*[41] is illustrated in Figure 14. The reported half-lives for the hydrolysis of **7**, **8**, and **9** to release benzamide **10** at pH 7.4 were 6.7, 0.78 and 4.5 hours, respectively. Therefore, an increase in the rate of release of **10** through the hydrolysis of **8** and **9** in comparison to the free acid **7** of up to 8.5 times was observed, however, no explanation for this change in reaction rate was reported. This result was considered

surprising, as there is no obvious reason that can be derived from the mechanism (Figure 14) to explain the observed increase in the rate of amide release. The hydrolysis of *N*-benzoyl-α-hydroxyglycine methyl ester **8** was therefore studied and is discussed in Chapter 2 of the Results and Discussion section of this thesis in order to re-examine the results previously reported.[41]

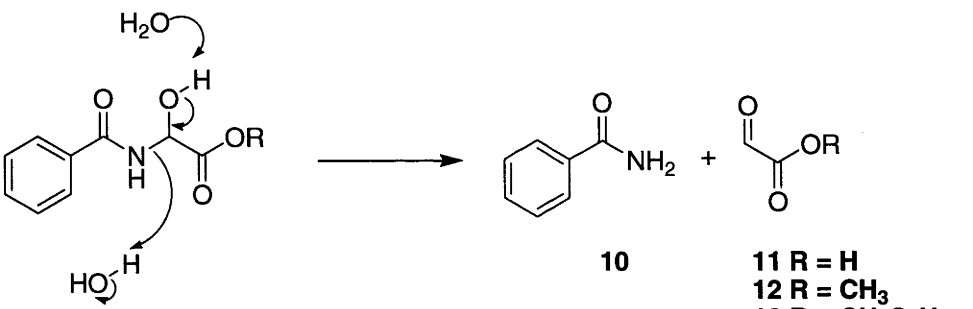

7 R = H
8 R = CH_3
9 R = $CH_2C_6H_5$

10

11 R = H
12 R = CH_3
13 R = $CH_2C_6H_5$

Figure 14. Mechanism of Hydrolysis of *N*-Benzoyl-α-hydroxyglycine **7**, *N*-Benzoyl-α-hydroxyglycine Methyl Ester **8** and *N*-Benzoyl-α-hydroxyglycine Benzyl Ester **9**.

In an attempt to extend the half-life of α-hydroxyglycine derivatives, Bundgaard *et al.*[41] protected **8** with various acyl groups. However, it was found that the acyl protected systems were highly unstable in aqueous conditions at biological pH, converting back to their α-hydroxyglycine analogues with a half-life of 1-3 seconds. A mechanism for the formation of **8** from *N*-benzoyl-α-acetoxyglycine methyl ester **14** is illustrated in Figure 15. The initial step in the hydrolysis of **14** is the formation of a transient *N*-acyliminium ion **15**, which in a subsequent fast step, undergoes attack by hydroxide to

give the α-hydroxyglycine **8**. The rate-determining step in the formation of **8** from **14** has been suggested to be the elimination of the carboxylate ion.

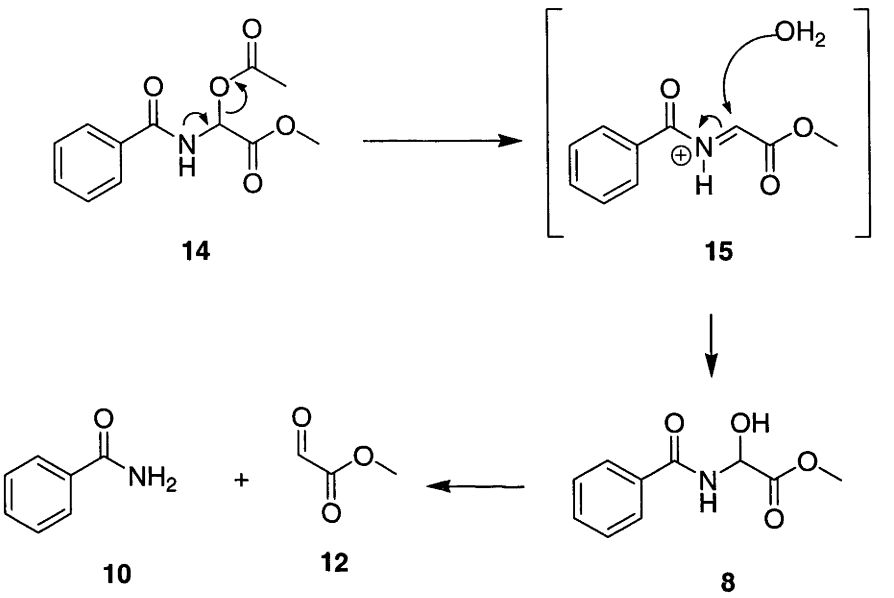

Figure 15. Mechanism of Hydrolysis of *N*-Benzoyl-α-acetoxyglycine Methyl Ester **14**.

The ability of acetate to stabilise a negative charge is reflected in the relatively low pK_a of acetic acid, which is 4.0.[43] As a result, acetate is a good leaving group. Therefore the instability of **14** may be due to the rate of elimination of the acyloxy anion being too fast. The hydrolysis of *N*-benzoyl-α-acetoxyglycine methyl ester **14** is investigated in Chapter 2 of the Results and Discussion section of this thesis to re-examine previously published results.[41] The development of α-substituted glycines, which hydrolyse to release amides slowly in comparison to *N*-benzoyl-α-acetoxyglycine methyl ester **14** in aqueous solution at biological pH, was desired. It seemed likely that this could be achieved if the rate of conversion of glycines such as **14** to **15** could be extended through the use of suitable alternatives to acyloxy groups as glycine α-substituents. In

Chapter 2 of the Results and Discussion section of this thesis, the α-substituted glycines which were investigated for their potential rates of hydrolysis in aqueous conditions or to compare with literature values,[41] are **8**, **14**, **17**, **19**, **21** and **22** (Figure 16).

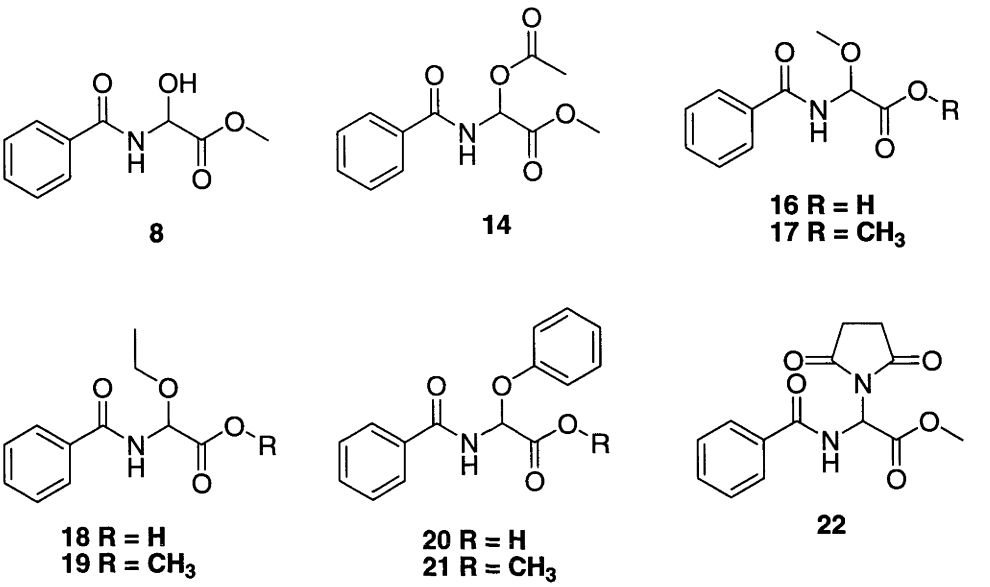

Figure 16. α-Substituted Glycine Derivatives **8**, **14** and **16 – 22**.

N-Benzoyl-α-methoxyglycine **16** and *N*-benzoyl-α-ethoxyglycine **18** have been previously synthesised in high yield via the base catalysed hydrolysis of *N*-benzoyl-α-methoxyglycine methyl ester **17** and *N*-benzoyl-α-ethoxyglycine methyl ester **19** respectively, with sodium hydroxide in aqueous methanol.[44] The high yield (96%) of *N*-benzoyl-α-methoxyglycine **16** obtained was surprising as the conditions used were aqueous. Using such conditions it would be reasonable to expect that, to some extent, *N*-benzoyl-α-methoxyglycine methyl ester **17** would have converted to the α-hydroxyglycine analogue **8** followed by the release of benzamide **10** in a similar manner to the hydrolysis of the α-acetoxyglycine **14** (Figure 15). The formation of the α-hydroxyglycine **8** would however, have required the generation of the transient *N*-acyliminium ion **15** to which water could then add. The yield of *N*-benzoyl-α-ethoxyglycine **18** was 94%. No evidence for the formation of the α-methoxyglycine **17**

or the α-hydroxyglycine **8** from **19** was reported. Exchange of **19** to give **17** or **8** would have also required the formation of the *N*-acyliminium intermediate **15**. Therefore, the formation of the *N*-acyliminium ion **15** from **17** or **19** seems unlikely. For **17** and **19** to form the *N*-acyliminium ion **15**, the respective methoxy and ethoxy groups would need to be displaced. Methanol and ethanol have pK_as of 15.0 and 17.5 respectively.[43] This reflects the poor ability of methoxide and ethoxide to stabilise a negative charge and as a result, they are poor leaving groups. This may explain the high yields of the α-methoxyglycine **16** and the α-ethoxyglycine **18** produced through the hydrolysis of **17** and **19** respectively under the conditions used by Kawai *et al.*[44] However, the fact that no *N*-acyliminium ion was then produced from **16** or **18** may be due to the short length of time over which the reactions were performed, which was one hour. The potential for hydrolysis of α-methoxy and α-ethoxyglycines in aqueous media over time periods greater than one hour had not been investigated. α-Alkoxyglycines are considered to be unstable due to an electronegative oxygen being directly attached to the α-carbon.[44] As a result it seemed reasonable to expect that the subjection of the α-methoxyglycine **17,** and the α-ethoxyglycine **19**, to aqueous conditions over extended periods of time, rather than one hour, might result in the slow formation of the free acid analogue of the α-hydroxyglycine **8**, this would then be expected to hydrolyse to release benzamide **10**. Studies evaluating the hypothesis that and **17** and **19** might slowly hydrolyse *via* an α-hydroxyglycine to release benzamide **10** in aqueous conditions over extended time periods are outlined in Chapter 2 of the Results and Discussion section of this thesis.

Attempts by Kawai *et al.*[44] at the base catalysed hydrolysis of *N*-benzoyl-α-phenoxyglycine methyl ester **21** by stirring in a solution of sodium hydroxide in

aqueous methanol were found not to yield the free acid, *N*-benzoyl-α-phenoxyglycine **20**, but rather the α-methoxyglycine **16**. This indicated that methanol was adding to the *N*-acyliminium ion **15** (which was most likely forming through the elimination of phenoxide) to give **17**. Saponification of **17** then gave the free acid **16**. It would also be expected that water would have added to the *N*-acyliminium ion **15** to give the α-hydroxyglycine **8** followed by subsequent hydrolysis to release benzamide **10**, however this possibility was not addressed. When the hydrolysis of *N*-benzoyl-α-phenoxyglycine methyl ester **21** was performed using sodium hydroxide in aqueous isopropanol, only benzamide **10** was isolated,[44] however no reasoning for its formation was provided. This may have been due to isopropanol being too poor a nucleophile (in comparison to methanol) to attack the *N*-acyliminium ion **15**. This would then allow water to add to **15**, forming the α-hydroxyglycine **8**, which presumably then hydrolysed to release benzamide **10**. It therefore seemed likely that under biological conditions, *N*-benzoyl-α-phenoxyglycine methyl ester **21** would also react, forming the α-hydroxyglycine **8**. Phenol has a pK_a of 10.0, which is in between that of acetic acid (4.0) and methanol and ethanol (15.0 and 17.5 respectively).[43] As a result phenoxide is a poorer leaving group than acetate and a better leaving group than both methoxide and ethoxide. It was therefore hypothesised that if *N*-benzoyl-α-phenoxyglycine methyl ester **21** was found to react to form the α-hydroxyglycine **8** in aqueous conditions, it would be at a slower rate than **14** and faster than the rates of the potential hydrolysis of **17** and **19**. Succinimide has a pK_a of 9.6 which is similar to that of phenol and as such, *N*-benzoyl-α-succinimidoglycine methyl ester **22** would also be expected to exchange to the α-hydroxyglycine **8** in aqueous conditions. Therefore the potential hydrolysis of **21** and **22** to release benzamide **10** in aqueous conditions was studied and the results are presented in Chapter 2 of the Results and Discussion section of this thesis.

In addition to hydrolytically cleavable derivatives of glycine, the *C*-terminal amide of peptide hormones could also be masked with photochemically removable groups resulting in photoactivatable hormone prodrugs. Chapter 3 of the Results and Discussion section of this thesis outlines research towards the photochemical release of *C*-terminal amidated peptide hormones. Therefore a short review of the chemistry of relevant photochemically cleavable groups follows.

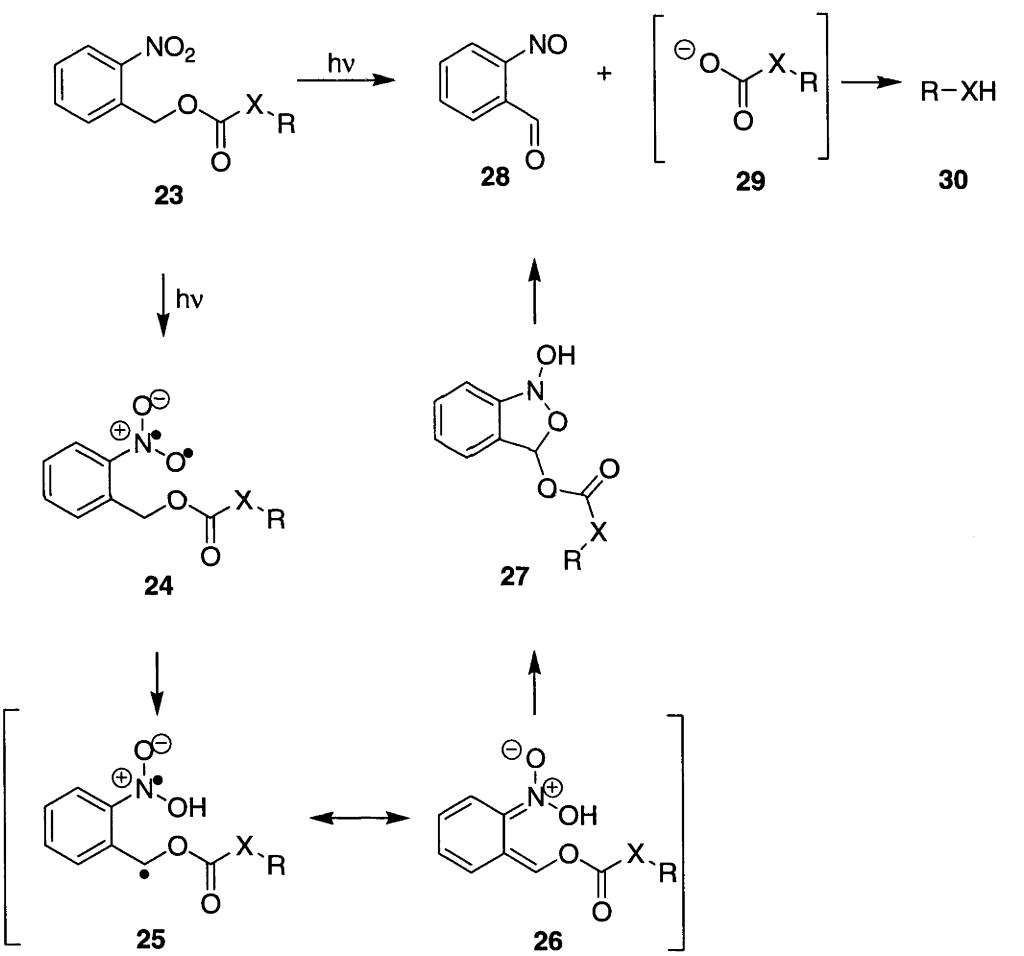

Figure 17. NBOC Photolysis Mechanism, X = NH or O.[45]

One of the most commonly used photolytic protecting groups is the 2-nitroveratroyloxycarbonyl group (NVOC), which was originally introduced by

Patchornik, Amit and Woodward.[45,46] NVOC and the analogous 2-nitrobenzyloxycarbonyl protecting group (NBOC)[46] have been used to protect alcohols and amines. NVOC and NBOC differ in that NVOC is methoxy substituted at the 4- and 5-positions of the aromatic ring. However, their mechanism of photolysis is the same. The mechanism of photolysis of NBOC is illustrated in Figure 17. Irradiation of **23** results in the formation of the diradical **24**. This is followed by abstraction of a hydrogen atom from the benzylic carbon by the oxygen-centred radical of **24** to give **25**. The *aci*-nitro intermediate **26**, which is a resonance form of **25**, then reacts to give the bicyclic species **27**. The bicyclic species **27** then spontaneously collapses[45] to release 2-nitrosobenzaldehyde **28** and the carbonate or carbamate anion **29** which through decarboxylation give the respective amine or alcohol **30**. The spontaneous degradation of the bicyclic species **27** is most likely related to the high efficiency of the resonance stabilised carbonate or carbamate anions to act as leaving groups. The rate determining step of NBOC photolysis is the ring closure of the *aci*-nitro species **26** to give the bicyclic intermediate **27**.[47] This is not surprising as the ring closure of **26** constitutes a 5-*endo-trigonal* process and as such is disfavoured.[48]

The 2-nitrophenethyloxycarbonyl group (NPEOC), which is a variant of NBOC, has been used to protect amines and alcohols and to mask carboxylic acids.[49,50] NPEOC differs from NBOC or NVOC in that it is derived from 2-(2-nitrophenyl)ethyl alcohol rather than 2-nitrobenzyl alcohol. The mechanism of NPEOC photolysis to unmask carbonate, carbamate or carboxylate anions is illustrated in Figure 18.

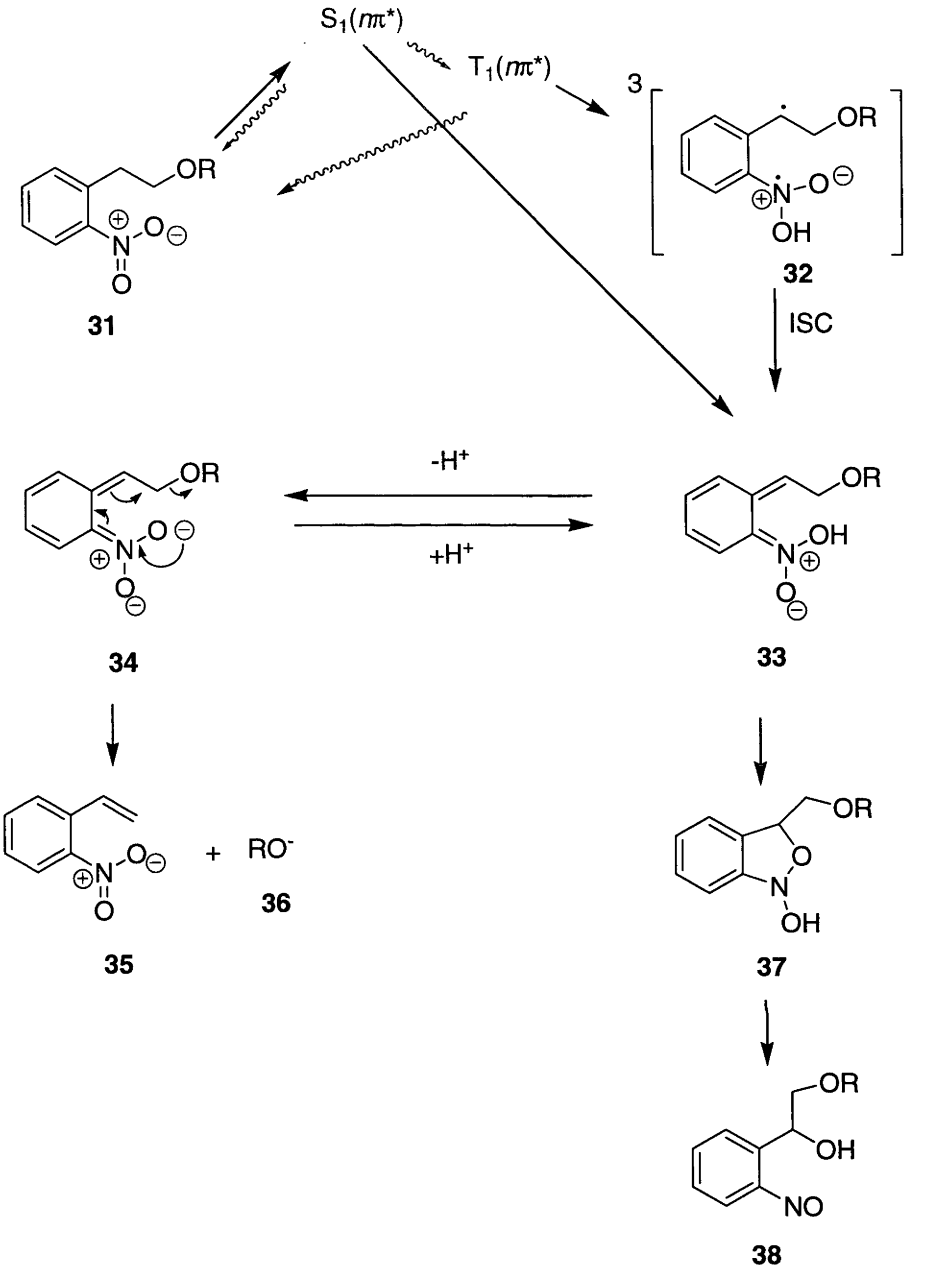

Figure 18. Mechanism of Photolysis of NPEOC R = Ac, COOMe, CO-5'-*O*-thymidine or CO-Phe-OH.[49,50]

Upon irradiation of **31** in the first absorption band, the $S_1(n\pi^*)$ of the NPEOC chromophore is populated. It decays by intersystem crossing to the triplet state $T_1(n\pi^*)$ and by internal conversion to the singlet ground state. It is believed that hydrogen atom transfer from the benzylic carbon to the nitro group is the mechanism by which the

triplet state relaxes. The primary product produced this way is a triplet biradical **32** that rapidly relaxes to the *o*-quinoid singlet ground state of the *aci*-nitro form **33**. Since the *aci*-nitro compound **33** represents an unstable tautomer of the starting compound **31**, its reversion to the stable tautomer **31** is also a possible pathway at this stage of the mechanism although other processes appear to out compete this. The *aci*-nitro form **33** can then either degrade to form unknown by-products, form the bicyclic compound **37** followed by degradation to the benzylic alcohol **38** or after deprotonation of the nitro group to give **34**, undergo elimination to form 2-nitrostyrene **35** and the anion **36**. In the case of **36** being a carbonate or carbamate anion, subsequent decarboxylation releases the alcohol or amine respectively.

The research described in Chapter 3 of the Results and Discussion section of this thesis is concerned with the release of amides through the photolysis of a photocleavable group. The protection of amides with NVOC, NBOC or NPEOC groups would not be viable as the corresponding acylcarbamates (Figure 19) would be too unstable.

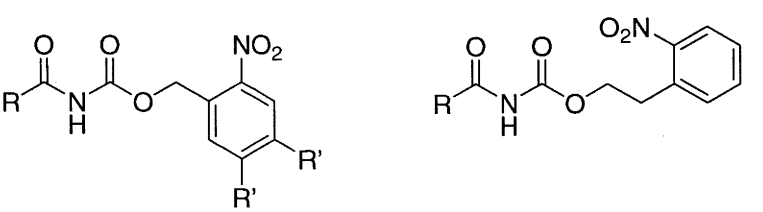

Figure 19. NVOC (R' = OCH_3), NBOC (R' = H), or NPEOC Protected Amides.

Amides have been masked using systems derived from NBOC such as 2-nitrobenzylamine **39**[51] and 2-nitrophenylglycine (Npg) **40**[52] (Figure 20). A review of the chemistry and applications of Npg **40** now follows.

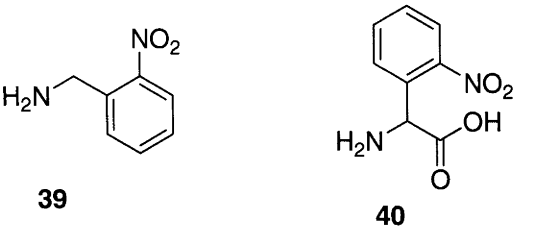

Figure 20. 2-Nitrobenzylamine **39** and Npg **40**.

The mechanism of photolysis of the Npg **41** (Figure 21) follows a similar pathway to that of NBOC **23** photolysis (Figure 17).

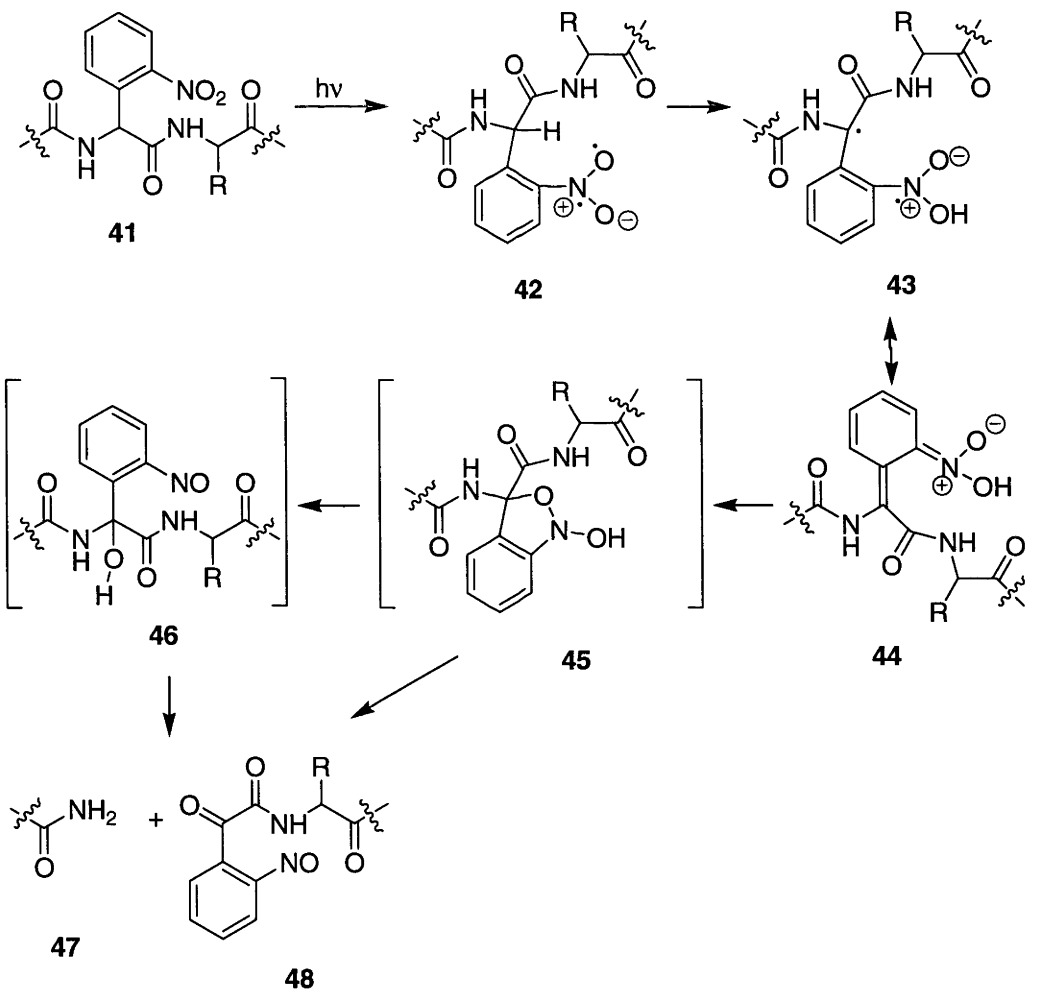

Figure 21. The Mechanism of Npg Photolysis.

Upon irradiation of the Npg **41**, the diradical **42** is formed. A hydrogen atom is then abstracted from the benzylic carbon of **42** by the oxygen centred radical to give **43**. The *aci*-nitro intermediate **44**, which is a resonance form of the diradical species **43**, then reacts further to give the transient bicyclic intermediate **45**. The degradation of the bicyclic species **45** has been thought to directly release an amide **47** and a nitrosoketone **48**, bypassing the formation of the α-hydroxy species **46**.[52] Alternatively, it has been suggested that the bicyclic intermediate **45** degrades via the transient formation of the α-hydroxy species **46** followed by hydrolysis to the amide **47** and the nitrosoketone **48**.[53]

The use of Npg **40** as a photochemically cleavable amino acid has been applied in a number of research areas, though with some limitations. Using the *in vivo* nonsense codon suppression method for incorporating unnatural amino acids into proteins expressed in *Xenopus oocytes*, England *et al.*[52] incorporated Npg **40** into two ion channels: the *Drosophila* Shaker B K^+ channel and the nicotinic acetylcholine receptor. Irradiation of the proteins *in vivo* led to peptide backbone cleavage at the site of the Npg residue. This method was used to investigate the functional role of the Cys128-Cys142 disulfide loop in the nAChR α subunit. Npg photolysis has also been utilised in the synthesis of *C*-terminal amidated peptides.[51] Micro-organisms lack the necessary enzymatic machinery to produce peptide hormones. As a result, in these systems, such hormones cannot be produced using gene technology. In order to overcome the difficulties in synthesising peptide hormones, a method was developed which involved their enzymatic synthesis (using the yeast derived carboxypeptidase-Y) with an Npg residue connected to their terminal amino acids. Irradiation of the peptides then cleaved the Npg residue, releasing the *C*-terminal amidated hormones. Production of hormones

via this method was achieved with high levels of efficiency provided the pH of the solution in which the photolysis of the Npg extended peptides was performed was basic. Although the photolysis of Npg has many novel applications, it has been reported to be very slow and inefficient at biological pH[53] with calls being made in the literature for the development of more efficient alternatives.[52] It seemed likely therefore, that the development of an unnatural amino acid, which could be photolysed to release amides efficiently at biological pH, was warranted. However, before this can be addressed, an understanding of why Npg photolysis is inefficient at biological pH is necessary.

The rate-determining step of the photolysis of NBOC **23** to release carbonate or carbamate anions has been established to be the degradation of the *aci*-nitro intermediate **26** to form the bicyclic system **27** (Figure 17).[47] The bicyclic species **27** then breaks down spontaneously to give the carbonate or carbamate anion **29** which decarboxylates to give the respective alcohol or amine **30**. In this way, NBOC groups can be efficiently photolysed to release the typical alcohols and amines **30**, which are poor leaving groups. It appears that the rate-determining step of the photolysis of the Npg **41** has been assumed to be the degradation of its equivalent *aci*-nitro intermediate **44**, [51,52,54,55] in spite of the fact that in this case cleavage releases an amide **47** which is a poor leaving group in comparison to a carbonate or carbamate anion **29**.

Recent work by Corrie *et al.*[47] on the photolysis of 1-(2-nitrophenyl)ethyl ethers (the photolysis mechanism of which is analogous to that of Npg in that the cleavage step involves the release of a poor leaving group) found that the degradation of its *aci*-nitro intermediate **49** was not rate-determining (Figure 22).

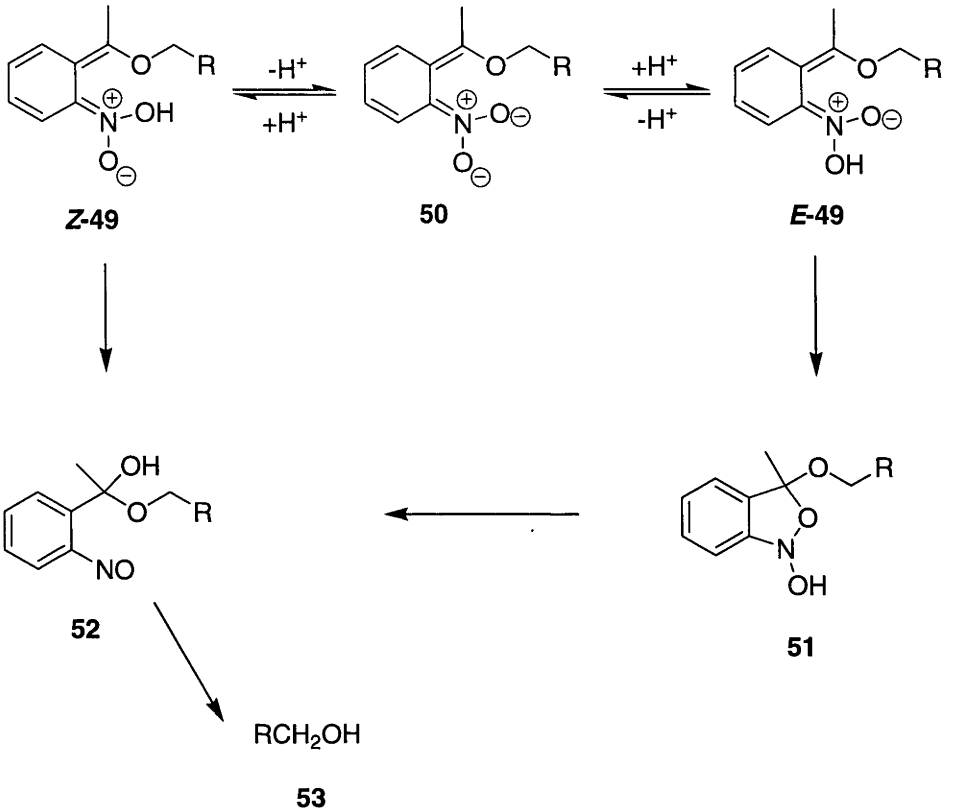

Figure 22. Proposed Two-Path Mechanism for Breakdown of the *aci*-Nitro Intermediate **49**, Generated Through the Photolysis of a 1-(2-Nitrophenyl) Ether.[47]

Flash photolysis studies performed by Corrie *et al.*[47] identified two elimination pathways from the *aci*-nitro species **49** generated through irradiation of a 1-(2-nitrophenyl)ethyl ether. In the mechanism outlined in Figure 22, the *aci*-nitro intermediate **49** can react *via* a 1,4- shift of the nitro OH to the benzylic carbon to give the hemiacetal intermediate **52** followed by hydrolysis to release the alcohol **53**. Alternatively the *aci*-nitro intermediate **49** can undergo a 5-*endo-trigonal*[48] ring closure to form the bicyclic species **51**, which then ring opens to give the hemiacetal **52**, followed by the hydrolysis of **52** to release the alcohol **53**. The *aci*-nitro dianion **50** was found to not undergo ring closure. It was found that in the case of 1-(2-

nitrophenyl)ethyl ether photolysis to release alcohols, the degradation of the hemi-acetal intermediate **52** rather than the *aci*-nitro intermediate **49** was rate-determining. Interestingly a similar intermediate to the hemi-acetal **52** was isolated during the photolysis of *N*-(2-nitrobenzyl)-1-napthalamide **54** to release an amide, except in this case the intermediate was a hemi-amidal **55** (Figure 23).[56]

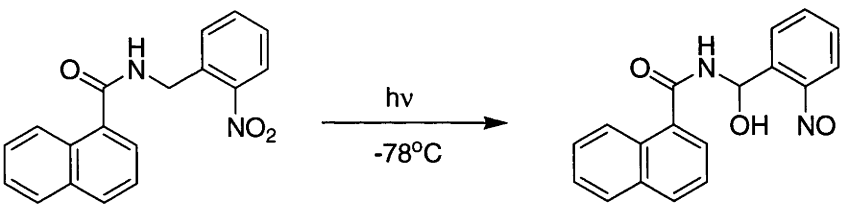

54 **55**

Figure 23. Photolysis of *N*-(2-Nitrobenzyl)-1-napthalamide **54** to Give the Hemi-amidal **55** Isolated by Itsuno *et al.*[56]

Corrie *et al.*[47] identified from the photolysis of 1-(2-nitrophenyl)ethyl ethers, that the hemi-acetal intermediate **52** was the precursor to cleavage (Figure 22) and that its hydrolysis to release the alcohol **53** was the rate-determining step. The fact that this step, rather than the disfavoured 5-*endo-trigonal* ring closure of **49** to give **51** was rate determining may be related to the instability of alkoxy anions. As was stated earlier, alkoxides are considered to be poor leaving groups. This was shown to be reflected in the pK_as of methanol and ethanol which are 15.0 and 17.5 respectively.[43] The pK_a of the alcohol **53** illustrated in Figure 22 would be expected to be similar to that of methanol and ethanol and as such it would also be a poor leaving group. This may explain why the degradation of the bicyclic intermediate **51** resulted in the formation of the hemi-acetal **52** rather than spontaneous release of the alcohol **53**. Primary amides have pK_as in the region and above that of acetamide which is 15.0.[43] Their pK_as are therefore of a

similar value to those of methanol and ethanol and correspondingly, amides are considered to be poor leaving groups. This may account for the ability of the hemi-amidal **55** to be isolated from the photolysis of **54**.[56] It is therefore apparent that in the photolysis of 2-nitrobenzyl groups (such as in the photolysis of **54**) or analogues (such as in the photolysis of a 1-(2-nitrophenyl)ethyl ether) to release poor leaving groups, the cleavage step is rate-determining. The photolysis of the Npg **41** releases an amide **47** *via* a similar mechanism to that of the release of the alcohol **53** through the irradiation of a 1-(2-nitrophenyl)ethyl ether compound. Therefore, as the amide **47** is a poor leaving group, the α-hydroxy system **46** would be expected to form during the photolysis of the Npg **41**. Furthermore, the hydrolysis of **46**, rather than the degradation of the *aci*-nitro intermediate **44**, would be expected to be rate-determining. The poor efficiency of photolysis of Npg at biological pH, as reported in the literature[52,53] may therefore be due to the formation of α-hydroxy intermediates such as **46** (Figure 21) and their subsequent slow hydrolysis. Indeed, in comparison to the rates of the other steps during the photolysis of Npg **41**, it would be reasonable to expect that the α-hydroxy intermediate **46** would hydrolyse slowly at biological pH in a similar manner to that of α-hydroxyglycines such as **7** and **8** which have half-lives of 6.7 and 0.78 hours, respectively.[41] It is therefore apparent that the development of a photochemically cleavable amino acid that does not involve the formation of intermediates that are slow to breakdown at biological pH is warranted.

NPEOC has been used to protect alcohols and amines. NPEOC has also been used to mask carboxylic acids, however no equivalent system based on NPEOC has been developed to mask amides. The cleavage step in the mechanism of photolysis of NPEOC **31** comes from the *aci*-nitro intermediate **34** and does not involve the

formation of species that would be expected to be slow to breakdown at biological pH (Figure 18). It was therefore hypothesised that, an amino acid, which was analogous to NPEOC might photolyse more efficiently at biological pH than Npg **40**. 2-Nitrophenylalanine was therefore designed and investigations into its potential photolysis to release amides are outlined in Chapter 3 of the Results and Discussion section of this thesis. A reaction scheme for the photolysis of a 2-nitrophenylalanine system **56** is illustrated in Figure 24.

By analogy to the mechanism of NPEOC photolysis (Figure 18), the photolysis of the 2-nitrophenylalanine **56** to cleave the N-C^{α} bond may release an amide **47** and a cinnamyl derivative **57** (Figure 24).

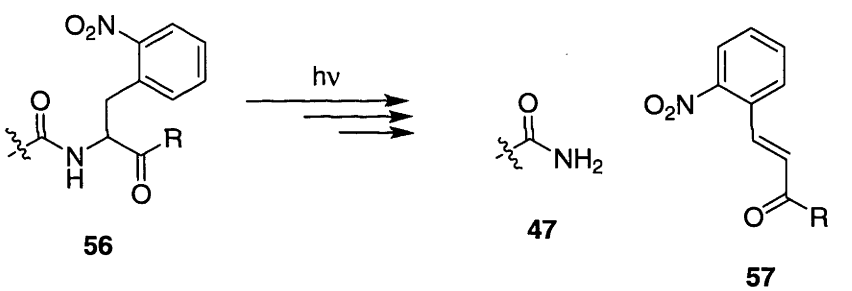

56 **47** **57**

Figure 24. Proposed Photolysis of a 2-Nitrophenylalanine System **56** to Unmask an Amide **47** and Release a Cinnamyl Derivative **57**, R = NH_2, NHR', OH or OR'.

The potential photolysis of 2-nitrophenylalanine to unmask amides efficiently at biological pH may have many applications. 2-Nitrophenylalanine could be use as an alternative to Npg in site-selective photochemical proteolysis. It would constitute a photocleavable linker, which could be used to connect hormones to the polymers, antibodies and immunotoxins that were described earlier for their potential to improve

the lifetime and selectivity of peptide hormones *in vivo*. Photodynamic therapy (PDT) involves the administration of a photosensitising drug, which preferentially accumulates in target tissues.[57] PDT is generally associated with the generation of singlet oxygen in cancer cells, which then results in their death. However, it may be that the technology used in PDT could also be utilised in 'Laser Photochemotherapy'.[58] Submillimeter diameter laser fibreoptics can be inserted via vascular or interstitial access providing a precise, minimally invasive method of activating light sensitive drugs in tumours. The masking of the *C*-terminal amide of peptide hormones with 2-nitrophenylalanine may result in light-activated hormone prodrugs that may find application in the area of 'Laser Photochemotherapy'. The potential photolysis of 2-nitrophenylalanine may be applied to a number of other research areas. Photoprobes are becoming increasingly common as remotely controllable tools in the drug discovery process.[59] The photochemical release of neurotransmitters (which are *C*-terminal amidated peptides) from 'caged' compounds can be used to study fast kinetic processes (in the submillisecond range) of neurotransmitter release and cell signalling through second messenger pathways. Such studies have allowed the elucidation of the activation mechanisms of learning and memory. This technique has also been used in the study of neurological disorders such as epilepsy and anxiety. The potential photolysis of 2-nitrophenylalanine might also be employed in the area of compound release from solid support.

This dissertation will now outline research towards the inhibition of peptide hormone production by PAM, the development of α- substituted glycines for the controlled hydrolytic release of *C*-terminal amidated peptides and the release of amides through the photolysis of 2-nitrophenylalanine residues.

Chapter 1. Inhibition of Peptidylglycine α–Amidating Monooxygenase by Exploiting Factors Affecting the Stability and Ease of Formation of Glycyl Radicals.

1.1 Project Rationale

As discussed in the Introduction, peptidylglycine α-amidating monooxygenase (PAM) catalyses the biosynthesis of a wide variety of *C*-terminal peptide amides through oxidative cleavage of the corresponding glycine-extended precursors (Figure 1). PAM has been implicated in a large number of disease states such as cancer,[6] asthma[8] and neurological disorders.[10] Therefore the development of systems for the inhibition of PAM could provide methods for the treatment of such diseases.[3]

The natural substrates of PAM all have in common an *N*-acylated glycine, and they are therefore comprised of acyl, amido, methylene and carboxyl groups. The common features possessed by PAM substrates, which contribute to α-carbon centred radical stability, were targeted for alteration in order to establish their effect on enzyme activity. The free carboxylate has been established as very important for substrate binding to PAM,[2] therefore all systems designed were to retain this functionality. PAM is known to accept a wide variety of acyl substituents and so variations of this group were investigated. Although derivatives of α-substituted amino acids tend not to bind to PAM, small α-alkyl substituents, such as the methyl group of (*R*)-alanine,[30,60] the vinyl moiety of (*R*)-vinylglycine[61] and the hydroxyethyl group of (*R*)-threonine are

accommodated.[60] The incorporation of a trifluoromethyl group was therefore studied since β,β,β-trifluoroalanine derivatives are known to be resistant to α-carbon centred radical formation.[21] Further to this, the amido group of PAM substrates was varied through substitution of the glycine unit with a glycolic acid or γ-keto acid. Glycolate inhibitors of PAM have been previously reported[13,61] in studies of broad ranges of compounds, but there has been no analysis of, nor explanation for, their behaviour. One γ-keto acid has been previously reported but it was found not to interact with PAM, either as a substrate or an inhibitor.[62]

The intention of these studies was to investigate factors affecting the formation of α-carbon centred glycyl radicals in order to design analogues of PAM substrates that competitively bind to but are not processed by the enzyme, and therefore inhibit the reaction of substrates. In order to achieve this, the results of ab initio calculations and studies of reaction rates in free radical brominations, which identify factors affecting the stability and ease of formation of α-carbon centred glycyl and related radicals, were compared with the kinetic parameters defining the interactions of analogous compounds with PAM.

1.2 Synthesis of Compounds for Investigation

A variety of compounds were required in order to study their reactivity in radical brominations or their interactions with PAM. The synthesis of these compounds will now be described.

1.2.1 Methyl O^{α}-Benzoylglycolate 59

The synthesis of methyl O^{α}-benzoylglycolate **59** was performed as depicted in Figure 25.

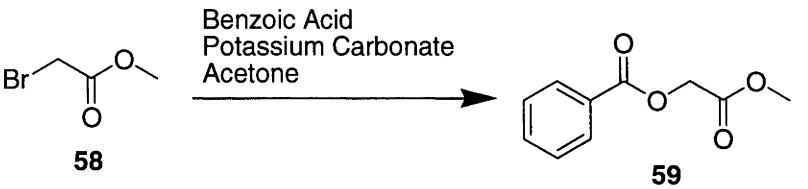

Figure 25. Synthesis of Methyl O^{α}-Benzoylglycolate **59**

Benzoic acid in acetone along with methyl bromoacetate **58** and potassium carbonate was heated at reflux overnight. The product **59** was purified by recrystallisation from ethyl acetate/hexanes. Characterisation of the product by ^{1}H NMR spectroscopy displayed resonances for the α-carbon, methyl ester and aromatic protons at δ4.87, δ3.80 and δ7.44 - 8.12 ppm, respectively.

1.2.2 *N*-Benzoylglycine Methyl Ester 61

The synthesis of *N*-benzoylglycine methyl ester **61** followed previously established chemistry (Figure 26).[63]

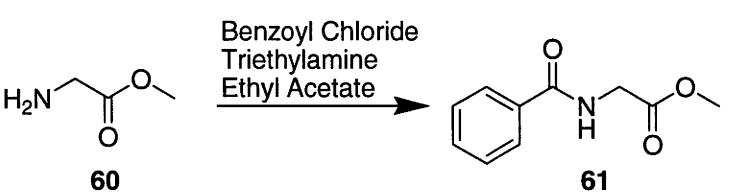

Figure 26. Synthesis of *N*-Benzoylglycine Methyl Ester **61**

Glycine methyl ester **60** along with benzoyl chloride and triethylamine was heated to reflux in ethyl acetate overnight to give *N*-benzoylglycine methyl ester **61**. The ^{1}H NMR spectrum of the product showed multiplet resonances for the aromatic protons at δ7.44 - 7.82 ppm confirming the presence of the benzoyl protecting group. This along with the glycine α-carbon protons' and methyl ester resonances at δ4.26 and δ3.79 ppm respectively indicated the reaction to have proceeded.

1.2.3 *O*$^{\alpha}$-(*N*-Acetyl-(*S*)-phenylalanyl-(*S*)-phenylalanyl)glycolic Acid 64

In the above synthesis of methyl *O*$^{\alpha}$-benzoylglycolate **59,** methyl bromoacetate **58** was used to install a methyl glycolate. However, as **64** is a free acid, synthesis via a methyl glycolate would not be suitable as the conditions required for methyl ester hydrolysis would also cleave the glycolate ester. Benzyl esters can be cleaved through hydrogenolysis, which could be performed without hydrolysis of the glycolate ester. Thus, benzyl bromoacetate was used to install the glycolate unit in compound **63**. The synthesis of *O*$^{\alpha}$-(*N*-acetyl-(*S*)-phenylalanyl-(*S*)-phenylalanyl)glycolic acid **64** is illustrated in Figure 27. *N*-Acetyl-(*S*)-phenylalanyl-(*S*)-phenylalanine **62** was purchased from Aldrich Chemical Company and converted to benzyl *O*$^{\alpha}$-(*N*-acetyl-(*S*)-phenylalanyl-(*S*)-phenylalanyl)glycolate **63** by reaction with benzyl bromoacetate and potassium carbonate in refluxing acetone. The ^{1}H NMR spectrum of the product displayed resonances for the benzylic protons of the benzyl ester at δ5.20 ppm and glycolate α-carbon protons at δ4.68 and δ4.75 ppm indicating that the glycolate unit had been installed. Hydrogenolysis of **63** in tetrahydrofuran with 10% palladium on carbon under an atmosphere of hydrogen gave the free acid **64**. The absence of a resonance in

the ^{1}H NMR spectrum of the product in the region of δ5.20 ppm characteristic of the benzylic protons of a benzyl ester indicated the loss of the benzyl group. The presence of the glycolic acid α-carbon protons was confirmed by the presence of a resonance at δ4.64 ppm. During the synthesis of **64**, racemisation was a possibility due to the basic conditions required for the installation of the benzyl glycolate moiety. However as the synthesis of **64** began with the chirally pure **62** and as there was only one set of resonances in the ^{1}H NMR spectrum of either **63** or **64** for each α-carbon proton the absence of diastereomers and therefore the retention of (*S*)-stereochemistry was established.

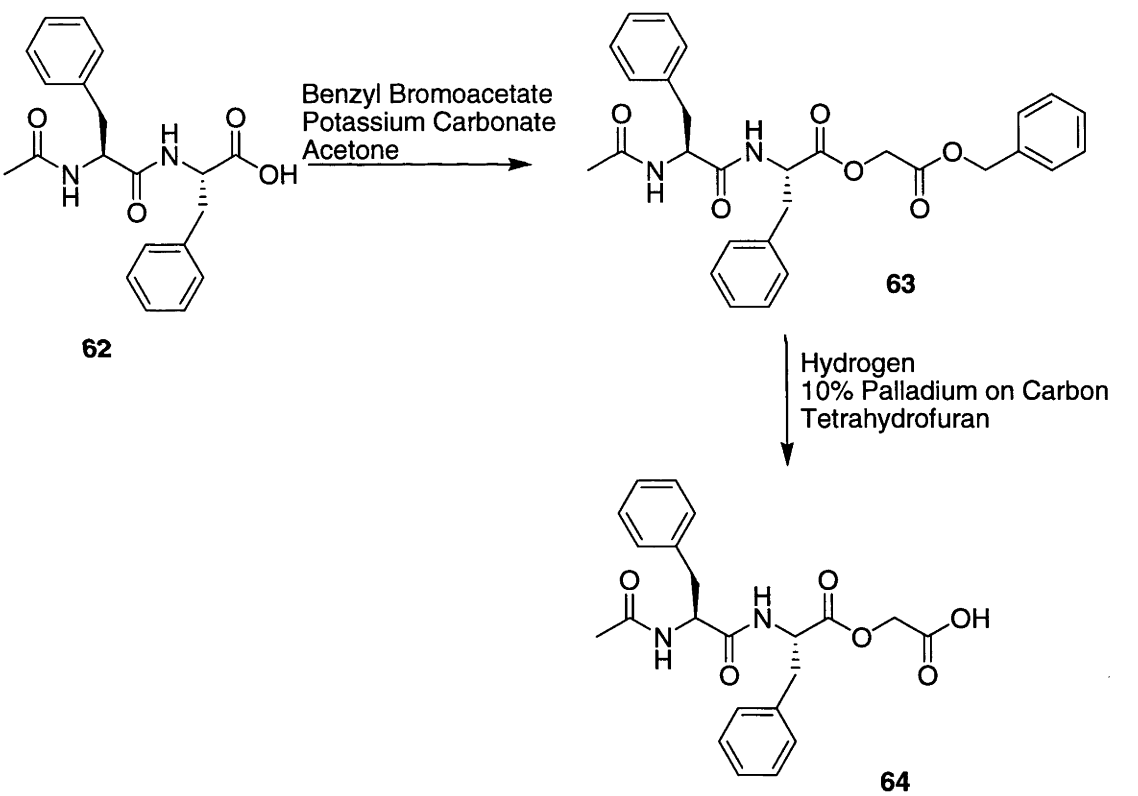

Figure 27. Synthesis of *O*$^{\alpha}$-(*N*-Acetyl-(*S*)-phenylalanyl-(*S*)-phenylalanyl)glycolic Acid **64**

1.2.4 O^{α}-(*N*-Benzoyl-(*S*)-valyl)glycolic Acid 70

The synthesis of O^{α}-(*N*-benzoyl-(*S*)-valyl)glycolic acid **70** is depicted in Figure 28. (*S*)-Valine **65** was stirred in methanol that had been pre-treated with thionyl chloride to give **66**. Compound **66** was then treated with benzoyl chloride in refluxing ethyl acetate to give *N*-benzoyl-(*S*)-valine methyl ester **67**. The ^{1}H NMR spectrum of the product displayed resonances for the aromatic protons at δ7.26-7.82 ppm, the α-carbon proton at δ4.79 ppm and the methyl ester protons at δ3.77 ppm. Compound **67** was then saponified in a 1:1 mixture of tetrahydrofuran and 1M sodium hydroxide to give *N*-benzoyl-(*S*)-valine **68**. The absence of a resonance indicative of methyl ester protons in the region of δ3.77 ppm in the products' ^{1}H NMR spectrum was evidence that the deprotection had occurred. The melting point of the product was 129 °C which corresponded closely with that recorded in the literature for *N*-benzoyl-(*S*)-valine **68** (127 °C).[64] *N*-Benzoyl-(*S*)-valine **68** along with benzyl bromoacetate and potassium carbonate in acetone were heated at reflux overnight to give **69**. The ^{1}H NMR spectrum of the product displayed resonances for the α-glycolate protons at δ4.64 and δ4.86 ppm, benzylic protons at δ5.21 ppm and the valine α-carbon proton at δ4.91 ppm. Hydrogenolysis of **69** using 10% activated palladium on carbon in tetrahydrodrofuran under an atmosphere of hydrogen gave **70**. The product was purified by HPLC using water and acetonitrile as solvents. Care was taken not to use 0.01% trifluoroacetic acid in water as an eluent as the glycolic acid ester was found to be acid labile. The ^{1}H NMR spectrum of the purified product showed resonances for the glycolic acid α-carbon protons at δ4.36 and δ4.64 ppm and the valine α-carbon proton at δ4.63 ppm.

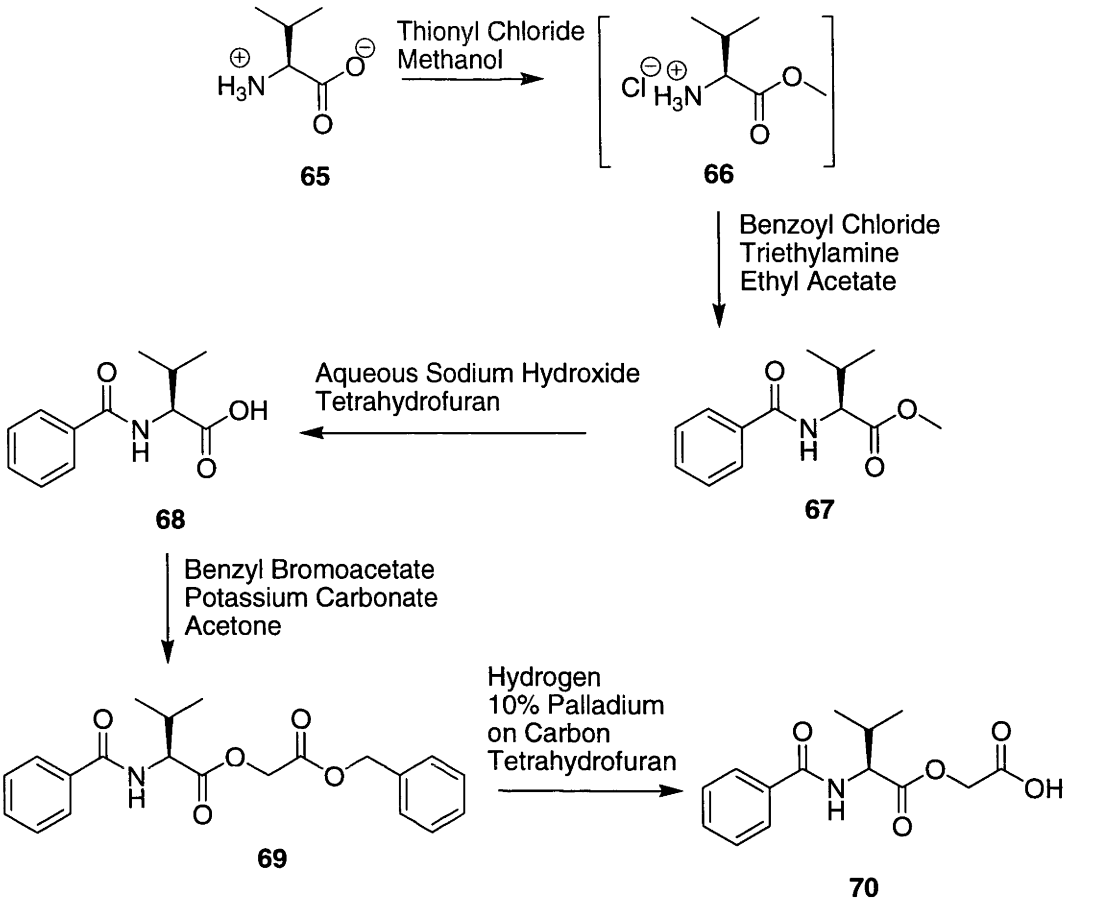

Figure 28. Synthesis of O^{α}-(*N*-Benzoyl-(*S*)-valyl)glycolic Acid **70**

The melting point recorded for *N*-benzoyl-(*S*)-valine **68** corresponded closely with that recorded in the literature indicating that racemisation up to this point in the synthesis had not taken place. The conditions used in the above synthesis of **64** were found not to cause racemisation. The methods used to install the glycolate moieties as part of the syntheses of **64** and **70** were similar. This, along with the fact that **70** was synthesised from chirally pure starting materials and was optically active with a rotation of -12.5° lead to the assumption that it was the single enantiomer.

1.2.5 *N*-Benzoyl-(*S*)-valylglycine 72

N-Benzoyl-(*S*)-valylglycine **72** was synthesised as outlined in Figure 29.

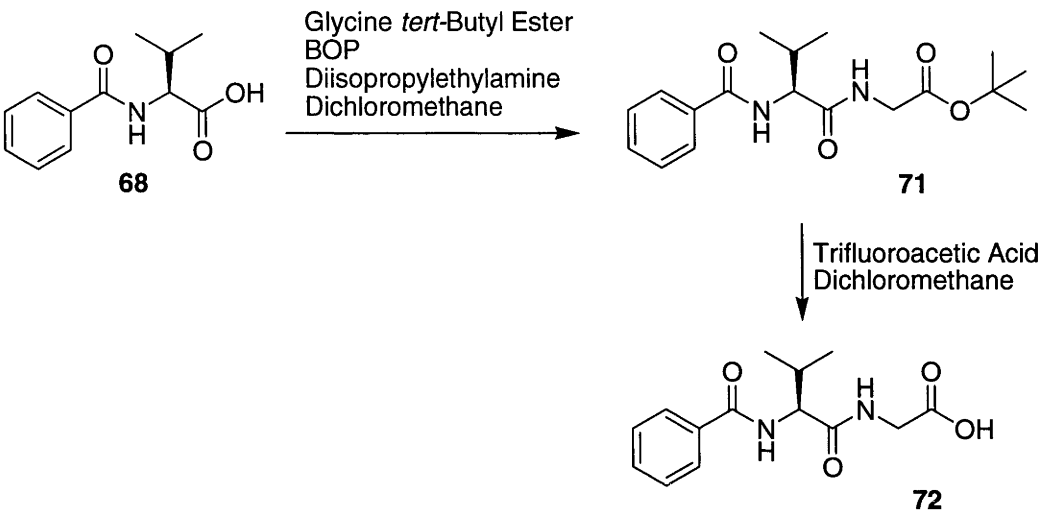

Figure 29. Synthesis of *N*-Benzoyl-(*S*)-valylglycine **72**

Compound **68** was synthesised following the method described above (Figure 28). *N*-Benzoyl-(*S*)-valine **68** was then stirred in dichloromethane along with BOP, diisopropylethylamine and glycine *tert*-butyl ester to give dipeptide **71**. The resonances in the ^{1}H NMR spectrum of the product for the glycine α-carbon protons at δ3.85 and δ4.04 ppm, the *tert*-butyl ester protons at δ1.46 ppm and the valine α-carbon proton at δ4.55 ppm indicated the coupling to have proceeded. Compound **71** was then deprotected by stirring in a mixture of dichloromethane and trifluoroacetic acid, removing the *tert*-butyl group. The ^{1}H NMR spectrum of the product **72** did not display a resonance for *tert*-butyl ester protons in the region of δ1.46 ppm indicating the deprotection to have been successful. The conditions selected for the reaction of **68** to give **71** are known to cause negligible levels of racemisation.[65] Furthermore, the conditions used to deprotect **71** to give **72** would not be expected to cause racemisation.

Therefore, as **72** was synthesised from chirally pure *N*-benzoyl-(*S*)-valine **68** and was optically active with an optical rotation of –32.2°, it was assumed that it was present as a single enantiomer.

1.2.6 N^{α}-Benzoyl-(*S*)-valinamide 73

N^{α}-Benzoyl-(*S*)-valinamide **73** was synthesised as shown in Figure 30.

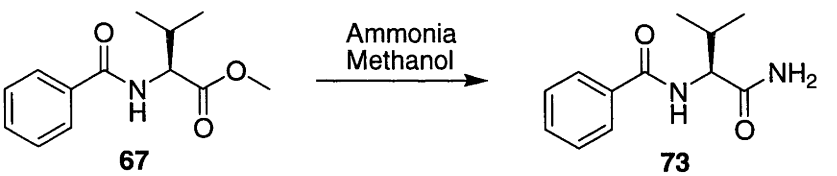

67 **73**

Figure 30. Synthesis of N^{α}-Benzoyl-(*S*)-valinamide **73**

N-Benzoyl-(*S*)-valine methyl ester **67**, synthesised by the method described in Figure 28, was treated with ammonia to give the amide **73**. The absence of resonances that could be attributed to methyl ester protons in the ^{1}H NMR spectrum of the product in the region of δ3.77 ppm along with a peak at *m/z* 221.1 in the electrospray mass spectrum for the protonated molecular ion and *m/z* 243.1 for the sodiated molecular ion indicated the reaction to have been successful. The melting point of compound **67** was 86 °C which corresponded with that provided in the literature for *N*-benzoyl-(*S*)-valine methyl ester **67** (86 °C).[66] Therefore as **73** was synthesised from the chirally pure **67** and the conditions used would not be expected to cause racemisation, **73** was assumed to be a single enantiomer. However, **73** was required purely for its retention time in UV-HPLC analysis and so the nature of its chiral centre was of no consequence to these studies.

1.2.7 O^{α}-(Decanoyl)glycolic Acid 76

O^{α}-(Decanoyl)glycolic acid **76** was synthesised as illustrated in Figure 31.

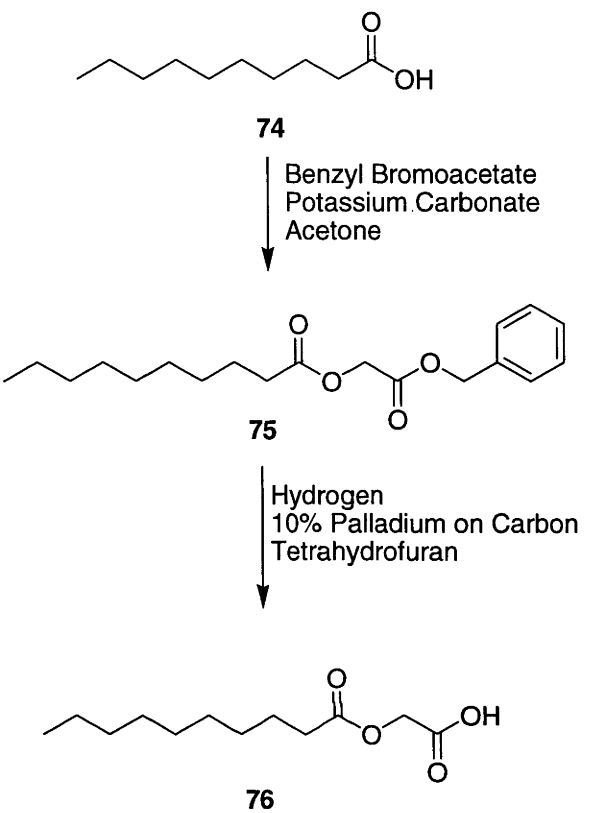

Figure 31. Synthesis of O^{α}-(Decanoyl)glycolic Acid **76**

Decanoic acid **74**, benzyl bromoacetate and potassium carbonate in acetone were heated at reflux overnight to give benzyl O^{α}-(decanoyl)glycolate **75.** The ^{1}H NMR spectrum of the product displayed resonances for the benzylic protons at δ5.19 ppm and the glycolate α-carbon protons at δ4.65 ppm. Hydrogenolysis of **75** by stirring in a suspension of 10% palladium on carbon in tetrahydrofuran under an atmosphere of hydrogen gave O^{α}-(decanoyl)glycolic acid **76**. The absence of a benzylic proton resonance in the region of δ5.19 ppm in the ^{1}H NMR spectrum of the product indicated the deprotection to have been successful.

1.2.8 O^{α}-(Benzoyl)glycolic Acid 79

The synthesis of O^{α}-(benzoyl)glycolic acid **79** is shown below in Figure 32. Benzoic acid **77** in acetone along with benzyl bromoacetate and potassium carbonate were heated at reflux overnight to give compound **78**. A benzylic protons' resonance at δ5.20 ppm and glycolate α-carbon protons' resonance at δ4.86 ppm were observed in the ^{1}H NMR spectrum of the product. Hydrogenolysis of compound **78** by stirring in a suspension of 10% palladium on carbon in tetrahydrofuran under an atmosphere of hydrogen gave the free acid **79**. The absence of a benzylic protons' resonance in the region of δ5.20 ppm in the ^{1}H NMR spectrum of the product indicated the reaction to have been successful.

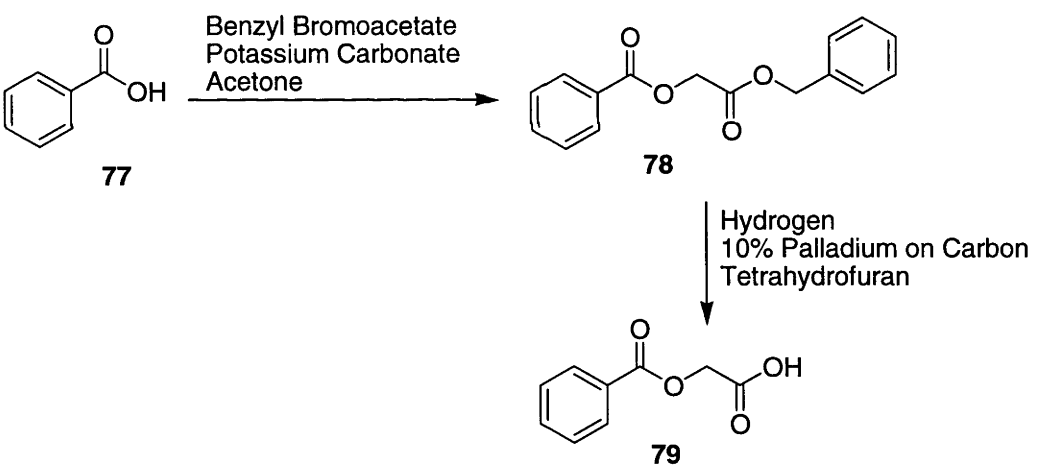

Figure 32. Synthesis of O^{α}-(Benzoyl)glycolic Acid **79**

1.2.9 3-(*N*-Acetylphenylalanyl)propionic Acid 85

The synthesis of 3-(*N*-acetylphenylalanyl)propionic acid **85** is illustrated below in Figure 33. *N*-Acetyl-(*S*)-phenylalanine **80**, purchased from Aldrich Chemical Company, was stirred in tetrahydrofuran along with 1,1'-carbonyldiimidazole to give the intermediate **81** which was then treated *in situ* with a solution of lithium *tert*-butyl acetate in tetrahydrofuran to give **82**. The ^{1}H NMR spectrum of the product displayed resonances for the *tert*-butyl ester protons at δ1.45 ppm and the phenylalanine α-carbon proton at δ4.92 ppm indicating the reaction to have been successful. Compound **82** was then stirred in tetrahydrofuran along with sodium hydride followed by treatment with a solution of benzyl bromoacetate in dichloromethane to give **83** as a mixture of diastereomers. The ^{1}H NMR spectrum of the product displayed resonances for the *tert*-butyl ester protons at δ1.37 and δ1.40 ppm, the phenylalanine α-carbon protons at δ4.04 and δ4.22 ppm and the benzyl ester benzylic protons at δ5.08 and δ5.10 ppm indicating the reaction to have proceeded. Compound **83** was then stirred in a solution of dichloromethane and trifluoroacetic acid and heated to reflux overnight to give **84**. The absence of resonances characteristic of *tert*-butyl ester protons in the ^{1}H NMR spectrum of the product in the region of δ1.37 or δ1.40 ppm indicated the deprotection to have been successful. Hydrogenolysis of compound **84** by stirring in a suspension of 10% palladium on carbon in tetrahydrofuran under an atmosphere of hydrogen gave the free acid **85**. The ^{1}H NMR spectrum of the product did not display resonances characteristic of benzyl ester benzylic protons in the region of δ5.08 or δ5.10 ppm indicating the deprotection to have proceeded. Although the synthesis of **85** began with chirally pure *N*-acetyl-(*S*)-phenylalanine **80**, it was not optically active and was probably therefore a racemate. Racemisation during the synthesis of **85** was most likely due to the use of the strong bases, sodium hydride and lithium diisopropylamine, as reagents.

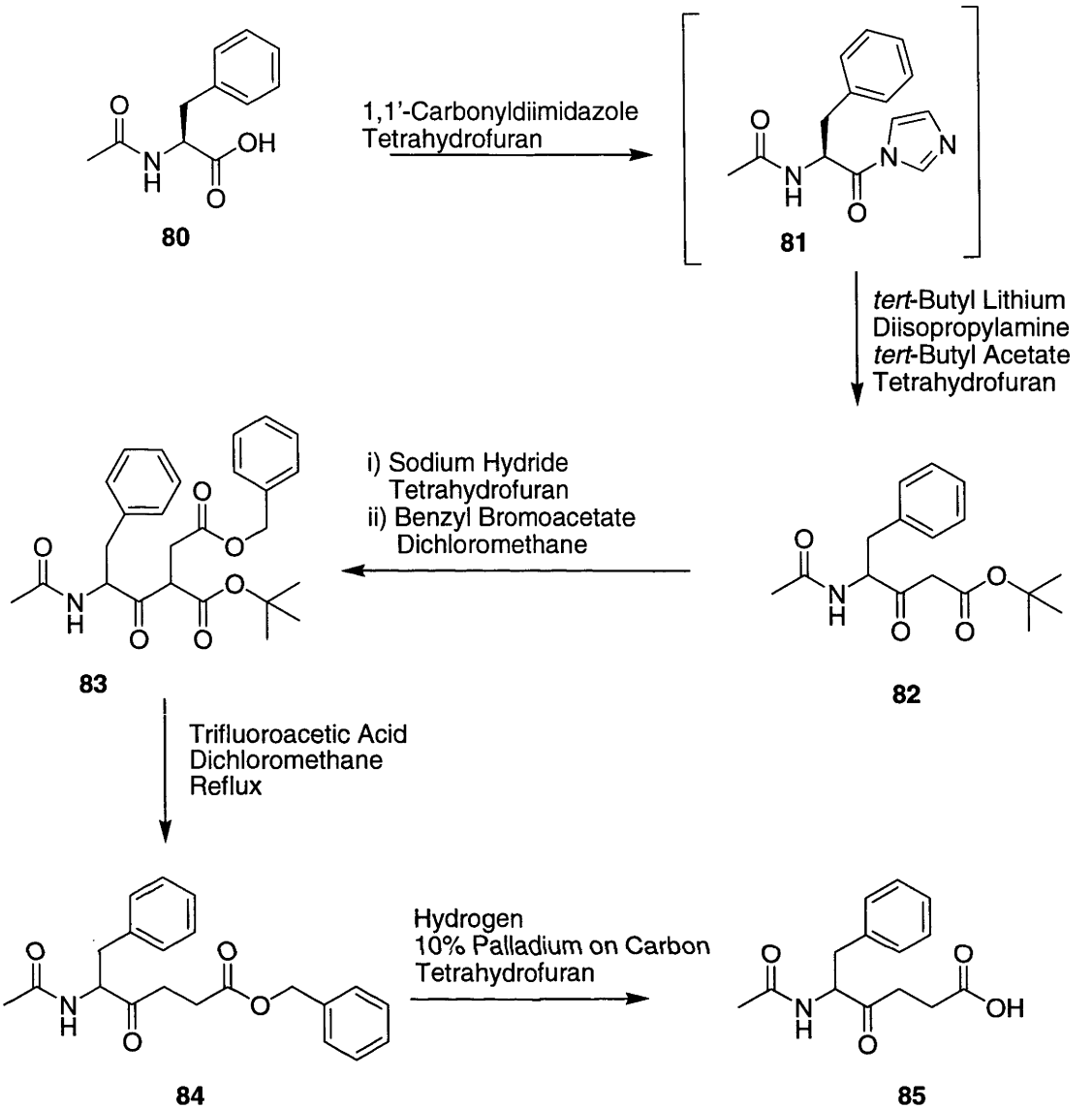

Figure 33. Synthesis of 3-(*N*-Acetylphenylalanyl)propionic Acid **85**

1.3 Relative Rates of Bromination, Radical Stablisation Energies and PAM Activity

As covered in the Introduction, rates of bromination of glycine derivatives and related compounds using NBS were to be used in the development of PAM inhibitors. The systems that were investigated for their rates of bromination are illustrated in Figure 34.

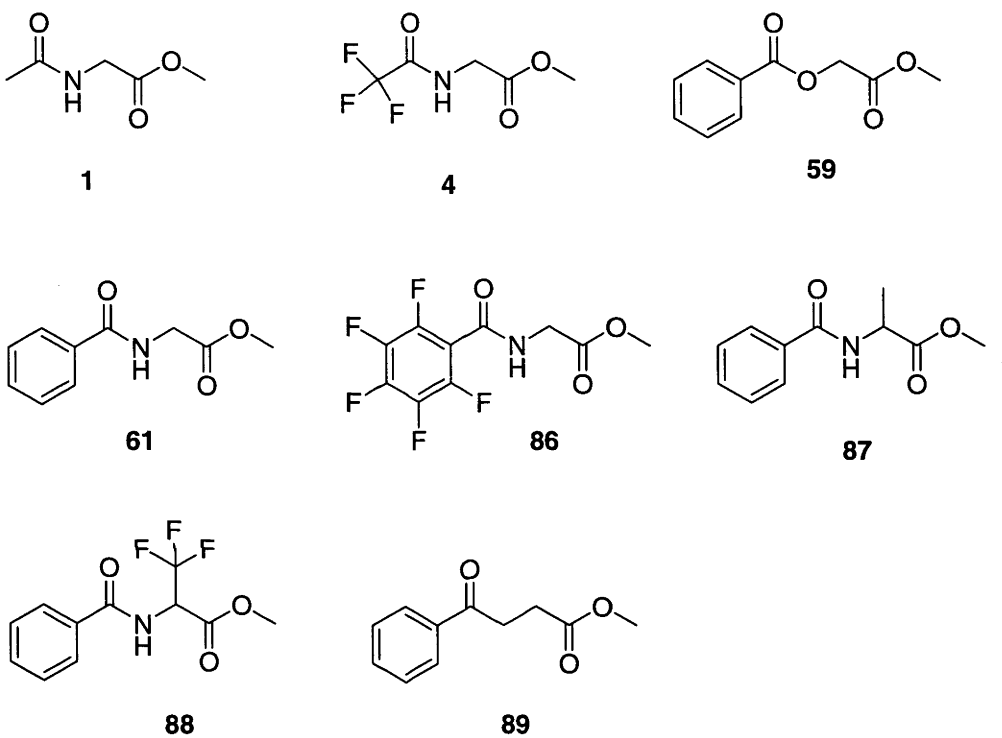

Figure 34. Systems Investigated for their Rates of Bromination.

The relative rates of bromination for compounds **1**, **4**, **61** and **86** - **89** were obtained from the literature.[21,27,67] However the bromination of **59** had not been studied. The treatment of methyl O^{α}-(benzoyl)glycolate **59** with NBS is illustrated in Figure 35 along with that of its glycine analogue **61**.

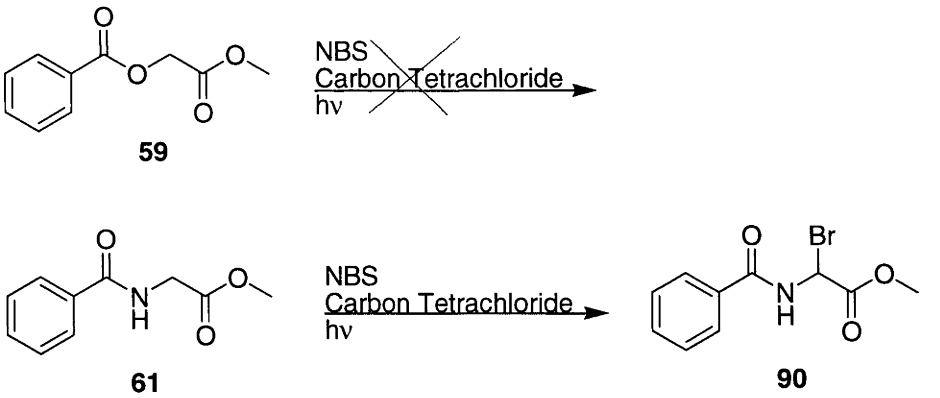

Figure 35. Reaction of *N*-Benzoylglycine Methyl Ester **61** and Treatment of Methyl O^{α}-Benzoylglycolate **59** with NBS

Compound **59** was stirred in carbon tetrachloride with NBS and the mixture was heated to reflux under irradiation from a 300W sun lamp. A sample of the crude solution was dissolved in deuterated chloroform and analysed by ^{1}H NMR spectroscopy. The ^{1}H NMR spectrum displayed resonances for the starting material **59** and no evidence for the formation of its α-brominated analogue. In order to eliminate the possibility that this result was caused by a contaminant inhibiting bromination, a competitive experiment was performed. Compound **59** along with **61** was treated with NBS under the same conditions as the previous experiment. A sample of the crude solution was dissolved in deuterated chloroform and analysed by ^{1}H NMR spectroscopy. The ^{1}H NMR spectrum showed a resonance at δ6.68 ppm characteristic of the α-carbon proton of **90** whilst there was no evidence of reaction of **59**. Therefore, the relative rate of bromination of **59** was determined to be < 0.005. The relative rates of bromination of **59** along with those for compounds **1**, **4**, **61** and **86** - **89** are provided in Table 1. Since the reactions involve radical brominations, with hydrogen atom transfer from the carbon adjacent to the ester group of each substrate determining the relative rate at which the

compound is brominated, the relative rates of reaction correspond to the relative ease of formation of the radicals **2**, **5**, **91**, **92** and **93b** – **96b** illustrated in Figure 36.

Table 1. Relative Rates of Reaction of the Amino Acid Derivatives **1**, **4**, **59**, **61** and **86** - **89** with NBS to give the Corresponding Radicals **2**, **5**, **95b**, **91**, **92**, **93b**, **94b** and **96b**

Compound	Relative Rate of Reaction
61	1.0[a]
86	0.25[b]
1	1.2[b]
4	0.05[b]
87	0.33[c]
88	<0.005[d,e]
59	<0.005[e]
89	<0.005[e]

[a]Assigned as unity. [b]Data from reference 27. [c]Data from reference 68. [d]Data from reference 21. [e]No detectable bromination.

For comparison with the relative rates of bromination of **1**, **4**, **59**, **61** and **86** - **89** and the relative ease of formation of the radicals **2**, **5**, **91**, **92** and **93b** – **96b** (Figure 36) in those reactions, RSEs for the radicals **2**, **5** and **93a** – **96a** (Figure 36) were determined (Table 2).

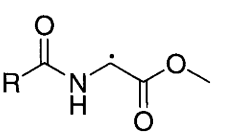

2 R = CH_3
91 R = C_6H_5

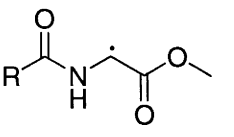

5 R = CF_3
92 R = C_6F_5

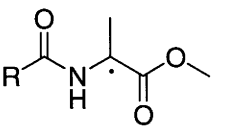

93a R = CH_3
93b R = C_6H_5

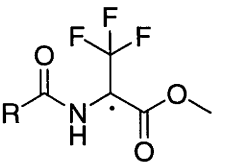

94a R = CH_3
94b R = C_6H_5

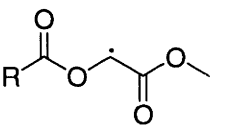

95a R = CH_3
95b R = C_6H_5

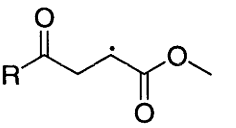

96a R = CH_3
96b R = C_6H_5

Figure 36. Radicals Investigated either for their RSEs (**2**, **5** and **93a – 96a**) or their Ease of Formation in Bromination Reactions (**2**, **5**, **91**, **92**, and **93b – 96b**).

Table 2. RSEs[a] [0 K, RMP2/G3large, kJ mol^{-1}] of Derivatives of Glycyl and Related Radicals

Radical	RSE
2	79.1
5	69.9
93a	78.8
94a	39.9
95a	44.4
96a	34.9
$^{\bullet}CH_2CO_2Me$	20.2
$MeCONHCH_2^{\bullet}$	41.3
$MeCO_2CH_2^{\bullet}$	17.1

[a]Radical stabilisation energies (RSEs) were calculated as the energy change in the isodesmic reaction $R^{\bullet} + CH_4 \rightarrow RH + {}^{\bullet}CH_3$. The RSEs correspond to the differences between the bond dissociation energies (BDEs) of methane and RH,[25,26,68] and reflect the stability of $R^{\bullet}$ compared with $^{\bullet}CH_3$, relative to the corresponding closed-shell systems. These RSEs correspond to values at 0 K.

As discussed in the Introduction, RSEs relate the stability of the radicals in question to that of the methyl radical (relative to the corresponding closed shell species), with a more stable radical having a more positive RSE.[25,26,68] The geometries and zero-point vibrational energies were determined at the B3-LYP/6-31G(d) level, while improved relative energies were obtained by carrying out single-point calculations on these optimised structures at the RMP2 level with the 6-311+G(2df,p) and G3large basis sets.[69] The results quoted in Table 2 correspond to RMP2/G3large//B3-LYP/6-31G(d) RSEs at 0 K. The radicals **91**, **92** and **93b** – **96b** (Figure 36) were not studied because their aryl groups would substantially increase the complexity of the calculations. The acetamides **93a** – **96a** were examined instead of the benzamides **93b** – **96b**. The effect of different acyl groups was examined with only **2** and **5** and not **91** and **92**.

The data compiled in Tables 1 and 2 were to be used to investigate whether relative rates of bromination and RSEs of various compounds could be related to PAM activity towards comparable systems. To this end the kinetic parameters that describe the activity of PAM towards a number of suitable compounds (illustrated in Figure 37) were obtained either through assay with the enzyme or from literature sources.

In Figure 37 the acetamides **97a,b**, the βββ-trifluoroalanines **98a,b**, the glycolates **64**, **70**, **76**, **79**, **100a** and **103a**, the glycines **72**, **99**, **100b**, **101**, **102** and **103b** and the γ-keto acids **85** and **104** are illustrated. The kinetic data for the interactions of compounds **97a,b**, **99**, **100a,b**, **101**, **102** and **103a,b** with PAM were obtained from the literature.[4,61,67] The kinetic parameters for the interactions of **64**, **70**, **72**, **76**, **79**, **85**, **98a,b** and **104** with PAM were unknown and therefore had to be obtained through assay with the enzyme. The assays of **64**, **70**, **72**, **76**, **79**, **85**, **98a,b** and **104** with PAM were

performed using modified literature procedures as outlined in the Experimental.[13,14,70] The results of the assays of compounds **64**, **70**, **72**, **76**, **79**, **85**, **98a,b** and **104** with PAM along with the literature data for compounds **97a,b**, **99**, **100**, **101a,b**, **102**, **103a,b** and **104** are supplied in Table 3.

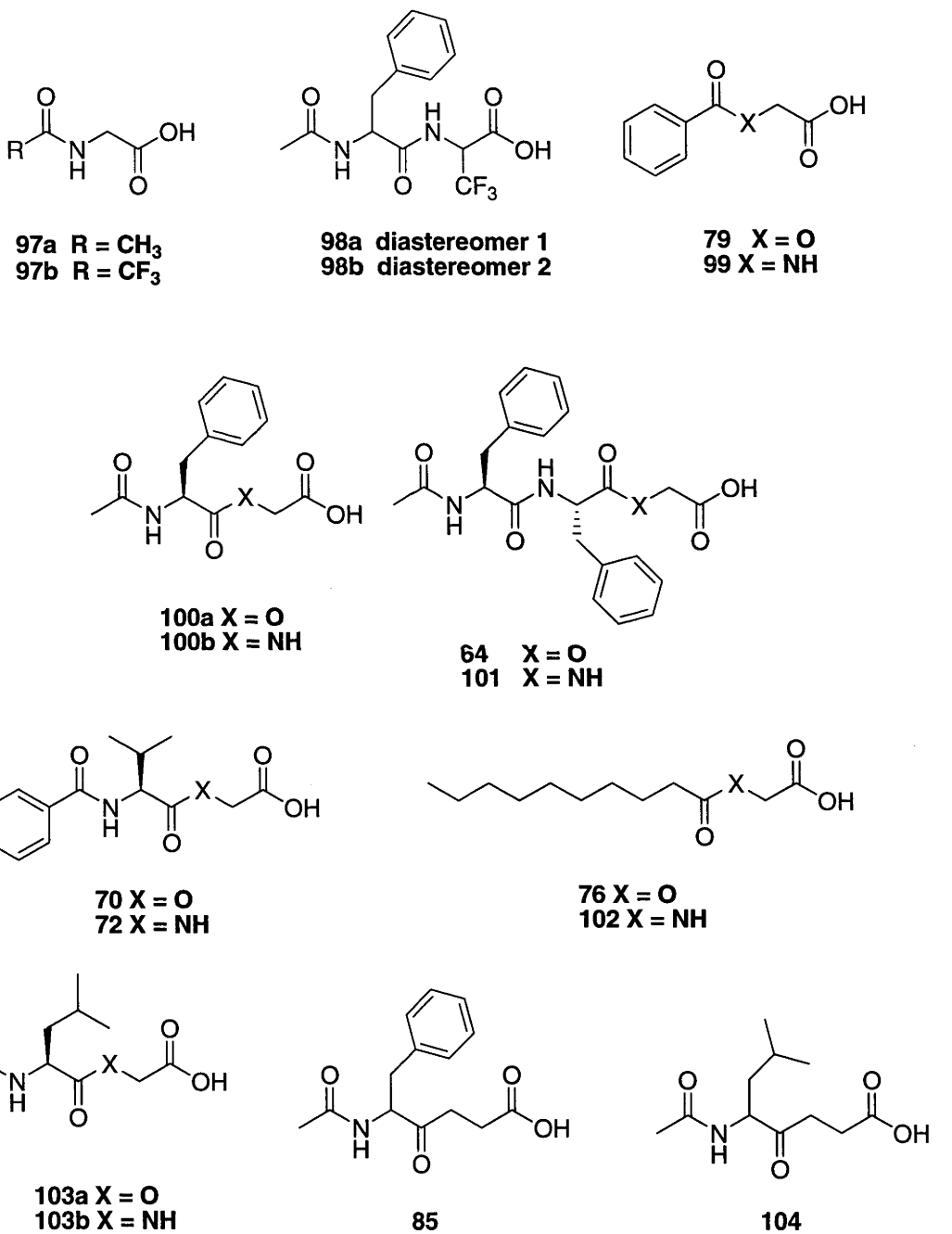

Figure 37. Systems Investigated for their Activity with PAM.

Table 3. Kinetic Parameters for Interactions of Various Substrates and Inhibitors with Peptidylglycine α-Amidating Monooxygenase

Compound	$V_{M,app}$ (μM min^{-1} mg^{-1})	$K_{M,app}$ (mM)	K_I (mM)	IC_{50}[a] (mM)
97a	6.4[b]	9.3[b]	-	-
97b	1.4[b]	4.1[b]	-	-
99	6.5[b]	1.3[b]	-	-
100b	5.6[b]	0.0079[b]	-	-
101	3.3[c]	0.0012[c]	-	-
72	-	0.03	-	-
102	12.6[b]	0.1[b]	-	-
103b	8.2[c]	0.096[c]	-	-
98a	Inhibitor	-	-	5
98b	Inhibitor	-	-	5
64	Inhibitor	-	-	0.05
70	Inhibitor	-	-	0.5
76	Inhibitor	-	-	0.04
79	Inhibitor	-	-	0.25
100a	Inhibitor	-	0.0452[c]	-
103a	Inhibitor	-	0.0598[c]	-
85	Inhibitor	-	-	3
104	Inhibitor	-	-	6

[a]Corresponds to loss of 50% of the catalytic activity of PAM in processing the substrate (*R*)-tyrosyl-(*S*)-valylglycine at a concentration of 0.1 mM, under conditions where the

$K_{M,app}$ for the substrate is 0.2 mM. Although $K_{M,app}$, K_I and IC_{50} values are not directly comparable as measures of enzyme binding affinity, they are adequate as used in this thesis to establish that compounds interact with PAM. [b]Data from reference 4. [c]Data from reference 61.

The data for the glycine derivatives **97a,b** and **99**, and the glycolate **79** allow for a direct comparison with the rates of bromination of the analogous esters **1**, **4**, **61** and **59** and the stability and ease of formation of the corresponding radicals **2**, **5**, **91** and **95b**. The properties of the glycolates **64**, **70**, **76**, **79**, **100a** and **103a** and the analogous glycine derivatives **101**, **72**, **102**, **99**, **100b** and **103b** allow for further analysis of the relationships between these two classes of compounds. It was not feasible to examine the interaction of the free acids *N*-benzoyl-βββ-trifluoroalanine or 3-benzoylpropionic acid with PAM for comparison with the glycine derivative **99**, due to their anticipated poor enzyme-binding affinities. Instead the effect of these substitutions was explored using the trifluoroalanine derivatives **98a,b** and the γ-keto acids **85** and **104** and relating their behaviour to that of the analogous glycinated dipeptide derivatives **100b** and **103b**.

The above results for rates of bromination, RSEs and PAM activity will now be discussed.

1.4 Relationship Between Relative Rates of Bromination, Radical Stabilisation Energies and PAM Activity

N-Acetyl-, trifluoroacetyl-, benzoyl-, and pentafluorobenzoyl-glycine methyl ester **1**, **4**, **61** and **86** differ only in their *N*-acyl substituents. In their reactions with NBS, the benzamide **61** is 4 times more reactive than the pentafluorobenzamide **86**, and the acetamide **1** is 24 times more reactive than the trifluoroacetamide **4** (Table 1). These relative reactivities can be attributed to differences between the π-electron-donating abilities of the various amido groups, to stabilise and therefore facilitate formation of the corresponding radicals **91**, **92**, **2** and **5**. The inductively electron-withdrawing fluorines of the pentafluorobenzamide **86** and the trifluoroacetamide **4** decrease the extent of resonance stabilisation of the radicals **92** and **5**, relative to those radicals **91** and **2** derived from the non-halogenated precursors **61** and **1**, respectively. This effect of the fluorines is reflected in the calculated RSEs in the cases of the radicals **2** and **5**, where the trifluoroacetamide **5** is less stable than the acetamide **2** by 9.2 kJ mol^{-1} (Table 2). The fluorines also exert an inductive effect that decreases the pK_as of the carboxylic acid analogues of the amido groups, due to stabilisation of the corresponding carboxylate anions (the pK_as of benzoic acid, pentafluorobenzoic acid, acetic acid, and trifluoroacetic acid are 4.2, 1.5, 4.8 and 0.6, respectively[71]). As a result, there is a strong correlation between the effect of the fluorines on the relative reactivity of the glycine derivatives **61**, **86**, **1** and **4**, the relative acidity of the acids, and the RSEs of the radicals **2** and **5**. The effect of the fluorines on the reactivity of **61**, **86**, **1** and **4** and the acidity of the corresponding carboxylic acids is greatest with the trifluoroacetamide **4** and trifluoroacetic acid, relative to the acetamide **1** and acetic acid, respectively.

In analogous systems, the fluorines have a related impact on the interactions of *N*-acetylglycine **97a** and *N*-trifluoroacetylglycine **97b** with PAM. They decrease the overall rate of turnover ($V_{M,app}$) of **97b** relative to **97a**, via the corresponding glycyl

radicals, by a factor of 4.5 (Table 3). Consequently, the correlation of the differences between RSEs of the *N*-acetyl- and trifluoroacetyl-glycyl radicals **2** and **5**, the relative rates of bromination of *N*-acetyl- and trifluoroacetyl-glycine methyl ester **1** and **4**, and the pK_as of acetic acid and trifluoroacetic acid extends to the relative rates of the enzyme-catalysed reactions of *N*-acetyl- and trifluoroacetyl-glycine **97a** and **97b**. The fluorines reduce the RSE of the radical **5** (by 9.2 kJ mol^{-1}), the rate of bromination of the ester **4** (by a factor of 24), the pK_a of trifluoroacetic acid (by 4.2 units), and the rate of turnover of the acid **97b** by the enzyme (by a factor of 4.5). By way of comparison, replacing the acetyl substituent of *N*-acetylglycine methyl ester **1**, *N*-acetylglycine **97a**, and acetic acid with the benzoyl group of *N*-benzoylglycine methyl ester **61**, *N*-benzoylglycine **99** and benzoic acid **77** has relatively little effect on any of these properties. It decreases the rate of bromination of the ester **61** by a factor of only 1.2, decreases the pK_a of benzoic acid **77** by only 0.6, and changes the rate of the enzyme catalysed reaction of the acid **99** by less than 2%.

The effect of the fluorines, although reducing the rate of turnover, is clearly insufficient to prevent the PAM catalysed reaction of *N*-trifluoroacetylglycine **97b**. On the basis of the calculations with the *N*-acetyl- and trifluoroacetyl-glycyl radicals **2** and **5**, this indicates that a reduction in the RSE of 9.2 kJ mol^{-1} is not sufficient to stop glycyl radical formation by the enzyme. This is consistent with reductions in the RSEs of alanyl and threonyl radicals relative to those of the corresponding glycyl radicals of 0.3 and 7-14 kJ mol^{-1}, respectively,[21,72] being too small to prevent the enzyme-catalysed reactions of alanine and threonine derivatives.[60] The effect of the trifluoromethyl substituent on the stability of the trifluoroalanyl radical **94a** is much larger, reducing the calculated RSE relative to that of the corresponding glycyl radical **2** by 39.2 kJ mol^{-1}

(Table 2). The substituent also prevents bromination of *N*-benzoyl-β,β,β-trifluoroalanine methyl ester **88** (Table 1) and the processing of the trifluoroalanine containing dipeptides **98a,b** by PAM (Table 3). *N*-Benzoyl-β,β,β-trifluoroalanine methyl ester **88** was inert on treatment with *N*-bromosuccinimide, either alone or as a mixture with *N*-benzoylglycine methyl ester **61**, that nevertheless reacted smoothly to give the corresponding α-bromoglycine derivative **90**. There was no evidence of reaction of either of the trifluoroalanine-containing dipeptides **98a** or **98b** being catalysed by PAM, even though competitive experiments with (*R*)-tyrosyl-(*S*)-valylglycine established that both **98a** and **98b** bind to the enzyme, albeit with IC_{50} values of around 5 mM (Table 3). It is therefore apparent that the decrease in RSE brought about by introducing the trifluoromethyl group is sufficient to prevent radical formation by PAM. However, this does not give effective enzyme inhibitors, as the trifluoromethyl substituent prevents tight binding to the enzyme. This is seen from the IC_{50} value of 5 mM for each of the trifluoroalanine derivatives **98a** and **98b**. As an indirect comparison, the $K_{M,app}$ value of the corresponding glycine derivative **100b** is 7.9 μM.

In a manner similar to the effect of introducing the trifluoromethyl group, replacing the glycine moiety with glycolate, which is a simple substitution of the glycine NH by O, reduces the RSE of the glycolyl radical **95a** compared with that of the corresponding glycyl radical **2** by 34.7 kJ mol^{-1} (Table 2). This can be attributed to the decreased π-electron-donating and increased σ-electron-withdrawing ability of the acetoxy group of **95a** relative to the acetamido substituent of **2**, as reflected in the RSEs of the radicals $MeCONHCH_2^{\bullet}$ and $MeCO_2CH_2^{\bullet}$ of 41.3 and 17.1 kJ mol^{-1}, respectively.[73] The effect is magnified in the captodatively stabilised[74,75] glycyl and glycolyl radicals **2** and **95a**

where the extent of synergy displayed by the acetamido and acetoxy substituents in combination with the carboxyl group corresponds to 17.6 and 7.1 kJ mol^{-1}. These values are based on the differences between the RSEs of $MeCONHCH_2^{\bullet}$ (41.3 kJ mol^{-1}), $^{\bullet}CH_2CO_2Me$ (20.2 kJ mol^{-1}), and **2** (79.1 kJ mol^{-1}) and $MeCO_2CH_2^{\bullet}$ (17.1 kJ mol^{-1}), $^{\bullet}CH_2CO_2Me$, and **95b** (44.4 kJ mol^{-1}), respectively. The substitution of glycine by glycolate prevents bromination of methyl O^{α}-benzoylglycolate **59** (Table 1). It also prevents catalysis of the reactions of the glycolates **64**, **70**, **76**, **79**, **100a** and **103a** by PAM (Table 3). The glycine derivatives **101**, **72**, **102**, **99**, **100b** and **103b** are all turned over by the enzyme, but there is no evidence of reaction of the corresponding glycolates **64**, **70**, **76**, **79**, **100a** and **103a**. In this case substitution does not severely disrupt binding to the enzyme. The IC_{50} and K_I values of the glycolates **64**, **70**, **76**, **79**, **100a** and **103a** are all in the 0.04-0.5 mM range. The corresponding glycine derivatives **101**, **72**, **102**, **99**, **100b** and **103b** have $K_{M,app}$ values between 1 μM and 1 mM. Therefore, the glycolates constitute a general class of inhibitors of the enzyme because they do not readily undergo hydrogen atom transfer, yet they bind effectively to PAM, the further implication being that the substitution of the terminal glycine of tight binding PAM substrates with glycolate should yield inhibitors of the enzyme with high binding affinity.

Replacing the acylglycine with a γ-keto acid or ester, through substitution of the glycine NH by CH_2, has similar effects to the swapping of glycine for glycolate. The RSE of the keto ester radical **96a** is less than that of the analogous glycyl radical **2** by 44.2 kJ mol^{-1} (Table 2). The γ-keto ester **89** is inert to bromination (Table 1), and the γ-keto acids **85** and **104** are not processed by PAM (Table 3), even though, unlike the example

reported previously,[62] these keto acids **85** and **104** do bind to some extent with the enzyme, with IC_{50} values of 3 and 6 mM, respectively. Again it is apparent that a reduction in the RSE of around 35-45 kJ mol^{-1} is sufficient to stop both the bromination with NBS and the catalysis by the monooxygenase.

From the $K_{M,app}$ values of the glycine derivatives **100b** and **103b** of 7.9 and 96 μM, respectively, the K_I values of the corresponding glycolates **100a** and **103a** of 45.2 and 59.8 μM, and the IC_{50} values of the analogous γ-keto acids **85** and **104** of 3 and 6 mM (Table 3), it appears that the replacement of an acylglycine with a γ-keto acid has a more adverse effect on the binding to PAM than does the substitution of glycine by glycolate.

1.5 Comparisons of the Binding Strengths of PAM Substrates and βββ-Trifluoroalanine, Glycolate and γ-Keto Acid Enzyme Inhibitors and the Implications for Inhibitor Design

The substitution of the acylglycine of a typical PAM substrate with a trifluoroalanine or γ-keto acid results in a reduction in binding affinity to the enzyme. This loss of binding affinity with PAM was not observed for the conversion of the acylglycine of the PAM substrates **101**, **72**, **102**, **99**, **100b** and **103b** to their equivalent glycolates **64**, **70**, **76**, **79**, **100a** and **103a**, respectively. The poor binding affinity of the α-trifluoromethyl systems **98a** and **98b** can be rationalised as being due to the intolerance of PAM towards increased steric bulk on the α-carbon of glycine. However an understanding of the

reasons that acylglycines and acylglycolates exhibit similar binding affinities for PAM, whilst the γ-keto acids do not requires more consideration.

In the Introduction, the features of a crystal structure of PAM with bound substrate (Figure 3) were discussed. The crystal structure indicated that the acylglycine NH was acting as a hydrogen bond donor to the enzyme through interactions with an asparagine residue's side chain amide. The ability of glycolates to bind effectively to PAM may be due to hydrogen bonding interactions between a glycolate ester O and the side chain amide of the same asparagine residue. In this case, the asparagine side chain amide would be acting as a hydrogen bond donor (Figure 38).

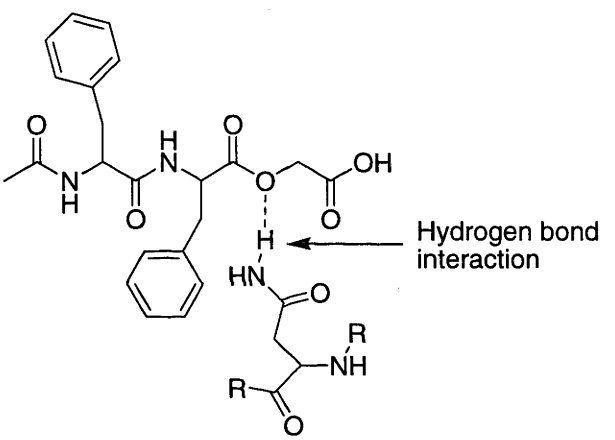

Figure 38. Hypothesised Hydrogen Bond Interaction between a Glycolate Ester Oxygen and the Side Chain Amide of an Asparagine Residue in the PHM Active Site.

A γ-keto acid possesses a methylene at the position which is equivalent to an acylglycines amido NH. This methylene could not form a hydrogen bond such as illustrated in Figure 38, therefore reducing a γ-keto acid's binding strength in comparison to analogous glycines and glycolates.

However it has been hypothesised that hydrogen bonds such as illustrated in Figure 38 have a minimal contribution to the overall binding strength of a substrate or inhibitor with an enzyme.[76] In the absence of bound substrate or inhibitor, PAM would be fully hydrated, with all possible hydrogen bonds in the active site being formed either between amino acids or between residues and water. As was covered in the Introduction, the asparagine (N316, Figure 3) must break a hydrogen bond with a neighbouring tyrosine (Y318, Figure 3) in order to form a new hydrogen bond with the glycine amido NH of bound substrate. Therefore, there may be no net change in overall energy. If this is the case, further therories are required to rationalise why acylglycines and acylglycolates exhibit similar binding affinities for PAM, whilst the γ-keto acids do not.

The hybridisation of a secondary carbon radical is sp^2 adopting a trigonal planar geometry. α-Carbon centred glycyl radicals preferentially adopt near planar orientations. It is therefore likely that PAM, in order to reduce the activation energy required for the formation of an α-carbon centred glycyl radical, binds its substrates in a complimentary way. As a result of the conjugation of the amide NH of an acylglycine and the analogous ester O of an acylglycolate, in each case there is free rotation only around the bonds to the α-carbon. In the case of a γ-keto acid there is free rotation around the bonds to the α- and β-carbons. This may allow acylglycines and acylglycolates to adopt conformations which are closer to the planar conformation preferred by the enzyme than a γ-keto acid. Further, assuming that acylglycines, acylglycolates and analogous γ-keto acids bind to PAM with similar orientations, and

that the planarity of the amide and ester groups of acylglycines and acylglycolates is maintained, there would be a greater degree of conformational constraint and loss of entropy on binding of a γ-keto acid. A direct comparison of the kinetic parameters that describe the interactions of the glycines **100b** and **103b** and their analogous glycolates **100a** and **100b** and γ-keto acids **85** and **104** with PAM along with the bond angles of their atoms which are at the position of (or equivalent position to) an acylglycines amido N (Figure 39 and Table 4), may help to elucidate a further theory.

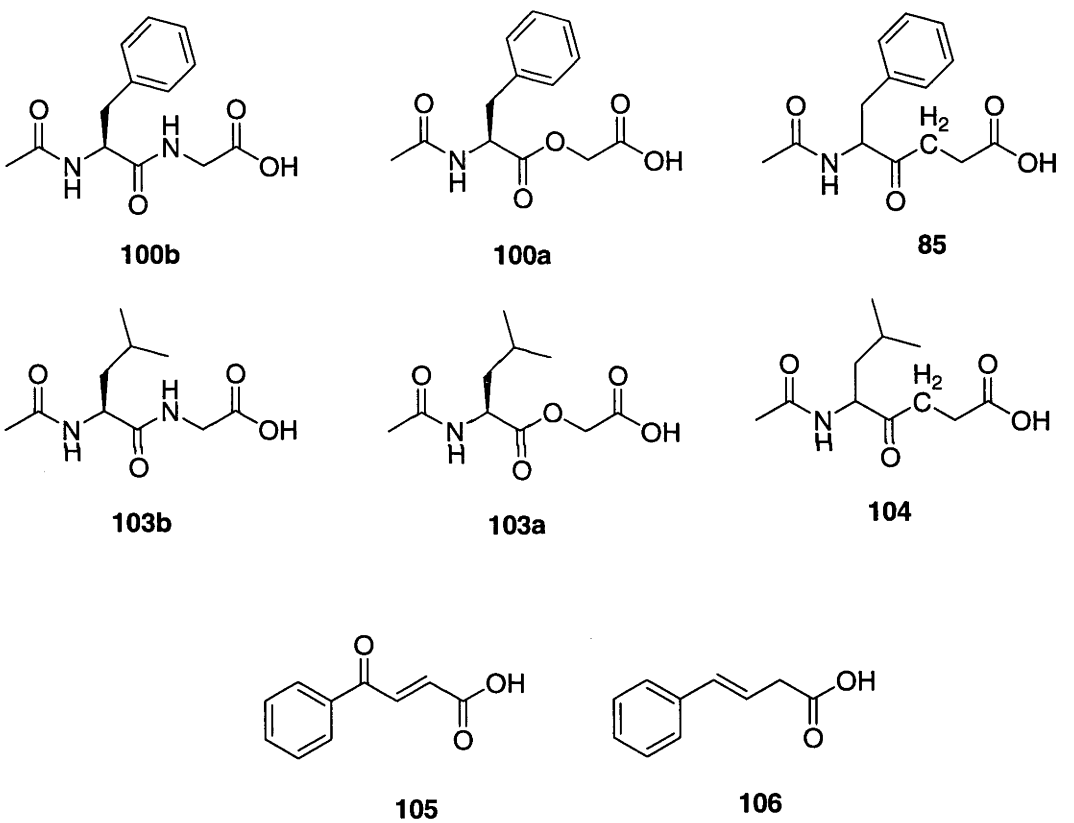

Figure 39. PAM Inhibitors and Substrates for Comparison of Bond Angles and Binding Affinities

Table 4. Binding Affinities of Compounds and Relevant Bond Angles

Compound	$IC_{50}/K_I/K_{M,app}$	Angle (α-N-C(O) or analogue)
100a	0.0452[a]	115
100b	0.0079[b]	120
85	3[c]	109.6
103a	0.0598[a]	115
103b	0.0096[d]	120
104	6[e]	109.6
105	0.001[a]	120
106	0.16[b]	120

IC_{50} and K_I values are quoted as mM concentrations. Data for **85**, **100a,b**, **103a,b** and **104** taken from Table 3, [a]apparent K_I value obtained from reference [13], [b]K_I value obtained from reference [13]. Bond angles are quoted as those typical of sp^2 and sp^3 hybridised atoms[77,78] and were not calculated *via* computational methods.

The nitrogen of amides and ether oxygens of esters are known to be sp^2 hybridised, adopting trigonal planar geometries.[78] The acyglycine N of **100b** and **103b** is sp^2 hybridised, adopting a trigonal planar geometry with bond angles to the adjacent carbons of 120°. In the equivalent position to an acylglycines N, the glycolates **100a** and **103a** possess an oxygen atom which is sp^2 hybridised, also adopting a trigonal

planar geometry with bond angles to the adjacent carbons of 115°. These compounds, **100a,b** and **103a,b** possess binding affinities with PAM of 0.0452, 0.0079, 0.0598 and 0.096 mM respectively (Table 4). The inhibitors **85** and **104** possess, at the position equivalent to an acyglycines N, a carbon atom that is sp^3 hybridised adopting a tetrahedral geometry with a bond angle between the adjacent carbons of 109.6°. The IC_{50}s of **85** and **104** of 3 and 6 mM respectively, are significantly higher than the K_Is of the corresponding glycines and glycolates **100a,b** and **103a,b** (Table 4). Therefore a reduction in binding affinity of two to three orders of magnitude is incurred when the sp^2 hybridised atoms in **100a,b** and **103a,b**, that are at the position (or equivalent) of an acylglycines N, are substituted for an sp^3 hybridised carbon. The simple inhibitors **105** and **106** possess carbon atoms at the equivalent position to an acyl-glycines N which are sp^2 hybridised and possess a trigonal planar geometry with bond angles to the adjacent carbons of 120°. The binding strengths of **105** and **106** to PAM are 0.001 and 0.16 mM, respectively. Although their binding affinities with PAM are not directly comparable with those of **100a,b**, **103a,b**, **85** and **104**, the fact that such simple systems with sp^2 hybridised atoms at the equivalent position to an acylglycines N, exhibit tighter binding than the more complex **85** and **104** may be significant. It was therefore hypothesised that the poor binding affinities exhibited by **85** and **104** to PAM may be due to the change in geometry that is incurred when substituting an acylglycine with a γ-keto acid, thereby resulting in the displacement of the recognition points required for tight binding with the enzyme. As a result it seems apparent that PAM is tolerant of the substitution of an acylglycines NH, providing that the geometry of the new substituent does not significantly deviate from an sp^2 hybridised trigonal planar conformation.

Chapter 2. α-Substituted Glycines for the Controlled Hydrolytic Release of *C*-Terminal Amidated Peptide Hormones.

2.1 Project Rationale

The PAM enzyme was discussed in the Introduction with respect to its role in the production of *C*-terminal amidated peptide hormones. Chapter 1 of the Results and Discussion outlined the development of inhibitors of this enzyme with the aim to their use in the treatment of conditions resultant from an over-production of hormones. However, a deficiency of peptide hormones can also lead to various disease states. Such disease states are commonly treated through the direct administration of peptide hormones or suitable analogues.[34] For example, growth hormone is administered in the treatment of cardiac failure, sepsis, burns, cancer cachexia, end-stage renal failure, trauma and AIDs.[35] The somatostatin analogues, octreotide, lanreotide and vapreotide are used clinically in the treatment of pituitary and gastrointestinal cancers.[38] The need for the development of hormone prodrugs, which, upon administration to a patient, slowly release active hormones in a controlled manner was outlined in the Introduction.

The *C*-terminal amide of peptide hormones is essential to their bioactivity,[1] and as such it constitutes an appropriate site to block in the design of hormone prodrugs. However, any method used to block the *C*-terminal amide of peptide hormones would need to allow for the eventual liberation of the hormone. α-Substituted glycines that hydrolyse

slowly at biological pH to release amides were proposed as suitable masking groups which could be used for this purpose. The conjugation of peptide hormones through the linking of their *C*-terminal amide with molecules such as large polymers, antibodies and immunotoxins has also been proposed as a suitable approach towards the development of hormone prodrugs.[38] To this end, α-substituted glycines which hydrolyse in a controllable manner at biological pH were proposed as potentially suitable systems that could be used to transiently link peptide hormones with other molecules. The intention of these studies was to determine whether the rate of hydrolysis of α-substituted glycines in aqueous solution to release amides might be controlled through the variation of the glycine α-substituent.

2.2 Synthesis of α-Substituted Glycine Derivatives

A variety of compounds were required in order to investigate the extent to which the rate of hydrolysis of α-substituted glycines to release amides in aqueous solution might be controlled through variation of the glycine α-substituent. *N*-Benzoyl-α-hydroxyglycine **7** and *N*-benzoyl-α-hydroxyglycine methyl ester **8** used in these studies were donated as generous gifts.[79,80] The synthesis of the other systems chosen for investigation will now be outlined.

2.2.1 *N*-Benzoyl-α-acetoxyglycine Methyl Ester 14

The synthesis of *N*-benzoyl-α-acetoxyglycine methyl ester **14** is depicted in Figure 40. *N*-benzoylglycine methyl ester **61** and NBS in carbon tetrachloride were heated with stirring at reflux whilst being irradiated by a 300W sun lamp. The bromide **90** was

then treated *in situ* with sodium acetate to give **14**. The ^{1}H NMR spectrum of the product displayed resonances for the α-carbon proton at δ6.77 ppm, the methyl ester protons at δ3.81 ppm and the acetyl protons at δ2.77 ppm indicating the reaction to have been successful.

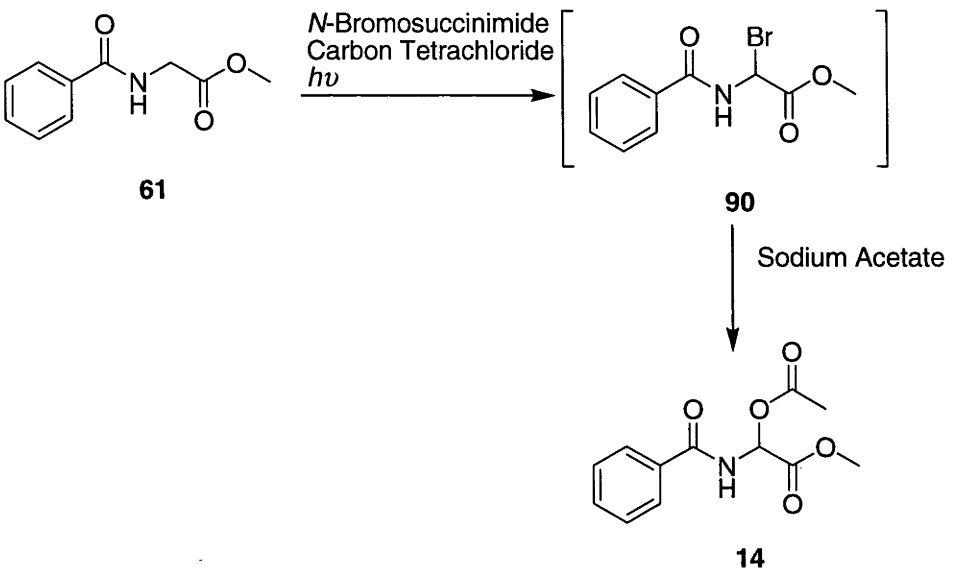

61 **90** **14**

Figure 40. Synthesis of *N*-Benzoyl-α-acetoxyglycine Methyl Ester **14**

2.2.2 *N*-Benzoyl-α-methoxyglycine Methyl Ester 17

The synthesis of *N*-benzoyl-α-methoxyglycine methyl ester **17** is now described (Figure 41). The bromide **90**, synthesised as described above, was treated *in situ* with a solution of methanol and diisopropylethylamine to give **17**. The ^{1}H NMR spectrum of the product displayed resonances for the α-carbon proton at δ5.77 ppm, the methyl ester protons at δ3.81 ppm and the α-methoxy protons at δ3.50 ppm.

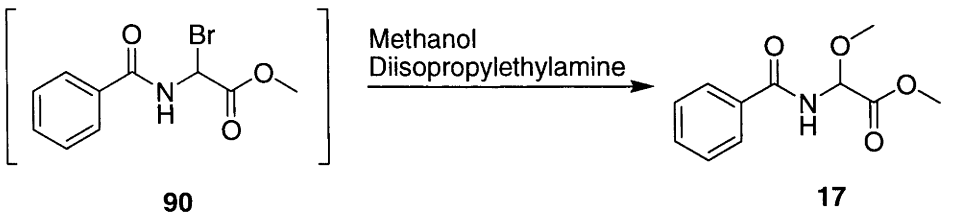

90 17

Figure 41. Synthesis of *N*-Benzoyl-α-methoxyglycine Methyl Ester **17**

2.2.3 *N*-Benzoyl-α-ethoxyglycine Methyl Ester 19

The synthesis of *N*-benzoyl-α-ethoxyglycine methyl ester **19** is illustrated in Figure 42. The bromide **90**, synthesised as illustrated in Figure 40, was treated *in situ* with a solution of ethanol and diisopropylethylamine to give **19**. Excess diisopropylethylamine was added to act as an acid scavenger to prevent acid catalysed transesterification of the methyl ester of **19** with ethanol. The ^{1}H NMR spectrum of the product displayed resonances for the α-carbon proton at δ5.85, the methyl ester protons at δ3.85, the ethoxy methyl and the ethoxy methylene protons at δ1.25 and δ3.79 ppm, respectively.

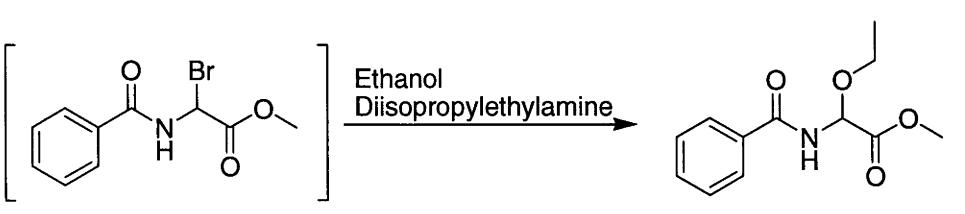

90 19

Figure 42. Synthesis of *N*-Benzoyl-α-ethoxyglycine Methyl Ester **19**

2.2.4 *N*-Benzoyl-α-phenoxyglycine Methyl Ester 21

The synthesis of *N*-benzoyl-α-phenoxyglycine methyl ester **21** is depicted in Figure 43.

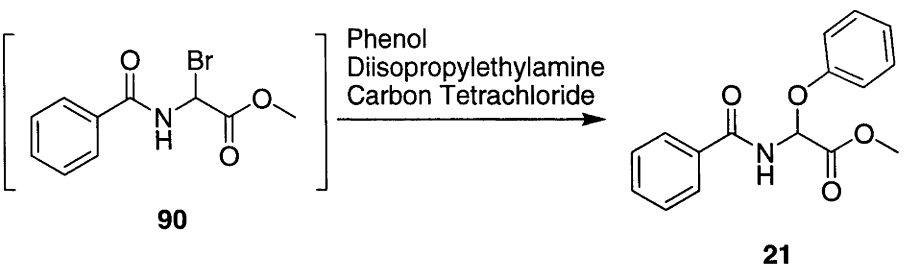

Figure 43. Synthesis of *N*-Benzoyl-α-phenoxyglycine Methyl Ester **21**

The bromide **90**, synthesised as described above, was treated *in situ* with a solution of phenol and diisopropylethylamine in carbon tetrachloride to give **21**. The ^{1}H NMR spectrum of the product displayed resonances for the α-carbon proton at δ6.44 ppm and the methyl ester protons at δ3.85 ppm. The electrospray mass spectrum of the product showed a peak for the protonated molecular ion at *m/z* 286 and the sodiated molecular ion at *m/z* 308 providing further evidence for the success of the synthesis.

2.2.5 *N*-Benzoyl-α-succinimidoglycine Methyl Ester 22

The synthesis of *N*-benzoyl-α-succinimidoglycine methyl ester **22** is shown in Figure 44. The bromide **90**, synthesised as illustrated in Figure 40, was treated *in situ* with a solution of succinimide and diisopropylethylamine in carbon tetrachloride to give **22**. The ^{1}H NMR spectrum of the product displayed resonances for the α-carbon proton at

δ6.77 ppm, the methyl ester protons at δ3.81 ppm and the succinimido methylene protons at δ2.78 ppm.

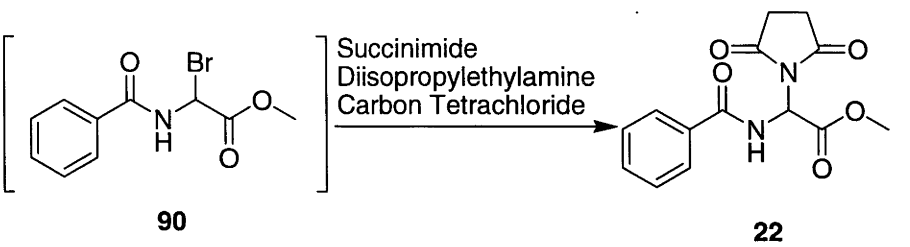

90 **22**

Figure 44. Synthesis of *N*-Benzoyl-α-succinimidoglycine Methyl Ester **22**

2.3 Hydrolysis of α-Substituted Glycines to Release Benzamide

Solutions of the α-substituted glycines **8**, **14**, **17**, **19**, **21** and **22** were made up in 25% acetonitrile and 75% 50 mM carbonate buffer (made up in deuterated water at pD 4.4, 7.9 and 10.4; pD corresponds to pH + 0.4) and were incubated at 37 °C. The hydrolysis experiments were analysed by ^{1}H NMR spectroscopy. The starting concentration of **8** was 5 mM, whilst the starting concentrations of **14**, **17**, **19**, **21** and **22** were 20 mM. This was to aid analysis, due to the hydrolysis reactions of **14**, **17**, **19**, **21** and **22** producing more products, at lower concentrations, than those formed during the reaction of **8**.

The aim of these studies was to develop α-substituted glycines that would hydrolyse to release amides in a slow and controlled manner *in vivo* and so hydrolysis experiments were performed on the α-substituted glycines **8**, **14**, **17**, **19**, **21** and **22** at pH 7.5 to approximate biological conditions. Studies were also performed at pH 4.0 and 10.0 to investigate their reactions over a range of pH. No evidence for the hydrolysis of **8**, **14**, **17**, **19**, **21** or **22** at pH 4.0 was obtained over three weeks of reaction monitoring, indicating that their half-lives at this pH are conservatively greater than 500 hours corresponding to pseudo-first order rate constants of $<4 \times 10^{-7}$ sec^{-1}. The estimation of the psuedo-first order rate constants for the hydrolysis of **8**, **14**, **17**, **19**, **21** and **22** at pH 4.0 was calculated from Equation 1 (where $t_{½}$ is 18×10^5 seconds (504 hours)).[81] A hypothesis as to why no reactions were observed for the hydrolysis of **8**, **14**, **17**, **19**, **21** or **22** at pH 4.0 is provided later in this Chapter.

Equation 1. $t_{½} = \ln 2/k$

The ^{1}H NMR spectra obtained for the hydrolysis of **8** at pH 7.5 and 10.0 over three weeks showed evidence for the hydrolysis of **8** to give benzamide **10**. A ^{1}H NMR spectrum of the pH 10.0 reaction solution after 30 minutes is provided in Figure 45.

The ^{1}H NMR spectrum illustrated in Figure 45 displays resonances for the α-carbon proton of **8** at δ5.52 ppm. The resonances at δ5.21 ppm and δ4.88 ppm were attributed to the α-carbon proton of **7** and the acetal proton of **108**, respectively by spiking of the reaction solution with authentic samples.[79] The resonances at δ5.33 and δ3.61 ppm were assigned to the α-carbon and methyl ester protons of the acetal **107** respectively.

These resonances were also observed in the ^{1}H NMR spectra obtained during the hydrolysis reaction of **8** performed at pH 7.5, although they formed at different rates.

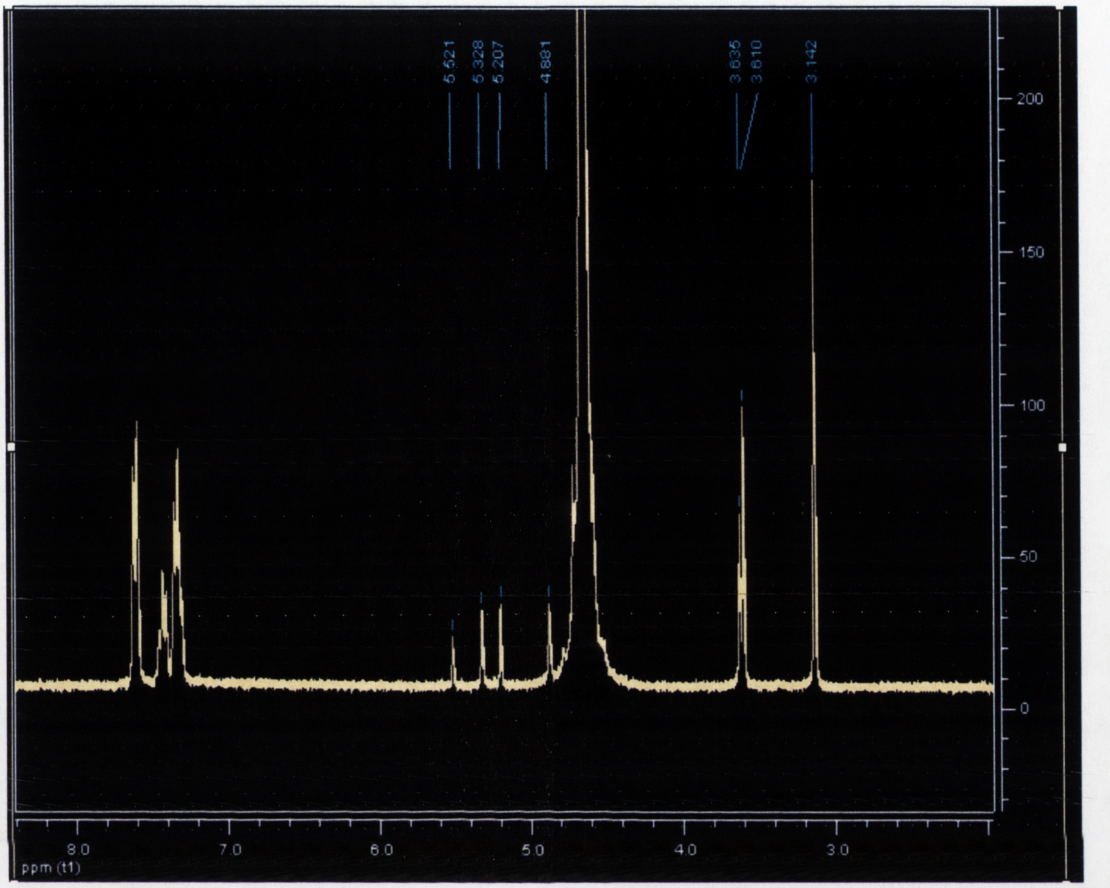

Figure 45. ^{1}H NMR Spectrum of a Solution of *N*-Benzoyl-α-hydroxyglycine Methyl Ester **8** at pH 10 after 30 Minutes.

In order to investigate the kinetics of the hydrolysis of **8** at pH 7.5 and 10.0, ^{1}H NMR spectra were taken after various reaction times. The integration of the characteristic resonances of **7**, **8**, **107** and **108** at δ5.21, δ5.52, δ5.33 and δ4.88 ppm, respectively, was used to determine the ratios/concentrations of the individual components. From analysis of the ^{1}H NMR spectra it was apparent that the hydrolysis of **8** at pH 7.5 and 10.0 proceeded *via* two separate pathways (Figure 46). Firstly, **8** hydrolysed to give benzamide **10** and hydrated methyl glyoxylate **107** (k_1). Alternatively **8** hydrolysed to

give the free acid **7** (k_2) which then reacted further to give the amide **10** and **108** (k_3). As these studies were concerned with the control of the rate of release of amides from α-substituted glycines, the hydrolysis of **107** to give **108** (k_4) will not be discussed in detail. A description of the methods used to determine the combined rate constant k_1 + k_2, and the pseudo-first order rate constants k_1 and k_2 for the hydrolysis of **8** and k_3 for the hydrolysis of **7** at pH 7.5 follows.

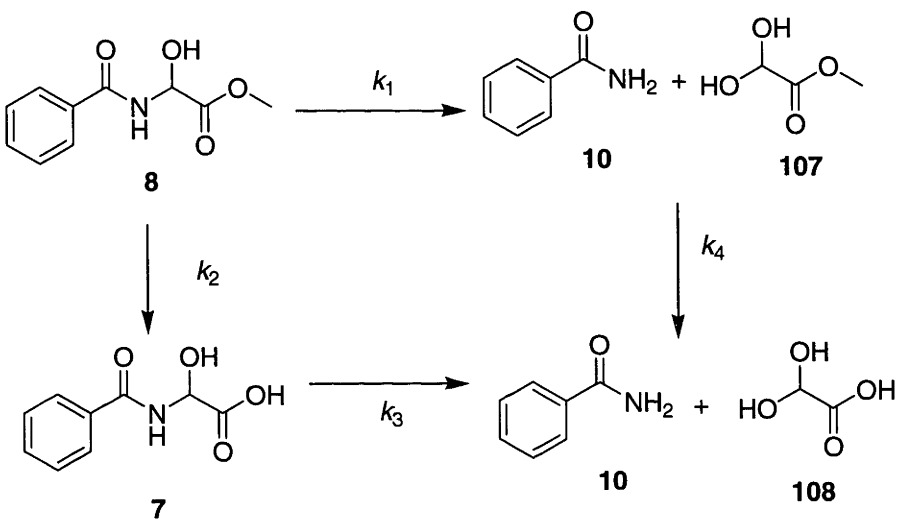

Figure 46. Routes for Hydrolysis of **8** at pH 7.5 and 10.0

A graph of $\ln([A]/[A]_0)$ versus time (where [A] is the concentration of **8** at a given time and $[A]_0$ is the original concentration of **8**) for the hydrolysis of **8** at pH 7.5 was plotted (Figure 47). The rate constant for the consumption of starting material (k_1 + k_2) was determined from the gradient of the line of best fit. The individual values of k_1 and k_2 were determined from the ratio of the concentrations of **107** and **7** respectively after 30 minutes, as no concentration of **108** could be detected by this time. A graph of $\ln([A]/[A]_0)$ versus time (where [A] is the concentration of **7** at a given time and $[A]_0$ is the concentration of **7** after 11.25 hours) is illustrated in Figure 48. The zero point concentration ($[A]_0$) of **7** was taken at 11.25 hours as by this time the amount of **8** remaining was negligible and so no significant amount of **7** was being produced. The

rate of hydrolysis of **7** to give **10** and **108** (k_3) was then determined from the gradient of the line of best-fit in Figure 48. A similar method was used to determine the combined rate constant $k_1 + k_2$, and the pseudo-first order rate constants k_1 and k_2 for the hydrolysis of **8** and k_3 for the hydrolysis of **7** at pH 10.0. The combined rate constants $k_1 + k_2$ and the psuedo-first order rate constants k_1 and k_2 for the hydrolysis reaction of **8** to give **10** and k_3 for the reaction of **7** to give **10** at pH 7.5 and 10.0 are provided in Tables 5 and 6, respectively.

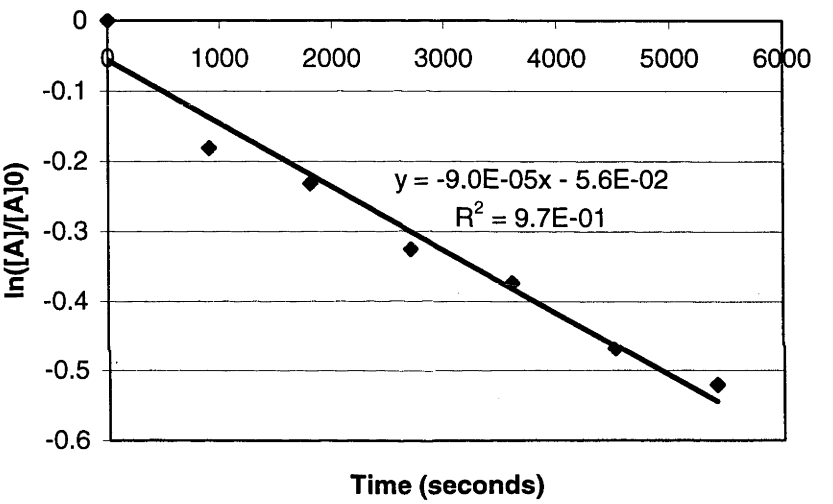

Figure 47. Plot of $\ln([A]/[A]_0)$ *versus* Time (seconds) for the Degradation of **8** at pH 7.5

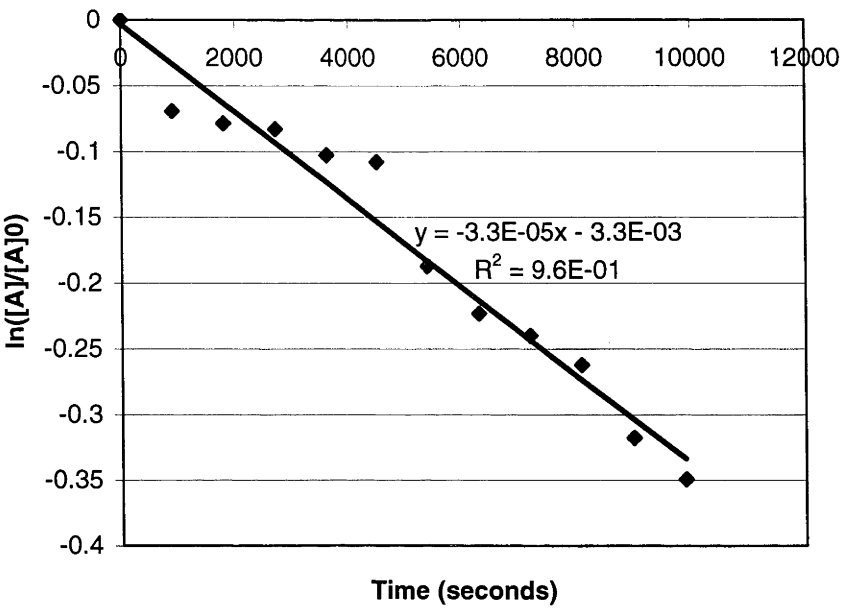

Figure 48. Plot of $\ln([A]/[A]_0)$ *versus* Time (seconds) for the Degradation of **7** at pH 7.5

Table 5. Rate Constants k_1+k_2 and $k_1 - k_3$ for the Hydrolysis of **8** at pH 7.5 Along with Corresponding Half-lives for the Consumption of **8** and the Hydrolysis of **7** to Give the Amide **10**.

Rate Constant	sec^{-1}	Half-life (hrs)
$k_1 + k_2$	9.0×10^{-5}	2.1
k_1	3.6×10^{-5}	-
k_2	5.4×10^{-5}	-
k_3	3.3×10^{-5}	5.8

Table 6. Rate Constants k_1+k_2 and $k_1 - k_3$ for the Hydrolysis of **8** at pH 10.0 Along with Corresponding Half-lives for the Consumption of **8** and the Hydrolysis of **7** to Give the Amide **10**.

Rate Constant	sec^{-1}	Half-life (hrs)
$k_1 + k_2$	2.6×10^{-4}	0.64
k_1	5.8×10^{-5}	-
k_2	1.9×10^{-4}	-
k_3	5.4×10^{-5}	3.5

The psuedo-first order rate constants k_1 and k_3 relate to the release of amide **10** from **8** and **7** respectively. Their values of 3.6×10^{-5} sec^{-1} (k_1) and 3.3×10^{-5} sec^{-1} (k_3) provided in Table 5 are very similar, indicating that there is minimal difference between the rates of release of **10** from **8** or **7** at pH 7.5. However, the rate constant k_2 was found to increase 3.5 fold when increasing the pH from 7.5 to 10.0, which would be expected for the base catalysed hydrolysis of a methyl ester. No marked increase in k_1 or k_3 was observed between reactions at pH 7.5 and 10.0, indicating minimal base sensitivity. The amide **10** can be considered to be a poor leaving group, in accordance with its pK_a which could reasonably be expected to be similar to that of acetamide (15.0).[43] The cleavage mechanism of **8** and **7** to release the amide **10** most likely involves the deprotonation of the α-hydroxy group and the protonation of the amide upon leaving in a concerted manner. Therefore, as this step requires a basic proton abstraction and an acidic protonation, it is not suprising that the hydrolysis reactions of **8** and **7** to give **10** show little base sensitivity over this range of pH.

In independent experiments, Bundgaard *et al.*[41] determined the half-lives for the hydrolysis reactions of **7** and **8** to give the amide **10** at pH 7.4 to be 6.7 and 0.78 hours respectively (Figure 49). However, no explanation was provided as to why the methyl ester **8** hydrolysed 8.6 times faster than the free acid **7**. The half-life of the hydrolysis of **7** to give **10** at pH 7.5 (Table 5) of 5.8 hours is comparable with the value obtained by Bundgaard *et al.*[41] of 6.7 hours at pH 7.4. However, the half-life determined from the psuedo-first order rate constant k_1 for the hydrolysis of **8** to give **10** at pH 7.5 (Table 5) of 5.3 hours is in contradiction to the value quoted by Bundgaard *et al.*[41] of 0.78 hours at pH 7.4. Although the pH used by Bungaard *et al.*[41] for these experiments was 7.4 rather than 7.5, this would not be expected to result in such a large difference in reaction rate for the hydrolysis of **8** to give **10**. It seems likely that this discrepancy is due to Bundgaard *et al.*[41] having monitored starting material consumption rather than amide production. The results for the hydrolysis of **8** at pH 7.4 reported by Bundgaard *et al.*[41] were obtained by monitoring the rate of starting material consumption by UV-HPLC. However, this method of reaction monitoring for the hydrolysis of **8** would be following both the direct release of the amide **10** (k_1) and the saponification of **8** to give the free acid **7** (k_2). Thus, the half-life for the release of **10** from **8** at pH 7.4, as reported by Bungaard *et al.*[41] is actually the value of the combined rate constant, $k_1 + k_2$, and as such it is invalid with respect to the rate of the direct release of amide **10** (k_1). Indeed the reaction scheme for the hydrolysis of **8** illustrated in the paper published by Bundgaard *et al.*[41] (represented in Figure 49) does not depict hydrolysis of the methyl ester of **8** to give the free acid **7**. The combined rate constant $k_1 + k_2$ for the hydrolysis of **8** at pH 7.5 provided in Table 5 corresponds to a half-life of 2.1 hours which is 2.8 times longer than the rate of hydrolysis of **8** at pH 7.4 reported by Bundgaard *et al.*[41] This error may be due to the different experimental conditions used, however, it

remains apparent that the previously published rate of hydrolysis of **8** to give **10** in the region of pH 7.5 was incorrect and has now been addressed.

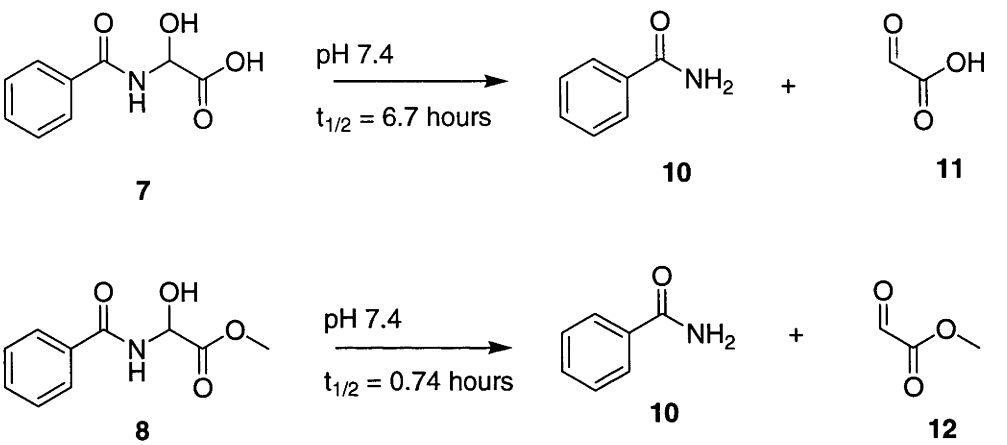

Figure 49. Reactions Schemes for the Hydrolysis of **8** and **7** and their Half-lives as Reported by Bundgaard *et al.*[41] in Independent Experiments.

The proposed use of α-substituted glycines to transiently link peptide hormones with other molecules has been outlined in the Introduction. The mechanism of hydrolysis of the α-acetoxyglycine **14** involved the formation of the α-hydroxyglycine **8** followed by hydrolysis to release the amide **10** (Figure 15). Accordingly it would be expected that the α-substituted glycines **17**, **19**, **21** and **22** would also hydrolyse to release the amide **10** *via* the formation of an α-hydroxyglycine intermediate. The α-hydroxyglycine methyl ester **8** can be considered to be a system where a methyl group and a benzoyl group are transiently linked by an α-hydroxyglycine residue. The α-hydroxyglycine **7** can be considered to be a system where benzamide **10** is masked by α-hydroxyglycine. As outlined above, rates of hydrolysis of **7** and **8** to release **10** at biological pH reported by Bundgaard *et al.*[41] differed by a factor of 8.6. This implied that the hydrolysis of α-

substituted glycines would be significantly different when used to transiently link peptide hormones with other molecules in comparison to when they were being used to mask hormone *C*-terminal amides. However, the rates of hydrolysis of **7** and **8** to release **10** at pH 7.5 (outlined above) have been found to be essentially identical. Therefore the studies of the α-substituted glycines **14**, **17**, **19**, **21** and **22** outlined below can be considered to be suitable for modelling both the hydrolysis of their α-substituted glycine residues when being used as amide masking agents and as transient linkers between molecules.

The hydrolyses of the α-substituted glycines **14**, **17**, **19**, **21** and **22** in aqueous solution at pH 7.5 and 10.0 were then performed using the method described above. Due to the complexity of the ^{1}H NMR spectra obtained for the hydrolysis of **22**, UV-HPLC was used to analyse these reactions. The concentration of **22** used for the reactions monitored by UV-HPLC was 1 mM, all other conditions remained the same as described above. The results of these experiments are summarised in Table 7 and a description of how these values were obtained follows.

The hydrolysis of **14** at pH 7.5 and 10.0 to the α-hydroxyglycine **8** was extremely rapid such that 100% of the starting material had reacted within the time required to begin reaction monitoring. Therefore the half-lives of **14** at pH 7.5 and 10.0 were estimated to be <2 minutes (Table 7). Correspondingly the psuedo-first order rate constant for the hydrolysis of **14** to give **8** must be >5 x 10^{-3} sec^{-1}. The mechanism of hydrolysis of **14** at basic pH is illustrated in Figure 50. The hydrolysis of **14** to give **109** followed by **110** was a possibile outcome of this experiment and as such is depicted in Figure 50,

however, this was not observed as the rate of conversion of **14** to **15** was too fast. The α-hydroxyglycines **8** and **7** formed during this reaction hydrolysed to release benzamide **10** in accordance with the mechanism illustrated in Figure 46.

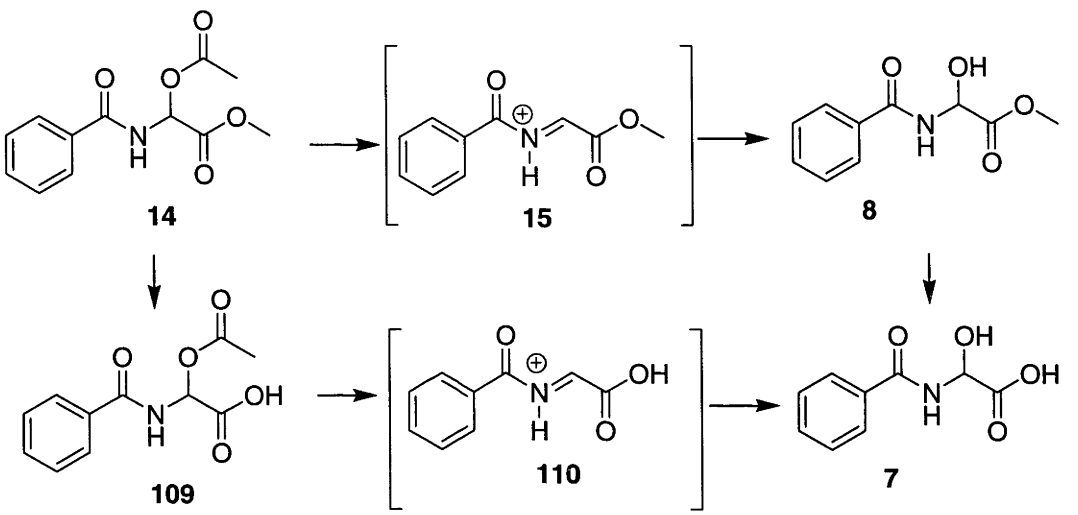

Figure 50. Mechanism of Hydrolysis of **14** at pH 7.5 and 10.0

The ^{1}H NMR spectra obtained for the reactions of **17** and **19** in aqueous solution at pH 7.5 and 10.0 over three weeks showed only the hydrolysis of their methyl esters to give their respective free acids **16** and **18** and no evidence for the release of amide **10** was observed. Therefore, the half-lives for the hydrolysis reactions to release the amide **10** from **16** and **18** at pH 7.5 and 10.0 must be >500 hours (Table 7). Correspondingly, the psuedo-first order rate constants of these reactions must be $<4.0 \times 10^{-7}$ sec^{-1}.

The ^{1}H NMR spectra obtained for the hydrolysis of the α-succinimidoglycine **22** performed at pH 7.5 and 10.0 showed the formation of new resonances, although none were attributable to the methyl ester **8** or the free acid **7**. Evidence for the formation of

the amide **10** was not observed. It is likely that at pH 7.5 and 10.0 the succinimido ring of **22** is hydrolysing to give the new species **113**, the proposed routes to which is illustrated in Figure 51. The hydrolysis of **22** could give the ring opened intermediate **111** followed by saponification to give **113**. Alternatively, saponification of **22** may yield **112**, followed by hydrolysis to produce **113**. Evidence for the formation of **113** was obtained by electrospray mass spectrometry of the reaction solution, which showed a peak for the protonated molecular ion at *m/z* 277. As no evidence for the formation of the amide **10** was observed, the half-life for the hydrolysis of **113** to release **10** must be conservatively >500 hours, corresponding to a pseudo-first order rate constant <4.0 x 10^{-7} sec^{-1}.

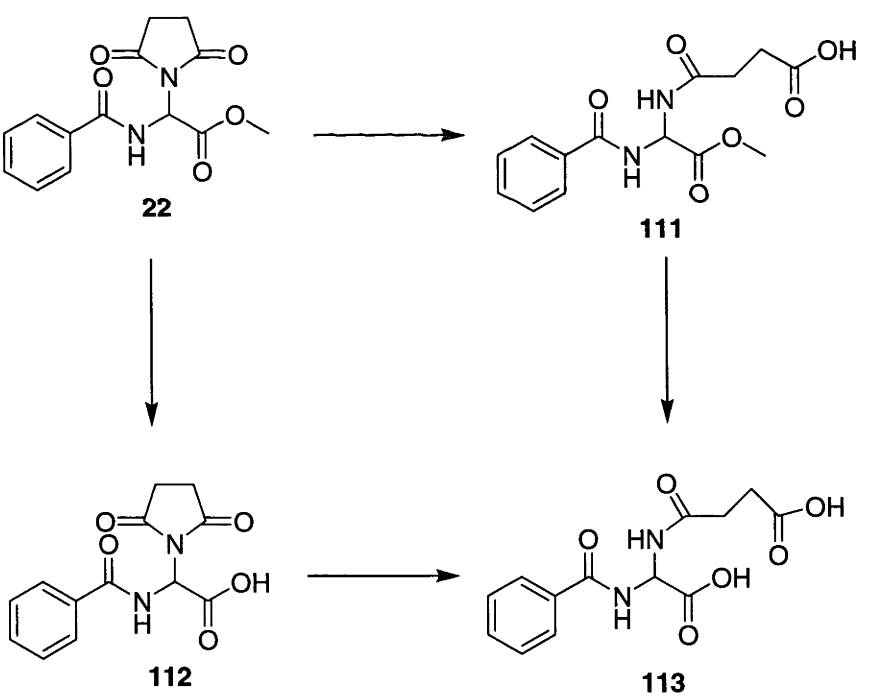

Figure 51. Mechanism of Hydrolysis of **22** at pH 7.5 and 10.0

Traces obtained by UV-HPLC of the reactions of **21** at pH 7.5 and 10.0 are provided in Figures 52 and 53. The peaks in Figures 52 and 53 with a retention time of 5.6 minutes are attributable to the starting material **21**. Through comparison to the UV-HPLC trace of an injection of an authentic sample, the peak with a retention time of 2.9 minutes was assigned to the amide **10**. The peak with a retention time of 4.0 minutes in Figure 52 and 3.9 minutes in Figure 53 was assigned to phenol through comparison to the retention time and UV-absorbance profile of the peak in a UV-HPLC trace of an injection of an authentic sample. The peak with a retention time of 5.0 minutes was assumed to be the free acid **20** as it possessed the same UV absorbance profile as the starting material **21**. Furthermore, this peak was larger in the UV-HPLC traces in Figure 53 than in Figure 52, which would be consistent with increased base catalysed methyl ester hydrolysis at pH 10.0 in comparison to pH 7.5. This peak in Figures 52 and 53 never reached a substantial size, indicating that **20** did not reach a high concentration during the hydrolysis of **21** at pH 7.5 and 10.0. This was consistent with the ^{1}H NMR spectra obtained during the hydrolysis of **21** at pH 7.5 and 10.0, which also did not show any significant evidence for the formation of **20**. Therefore, any effect that that rate of hydrolysis of **21** to give **20** might have on the calculated rate of formation of **8** from the rate of starting material consumption would not be substantial. The rate of formation of **8** from **21** at pH 7.5 and 10.0 was therefore estimated from the rate of starting material consumption and the values are provided in Table 7.

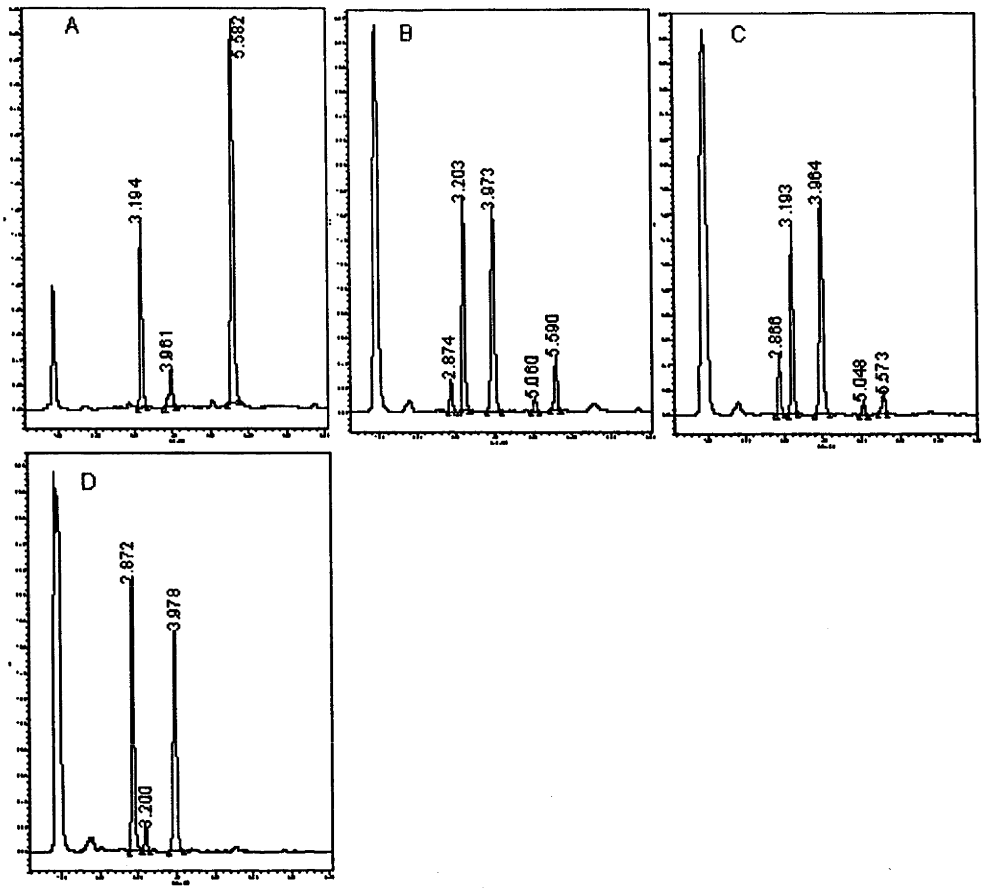

Figure 52. UV-HPLC Traces (225 nm) Obtained During the Hydrolysis of **21** at pH 7.5, **A** = 5 min, **B** = 35 min, **C** = 65 min and **D** = 155 min

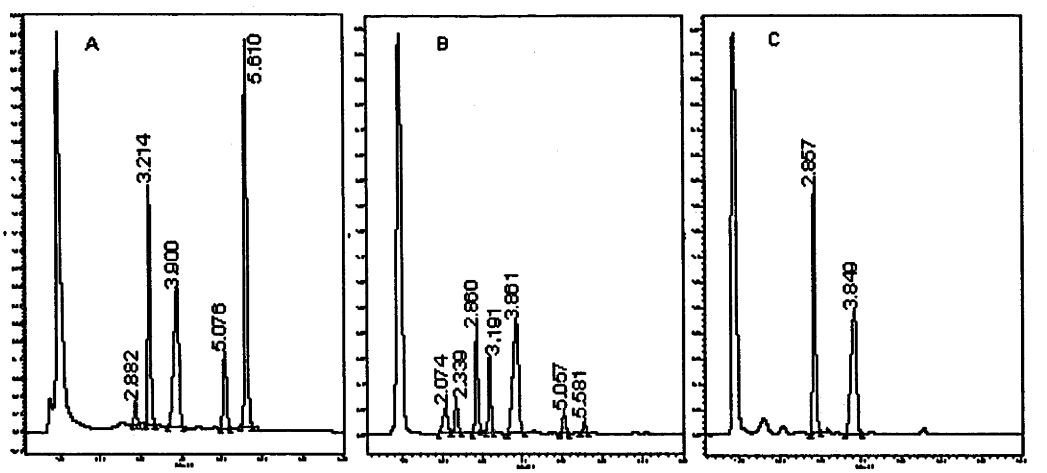

Figure 53. UV-HPLC Traces (225 nm) Obtained During the Hydrolysis of **21** at pH 10.0, **A** = 5 minutes, **B** = 20 minutes and **C** = 155 minutes

The half-lives for the hydrolysis of **21** to release the α-hydroxyglycine **8** at pH 7.5 and 10.0 were estimated to be 0.40 hours and 0.08 hours respectively (Table 7). The psuedo-first order rate constants for the hydrolysis of **21** to give the α-hydroxyglycine **8** at pH 7.5 and 10.0 were therefore estimated to be 4.7 x 10^{-4} sec^{-1} and 2.4 x 10^{-3} sec^{-1} respectively by applying the corresponding half-lives to Equation 1. The yield of amide **10** from the hydrolysis of **21** at pH 10.0 and 7.5 was found to be quantitative through comparison of the area of the peak for **10** in reaction UV-HPLC traces to that in the UV-HPLC trace of an injection of a standard solution of an authentic sample. Therefore the hydrolysis of **22** to give **10** was found to be efficient and high yielding. The routes for hydrolysis of **21** at basic pH is illustrated in Figure 54. This is derived from the proposed ways in which the α-acetoxyglycine **14** hydrolyses (Figure 50). The hydrolysis of **21** to produce the α-hydroxyglycines **8** and **7** was proposed to have proceeded via the *N*-acyliminium ions **15** (directly) and **110** (indirectly). The α-hydroxyglycines **8** and **7** then hydrolysed further to ultimately release the amide **10** in accordance with the mechanism illustrated in Figure 46.

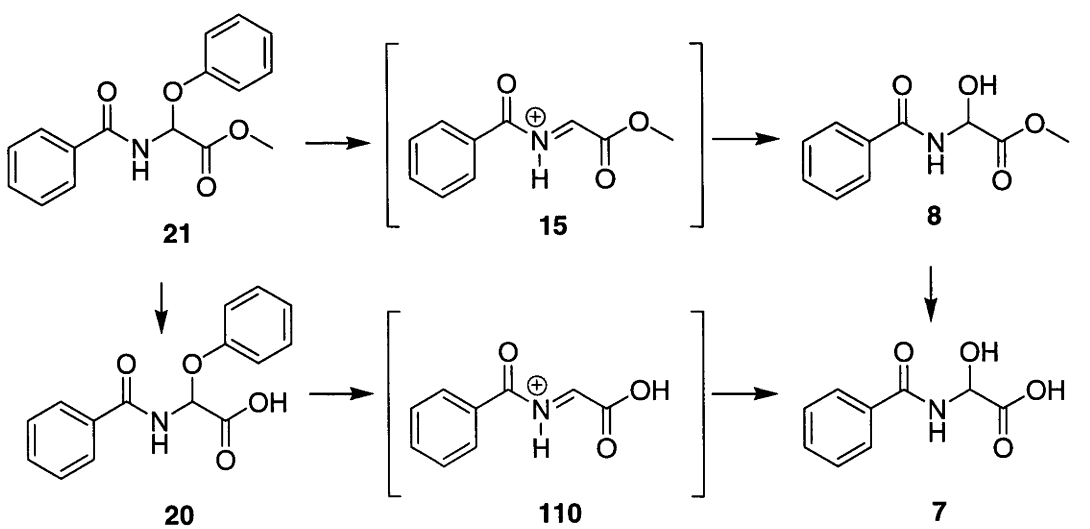

Figure 54. Mechanism of Hydrolysis of **21** at pH 7.5 and 10.0.

Table 7. Half-lives of **14**, **16**, **18**, **21** and **113** at pH 7.5 and 10.0 in Aqueous Solution.

Compound	pH 7.5	pH 10.0
14	<2 min	<2 min
16	>504 hrs	>504 hrs
18	>504 hrs	>504 hrs
113	>504 hrs	>504 hrs
21	0.40 hrs	0.08 hrs

The hydrolysis reactions of **8**, **14**, **17**, **19**, **21** and **22** to release the amide **10** at pH 4.0 were unsuccessful. The mechanism of hydrolysis of **8**, **14**, **17**, **19**, **21** and **22** at acidic pH would most likely involve the protonation of the amide and release of the amide tautomer **114** as illustrated in Figure 55. This may not readily occur at pH 4.0 thus explaining the resistance of **8**, **14**, **17**, **19**, **21** and **22** to hydrolysis under these conditions.

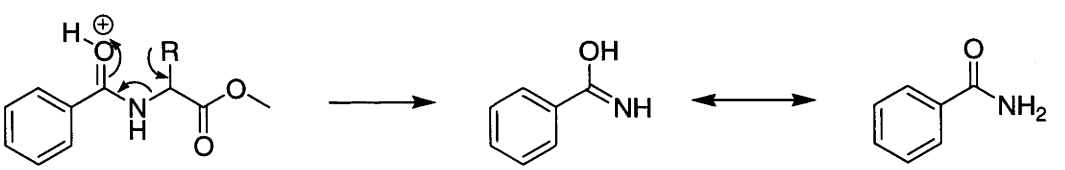

8 R = Hydroxy
14 R = Acetoxy
17 R = Methoxy
19 R = Ethoxy
21 R = Phenoxy
22 R = Succinimido

114

10

Figure 55. Proposed Mechanism of Hydrolysis of the α-Substituted Glycines **8**, **14**, **17**, **19**, **21** and **22** to Release Amide **10** at Acidic pH.

The hydrolysis of the α-acetoxyglycine **14** at pH 7.5 and 10.0 to form the α-hydroxyglycine **8** was very fast with a half-life of <2 minutes. This was rationalised in accordance with acetate being a good leaving group, resulting in the reaction of **14** to give the *N*-acyliminium ion **15** being very fast. Although the hydrolysis of **14** at pH 7.5 and 10.0 gave **8** which then hydrolysed to release benzamide **10**, the rate of conversion of **14** to **8** was too fast. Therefore, α-acetoxyglycines would be unsuitable to use as hydrolytically cleavable masking groups of the *C*-terminal amide of peptide hormones, or to transiently link hormones with other molecules. The hydrolysis reactions of the α-methoxyglycine **17** and the α-ethoxyglycine **19** at pH 7.5 and 10.0 formed only their respective free acids **16** and **18**. By analogy to the mechanism of hydrolysis of **14**, the hydrolysis of **16** and **18** to give the α-hydroxyglycine **7** would have to involve the formation of the *N*-acyliminium ion **110**. However, this would involve the elimination of methoxide from **16** and ethoxide from **18**. As both **16** and **18** did not hydrolyse to release the α-hydroxyglycine **7**, methoxide and ethoxide must be too inefficient as leaving groups to allow the *N*-acyliminium ion **110** to form, even over extended periods of time. The hydrolysis of the α-succinimidoglycine **21** at pH 7.5 and 10.0 was unsuccessful with respect to the release of the amide **10**. The reaction of **21** at pH 7.5 and 10.0 was found to give the ring opened product **113**. The hydrolysis of **113** to give the α-hydroxyglycine **7** would have to involve the formation of the *N*-acyliminium ion **110**. Acetamide is considered a poor leaving group in accordance with its pK_a of 15.0.[43] The α-carbon substituent of **113** can be considered to be analogous to acetamide and as such it would also be a poor leaving group. Therefore, as the hydrolysis of **113** at pH 7.5 and 10.0 to release the amide **10** was unsuccessful, the α-carbon substituent of **113** must be too inefficient as a leaving group to allow for the formation of the *N*-acyliminium ion **110**. The hydrolysis of the α-phenoxyglycine **21** at pH 7.5 and 10.0 to

release benzamide **10** was successful. The half-lives for the release of the α-hydroxyglycine **8** from the hydrolysis of α-phenoxyglycine **21** at pH 7.5 and 10.0 were 0.40 and 0.08 hours respectively. This result was rationalised in accordance with the pK_a of phenol (10.0)[43] being sufficient to allow phenoxide to be eliminated from **21** resulting in the formation of the *N*-acyliminium ion **15**. A discussion of how the results for the hydrolysis of **14**, **18**, **19**, **21** and **22** at pH 7.5 and 10.0 relate to each other follows.

The pK_as of ethanol, methanol, acetamide, phenol and acetic acid are 17.5, 15.0, 15.0, 10.0 and 4.0, respectively.[43] This reflects the ability of ethoxide, methoxide, acetamide, phenoxide and acetate to stabilise a negative charge which increases in the order ethoxide < methoxide, acetamide < phenoxide < acetate. Their efficiencies as leaving groups therefore increase in the same order. The α-phenoxyglycine hydrolysed at pH 7.5 and 10.0 faster than the α-alkoxyglycines **16** and **18** and slower than the α-acetoxyglycine **14**. This correlates with the pK_a of phenol being lower than for methanol and ethanol and higher than for acetic acid. It is therefore apparent that the rate of hydrolysis of α-substituted glycines at pH 7.5 and 10.0 is related to the pK_a of the α-substituents corresponding acid. Therefore, the initial hypothesis that the rate of hydrolysis of α-substituted glycines could be controlled through variation of the α-substituents was correct.

The aim of this research was to increase the time required for amides to be hydrolytically released from α-substituted glycines. The half-life of the α-phenoxyglycine **21** at biological pH was 0.40 hours. Therefore, it would be reasonable to expect that, the use of α-phenoxyglycine as a hydrolytically cleavable masking group

of the *C*-terminal amide of clinically administered peptide hormones would allow suitable time for drug dispersal and transport across cell membranes before exposure of the active drug form. Methods by which the rate of hydrolysis of α-substituted glycines to release amides could be extended further will be outlined in the Future Work and Conclusions section of this thesis.

Chapter 3. 2-Nitrophenylalanine - a Photochemically Cleavable Amino Acid for Efficient Amide Release Under Biological Conditions.

3.1 Project Rationale

In Chapter 2 of the Results and Discussion, research towards the development of α-substituted glycines as hydrolytically cleavable amide masking groups or as systems that could be used to transiently link the *C*-terminal amide of peptide hormones to other molecules was outlined. As covered in the Introduction, the development of photocleavable amino acids that could be used for similar purposes is warranted. Npg **40** has been used to mask the *C*-terminal amide of peptide hormones and to transiently link amides with other molecules, however, its photolysis at biological pH is known to be inefficient.[51,52,82] It was reasoned that Npg photolysis was inefficient at biological pH due to the formation of α-hydroxy intermediates such as **46** (Figure 21) which would be slow to hydrolyse under these conditions.

The photolysis of the NPEOC **31** (Figure 18) did not involve the formation of reaction intermediates which would be expected to be slow to breakdown at biological pH. It was therefore hypothesised that 2-nitrophenylalanine derivatives, which were designed through analogy to NPEOC, would photolyse more efficiently at biological pH in comparison to Npg. The potential applications of the photolysis of 2-nitrophenylalanine derivatives include, light activated peptide hormone drugs for use in PDT, site-selective photochemical proteolysis, photoprobe research, peptide hormone synthesis and the release of molecules from solid support. Therefore, studies were performed to determine whether 2-nitrophenylalanine derivatives could be photolysed to unmask amides.

3.2 Synthesis of 2-Nitrophenylalanine Peptidic Systems and Analogues

A variety of compounds were required in order to investigate the potential photolysis of 2-nitrophenylalanine derivatives to unmask amides. *N*-Benzoyl-(*R,S*)-valine purchased from Aldrich Chemical Company was used throughout the syntheses described in this Chapter. The synthesis of the systems chosen for investigation will now be outlined.

3.2.1 *N*-Benzoylvalyl-2-nitrophenylalanine Methyl Ester 119

The synthesis of *N*-benzoylvalyl-2-nitrophenylalanine methyl ester **119** is now described (Figure 56).

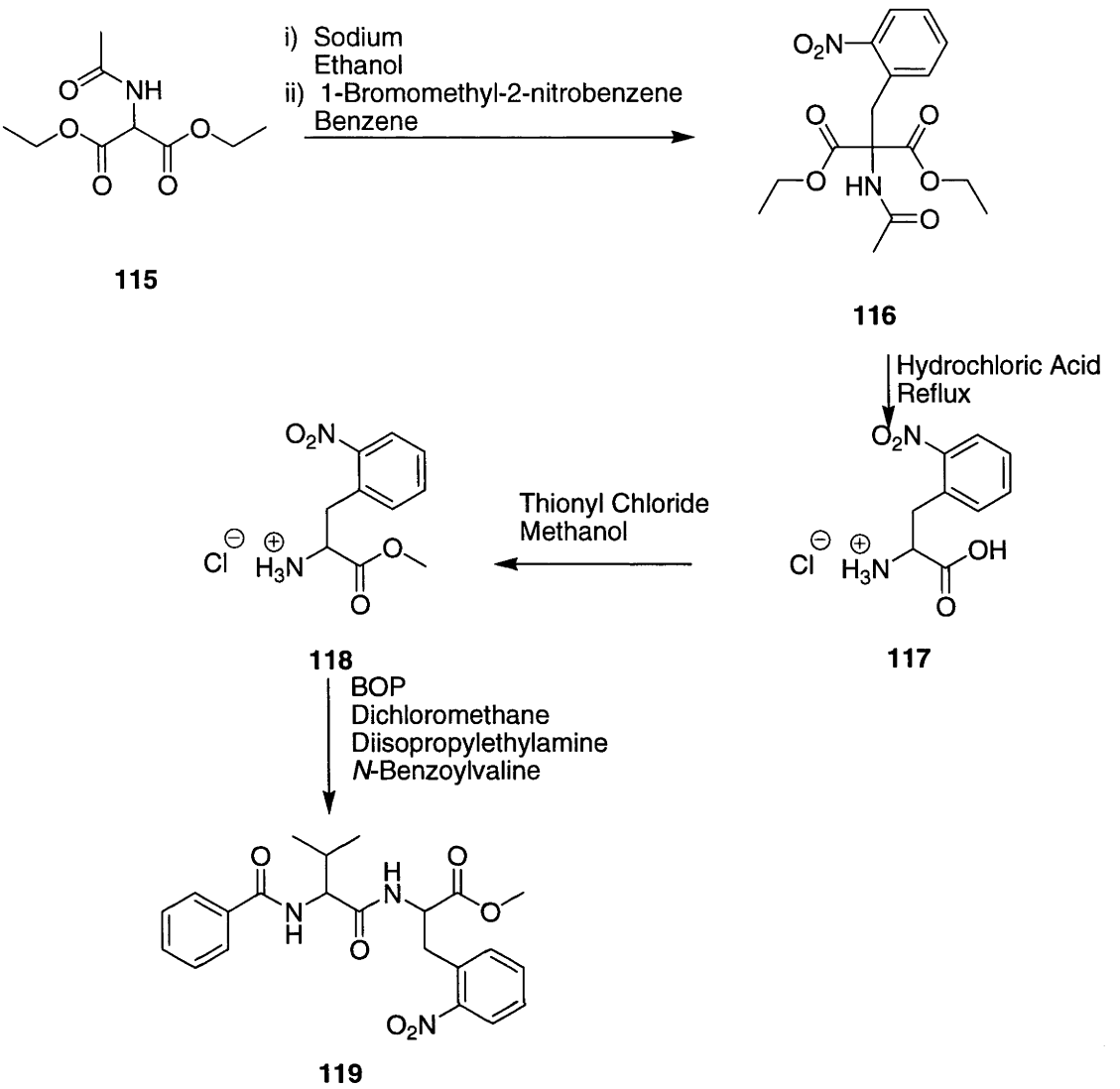

Figure 56. Synthesis of *N*-Benzoylvalyl-2-nitrophenylalanine Methyl Ester **119**

Diethyl 2-acetamidomalonate **115** was stirred in a solution of sodium ethoxide in ethanol and treated with 1-bromomethyl-2-nitrobenzene in benzene to give **116**. The ^{1}H NMR spectrum of the product showed resonances for the acetyl protons at δ1.16 ppm and the aromatic protons at δ7.25 – 7.90 ppm. Compound **116** was heated to reflux in concentrated hydrochloric acid to give 2-nitrophenylalanine **117**. The ^{1}H

NMR spectrum of the product showed resonances for the 2-nitrophenylalanine α-carbon proton at δ4.35 ppm and the β-carbon protons at δ3.42 and δ3.67 ppm respectively. 2-Nitrophenylalanine **117** was stirred in methanol which had been pretreated with thionyl chloride to give **118**. The appearance of the methyl ester protons' resonance at δ3.71 ppm in the ^{1}H NMR spectrum of the product indicated the reaction to have been successful. 2-Nitrophenylalanine methyl ester **118** was stirred in dichloromethane along with BOP, diisopropylethylamine and *N*-benzoylvaline to give **119** as diastereomers in a ratio of 1:4 as determined by ^{1}H NMR spectroscopy. The ^{1}H NMR spectrum of the product showed resonances for the valine α-carbon proton at δ4.91 ppm and methyl ester protons at δ3.70 and δ3.76 ppm.

3.2.2 *N*-Benzoyl-2-nitrophenylalanylalanine Methyl Ester 122

The synthesis of *N*-benzoyl-2-nitrophenylalanylalanine methyl ester **122** is now described (Figure 57). 2-Nitrophenylalanine methyl ester **118** was synthesised *via* the established method illustrated in Figure 56. The ester **118** was then heated at reflux in ethyl acetate along with benzoyl chloride and triethylamine to give compound **120**. The ^{1}H NMR spectrum of the product displayed resonances for the aromatic protons at δ7.48 – 7.92 ppm and the 2-nitrophenylalanine α-carbon proton at δ5.10 ppm and the β-carbon protons at δ3.46 and δ3.58 ppm. *N*-Benzoyl-2-nitrophenylalanine methyl ester **120** was then saponified by stirring in aqueous sodium hydroxide and tetrahydrofuran to give the free acid **121**. The ^{1}H NMR spectrum of the product did not display any resonances characteristic of methyl ester protons in the region of δ3.00 - δ4.00 ppm indicating the deprotection to have proceeded. The free acid **121** was then stirred in dichloromethane along with BOP, diisopropylethylamine and alanine methyl ester,

which was purchased from Aldrich Chemical Company, to give **122** as diastereomers in a 1:2 ratio as determined by ^{1}H NMR spectroscopy. The appearance of resonances for the alanine α-carbon protons at δ4.36 and δ4.45 ppm, β-carbon protons at δ1.31 and δ1.39 ppm and methyl ester protons at δ3.68 and δ3.70 ppm in the ^{1}H NMR spectrum of the product indicated the reaction to have proceeded.

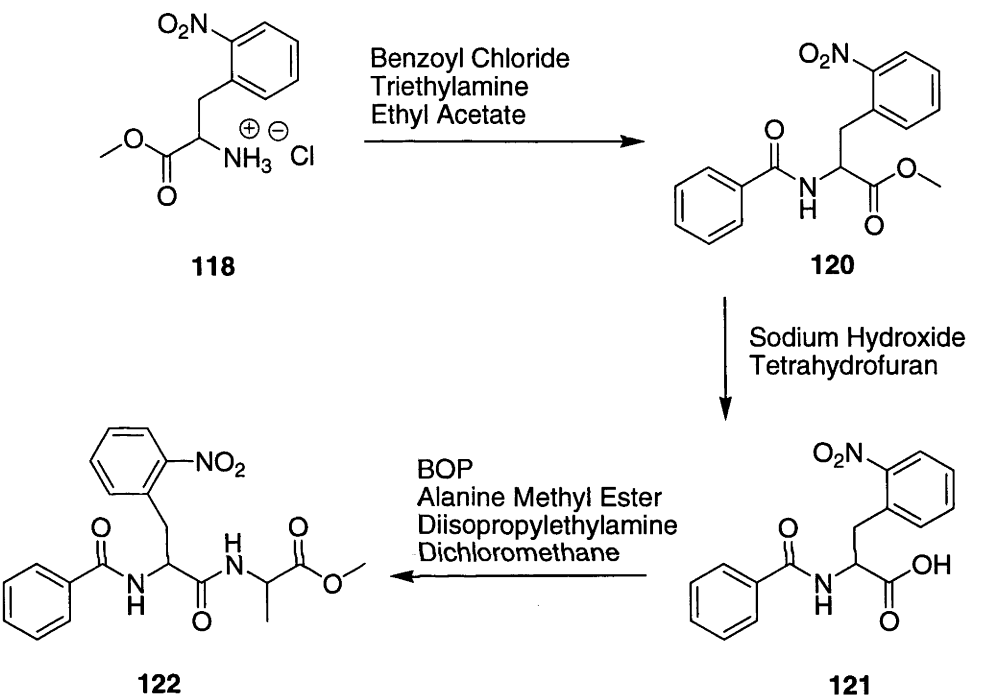

Figure 57. Synthesis of *N*-Benzoyl-2-nitrophenylalanylalanine Methyl Ester **122**

3.2.3 *N*-Benzoylvalyl-2-nitrophenylalanine 123

N-Benzoylvalyl-2-nitrophenylalanine **123** was synthesised as depicted in Figure 58. *N*-Benzoylvalyl-2-nitrophenylalanine methyl ester **119** was synthesised as illustrated in Figure 56 and then saponified by stirring in aqueous sodium hydroxide and

tetrahydrofuran to give **123** as diastereomers in a ratio of 1:4 as determined by ^{1}H NMR spectroscopy. The ^{1}H NMR spectrum of the product did not display any resonances for methyl ester protons in the region of δ3.70 - δ3.76 ppm indicating the deprotection to have proceeded.

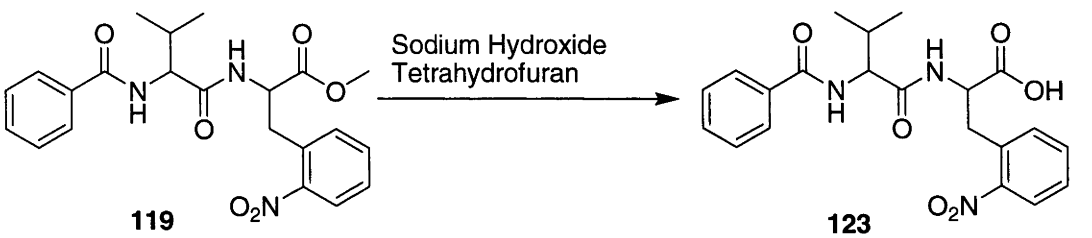

Figure 58. Synthesis of *N*-Benzoylvalyl-2-nitrophenylalanine **123**

3.2.4 *N*-(2-Nitrophenylethyl)-N^{α}-benzoylvalinamide 128

N-(2-Nitrophenylethyl)-N^{α}-benzoylvalinamide **128** was synthesised as depicted in Figure 59. 2-Phenylethylamine **124** was stirred in water along with acetic anhydride and triethylamine to give the amide **125**. The ^{1}H NMR spectrum of the product showed resonances for the acetyl protons at δ1.93 ppm and the aromatic protons at δ7.17 – δ7.33 ppm indicating the reaction to have proceeded. Nitration of compound **125** by stired in a mixture of nitric acid and sulfuric acid gave the two isomers, *N*-acetyl-2-(2-nitrophenyl)ethylamine **126** and *N*-acetyl-2-(4-nitrophenyl)ethylamine. The desired *ortho* isomer **126** was separated from *N*-acetyl-2-(4-nitrophenyl)ethylamine by HPLC. The ^{1}H NMR spectrum of the product showed resonances for the protons of an ortho substituted aromatic ring in the region of δ7.67 – 8.78 ppm. Compound **126** was stirred in hydrochloric acid and the mixture was heated to reflux to give the amine **127**. The ^{1}H NMR spectrum of the product did not display a resonance characteristic of acetyl

protons in the region of δ1.97 ppm indicating the reaction to have been successful. 2-Nitrophenethylamine **127** was stired in dichloromethane along with BOP, diisopropylethylamine and *N*-benzoylvaline to give *N*-benzoylvalyl-2-nitrophenethylamide **128**. The ^{1}H NMR spectrum of the product displayed resonances for the valine α- and β-carbon protons at δ4.95 ppm and δ2.10 ppm and the benzylic protons at δ4.46 ppm.

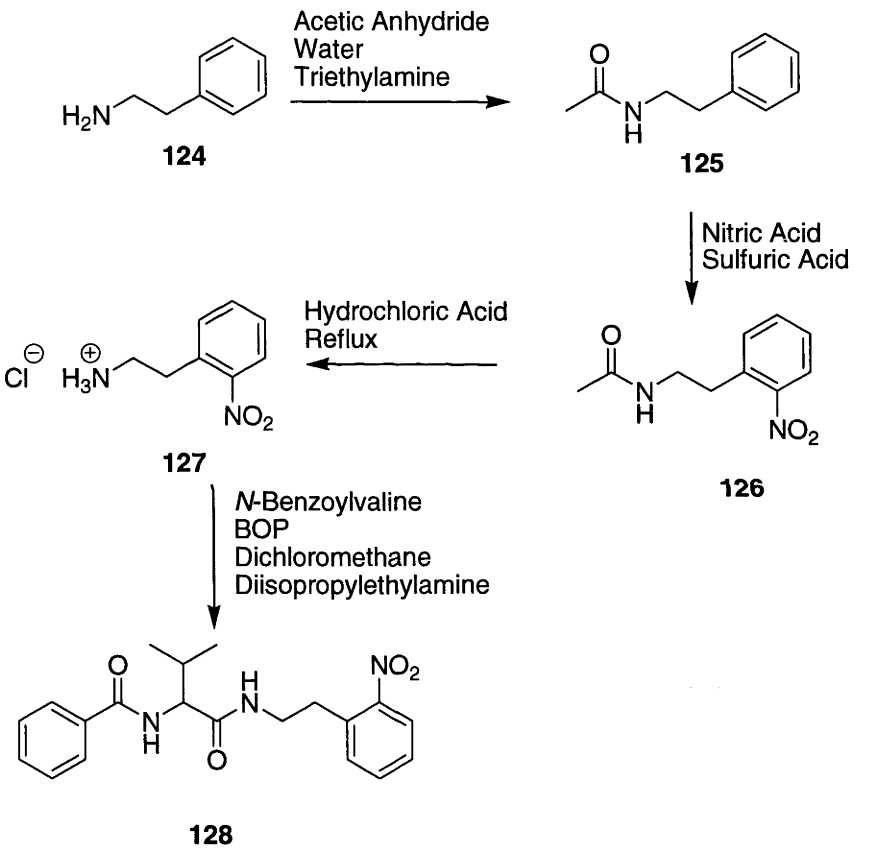

Figure 59. Synthesis of *N*-(2-Nitrophenylethyl)-N^{α}-benzoylvalinamide **128**

3.2.5 *N*-Benzoylvalyl-2-nitrophenylalanylalanine Methyl Ester 129

N-Benzoylvalyl-2-nitrophenylalanylalanine methyl ester **129** was synthesised as illustrated in Figure 60. Alanine methyl ester was stirred in dichloromethane along with BOP, diisopropylethylamine and the free acid **123** (the synthesis of **123** is described above in Figure 58) to give the tripeptide **129** as diastereomers in a ratio of 1:1:2:2.5 as determined by ^{1}H NMR spectroscopy. The spectrum obtained by high resolution fast atom bombardment mass spectrometry of the product showed a peak for the protonated molecular ion at *m/z* 499.2186 which corresponds closely with the calculated accurate mass of *m/z* 499.2193.

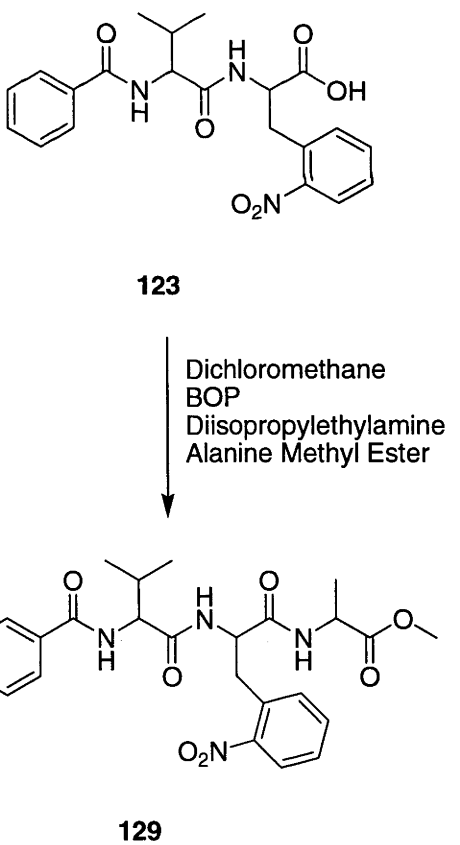

123

129

Figure 60. Synthesis of *N*-Benzoylvalyl-2-nitrophenylalanylalanine Methyl Ester **129**.

3.2.6 *N*-Benzoylvalyl-2-nitro-4,5-dimethoxyphenylalanine Methyl Ester 133

N-benzoylvalyl-2-nitro-4,5-dimethoxyphenylalanine methyl ester **133** was synthesised as illustrated in Figure 61.

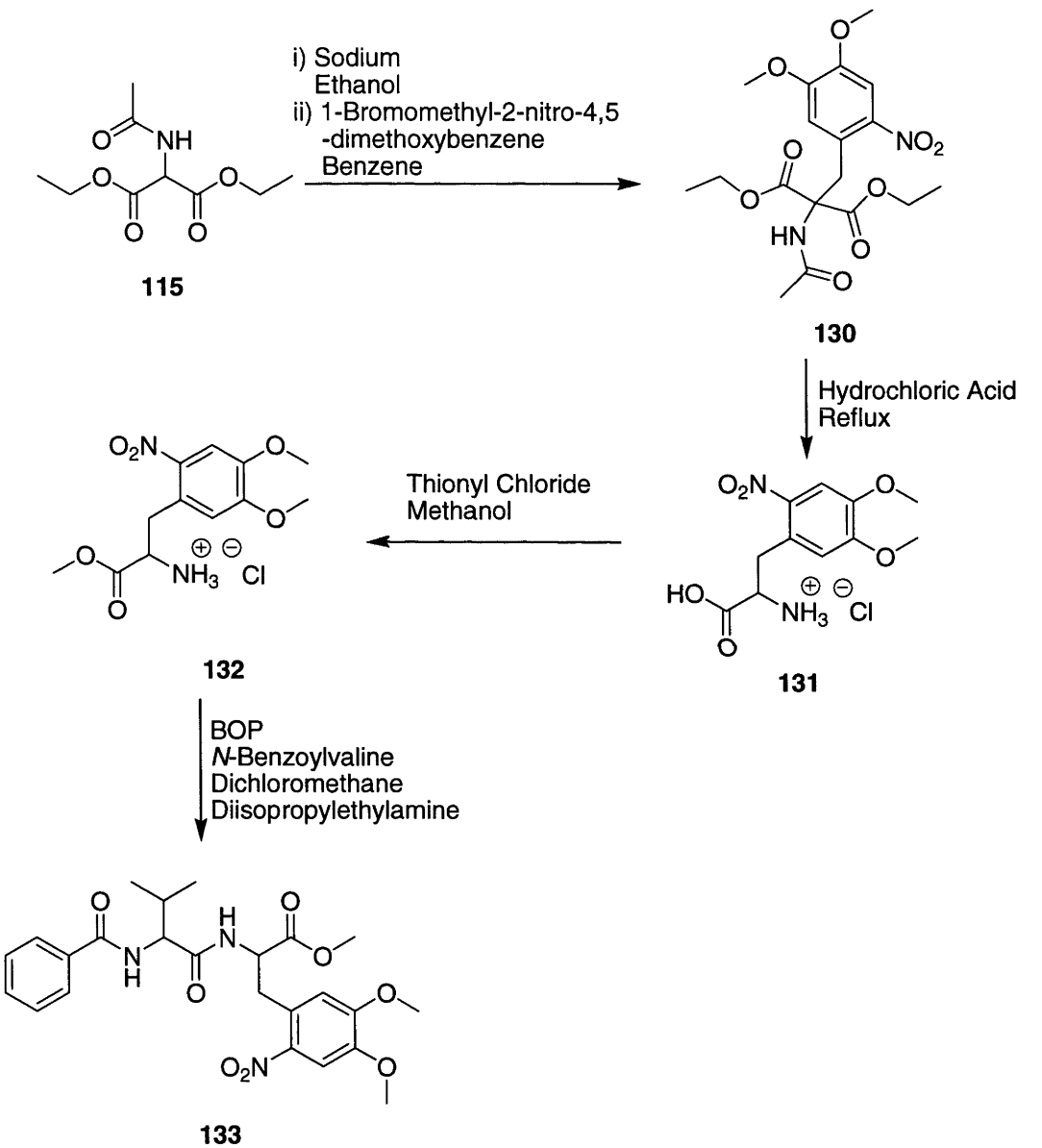

Figure 61. Synthesis of *N*-Benzoylvalyl-2-nitro-4,5-dimethoxyphenylalanine Methyl Ester **133**.

The malonate **115** was stirred in sodium ethoxide in ethanol and then treated with 1-bromomethyl-2-nitro-4,5-dimethoxybenzene in benzene to give **130**. The ^{1}H NMR spectrum of the product displayed singlet resonances for the aromatic protons at δ6.76 and δ7.57 ppm and the acetyl protons at δ1.37 ppm. Compound **130** was heated at reflux in concentrated hydrochloric acid to give 2-nitro-4,5-dimethoxyphenylalanine **131**. The ^{1}H NMR spectrum of the product displayed resonances for the α-carbon proton at δ4.34 ppm, the β-carbon protons at δ3.39 and δ3.72 ppm and the methoxy protons at δ3.91 and δ3.97 ppm. Compound **131** was stirred in methanol that had been pretreated with thionyl chloride to give the ester **132**. The ^{1}H NMR spectrum of the product displayed a resonance for the methyl ester protons at δ3.98 ppm indicating the reaction to have proceeded. Compound **132** was stirred in dichloromethane along with BOP, diisopropylethylamine and *N*-benzoylvaline to give the dipeptide **133** as diastereomers in a ratio of 1:2 as determined by ^{1}H NMR spectroscopy. The ^{1}H NMR spectrum of the product displayed resonances for the valine α-carbon proton at δ4.94 ppm, along with the 2-nitrophenylalanine α-carbon proton at δ4.56 and the β-carbon protons at δ3.28 and δ3.51 ppm, respectively, indicating the reaction to have been successful.

3.3 Photolysis of 2-Nitrophenylalanine Systems and Analogues

The aim of these studies was to design an unnatural amino acid, which could be photolysed efficiently under biological conditions. Photolysis experiments were therefore performed in a solution containing 75% 50 mM HEPES buffer at pH 7.4. Due to the solubility requirements of the systems outlined in this chapter, 25%

acetonitrile was also used. Photolysis experiments were performed at a concentration of 50 μM to minimise possible intermolecular interactions and internal filtering by reaction intermediates and side products. The irradiation of solutions was performed in a Luzchem Photoreactor using three different lamp types which emit radiation at 254, 300 or 350 nm and the level of light flux was controlled by manipulation of the number of lamps used with the maximum number being ten. Although irradiating 2-nitrophenylalanine derivatives at 254, 300 and 350 nm would not be ideal in biological experiments, they are used in these studies for method and system development. Experiments were analysed by UV-HPLC at 225 nm through comparisons of injections of reaction mixtures with those of 50 μM standards of authentic samples of starting material and the amides to be released.

The anticipated mechanism of photolysis of the 2-nitrophenylalanine derivative **56** (Figure 62) was derived from that of the NPEOC **31** (Figure 18). The irradiation of **56** would give the diradical **134**. The oxygen centered radical of **134** would then abstract a hydrogen atom from the benzylic carbon to give the diradical **135**. After abstraction of a proton from the *aci*-nitro intermediate **136**, which is a resonance form of **135**, to give **137**, elimination of the amide **47** and a cinnamyl derivative **57** would occur.

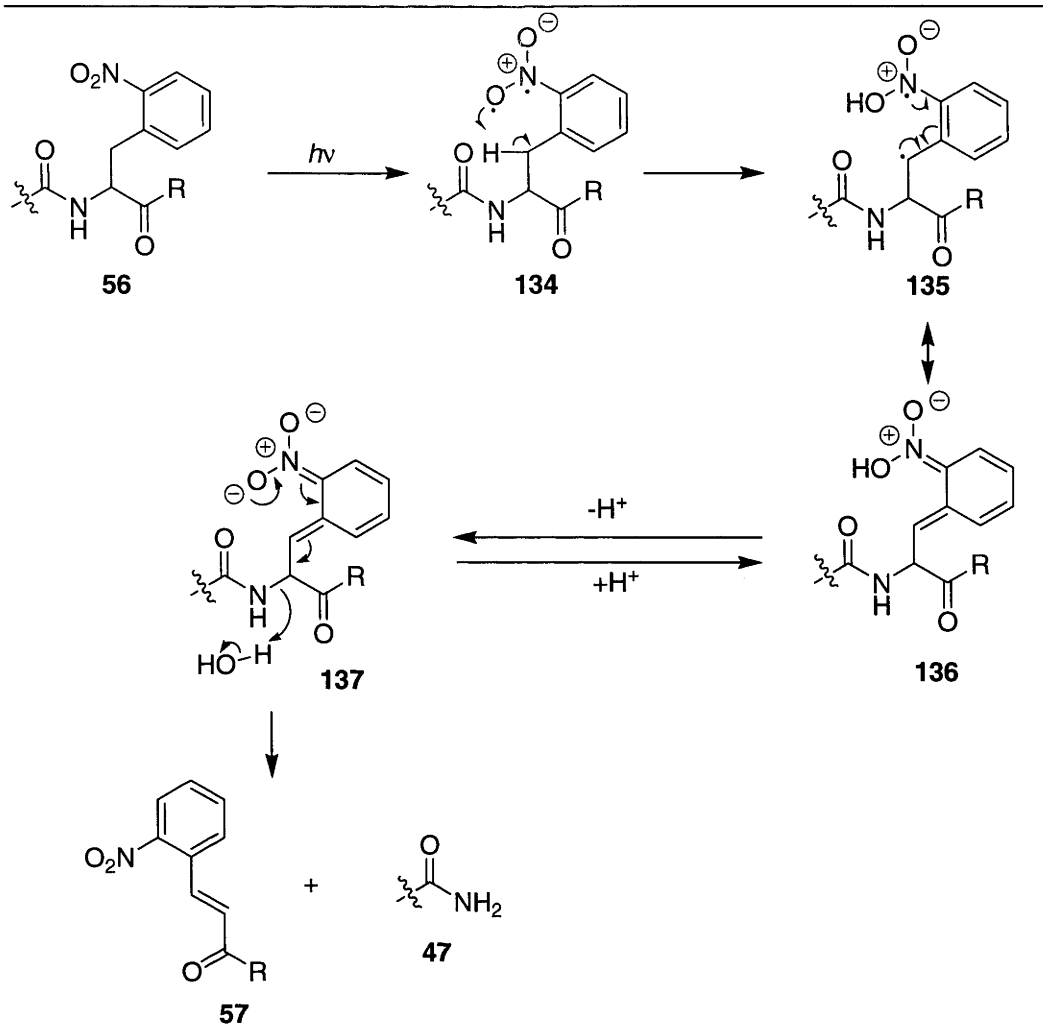

Figure 62. Anticipated Mechanism of 2-Nitrophenylalanine Photolysis. R = NH_2, NHR', OH, OR'

Initial studies to determine whether 2-nitrophenylalanine derivatives could be photolysed to release amides were performed on *N*-benzoylvalyl-2-nitrophenylalanine methyl ester **119**. In the Introduction it was outlined that the generation of the *aci*-nitro dianion **34** during NPEOC **31** photolysis was necessary for the desired cleavage mechanism to proceed (Figure 18). It was hypothesised that this process would be facilitated through the presence of a protic solvent, such as water, in the reaction media.

N-Benzoylvalyl-2-nitrophenylalanine methyl ester **119** was therefore selected for these initial studies as it possessed a suitable level of solubility in water.

A reaction scheme for the photolysis of **119** is illustrated in Figure 63. The photolysis of **119** was anticipated to release *N*-benzoylvalinamide **73** and the cinnamate **138** in accordance with the mechanism of photolysis of the 2-nitrophenylalanine derivative **56** (Figure 62).

The photolysis of **119** was performed using the conditions described above at 254 nm using 2 lamps. The UV-HPLC trace of the reaction solution after 55 minutes of irradiation and that for 50 μM standard solutions of *N*-benzoylvalinamide **73** and the starting material **119** are provided in Figures 64, 65 and 66, respectively.

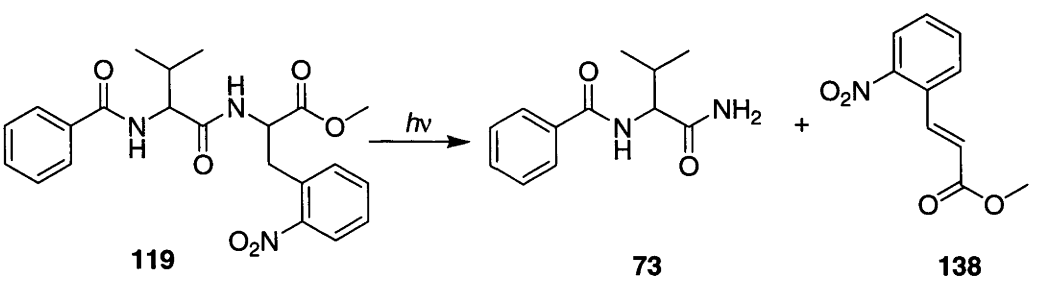

Figure 63. Reaction Scheme for the Photolysis of **119**

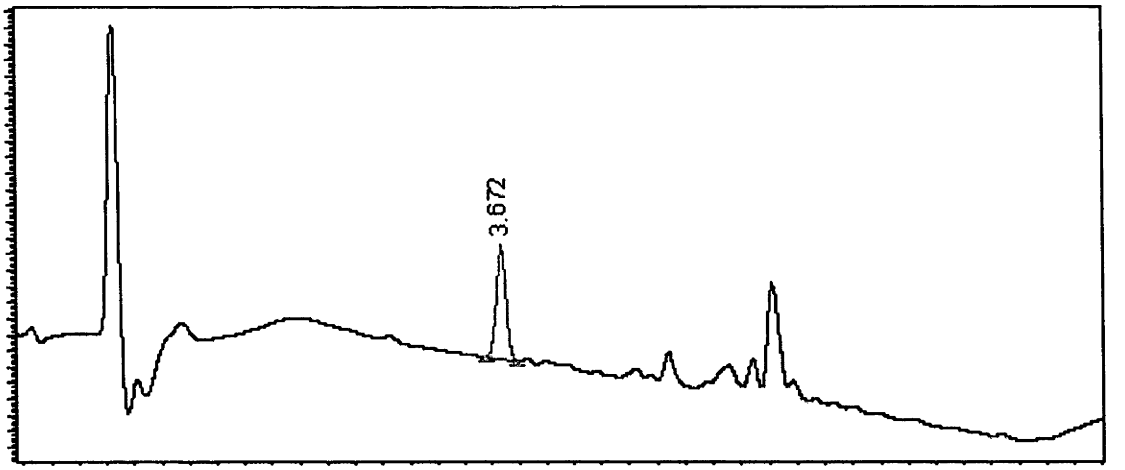

Figure 64. UV-HPLC Trace of the Reaction Solution of *N*-Benzoylvalyl-2-nitrophenylalanine Methyl Ester **119** after 55 Minutes of Irradiation at 254 nm using 2 Lamps

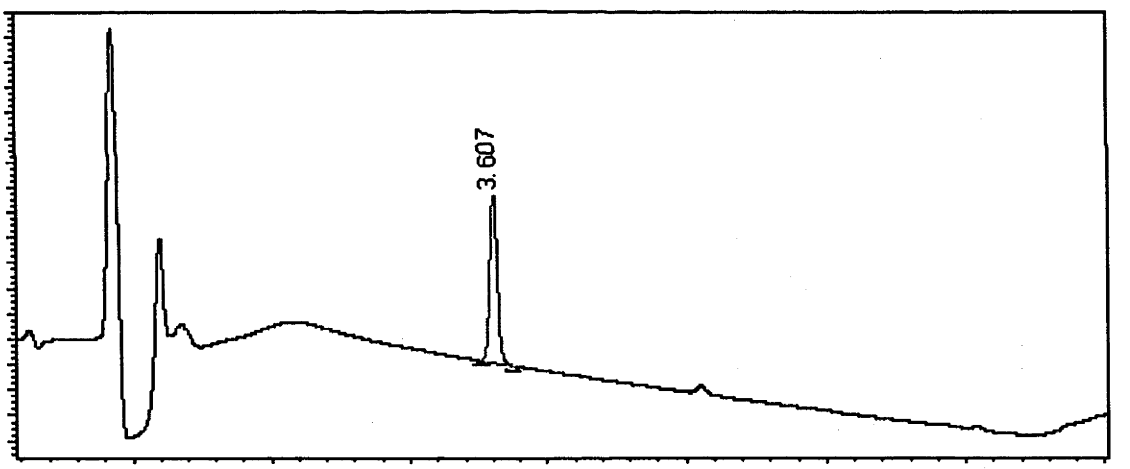

Figure 65. UV-HPLC Trace of a 50 μM Standard Solution of *N*-Benzoylvalinamide **73**

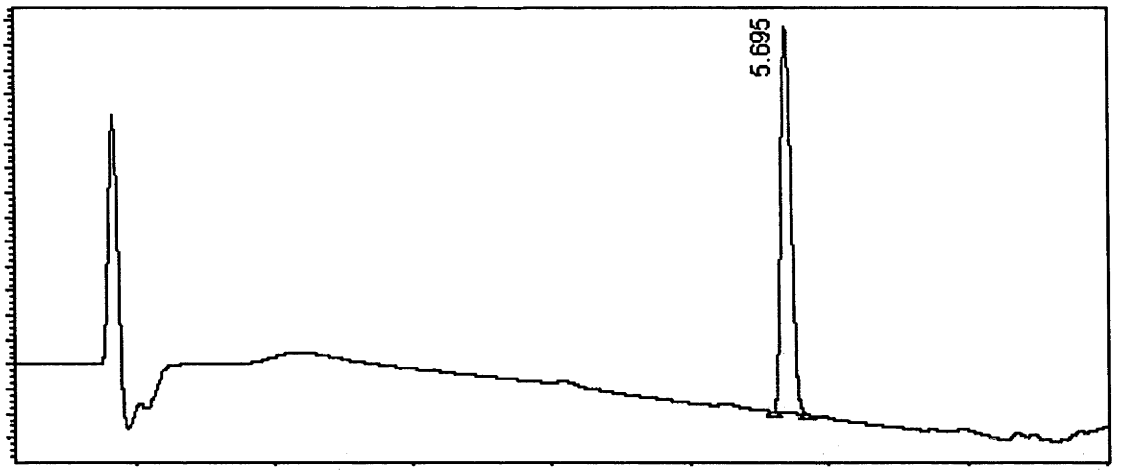

Figure 66. UV-HPLC Trace of a 50 μM Standard Solution of *N*-Benzoylvalyl-2-nitrophenylalanine Methyl Ester **119**

The peak at 3.67 minutes in Figure 64 was of a similar retention time to that for **73** in Figure 65. Spiking of the reaction solution with an authentic sample of **73** resulted in an increase in the area of the peak at 3.67 minutes. Furthermore, the UV-absorbance profiles of the peaks at 3.67 minutes in Figure 64 and 3.60 minutes in Figure 65 were identical. Therefore the peak at 3.67 minutes in Figure 64 was assigned to **73** proving the photolysis of **119** to have been successful. It was anticipated that the photolysis of **119** would also result in a large peak due to the formation of the 2-nitrocinnamate **138**. However, no large peak was observed that could be assigned to the cinnamate **138**. It was hypothesised that this might be a consequence of **138** being photoactive due to the presence of the nitro functionality, thereby resulting in its degradation *via* other photochemical pathways as yet not elucidated. Therefore, future studies of the photolysis of 2-nitrophenylalanine systems concentrated on the release of amides exclusively.

The release of the amide **73** from the photolysis of **119** at 225, 300 and 350 nm using 1, 10 and 10 lamps, respectively, was then studied through continuous reaction monitoring by UV-HPLC (Figure 67). The photolysis of **119** at 254 nm using 10 lamps was found to give **73** in ~ 50% yield with complete loss of starting material after 10 minutes. Therefore 1 lamp was used at this wavelength as the resultant slower rate of photolysis was more suitable for reaction monitoring.

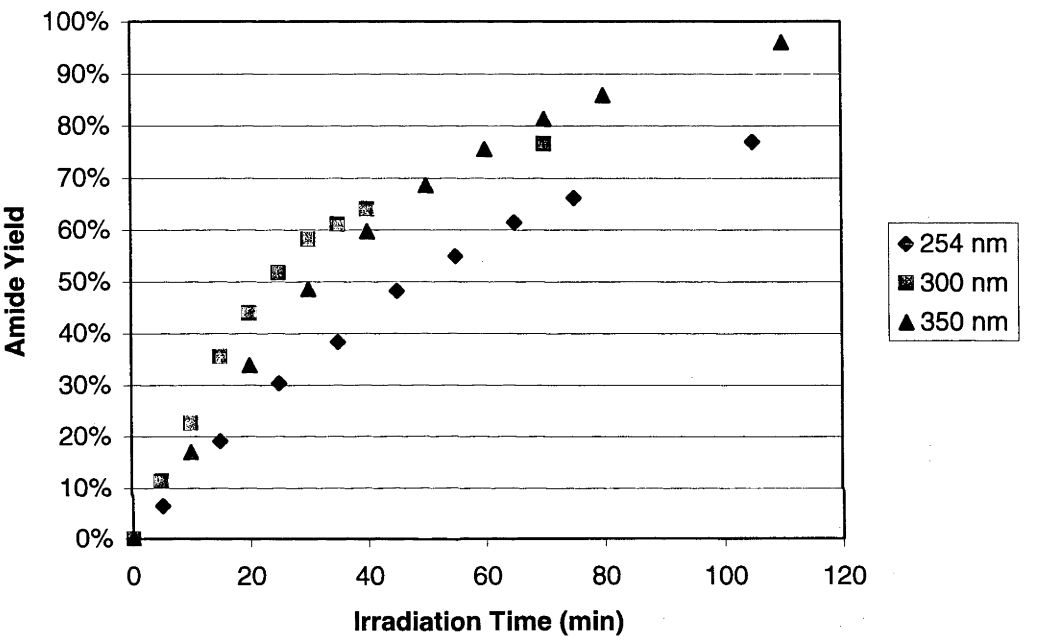

Figure 67. Release of Amide **73** from the Photolysis of **119** at 254, 300 and 350 nm using 1, 10 and 10 Lamps, Respectively.

The photolysis of **119** at 254, 300 and 350 nm gave yields of **73** of 80 – 100% over a 2 hour period (Figure 67). The rate of amide **73** release at the three different wavelengths was found to be similar. In order to rationalise this result, the UV absorbance profile of **119** was analysed (Figure 68). The UV-absorbance profile of **119** shows a maximum absorbance at 234 nm and minimal absorbance at 300 nm and above. Although only 1

lamp was used at 254 nm and 10 lamps were used at 300 and 350 nm, the reaction rates were similar due to **119** having a larger level of absorbance at 254 nm.

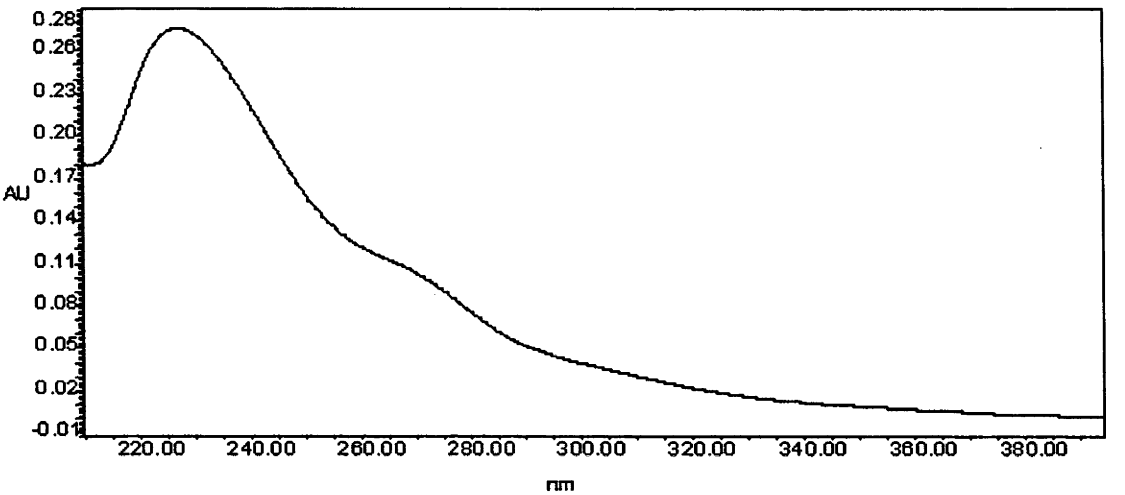

Figure 68. Absorbance Profile of *N*-Benzoylvalyl-2-nitrophenylalanine Methyl Ester **119**

The high yields obtained for the photolysis of **119** are significant when compared to those obtained by Henriksen *et al.*[53] for the photolysis of the Npg derivative **139** shown in Figure 69.

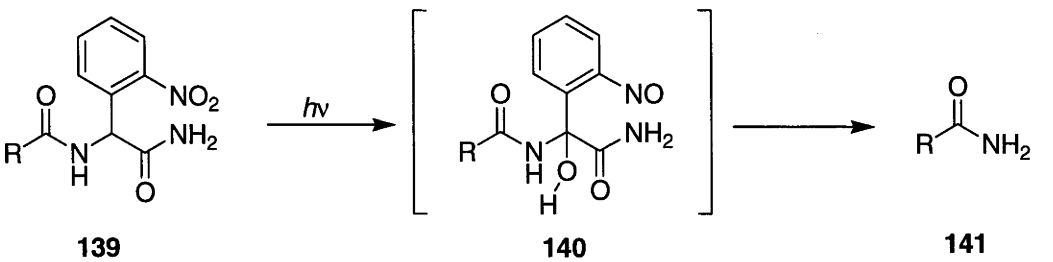

139 **140** **141**

Figure 69. Photolysis of a 2-Nitrophenylglycine Derivative, R = *N*-Benzoylalanyl.

The photolysis of the Npg **139** (Figure 69) was found to exhibit a large degree of pH dependence.[53] At pH 9.5, a quantitative yield of amide **141** was observed over two hours of photolysis, however at pH 7.4 only 30% of **141** was produced over the same time period. As 100% of the starting material was consumed over two hours in both experiments, the poor yield of amide at biological pH is most likely due to the slow hydrolysis of the α-hydroxy intermediate **140**. By contrast, the photolysis of **119** at pH 7.4 gave yields of the amide **73** in the region of 70-80% after 1 hour and up to 100% after 2 hours (Figure 67). Therefore the photolysis of the 2-nitrophenylalanine **119** was more efficient than that of the Npg **139** at biological pH, indicating that photocleavage of 2-nitrophenylalanine is more efficient that Npg under these conditions. This is presumably due to their being no formation of intermediates that are slow to break down at biological pH during the photolysis of the 2-nitrophenylalanine **119**.

In the Introduction, the use of photolysis to release biologically active molecules from inactive precursors in PDT and photoprobe research was discussed. It may be advantageous to such research if the rate of release of biologically active compounds from inactive precursors could be controlled through the manipulation of light intensity. In order to achieve such flexibility the rate of photochemical consumption of a biologically inactive precursor must be closely related to the release of the active form. In other terms, the rate determining step must be the initial photochemical step. This would require there to be no formation of intermediates during the photolysis of 2-nitrophenylalanine systems that have half-lives which are significantly longer than the rate of the initial photochemical step. In the Introduction, the mechanism of photolysis of Npg **41** was discussed with respect to the slow hydrolysis of the α-hydroxy intermediate **46** at biological pH (Figure 21). Therefore the rate of photolysis of Npg

systems at biological pH cannot be enhanced through manipulation of light intensity or wavelength as the rate determining step is hydrolytic rather than photochemical. Studies were therefore performed to investigate the extent to which the manipulation of light intensity and wavelength influences the rate of amide release in 2-nitrophenylalanine derivative photolysis. This was performed by monitoring the effect that doubling the number of lamps used to photolyse **119** at 254 and 300 nm has on the rate of release of the amide **73** (Figure 70 and 71).

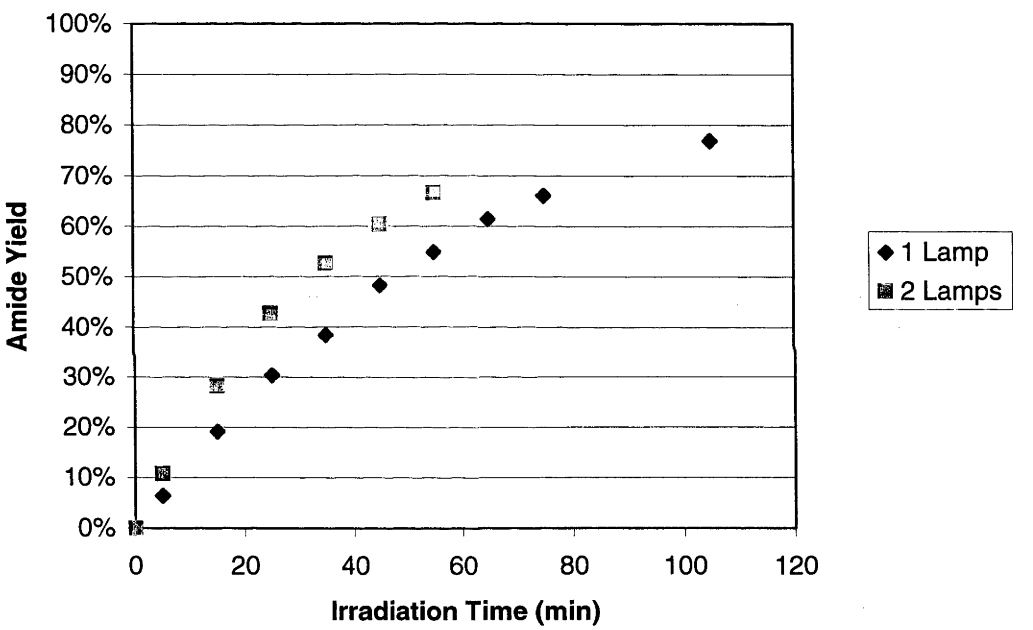

Figure 70. Release of Amide **73** Through Photolysis of **119** at 254 nm using 1 and 2 Lamps

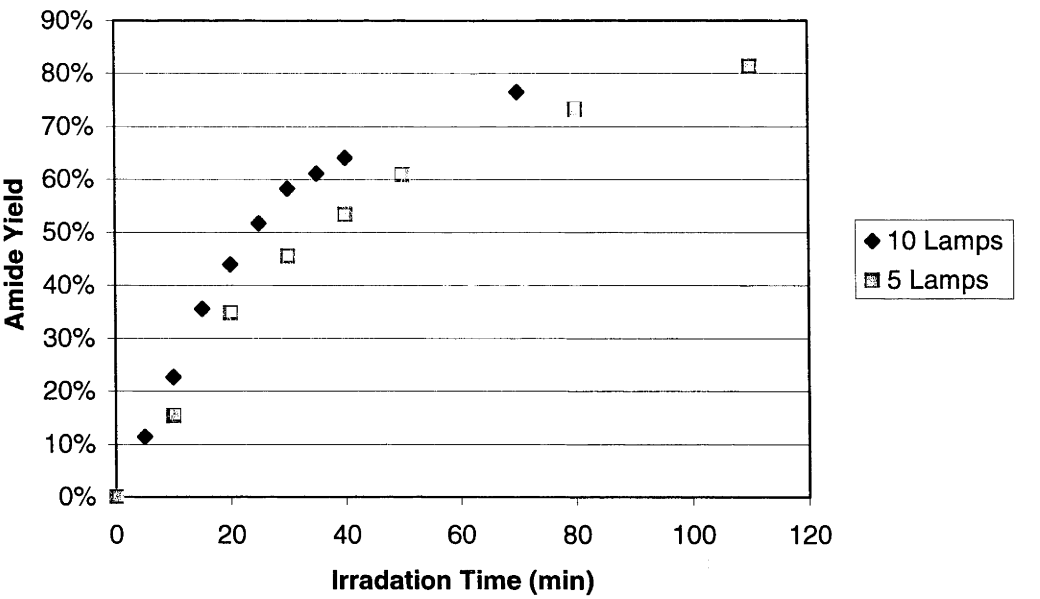

Figure 71. Release of Amide **73** Through Photolysis of **119** at 300 nm using 5 and 10 Lamps.

If the rate of amide production during 2-nitrophenylalanine photolysis is directly related to light intensity, a doubling of the number of lamps used would result in a two fold increase in the yield of **73** from **119** at any given time in the initial stages of the reaction. However, it is clear from the curves illustrated in Figures 70 and 71 that this was not the case. The photolysis of **119** at 254 nm using 1 lamp for 25 minutes gave a 30% yield of **73** whilst increasing the number of lamps used to 2 resulted in only a 42% yield of **73** over the same time period. Similarly, the photolysis of **119** at 300 nm using 5 lamps for 20 minutes gave a 35% yield of **73** whilst increasing the number of lamps to 10 resulted in only a 44% yield of **73** over the same time period. It was hypothesised that this discrepancy might be due to the formation of an intermediate during the photolysis of **119**, the rate of breakdown of which was of a similar order to that of starting material consumption. To further investigate this theory the rate of

consumption of **119** and production of amide **73** were compared at 254 nm using 1 and 2 lamps (Figure 72).

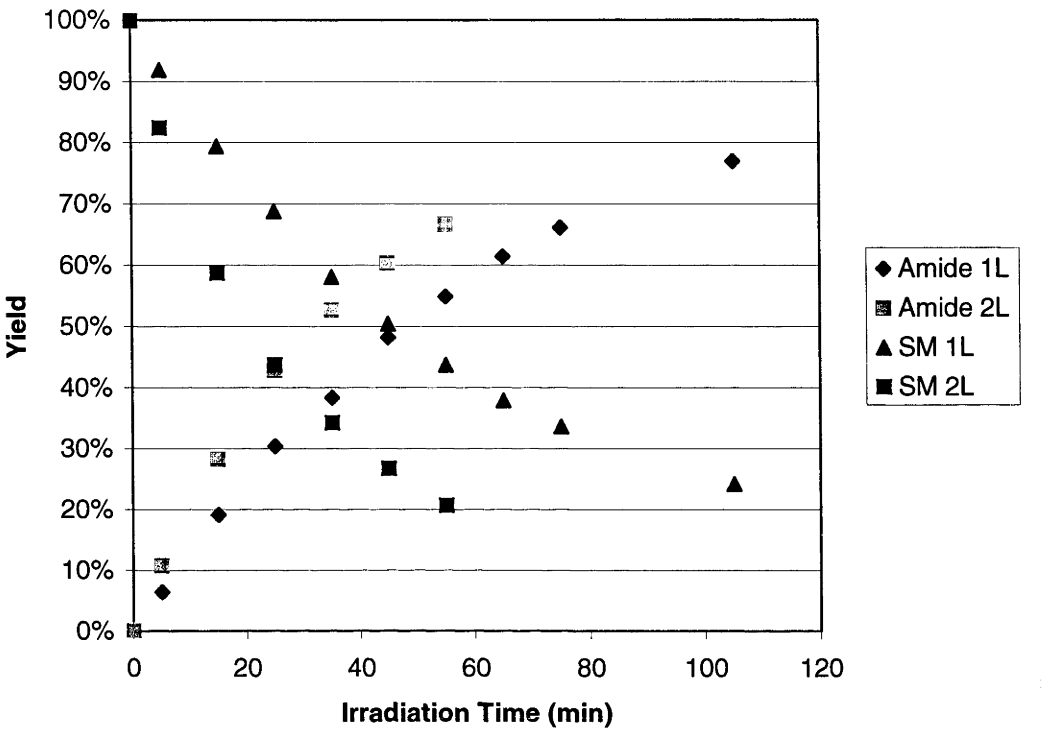

Figure 72. Consumption of **119** *vs* Amide **73** Production Through Irradiation at 254 nm using 1 and 2 Lamps. L = Lamp, SM = Starting Material

Through comparison of the curves in Figure 72, a discrepancy is observed between the rate of consumption of **119** and the respective rate of release of the amide **73**. After 15 minutes of irradiation, 20% and 40% of **119** was consumed using 1 lamp and 2 lamps, respectively. This indicated a ratio of 1:2 as expected if the rate of the loss of starting material during 2-nitrophenylalanine photolysis is directly related to the level of light intensity used. However, after 15 minutes of irradiation a 19% and 28% yield of the amide **73** was obtained using 1 and 2 lamps, respectively. This indicated a ratio of

1:1.5 as might be expected if the rate of amide release during 2-nitrophenylalanine photolysis is not directly related to the intensity of light used. Therefore although the rate of consumption of **119** appeared to be directly related to light intensity, the rate of amide **73** production was not. These results are consistent with the hypothesis that an intermediate is forming during the photolysis of **119** and that the rate of its breakdown is of a similar order to that of starting material consumption.

After photolysing **119** for 15 minutes at 254 nm using 1 lamp, a 19% yield of the amide **73** was observed, whilst 20% of **119** had been consumed (Figure 72). This essentially constitutes a complete mass balance, indicating that any intermediate formed during the photolysis of **119** had reacted to completion before analysis of the reaction was performed. After 15 minutes of photolysis of **119** with 2 lamps the mass balance was approximately 75%. If all the intermediate had been produced at t = 0, this would correspond to 2 half lives and so $t_{½}$ would be equal to 7.5 mintues. However, as intermediate is continually being produced during irradiation, the half life must be significantly <7.5 minutes. Further discussion of this intermediate with respect to its structure, and implications to the photolysis of 2-nitrophenylalanine systems, is provided later in the chapter.

In order to extend the series of 2-nitrophenylalanine systems studied, the photolysis of *N*-benzoyl-2-nitrophenylalanylalanine methyl ester **122** was performed. The reaction scheme for the photolysis of **122** is illustrated in Figure 73. The photolysis of **122** was expected to release benzamide **10** and the cinnamide **142**.

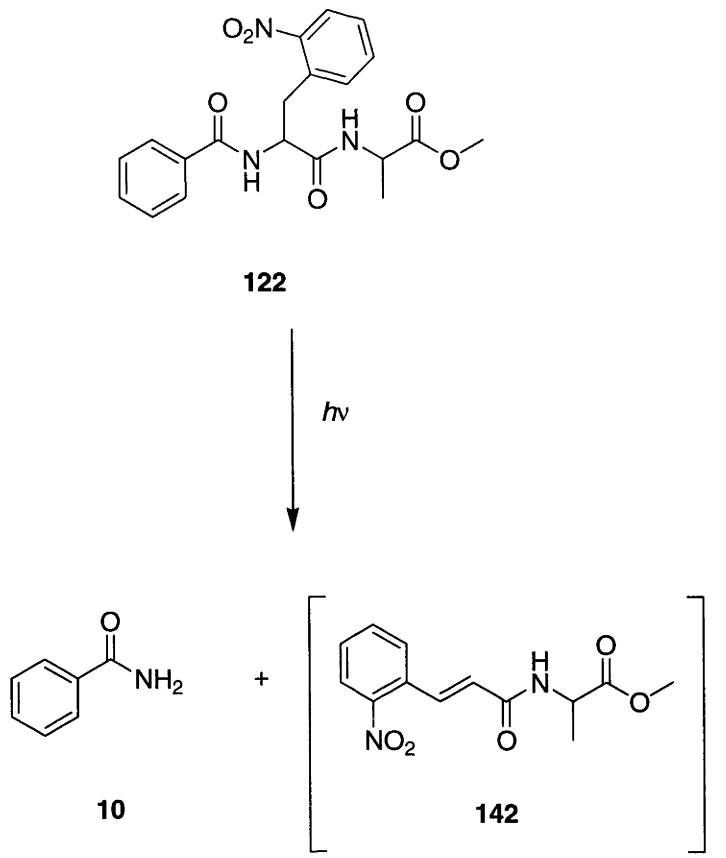

Figure 73. Reaction Scheme for the Photolysis of **122**.

The photolysis of **122** was performed using the conditions described above at 254 nm using 2 lamps. A UV-HPLC trace of the reaction solution after irradiation for 70 minutes along with that for 50 μM standard solutions of benzamide **10** and starting material **122** are provided in Figures 74, 75 and 76, respectively.

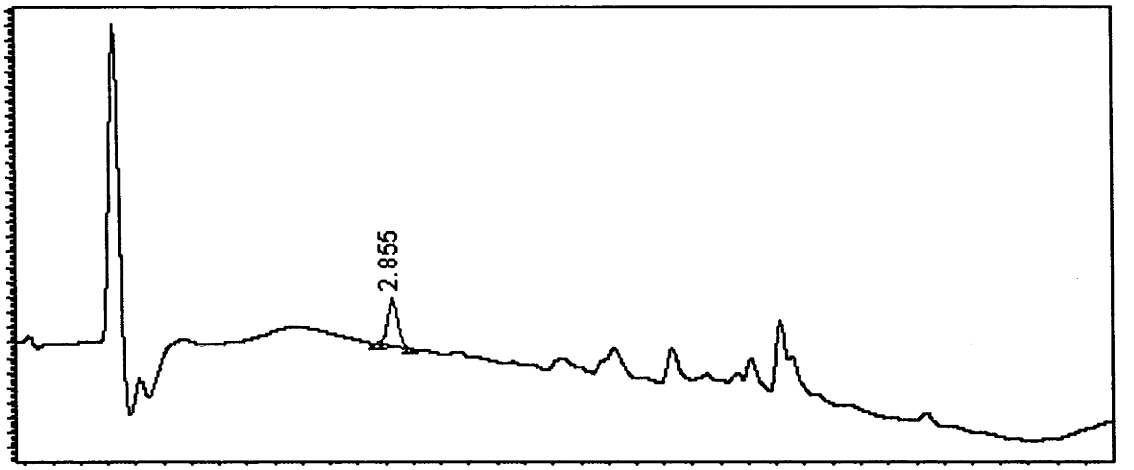

Figure 74. UV-HPLC Trace of a Solution of *N*-Benzoyl-2-nitrophenylalanylalanine Methyl Ester **122** after 70 Minutes of Irradiation at 254 nm using 2 Lamps.

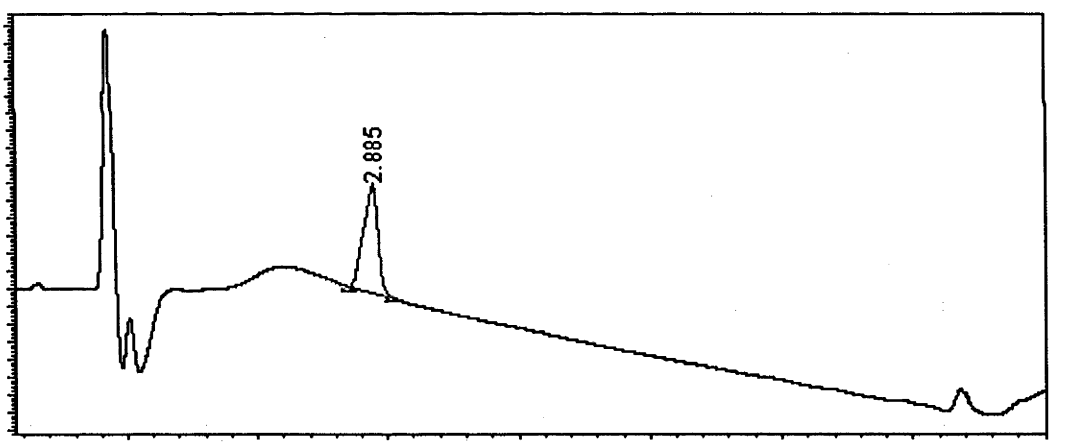

Figure 75. UV-HPLC Trace of a 50 μM Standard Solution of Benzamide **10**

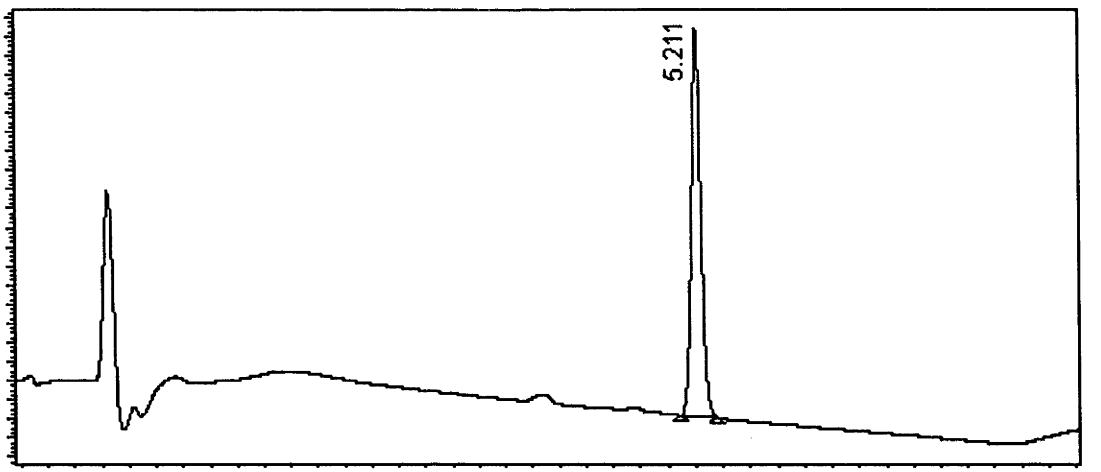

Figure 76. UV-HPLC Trace of a 50 μM Standard Solution of *N*-Benzoyl-2-nitrophenylalanylalanine Methyl Ester **122**

The peak at 2.89 minutes in Figure 74 was assigned to benzamide **10** through comparison with an authentic sample by the established method used to identify the *N*-benzoylvalinamide **73** peak at 3.67 minutes in Figure 64. It was therefore apparent that the photolysis of **122** to release the amide **10** at 254 nm using 2 lamps was successful and so further studies of this reaction were performed. Compound **122** was photolysed at 254, 300 and 350 nm using 2, 10 and 10 lamps, respectively, and the rate of release of the amide **10** was plotted (Figure 77).

The highest yield of the amide **10** through the photolysis of **122** was obtained at 300 nm with 10 lamps, reaching 38%. The rate of release of benzamide **10** from the photolysis of **122** as illustrated in Figure 77 increases in the order 350<254<300 nm. The UV-absorbance profile of **122** is provided in Figure 78. Although **122** is more absorbent at 254 nm than at 300 nm, the increased number of lamps used at 300 nm resulted in the rate of amide production being faster.

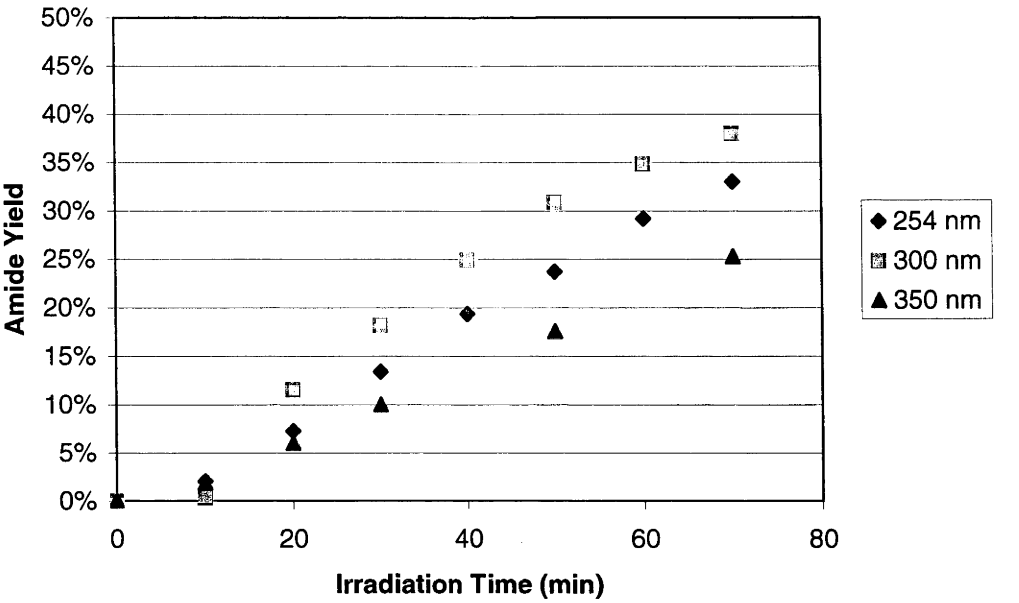

Figure 77. Release of Benzamide **10** Through the Photolysis of **122** at 254, 300 and 350 nm using 2, 10 and 10 Lamps, Respectively.

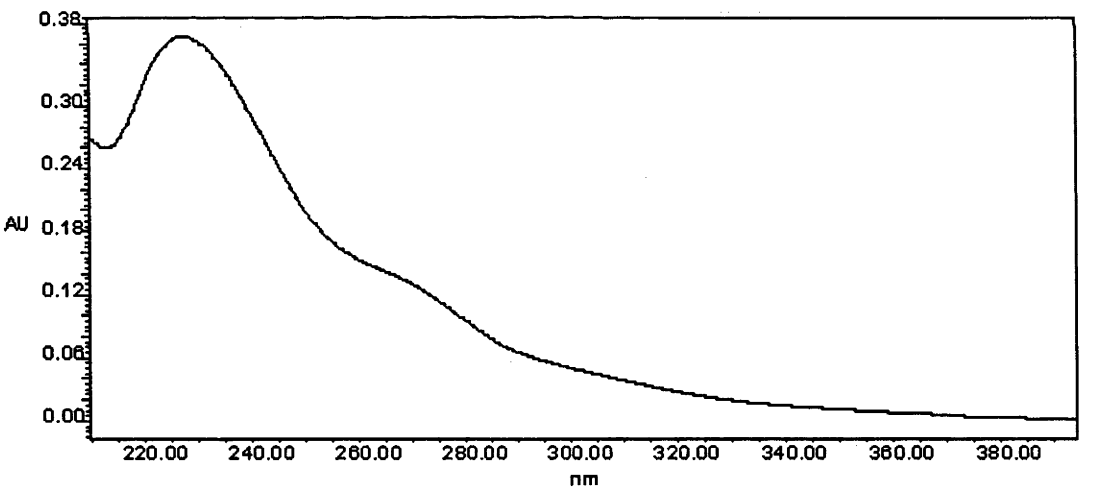

Figure 78. Absorbance Profile of *N*-Benzoyl-2-nitrophenylalanylalanine Methyl Ester **122**

As outlined above, the photolysis of **119** was believed to involve the formation of an intermediate, the breakdown of which was at a similar rate to that of starting material consumption. Through comparison of the plots for the photolysis of **122** and **119** in Figures 77 and 67, respectively, it can be seen that the rate of release of amide from **122** was slower. It therefore seemed likely that in the case of the photolysis of **122** the half-life of the intermediate formed might be longer. In order to test this hypothesis, the consumption of **122** and the release of **10** during photolysis at 254 and 350 nm using 2 and 10 lamps, respectively, was plotted (Figure 79). Only the experiments performed at 254 and 350 nm were selected for this study as the UV-HPLC traces obtained from these experiments were the cleanest at lower starting material yields, making integration of the starting material peak more reliable.

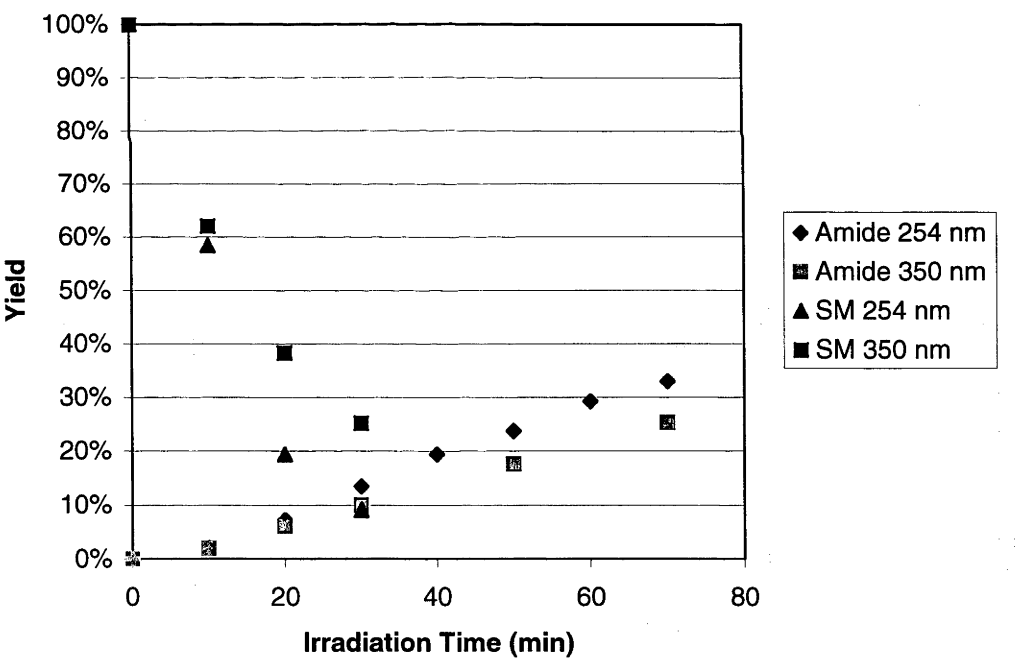

Figure 79. Release of the Amide **10** and the Consumption of **122** Through Photolysis at 254 and 350 nm using 2 and 10 Lamps Respectively.

After 20 minutes of photolysis of **122** at 254 nm, 80% of the starting material was consumed, however only a 7% yield of **10** was recorded (Figure 79). Similarly photolysis of **122** for 20 minutes at 350 nm resulted in 60% of the starting material having been consumed, however only a 6% yield of **10** was recorded. These results show that there is minimal relationship between the rate of starting material consumption during the photolysis of **122** and the rate of release of the amide **10**. It was therefore apparent that starting material consumption during the photolysis of **122** to release the amide **10** was not rate determing. It is clear from the data illustrated in Figure 79 that after 30 minutes when the consumption of **122** was almost complete, the yield of amide **10** continued to increase. These results are consistent with the slow breakdown of an intermediate during the photolysis of **122**. In order to test this hypothesis further, **122** was photolysed for 70 minutes at 300 nm using 10 lamps, after which the yield of amide **10** was continuously monitored by UV-HPLC (Figure 80). It was anticipated that if an intermediate was forming during the photolysis of **122** and its half-life was sufficiently long, the yield of amide **10** would continue to increase after irradiation had ceased.

Through continuous monitoring after the photolysis of **122** had ceased, an increase in the yield of amide **10** from 38% to approximately 53% was observed (Figure 80). This result indicates that the photolysis of **122** can be used to release benzamide **10** in satisfactory yield. The monitoring of the release of the amide **10**, after irradiation had ceased, began at approximately 38% yield, increasing by 14% to level out at approximately 52%. The half-life for the breakdown of the intermediate formed during the photolysis of **122** was calculated as the time required for the yield of amide to increase by 7% which was 1 hour. Therefore the half-life of the intermediate formed

during the photolysis reaction of **122** was at least an order of magnitude longer than for the intermediate formed from the irradiation of **119** which was <7.5 minutes. An hypothesis as to why the intermediates formed during the photolysis of **119** and **122** possess different half-lives and the consequences of this to the photolysis of 2-nitrophenylalanine systems will be provided later in this Chapter.

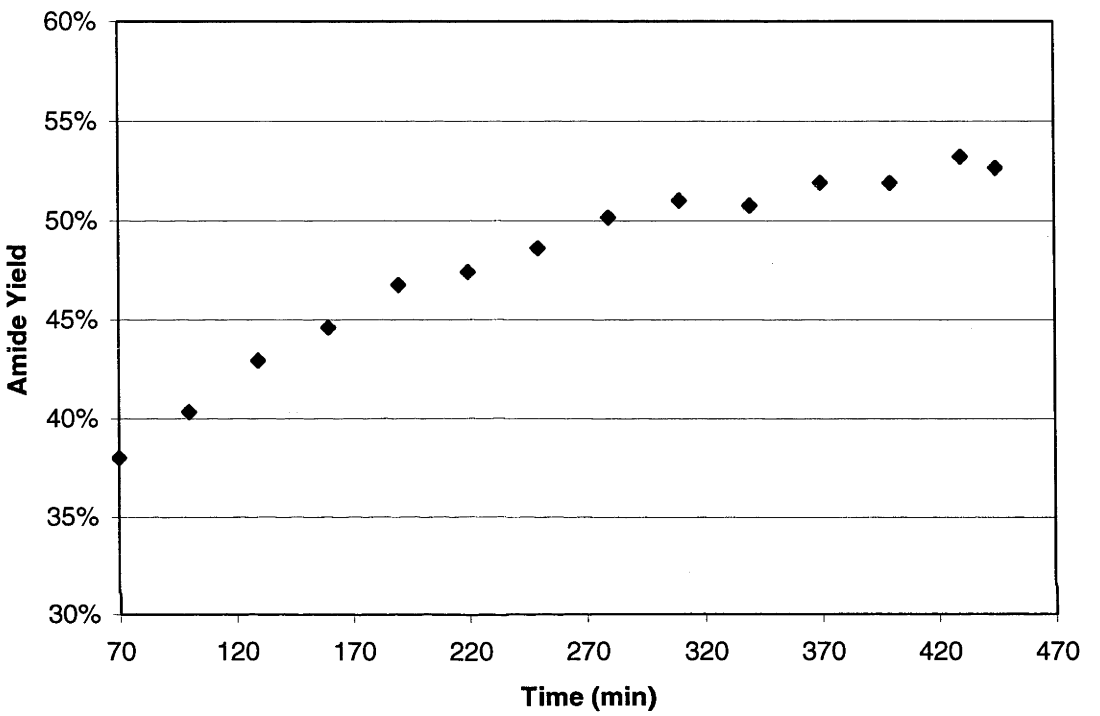

Figure 80. Release of the Amide **10** After the Photolysis of **122** at 300 nm using 10 Lamps had Ceased.

Through continuous monitoring after the photolysis of **122** had ceased, an increase in the yield of amide **10** from 38% to approximately 53% was observed (Figure 80). This result indicates that the photolysis of **122** can be used to release benzamide **10** in satisfactory yield. The monitoring of the release of the amide **10**, after irradiation had ceased, began at approximately 38% yield, increasing by 14% to level out at

approximately 52%. The half-life for the breakdown of the intermediate formed during the photolysis of **122** was calculated as the time required for the yield of amide to increase by 7% which was 1 hour. Therefore the half-life of the intermediate formed during the photolysis reaction of **122** was at least an order of magnitude longer than for the intermediate formed from the irradiation of **119** which was <7.5 minutes. An hypothesis as to why the intermediates formed during the photolysis of **119** and **122** possess different half-lives and the consequences of this to the photolysis of 2-nitrophenylalanine systems will be provided later in this Chapter.

The photolysis of *N*-benzoylvalyl-2-nitrophenylalanylalanine methyl ester **129** was also studied. The reaction scheme for the photolysis of **129** is illustrated in Figure 81.

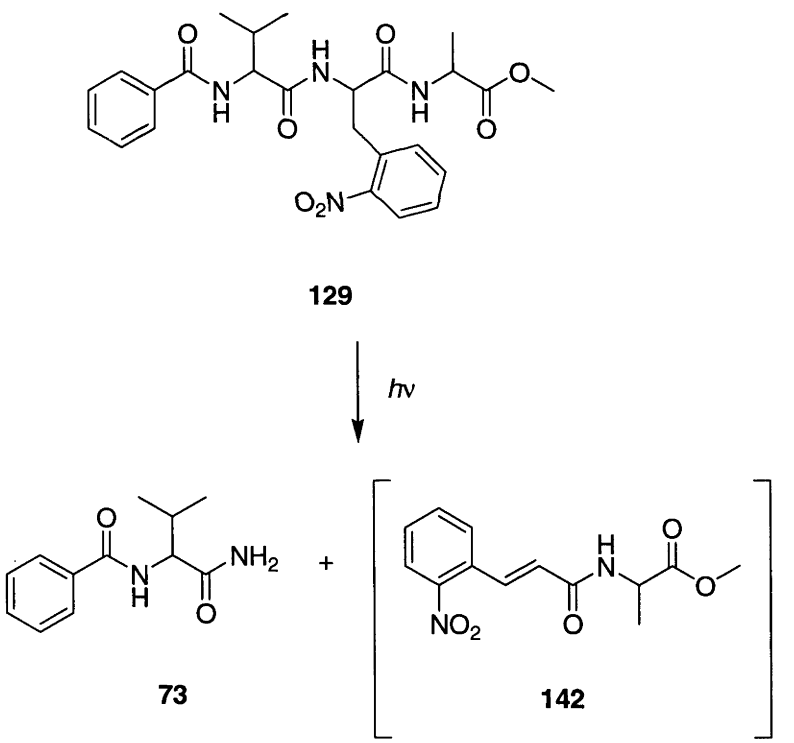

Figure 81. Reaction Scheme for the Photolysis of **129**

The photolysis of **129** was expected to give *N*-benzoylvalinamide **73** and the cinnamide **142**. The photolysis of **129** was to be used as a comparison to that of **119** and **122**.

This was because the photolysis of **129** would release **73** (as observed with **119**) and the cinnamide **142** (as expected with **122**). In this way it was reasoned that potential causes of the differences observed between the reactions of **119** and **122** might be elucidated.

The photolysis of **129** was performed using the conditions described above at 254 nm using 2 lamps. A UV-HPLC trace of the reaction solution after 105 minutes of irradiation along with that for a 50 μM standard solution of the starting material **129** are provided in Figures 82 and 83, respectively. For comparison, the UV-HPLC trace of a 50 μM standard solution of *N*-benzoylvalinamide **73** is provided above in Figure 65. The photolysis of **129** resulted in a peak at 3.67 minutes which was attributed to *N*-benzoylvalinamide **73** through comparison to an authentic sample by means of the standard procedure outlined above. It was therefore apparent that the photolysis of **129** to release **73** at 254 nm using 2 lamps was successful and as a result further studies of this reaction were performed.

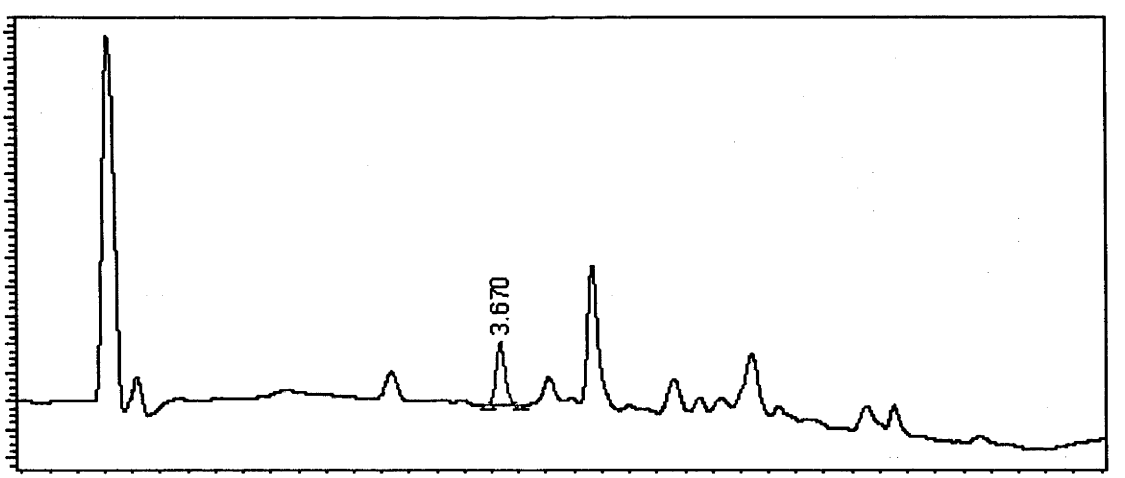

Figure 82. UV-HPLC Trace of a Solution of *N*-Benzoylvalyl-2-nitrophenylalanylalanine Methyl Ester **129** after 105 Minutes of Irradiation at 254 nm using 2 Lamps

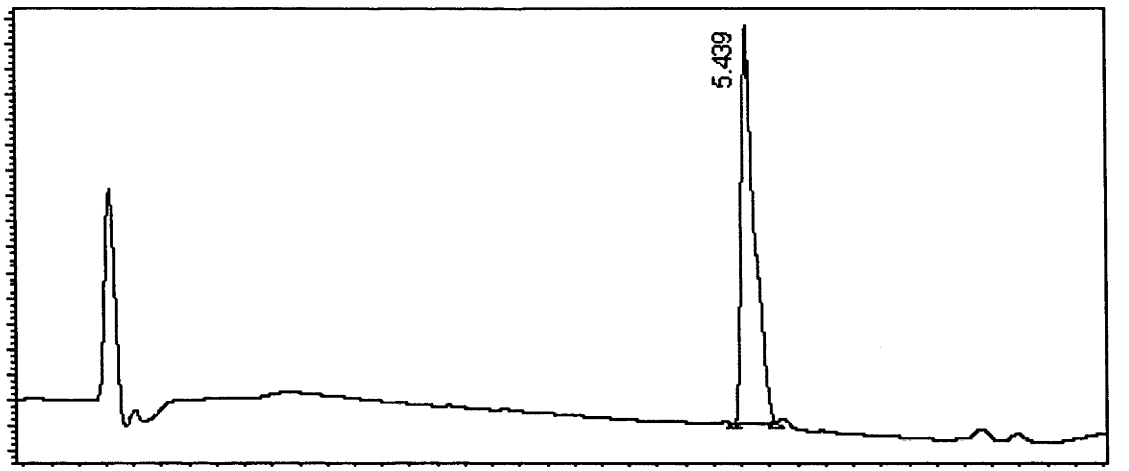

Figure 83. UV-HPLC Trace of a 50 μM Standard Solution of *N*-Benzoylvalyl-2-nitrophenylalanylalanine Methyl Ester **129**

The photolysis of **129** at 254, 300 and 350 nm using 2, 10 and 10 lamps, respectively, was then monitored by UV-HPLC and the release of amide **73** plotted with respect to time (Figure 84).

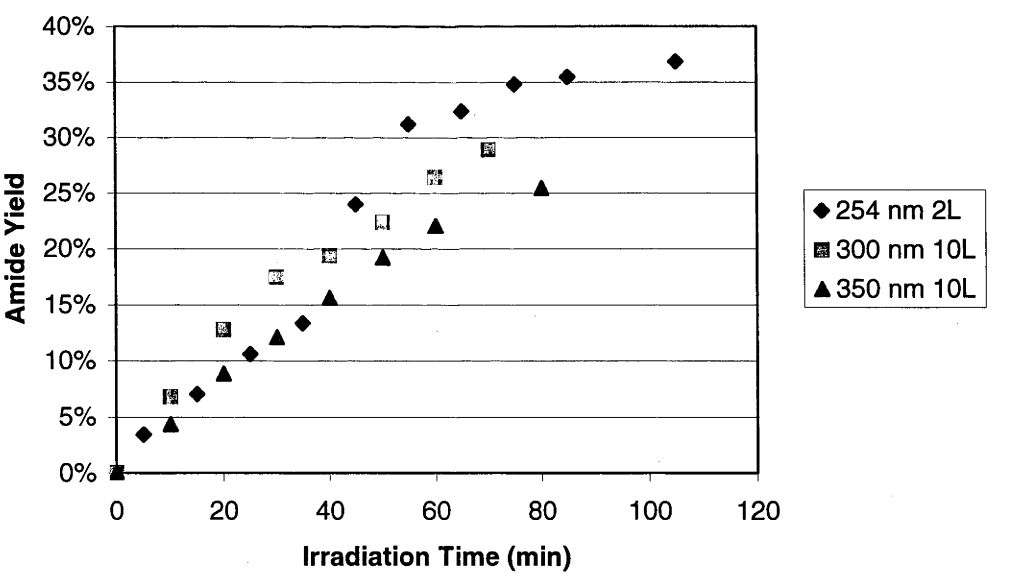

Figure 84. Release of the Amide **73** Through the Photolysis of **129** at 254, 300 and 350 nm, L = Number of Lamps

The highest yield of amide **73** obtained through the irradiation of **129** was at 254 nm after 110 minutes, reaching 37% (Figure 84). Through comparison of the plots for the release of **73** from **119** and **129** in Figures 67 and 71, respectively, it is apparent that the rate of release of amide **73** from the photolysis of **129** at 254, 300 and 350 nm was slower. It was hypothesised that the slower rate of amide release was due to a reaction intermediate being formed that possessed a similar half-life to that observed during the irradiation of **122**. The tripeptide **129** was therefore photolysed at 300 nm using 10 lamps for 20 minutes after which the yield of amide **73** was continuously monitored by UV-HPLC and plotted (Figure 85).

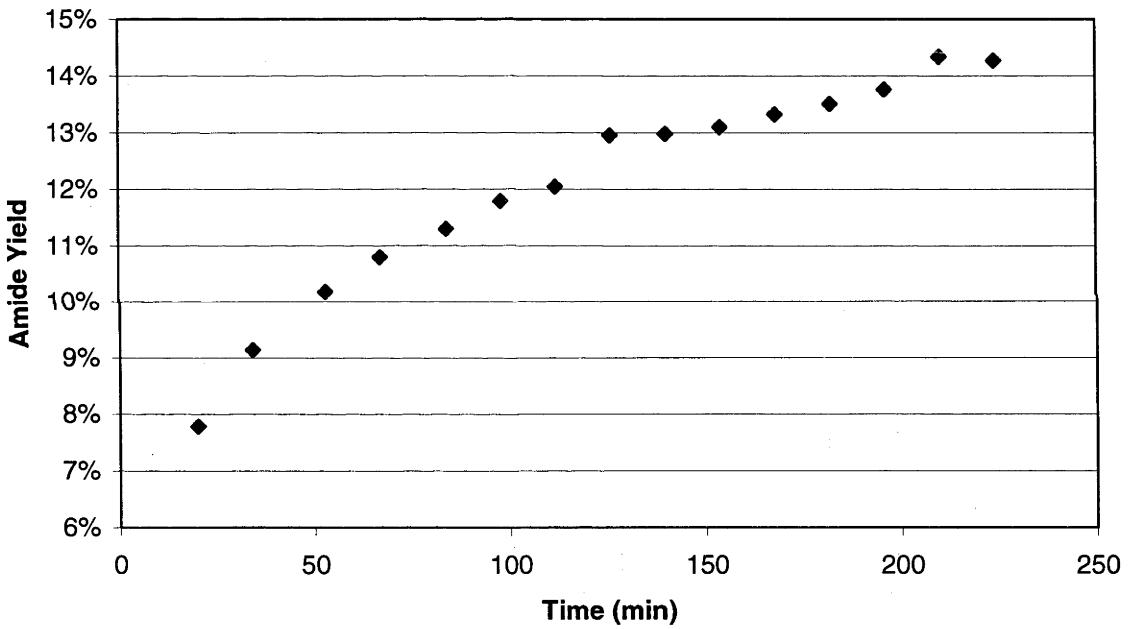

Figure 85. Release of Amide **73** After the Photolysis of **129** at 300 nm for 20 minutes had Ceased.

The yield of amide **73** was observed to increase by 6% from 8% to 14% after photolysis of the tripeptide **129** at 300 nm for 20 minutes had ceased (Figure 85). The half-life of the intermediate was calculated as the time required for the yield of amide

to increase to 11% which was 1 hour. Therefore the half-life for the intermediate formed during the photolysis of **129** is similar to that observed for the intermediate formed during the irradiation of **122**.

By analogy to the mechanism of 2-nitrophenylalanine photolysis illustrated in Figure 62, a hypothesis was formed that the intermediates observed to build up in concentration during the irradiation of **119**, **122** and **129** were the respective *aci*-nitro systems **143**, **144** and **145**, respectively (Figure 86).

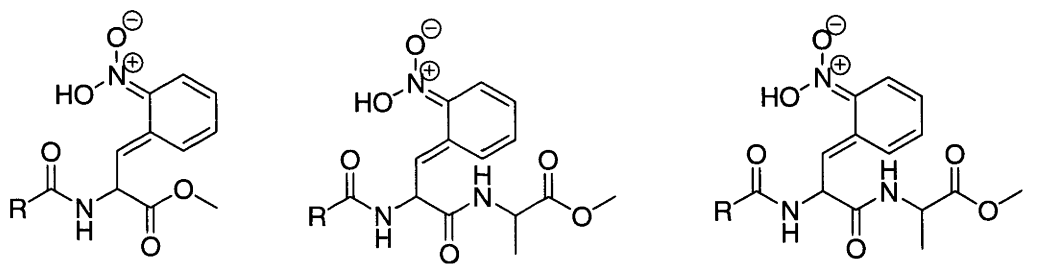

143 R = *N*-Benzoylvalyl **144** R = Phenyl **145** R = *N*-Benzoylvalyl

Figure 86. *aci*-Nitro Intermediates **143**, **144** and **145** Hypothesised to Form During the Photolysis of **119**, **122** and **129** Respectively

Intermediates such as **143**, **144** and **145** would also be resonance stabilised. Figure 87 illustrates how the *aci*-nitro intermediate **136**, proposed to form as part of the mechanism of photolysis of the 2-nitrophenylalanine **56** (Figure 62), could be resonance stabilised through extensive delocalisation of the charges on the nitro group through the aromatic ring to the benzylic carbon. Due to this delocalisation of charge it would not be surprising if the *aci*-nitro systems **143**, **144** and **145** were found to be stable enough to be the intermediates observed during the photolysis reactions of **119**, **122** and **129**, respectively.

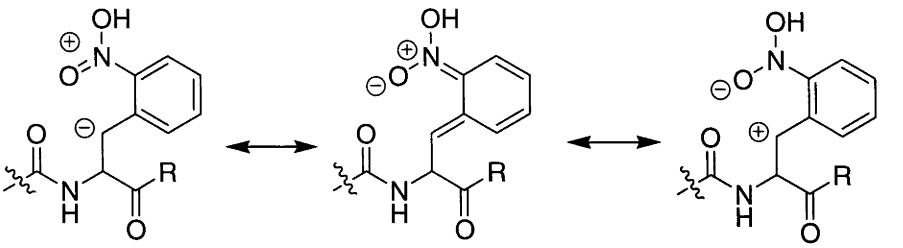

146 136 147

Figure 87. Resonance Forms for the *aci*-Nitro Intermediate **136**, R = NH_2, NHR', OH, OR'.

Investigations into the mechanism of photolysis of the NPEOC **31** (Figure 18) performed by Walbert *et al.*[49] found that an alternative product of the reaction was the benzylic alcohol. The mechanism of this proposed step as applied to 2-nitrophenylalanine photolysis is illustrated in Figure 88.

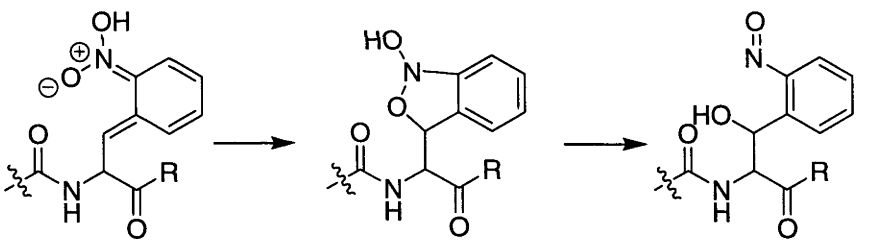

136 148 149

Figure 88. Alternative Pathway for the Breakdown of the *aci*-Nitro Intermediate **136**.

The nitro oxy-anion of **136** attacks the benzylic carbon to give the bicyclic species **148** *via* a 5-*endo-trigonal* ring closure. However, on formation of the benzylic alcohol **149** the mechanism cannot proceed towards amide release. This intermediate **149** may still

be photoactive due to the presence of the nitroso functional group and may degrade *via* further photochemical pathways not yet elucidated. Therefore the intermediate **136** may constitute a point of partition in the mechanism of 2-nitrophenylalanine photolysis in that it can either proceed to form a benzylic alcohol **149** or cleave to release the amide **47**. As amides are poor leaving groups and the mechanism of photolysis of the NPEOC **31** released the anion **36**, amide release during 2-nitrophenylalanine photolysis could reasonably be considered surprising in light of there being an alternative reaction pathway. However, as 5-*endo-trigonal* ring closures are disfavoured processes,[48] it appears that amide release is able to out-compete this during 2-nitrophenylalanine photolysis.

The photolysis of **119** released the amide **73** in high yield and the half-life of the intermediate formed during the reaction was <7.5 minutes. The photolysis reactions of **122** and **129** released the amides **10** and **73** respectively in lower yields and the half-lives of the intermediates formed during their reactions were approximately 1 hour. It was therefore apparent that the slower the rate of breakdown of the intermediate formed during the photolysis of a 2-nitrophenylalanine system, the less efficient the reaction may be with respect to amide release. It may be that the longer half-lives of the proposed intermediates **144** and **145** formed during the photolysis of **122** and **129**, respectively, may result in the disfavoured 5-*endo-trigonal* ring closure having more time to occur, thus lowering the yield of amide from these reactions in comparison to that of **119**.

The differences in the half-lives of the *aci*-nitro intermediates **143**, **144**, and **145** proposed to form during the photolysis of **119**, **122** and **129**, respectively, may be

related to differences in the stabilities of the products released during their reactions. The photolysis of the dipeptide **119** and the tripeptide **129** released the amide **73** in different yields and at different rates. It was therefore considered unlikely that the stabilities of amide fragments released during 2-nitrophenylalanine photolysis would be responsible for differences in intermediate half-lives. Although no evidence for the formation of 2-nitrocinnamyl products from the photolysis reactions of **119**, **122** and **129** was observed, it is reasonable to expect that they were produced as part of the final cleavage step in accordance with the mechanism of 2-nitrophenylalanine photolysis illustrated in Figure 62. The stabilities of the cinnamate **138** and the cinnamide **142** were therefore considered. The peptides **122** and **129** possess an amide at the equivalent position to the ester of **119**. This results in the photolysis of **122** and **129** producing the proposed cinnamide **142**, whereas the irradiation of **119** would produce the proposed cinnamate **138**. It was therefore hypothesised that the formation of cinnamides might be less favoured as products of 2-nitrophenylalanine photolysis than cinnamates. This implied that the nature of the carbonyl group of 2-nitrophenylalanine (either being an ester or an amide) may have a large effect on the success of its photolysis. Therefore, the effect of variations of this group on 2-nitrophenylalanine photolysis was studied.

A reaction scheme for the photolysis of **128** is illustrated in Figure 89. The photolysis of **128** would release *N*-benzoylvalinamide **73** which was also a product of the irradiation of the dipeptide **119.** The two systems **128** and **119** vary in that the proposed nitro fragments released from their photolysis are 2-nitrostyrene **35** and methyl 2-nitrocinnamate **138** respectively. The peptide **119** possesses a methyl ester and **128** does not possess an equivalent carbonyl group. Therefore, studies of the

photolysis of **128** would allow for further insight into the importance of the carbonyl group of 2-nitrophenylalanine to its photolysis.

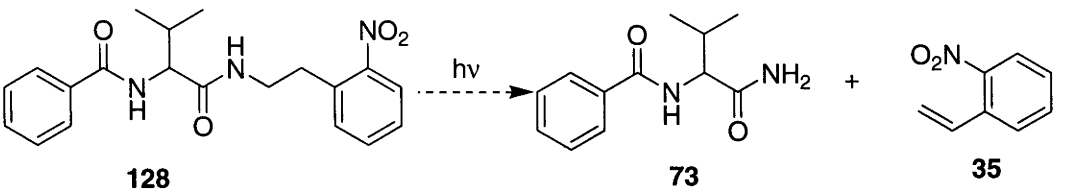

128 **73** **35**

Figure 89. Proposed Reaction Scheme for the Photolysis of *N*-2-(Nitrophenylethyl)-N^{α}-benzoylvalinamide **128**.

A solution of *N*-2-(Nitrophenylethyl)-N^{α}-benzoylvalinamide **128** was irradiated at 300 nm for 20 minutes using 10 lamps and the reaction was analysed by UV-HPLC. Analysis of the reaction mixture, whilst showing complete loss of starting material, provided no evidence for the formation of the amide **73**. It was hypothesised that this result may have been due to the formation of an *aci*-nitro intermediate with a half-life much longer than previously observed during 2-nitrophenylalanine photolysis. The solution was therefore allowed to stand overnight and then analysed by UV-HPLC to test this theory. No evidence for the formation of **73** was observed proving the photolysis of **128** to have been unsuccessful. These results indicated that the carbonyl group of 2-nitrophenylalanine derivatives is critical to the success of their photolysis. It seems likely that the formation of styrene is disfavoured in comparison to cinnamate or cinnamide release. The cinnamyl derivatives **138** and **142** are stabilised through the conjugation of the π electrons of their carbonyl groups to their aromatic rings. As **119** photolysed more efficiently than **122** and **129**, this effect may be more pronounced with cinnamates than cinnamides.

To further investigate the importance of the carbonyl group of 2-nitrophenylalanine derivatives to their photolysis, the reaction of the free acid **123** was studied. The proposed reaction scheme for the photolysis of **123** is illustrated in Figure 90. The photolysis of **123** would produce *N*-benzoylvalinamide **73**, as was observed from the photolysis of **119**, and the cinnamic acid **150** rather than the methyl cinnamate **138** would be the nitro fragment released. Comparisons between the photolysis of **123** and **119** would therefore provide further insight into the contribution that the carbonyl group of 2-nitrophenylalanine makes to photolysis efficiency.

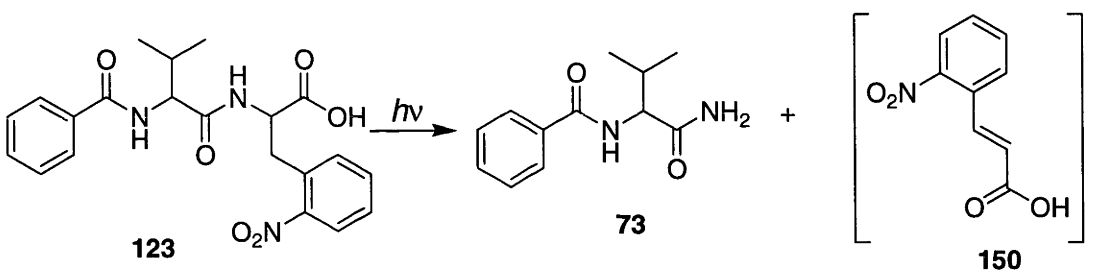

Figure 90. Proposed Reaction Scheme for the Photolysis of *N*-Benzoylvalyl-2-nitrophenylalanine **123**.

A solution of **123** was irradiated at 300 nm with 10 lamps for 20 minutes and analysed by UV-HPLC. The trace obtained revealed the complete loss of starting material, but only a 5% yield of **73**. The solution was allowed to stand overnight and then analysed by UV-HPLC, which showed a negligible increase in the yield of amide **73**. These results contrast with the efficiency of photolysis of the analogous methyl ester **119** at 300 nm using 10 lamps, which resulted in an 80% yield of amide **73** (Figure 67). In order to establish that this result was not attributable to some form of contaminant or other influence absent in previous experiments, a solution containing 25 μM concentrations of **123** and **119** was photolysed at 300 nm for 20 minutes. The UV-

HPLC trace of the reaction solution showed a 40% yield of the amide **73**. Therefore the photolysis of **123** to give the amide **73** was not unsuccessful due to contamination.

It may be possible to explain the different yields of the amide **73** obtained through the photolysis of **123** and **119** by consideration of their reaction mechanisms and a possible alternative pathway for the free acid **123** not possible for the methyl ester **119** (Figure 91).

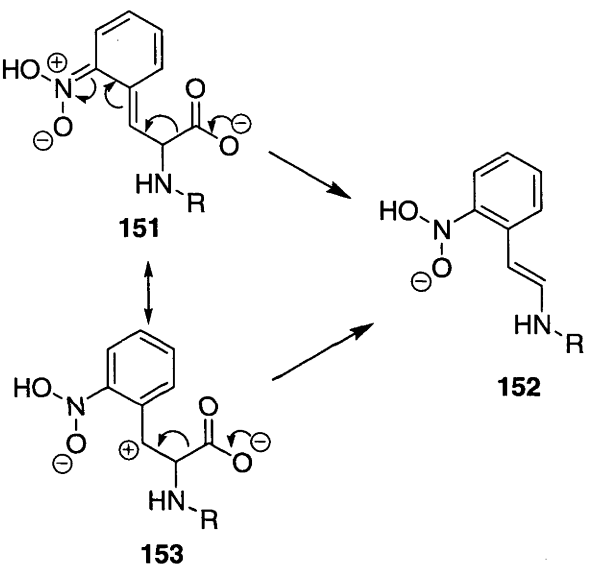

Figure 91. Potential Decarboxylation Pathways for Reaction of the *aci*-Nitro Intermediate **151** Proposed to Form During the Photolysis of **123**, R = *N*-Benzoylvalyl.

Figure 91 illustrates the *aci*-nitro intermediate **151** and its benzylic cation resonance contributor **153** proposed to form during the photolysis of **123**. At pH 7.4 carboxylic acids are deprotonated, forming the corresponding carboxylate anions. It is likely that

the compound represented by the resonance structures **151** and **153** undergoes decarboxylation as illustrated in Figure 91. The new product **152** is then unable to release the amide **73**. However, it would still be photoactive due to the presence of the nitro group and could possibly undergo further photochemical degradation. This may explain the absence of any evidence for the formation of compound **152** in the UV-HPLC trace obtained from the reaction solution. These results indicate that the use of 2-nitrophenylalanine free acids, to potentially increase water solubility, is not viable.

One of the aims of the development of 2-nitrophenylalanine as a photocleavable amino acid was that it would be efficiently photolysed under biological conditions. The use of 2-nitrophenylalanine as a photocleavable amino acid in biologically related experiments may ultimately require it to be photolysed efficiently at wavelengths above 300 nm. Analysis of the absorbance profiles of **119** and **122** (Figures 68 and 78) shows that the 2-nitrophenylalanine chromophore has minimal absorbance above 300 nm. It was believed that enhancing the absorbance of the 2-nitrophenylalanine chromophore above 300 nm may allow for faster photolysis at wavelengths more amenable to use in biological experiments. It has been established that the methoxy substituents of the NVOC group enhance its rate of photolysis at 350 nm in comparison to that of NBOC.[83] Therefore the dimethoxy substituted 2-nitrophenylalanine dipeptide **133** was designed (Figure 92). The photolysis of **119** was efficient and high yielding and so the dimethoxy system **133** was designed to be analogous. The dimethoxy system **133** and the anticipated products of its photolysis **73** and **154** are illustrated in Figure 92.

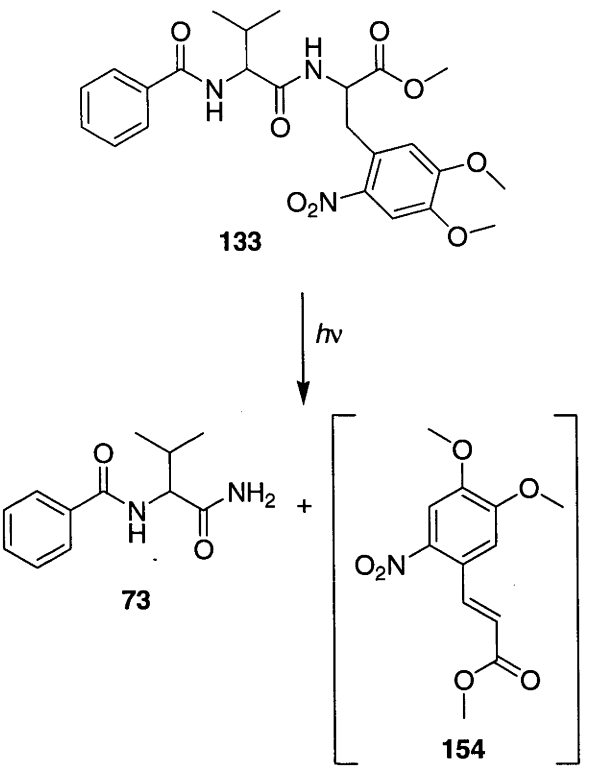

Figure 92. Reaction Scheme for the Photolysis of **133**

The photolysis of **133** was performed at 254, 300 and 350 nm. Initial studies at 254 nm using 2 lamps showed that the consumption of starting material was too slow for analysis with only 18% of the starting material **133** being consumed after 40 minutes of irradiation. Thus 4 lamps were used at this wavelength to allow for a reasonable analysis time frame. Other reaction conditions were identical to previous studies. The release of the amide **73** at the three different wavelengths along with the consumption of starting material **133** during photolysis was then plotted (Figures 93, 94 and 95).

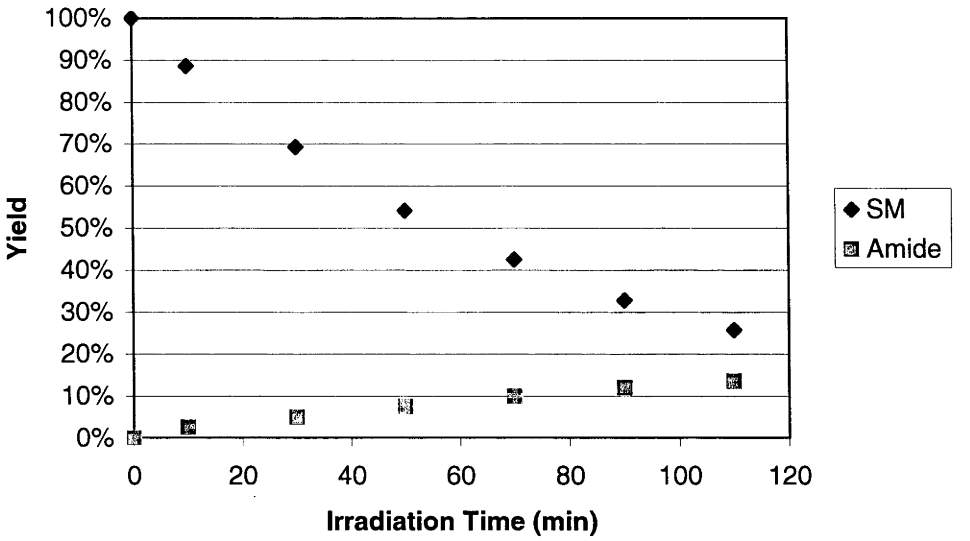

Figure 93. Photolysis of *N*-Benzoylvalyl-2-nitro-4,5-dimethoxyphenylalanine Methyl Ester **133** to give the Amide **73** at 254 nm using 4 Lamps, SM = Starting Material

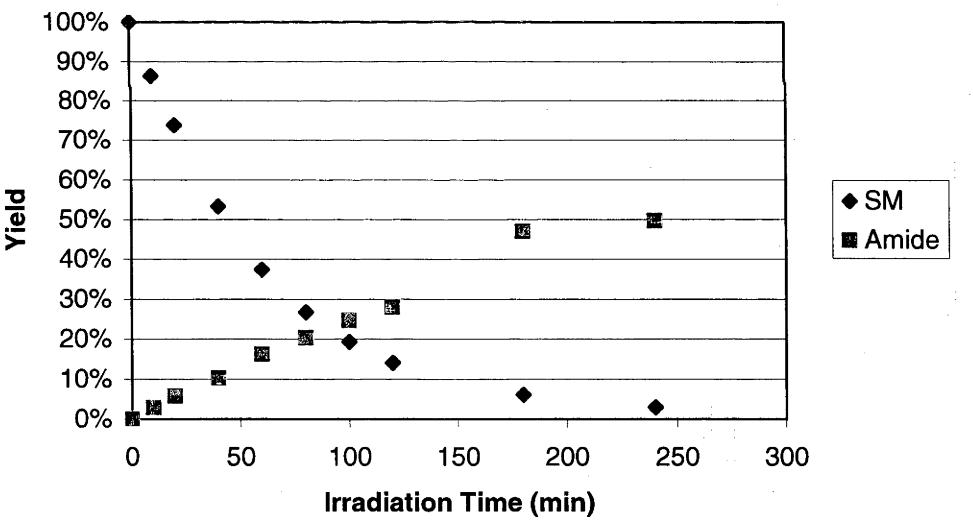

Figure 94. Photolysis of *N*-Benzoylvalyl-2-nitro-4,5-dimethoxyphenylalanine Methyl Ester **133** to give the Amide **73** at 300 nm using 10 Lamps, SM = Starting Material

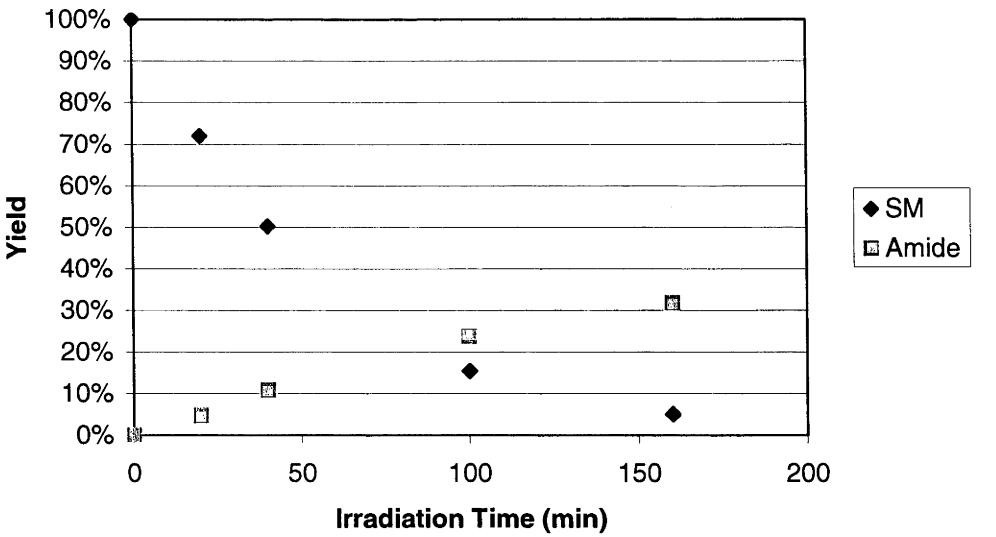

Figure 95. Photolysis of *N*-Benzoylvalyl-2-nitro-4,5-dimethoxyphenylalanine Methyl Ester **133** to give the Amide **73** at 350 nm using 10 Lamps, SM = Starting Material

The highest yield of the amide **73** obtained through the photolysis of **133** was observed after irradiation at 300 nm using 10 lamps (Figure 94) and was 50%. The yields of the amide **73** obtained through the photolysis of **133** at 254, 300 and 350 nm of 12, 50 and 32%, respectively, contrast significantly with those observed from the photolysis of the analogous dipeptide **119** which was at least 80% (Figure 67). The rate of starting material consumption illustrated in Figures 93, 94 and 95 is much faster than that of amide release. This indicated that starting material consumption was again not the rate determining step. The amide yields obtained from the reaction of **133** are comparable to those obtained for the photolysis of **122** and **129**. It was therefore hypothesised that the low yields of amide produced through the photolysis of **133** could be related to a long-lived reaction intermediate forming during photolysis as was observed for the reactions of **122** and **129**. In order to investigate this hypothesis, a new experiment was

performed where **133** was photolysed at 300 nm for 240 minutes, after which the release of the amide **73** was monitored continuously by UV-HPLC (Figure 96).

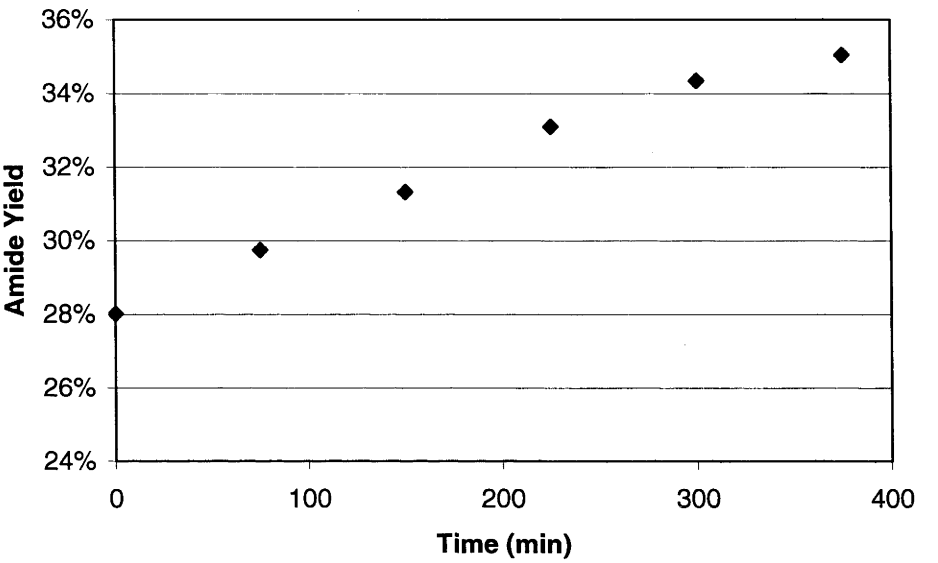

Figure 96. Release of Amide **73** after 240 minutes of Irradiation of **133** at 300 nm using 10 Lamps had Ceased.

The yield of the amide **73**, after irradiation of **133** had ceased, was observed to increase by 7% over six hours of continuous reaction monitoring (Figure 96). This indicated a half-life for the intermediate formed during the photolysis of **133** of at least 3 hours, which is significantly longer than that observed for the analogous **119**. These results are therefore consistent with the theory that extended intermediate half-lives result in lower amide yields from 2-nitrophenylalanine photolysis.

The intention of investigations into the photolysis of **133** was to determine whether the use of methoxy ring substituents on 2-nitrophenylalanine could enhance its rate of photolysis at wavelengths higher than 300 nm. A comparison of the rates of starting

material consumption during the photolysis of **119** and **133** at 350 nm using 10 lamps found that this was not the case (Figure 97).

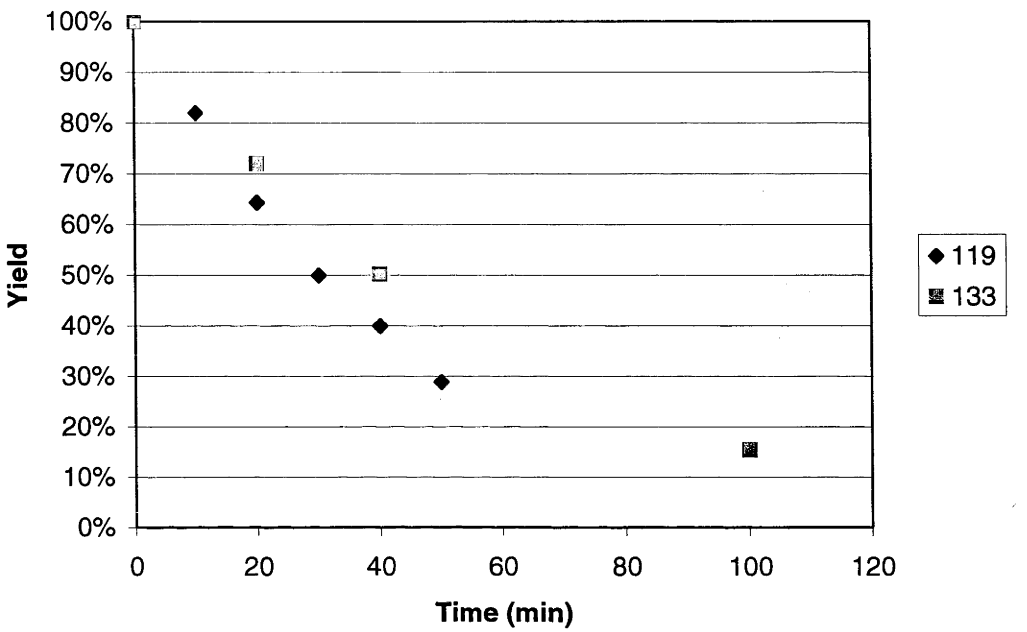

Figure 97. Starting Material Consumption for the Photolysis of **119** and **133** at 350 nm, using 10 Lamps.

It is apparent from Figure 97 that the rate of starting material consumption for the photolysis of **119** and **133** at 350 nm using 10 lamps is essentially the same. Indeed the consumption of **119** could be considered to be proceeding at a slightly faster rate. Comparison of the UV absorbance profile of **133** (Figure 98) to that of **119** (Figure 68) shows that the methoxy substituents of **133** enhanced its absorbance at 350 nm in relation to **119**. Therefore, the rates of starting material consumption for the photolysis of **119** and **133** at 350 nm appear to be in contradiction with those predictable from the

respective UV absorbance profiles. This decrease in the rate of starting material consumption might be due to the ability of methoxy-aromatic systems to fluoresce.

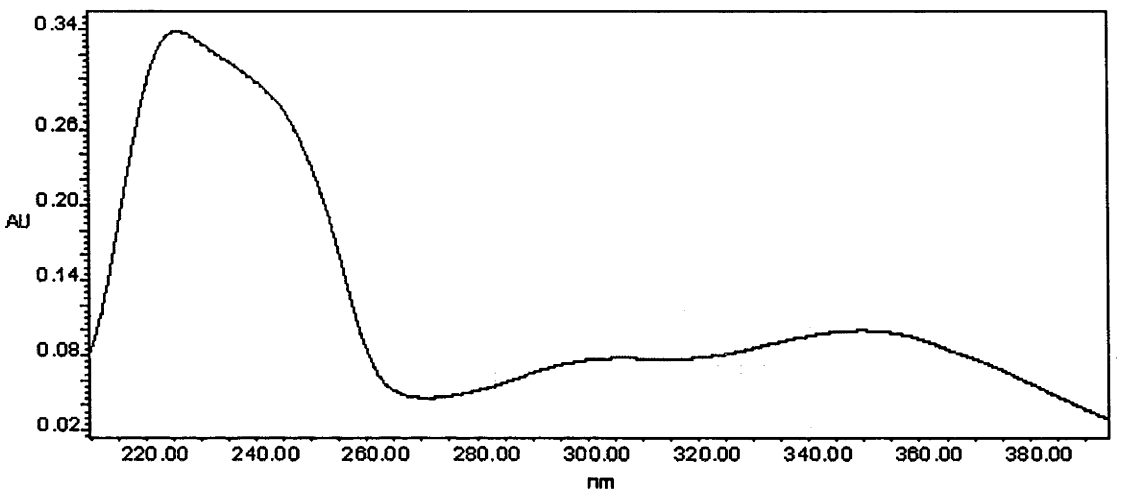

Figure 98. UV-absorbance Profile of **133**

The mechanism of NPEOC protecting group photolysis, as outlined in the Introduction (Figure 18), involves the intersystem crossing of the singlet state $S_1(n\pi^*)$ populated chromophore to the triplet state $T_1(n\pi^*)$. Fluorescence occurs through the relaxation of a singlet state excited species to the ground state.[43] The methoxy substitution of 2-nitrophenylalanine may enhance singlet state relaxation. Consequently, this relaxation may be out-competing intersystem crossing to the triplet state thereby inhibiting starting material consumption. This would correlate well with the findings of Hasan *et al.*[83] who found that although the methoxy substituents of the NVOC group enhanced its rate of photolysis at 350 nm in comparison to that of NBOC, they decreased the quantum yield of the reaction.

The half-life of the intermediate formed during the photolysis of **133** is of a similar order to that observed during the photolysis of **122** and **129** and therefore longer than

that observed from the reaction of **119**. The *aci*-nitro intermediate **155** proposed to form during the photolysis of **133** is illustrated in Figure 99. An understanding as to why the half-lives of the *aci*-nitro intermediates **155** and **143**, proposed to form during the photolysis of **133** and **119**, respectively, are different may come from a consideration of the resonance forms of **155** (Figure 99).

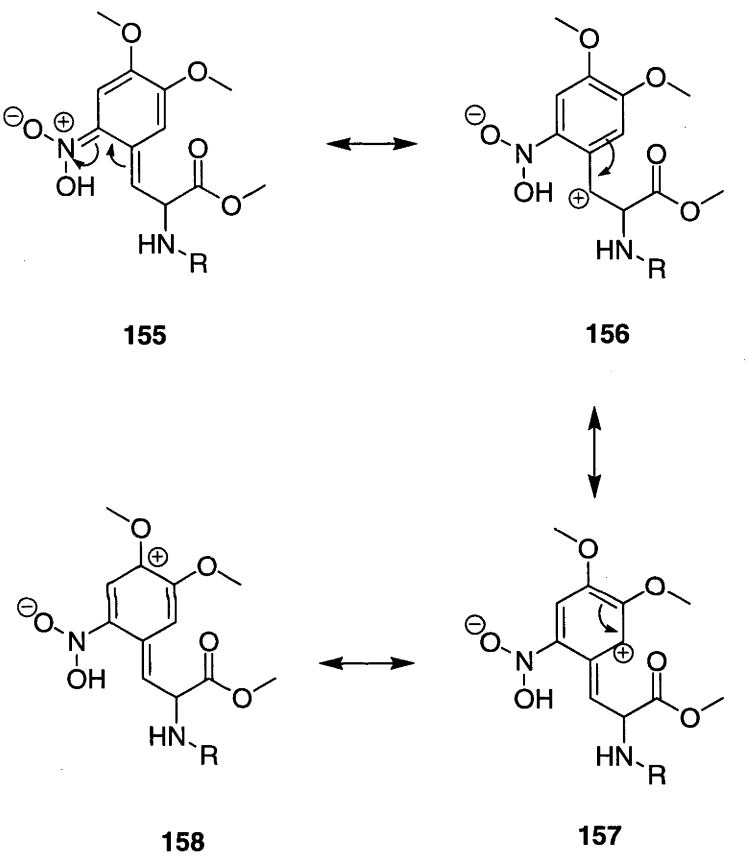

Figure 99. The *aci*-Nitro Intermediate **155** and Some of its Resonance Contributors **156**, **157** and **158**, R = *N*-Benzoylvalyl.

Methoxy substituents on aromatic rings are known to be σ electron withdrawing and π electron donating.[77] It is this feature which allows a positive charge to be stabilised

during electrophilic aromatic substitution of methoxy substituted aromatic rings and therefore governs the *ortho-para* selectivity of such reactions. The resonance forms illustrated in Figure 99 show that the 4-methoxy substituent of the aromatic ring may stabilise the *aci*-nitro intermediate **155** through similar π electron donation to the positively charged carbon.

In Figure 100, the *aci*-nitro intermediate **155** and its benzylic anion and benzylic cation resonance forms **159** and **156**, respectively, are illustrated. From the two resonance forms **155** and **159**, mechanisms can be drawn to allow for release of the amide **73**. However no reasonable mechanism can be drawn for the release of the amide **73** from the benzylic cation resonance form **156**. The ability of the 4-methoxy ring substituent to stabilise a positive charge (as illustrated in Figure 99) may make this resonance form of the *aci*-nitro intermediate **155** more dominant. This may therefore make the final cleavage step during the photolysis of **133** less likely, resulting in the extended *aci*-nitro intermediate half-life observed and consequently lower yield of amide **73** in comparison to the photolysis of the analogous **119**.

It is therefore apparent that the substitution of the ring of 2-nitrophenylalanine with methoxy substituents does not enhance its photolysis at wavelengths above 300 nm, although reasonable amide yields in the region of 50% may be obtained. These results indicate that in the design of future 2-nitrophenylalanine systems, ring substituents should be selected which would not stabilise an *aci*-nitro intermediates benzylic cation resonance form and should preferably enhance intersystem crossing to the triplet state $T_1(n\pi^*)$ chromophore. In the Future Work and Conclusions section of this thesis, methods by which this could be investigated are outlined.

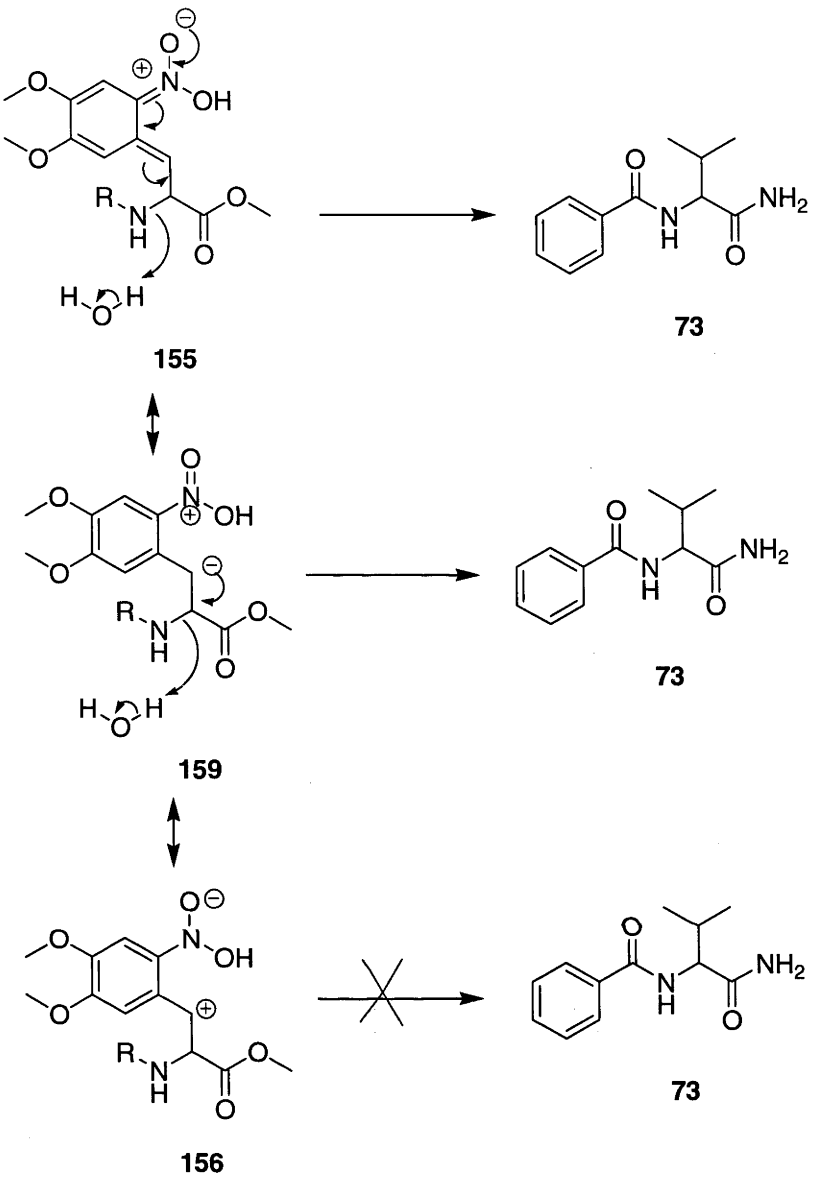

Figure 100. Mechanisms of Release of **73** from the *aci*-Nitro Intermediate **155** and its Resonance Form **159**. R = *N*-Benzoylvalyl

These studies have therefore established that amides can be released through 2-nitrophenylalanine photolysis. The photolysis of **119** was found to be efficient and

high yielding at pH 7.4. Therefore 2-nitrophenylalanine methyl ester may be a suitable photoremovable masking group for amides that could be used at biological pH in preference to Npg. Although the photolysis reactions of **122**, **129** and **133** were not as efficient as that of **119**, amide yields of up to 50% were obtained from their reactions. Potential methods by which the photolysis of 2-nitrophenylalanine to release amides might be enhanced will be outlined in the Future Work and Conclusions section of this thesis.

Chapter 4. Conclusions and Future Work

The research described in Chapter 1 of the Results and Discussion established that there are strong correlations between calculated radical stabilisation energies (RSEs), the ease of formation of glycyl and related radicals in free radical brominations, and the extent of catalysis of the reactions of analogous compounds by peptidylglycine α-amidating monooxygenase (PAM). A decrease in the RSE of around 10 kJ mol^{-1} relative to that of a normal peptide glycyl radical slowed, but did not stop, the rate of radical formation through either bromination or enzyme-catalysis. However, reducing the RSE by around 35-45 kJ mol^{-1}, through either introduction of a trifluoromethyl substituent at the α-position or by replacing the acylglycine NH with a glycolate O or a γ-keto acid CH_2, stopped both bromination and enzyme processing. Of these changes, only the glycolate substitution did not adversely affect the enzyme binding affinity. Consequently glycolates were found to be a general class of PAM inhibitors because they do not readily undergo hydrogen atom transfer, yet they bind effectively to the enzyme. The further implication of this observation is that the substitution of the

acylglycine of tight binding natural substrates of PAM with glycolate should afford enzyme inhibitors with high binding affinities.

In preliminary experiments, cell based assays were performed using the glycolate extended systems **63**, **64**, **75** and **76** to investigate whether they could be used to affect PAM activity in biological models.[84] The systems investigated are illustrated in Figure 101.

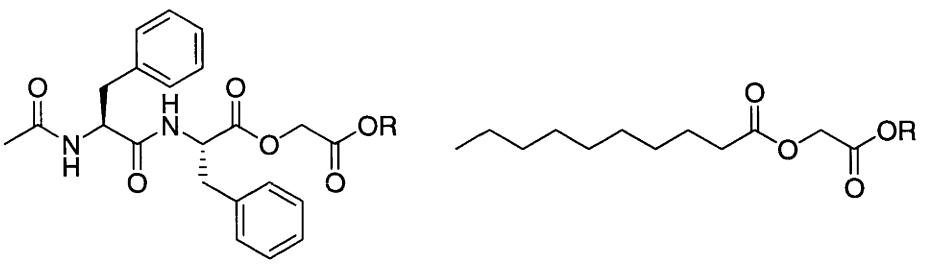

63 R = Benzyl
64 R = H

75 R = Benzyl
76 R = H

Figure 101. Systems Tested in Cell Based Assays.

Compounds **63**, **64**, **75** and **76** were selected for testing as they constituted different systems in that **75** and **76** are fatty acids and **63** and **64** are peptidic. The benzyl esters **63** and **75** were investigated as it was believed they would have enhanced transport into cells in comparison to the free acids **64** and **76**. Once inside the cells, it was anticipated that hydrolysis of **63** and **75** would occur to release the desired free acids **64** and **76**.

Compounds **63**, **64**, **75** and **76** were first studied for their capacity to affect proliferation of the human lung cancer cell line A549.[85] From these studies, IC_{50} and total growth inhibition (TGI) values were obtained. The IC_{50} for the free acids **64** and **76** were

>1000 μM and 257 μM and the TGI values were >1000 μM and >1000 μM, respectively. The IC_{50} values for the benzyl esters **63** and **75** were 64 and 81 μM and the TGI values were 324 and 211 μM respectively. Therefore the benzyl esters **63** and **75** were found to have significant activity as inhibitors of cancer cell growth. The enhanced activity of the benzyl esters **63** and **75** compared to their free acids **64** and **76** confirmed the importance of the benzyl ester moiety for the design of PAM inhibiting drugs.

The second system studied involved the monitoring of the effect that **63**, **64**, **75** and **76** have on substance P levels in rat dorsal root ganglian cells.[86] As was discussed in the Introduction, substance P levels are associated with inflammation and pain[7] and these studies attempted to establish the efficacy of compounds **63**, **64**, **75** and **76** to treat related physiological disorders. It was discovered that only the benzyl esters **63** and **75** were active, reducing substance P levels over a six hour period at a concentration of 50 μM. As the free acids **64** and **76** were not active these studies further established the importance of the benzyl ester design of compounds **63** and **75**.

Assays of **63**, **64**, **75** and **76** were also performed against an U87 cell line, using a radioimmunoassay (RIA) with 125I labelled adrenomedullin to establish whether levels of this hormone could be influenced.[87] Adrenomedullin is known for its activity in cardiovascular disease and renal faliure.[88] In these assays, the benzyl ester **75** was found to be the most active reducing the level of secreted adrenomedullin by 80% when used at a concentration of 0.1-1 nM.

PAM inhibition through the use of glycolate extended systems has therefore been shown to have potential in the development of therapeutic agents for the treatment of cancers, inflammation and pain and cardiovascular disorders. Future work will involve the development of more potent and specific inhibitors, tests of efficacy and toxicity in animal models and, subject to the satisfactory results of those studies, human trials.

Chapter 2 of the Results and Discussion section of this thesis described research towards the development of α-substituted glycines as hydrolytically cleavable amino acids. The hydrolysis reactions of the α-hydroxyglycines **7** and **8** to release benzamide **10** were found to have similar rates at pH 7.5. The psuedo-first order rate constant for the hydrolysis of the methyl ester **8** to release **10** directly at pH 7.5 was 3.6×10^{-5} sec^{-1} which corresponds to a half-life of 5.3 hours. Similarly the psuedo-first order rate constant for the hydrolysis of the free acid **7** to release **10** at pH 7.5 was 3.3×10^{-5} sec^{-1} which corresponds to a half-life of 5.8 hours. This was in contrast to the previously published half-lives for the hydrolysis of **7** and **8** to release benzamide **10** of 6.7 and 0.74 hours respectively.[41] The previously published half-life for the hydrolysis reaction of **8** to give the amide **10** was found to be valid only with respect to the rate of loss of starting material and not with respect to the rate of amide release. As a result the rate of the hydrolysis reaction of **8** to release **10** was previously incorrect and has now been addressed.

The half-lives for the hydrolysis reactions of the α-substituted glycines **14**, **16**, **18**, **21** and **133** to form α-hydroxyglycine moieties were found to correlate with the efficiency of the α-substituent to act as a leaving group. Through these studies it was established that α-phenoxyglycine (in comparison to α-hydroxyglycine), used as a masking group

for the *C*-terminal amide of peptide hormones or as a cleavable linker between such hormones with other molecules could reasonably be expected to extended the half-life of active drug release by 30 minutes at biological pH. The α-phenoxyglycine **21** hydrolysed to form an α-hydroxyglycine whilst the α-methoxyglycine **16** did not. This was correlated with the pK_as of methanol (15.0) and phenol (10.0) reflecting the inability of methoxide and the ability of phenoxide to act as leaving groups.[43] As **21** hydrolysed whilst **16** did not, the use of α-substituted glycines where the analogous acid of the α-substitutent possesses a pK_a in between 10.0 and 15.0, may therefore extend the half-lives of such systems at pH 7.5. Potential alcohols that could be used to this end include $C_3F_7CH_2OH$, $HCCCH_2OH$ and $CHCl_2CH_2OH$ which possess pK_as of 11.4, 13.55 and 12.89 respectively.[89,90] The use of such α-substituted glycines as masking groups for the *C*-terminal amide of peptide hormones, or as transient linkers between such hormones and macromolecules may afford greater control over the rate of release of active peptide drugs *in vivo* than possible with α-phenoxyglycine.

Chapter 3 of the Results and Discussion section of this thesis described research towards the development of a new photochemically cleavable amino acid. It was established that the 2-nitrophenylalanine systems **119**, **122**, **129** and **133** could be photolysed to release their respective amides **73**, **10**, **73** and **73** at biological pH. The most efficient system was *N*-benzoylvalyl-2-nitrophenylalanine methyl ester **119** which released the amide **73** at a rate comparable to that of starting material consumption in 80 – 100% yield. This result was significant in that it established that 2-nitrophenylalanine could be photolysed to release amides more efficiently than Npg at biological pH.

Preliminary studies were then performed to determine whether the *C*-terminal amide of oxytocin could be masked with a 2-nitrophenylalanine moiety, and unmasked through photolysis. Therefore, the masked oxytocin derivative **160** was designed and a reaction scheme for its photolysis is illustrated in Figure 102.

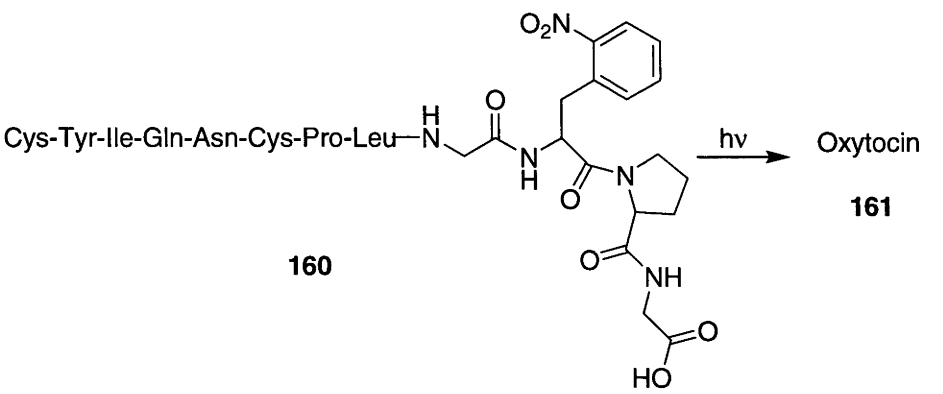

Figure 102. Photolysis of a Masked Oxytocin Derivative **160** to Release Oxytocin **161**

Polypeptide **160** was designed such that its irradiation would result in the cleavage of the 2-nitrophenylalanine N-C^{α} bond, thereby releasing oxytocin. The photolysis of the 2-nitrophenylalanine free acid **123** was unsuccessful. Therefore the 2-nitrophenylalanine of **160** was extended by a prolyl-glycine unit. This would also move the free acid far enough away from the 2-nitrophenylalanine residue such that any potential for it to interact with reaction intermediates formed during the photolysis would be eliminated.

In order that the polypeptide **160** could be synthesised by automated peptide synthesis, it was necessary to make the *N*-FMOC-2-nitrophenylalanine **162** (Figure 103).

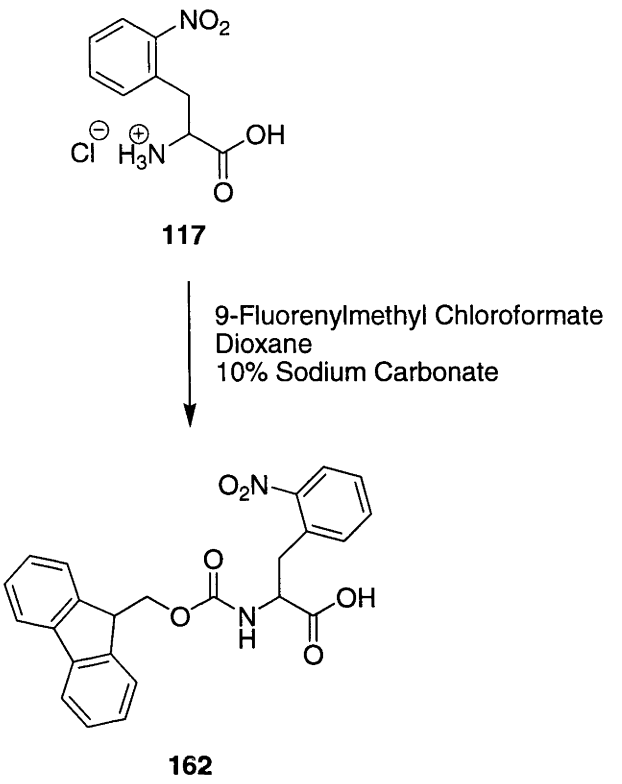

Figure 103. Synthesis of *N*-FMOC-2-Nitrophenylalanine **162**

2-Nitrophenylalanine **117** was stirred in dioxane and 10% sodium carbonate to which 9-fluorenylmethyl chloroformate was added to give the *N*-protected 2-nitrophenylalanine **162**. The ^{1}H NMR spectrum of the product showed a peak for the 2-nitrophenylalanine β-carbon protons at δ3.10 and δ3.67 ppm along with the α-carbon proton at δ4.62 ppm. Further the electrospray ionisation mass spectrum showed peaks for the protonated and sodiated molecular ions at *m/z* 432 and *m/z* 454 respectively indicating the reaction to have been successful. Compound **162** was then incorporated into the polypeptide **160** using automated peptide coupling procedures.[91] The electrospray mass spectrum of the product showed a peak for the protonated molecular ion at *m/z* 1353 indicating the synthesis to have been successful.

In a preliminary experiment, the polypeptide **160** was photolysed for 20 minutes at 300 nm using 10 lamps under the standard conditions established in Chapter 3 of the Results and Discussion section of this thesis. UV-HPLC traces of the starting material, an authentic sample of oxytocin[92] and the reaction solution are provided in Figures 104, 105 and 106, respectively. The photolysis of **160** resulted in the formation of two peaks (Figure 106). The peak at 2.85 minutes is due to an as yet not elucidated product. However, the peak at 3.15 minutes was attributed to oxytocin by comparison to authentic sample using the established procedure. Therefore the photolysis of **160** to give oxytocin **161** was successful although only a 5% yield of the hormone was recorded.

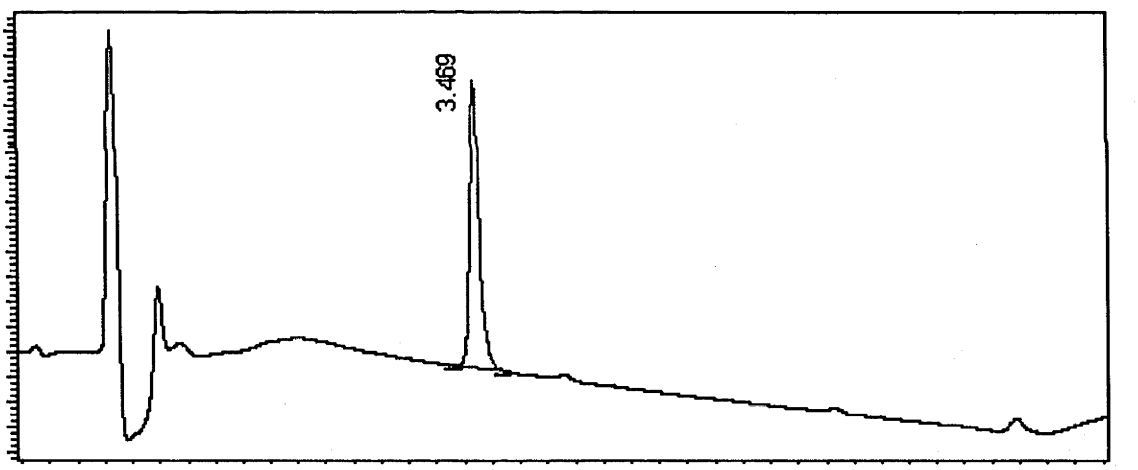

Figure 104. UV-HPLC Trace of a 50 μM Standard Solution of Polypeptide **160**

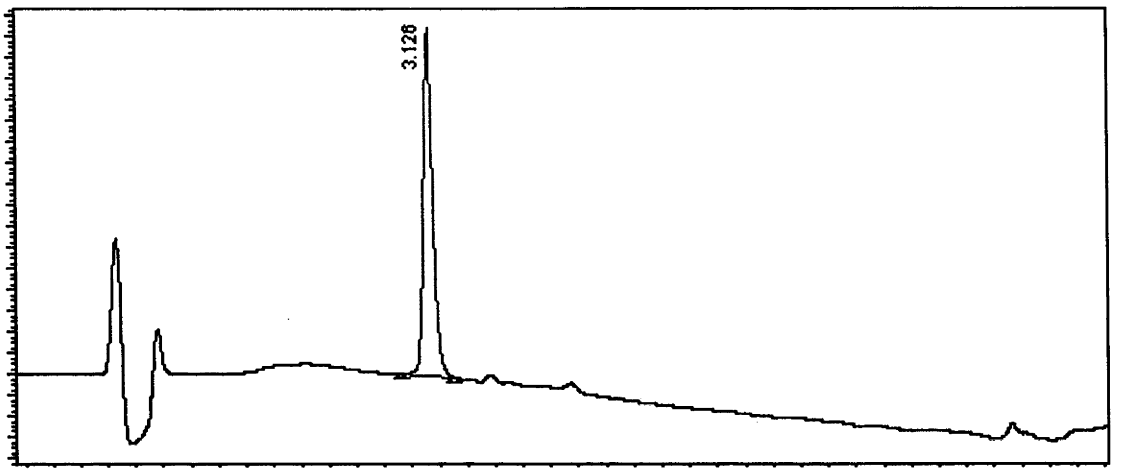

Figure 105. UV-HPLC Trace of a 50 μM Standard Solution of Authentic Sample of Oxytocin **161**

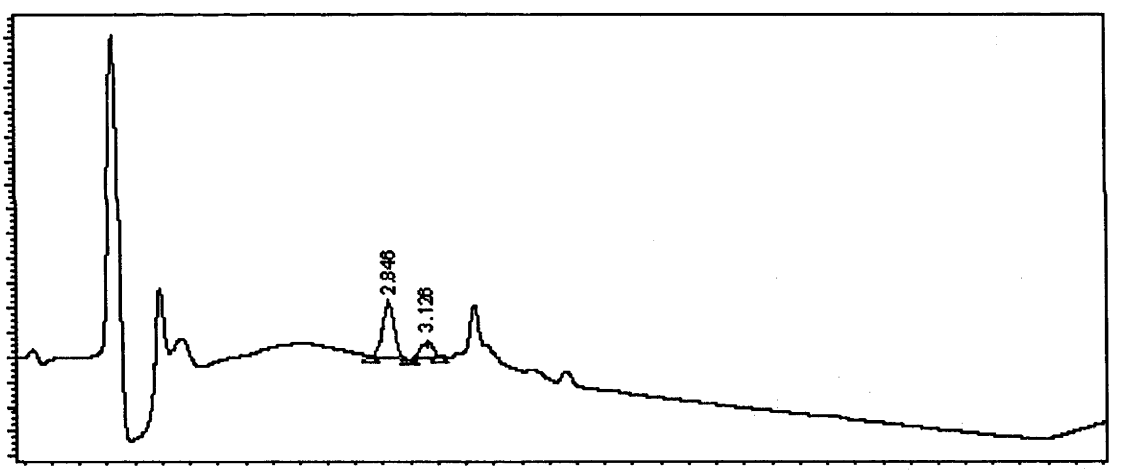

Figure 106. UV-HPLC Trace of Polypeptide **160** after Photolysis at 300 nm using 10 Lamps for 20 minutes.

In order to increase the yield of oxytocin released, future work may involve the incorporation of 2-nitrophenylalanine into a polypeptide as an ester **163** (Figure 107). This may take advantage of the potential high efficiency and yield of amide obtained

through the photolysis of 2-nitrophenylalanine esters as was observed for the reaction of the methyl ester **119**.

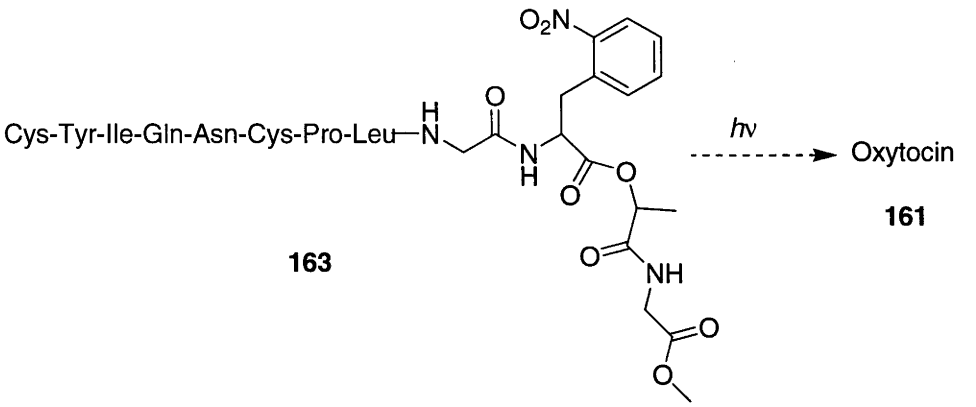

Figure 107. Reaction Scheme for the Potential Photolysis of the 2-Nitrophenylalanine Ester **163** to Release Oxytocin **161**.

Future work may also concentrate on increasing the reaction rate and efficiency of photolysis of 2-nitrophenylalanine. It was hypothesised that the efficiency of photolysis of 2-nitrophenylalanine systems was related to the nature of the 2-nitrophenylalanine carboxyl group. Therefore studies may be performed to determine the precise nature of this effect and methods by which the photolysis of 2-nitrophenylalanine systems could subsequently be improved. Furture studies could also include attempts at enhancing intersystem crossing from the excited singlet state $S_1(n\pi^*)$ populated chromophore formed upon irradiation to the triplet state $T_1(n\pi^*)$. In addition, studies towards increasing the yield and rate of release of amides from the *aci*-nitro intermediates formed during 2-nitrophenylalanine photolysis may also be performed. To this end, a number of 2-nitrophenylalanine analogues are proposed (Figure 108).

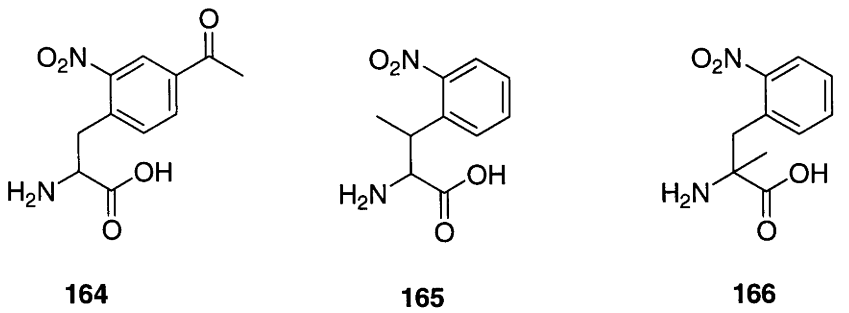

164 **165** **166**

Figure 108. Proposed 2-Nitrophenylalanine Analogues

Acetophenone has been widely used as a triplet energy transfer reagent in photochemical reactions.[93-96] Therefore the incorporation of an acetyl group at the *para* position of the ring to give the 2-nitrophenylalanine **164** may assist the intersystem crossing from the excited singlet state $S_1(n\pi^*)$ populated chromophore formed upon irradiation to the triplet state $T_1(n\pi^*)$. This may increase the rate of starting material consumption during the photolysis of 2-nitrophenylalanine systems. Further it would be reasonable to expect that the acetyl group of **164** would help to stabilise the benzylic anion resonance form of an *aci*-nitro intermediate whilst destablising the benzylic cation resonance form, potentially increasing the rate of the final cleavage step. The substitution of the β-carbon of 2-nitrophenylalanine with a methyl group to give **165** may also enhance the rate of starting material consumption during the irradiation of 2-nitrophenylalanine systems as the β-carbon centred radical formed would be tertiary rather than secondary. The substitution of the α-position of 2-nitrophenylalanine to give **166** and the β-position to give **165** may also help to stabilise the cinnamates and cinnamides formed during 2-nitrophenylalanine photolysis through greater substitution of the conjugated systems produced. This could potentially increase the rate of the final cleavage step.

Future work may also concentrate on the development of new potentially photocleavable amino acids such as the 2-acetylphenylalanine **167** which is illustrated in Figure 109. The 2-acetylphenylalanine was designed though analogy to the 1-[2-(2-hydroxyalkyl)phenyl]ethenone photoremovable protecting group which was developed by Atemnkeng *et al.*[97]

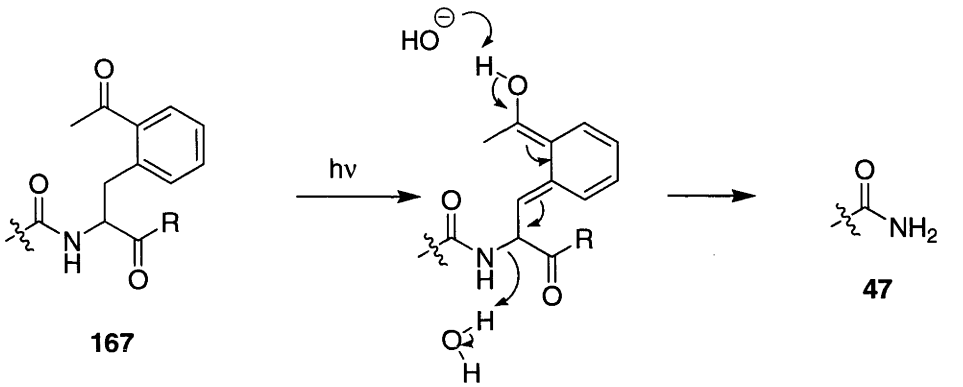

Figure 109. Potential Photolysis Mechanism of 2-Acetylphenylalanine. R = NH_2, NHR', OH, OR'.

Upon photolysis of **167** abstraction of a hydrogen atom from the β-carbon would occur in a similar manner to that observed in a Norrish Type II reaction. The resultant diradical would then rearrange in a similar manner to the mechanism of 2-nitrophenylalanine photolysis to give **168**. Compound **168**, which is an analogue of the *aci*-nitro compounds proposed as intermediates in 2-nitrophenylalanine photolysis, would then eliminate the amide **47**.

Experimental

General

Melting points were determined on a Kofler hot-stage melting point apparatus under a Reichert microscope and are uncorrected. ^{1}H and ^{13}C NMR spectra were recorded on Varian Gemini 300 and VRX 500S spectrometers. Electron impact (EI) mass spectra were obtained using a VG Autospec double-focussing trisector mass spectrometer operating at 70 eV. Electrospray ionization (ESI) mass spectra were recorded on a VG Quatro 2 triple-quadrupole mass spectrometer. Fast atom bombardment mass spectra (FAB) were obtained with a VG Analytical ZAB2-SEQ mass spectrometer. Microanalyses were performed by the Research School of Chemistry Microanalytical Service at the Australian National University, on a Carlo.Erba 1106 autoanalyser. Optical rotations were recorded using a Perkin Elmer 241 polarimeter.

High performance liquid chromatography (HPLC) was carried out on a Waters Alliance 2690 Chromatography Module, with a Waters 996 Photodiode Array Detector and a Waters Fraction Collector II, in conjunction with a Compaq Deskpro Data Station running Waters Millennium 32 chromatography management software. A Waters Symmetry Prep. C18 5 μm column (4.6 x 250 mm) was used for analytical separations and, and a YMC-Pack ODS-AQ 5 μm column (10 x 250 mm) for preparative separations described in Chapter 1 of the Results and Discussion. A Waters Symmetry C_{18} 3.5 μm column (4.6 x 75 mm) was used for the analytical separations described in Chapters 2 and 3 of the Results and Discussion. A Waters SymmetryPrep C_{18} 7 μm column (19 x 300 mm) was used for the preparative separation described in Chapter 2

of the Results and Discussion. Preparative chromatography was performed with Merck Kieselgel 60 (230.400 mesh ATSM). An Osram Ultra-Vitalux (240 V, 300 W, E27) sunlamp was used as the light source to initiate radical brominations, at a distance of between 5.10 cm from the reaction vessel. Organic extracts were dried using anhydrous $MgSO_4$. The photolysis of 2-nitrophenylalanine derivatives was performed in a Luzchem Photoreactor (LZC-ORG).

Recombinant peptidylglycine α-amidating monooxygenase (PAM) was purchased from Wako Pure Chemical Industries. Benzyl bromoacetate, decanoic acid, glycine hydrochloride *tert*-butyl ester and β,β,β-trifluoroalanine were bought from Sigma.Aldrich Chemical Co. *N*-Acetyl-(*S*)-phenylalanyl-(*S*)-phenylalanine and *N*-acetylphenylalanine were obtained from Auspep Pty. Ltd.

Experimental for Chapter 1

Theoretical Procedures

Standard ab initio molecular orbital theory and density functional theory calculations were performed using the GAUSSIAN 03 program. Geometries and zero-point vibrational energies (scaled by 0.9806) were determined at the B3-LYP/6-31G(d) level, while improved relative energies were obtained by carrying out single-point calculations on these optimized structures at the RMP2 level with the 6-311+G(2df,p) and G3large basis sets. Results quoted in the text correspond to RMP2/G3large//B3-LYP/6-31G(d) values at 0 K. Radical stabilisation energies (RSEs) of .CHXY radicals were calculated as the energies of the reactions:

$$CH_4 + {}^{\bullet}CHXY \rightarrow {}^{\bullet}CH_3 + CH_2XY \qquad (1)$$

This is equivalent to the difference between the C-H bond dissociation energy (BDE) in methane and the C-H BDE in the substituted methane (CH_2XY):

$$RSE({}^{\bullet}CHXY) = BDE(CH_4) - BDE(CH_2XY) \qquad (2)$$

Defined in this way, a positive RSE indicates that the radical $^{\bullet}CHXY$ is stabilised relative to $^{\bullet}CH_3$ (compared with the corresponding closed-shell systems).

Gaussian archive entries for the B3-LYP/6-31G(d) optimized structures are presented in Table E1. We note that the structures for **2**, **5**, **93b** and **94b** have been reported previously[21,27] but they are included here for completeness. Total energies at the RMP2/G3large//B3-LYP/6-31G(d) and RMP2/6-311+G(2df,p)//B3-LYP/6-31G(d) levels are included in Table E2, while corresponding RSEs at these two levels are listed in Tables E2 and E3.

Table E1. GAUSSIAN Archive Entries for the UB3-LYP/6-31G(d) Optimized Structures of Derivatives of Glycyl and Related Radicals

$MeCONHCH_2CO_2Me$ 1

```
1\1\GINC-VPP05\SP\RMP2-FC\6-31G(d)\C5H9N1O3\AKC501\28-Mar-1998\0\\# RM
P2/6-31G* SCF=DIRECT GUESS=CHECK GEOM=CHECK TEST MAXDISK=12582912\\CH3
O2CCH2NHCOCH3 sp RMP2/6-31G*//B3LYP/6-31G*\\0,1\C,-0.453984955,0.04227
64497,-0.4610673375\N,-0.434416958,-0.0062114363,0.9807989618\C,0.9689
```

096865,-0.0262498517,-0.9801271891\H,-0.9312052348,0.9609457186,-0.826
7029336\O,1.9556376518,-0.1077624508,-0.2773614955\O,0.9935745096,0.01
52606135,-2.320978703\C,2.3010407694,-0.0435036938,-2.9216242995\H,0.4
761138148,-0.0746290799,1.416180349\C,-1.5895703494,0.0400642778,1.704
2057359\O,-2.6876253658,0.1238515692,1.1654906135\C,-1.4223696652,-0.0
190545532,3.2149807124\H,-1.0363983067,-0.7867185427,-0.8840263162\H,2
.1281952796,0.0013801949,-3.9966976274\H,2.910140692,0.8022221855,-2.5
927965776\H,2.8040095293,-0.9749485721,-2.6499338831\H,-1.8698201152,0
.8775364171,3.6549097459\H,-1.9769883646,-0.8812328872,3.5979267627\H,
-0.3799758713,-0.0930690085,3.5401386944\\Version=Fujitsu-VP-Unix-G94R
evE.2\HF=-473.6480592\MP2=-474.9764903\RMSD=7.422e-09\PG=C01 [X(C5H9N1
O3)]\\@

MeCONHCH$^{\bullet}$CO$_2$Me 2

1\1\GINC-PC\SP\ROMP2-FC\6-31G(d)\C5H8N1O3(2)\AKC501\30-Mar-1998\0\\# R
OMP2/6-31G* SCF=DIRECT GUESS=CHECK GEOM=CHECK TEST MAXDISK=5242880000\
\CH3O2CCH'NHCOCH3 sp RMP2/6-31G*//B3LYP/6-31G*\\0,2\C,-0.3824700669,0.
0186723638,-0.37315618\N,-0.3645322925,-0.016000121,0.9905755085\C,0.8
977685159,-0.0135309135,-1.0327292927\H,-1.3377465782,0.0669329941,-0.
8738388169\O,1.9695412086,-0.0685718101,-0.4319076048\O,0.7849387732,0
.024138858,-2.3825116347\C,2.027964724,-0.0050705725,-3.0966484405\H,0
.5628675966,-0.0582000695,1.4044760017\C,-1.5024970986,0.0069307292,1.
7927967609\O,-2.6205637825,0.0512664451,1.3074769728\C,-1.2345521427,0
.0015144636,3.2849788804\H,1.7584939546,0.0303513968,-4.1527005464\H,2
.6479499822,0.8557621457,-2.8302527423\H,2.581666637,-0.921421798,-2.8
728909291\H,-1.3905122245,1.0110838402,3.6827324222\H,-1.9586461144,-0
.6581416589,3.7694459459\H,-0.2209603906,-0.320130371,3.5430878703\\Ve
rsion=SGI-G94RevE.2\HF=-473.0308985\MP2=-474.3466163\RMSD=7.089e-09\PG
=C01 [X(C5H8N1O3)]\\@

$CF_3CONHCH_2CO_2Me$ 4

1\1\GINC-VPP12\SP\RMP2-FC\6-31G(d)\C5H6F3N1O3\AKC501\30-Mar-1998\0\\#P
 RMP2/6-31G* SCF=DIRECT GUESS=CHECK GEOM=CHECK TEST MAXDISK=16777216\\
CH3O2CCH2NHCOCF3 sp RMP2/6-31G*//B3LYP/6-31G*\\0,1\C,-0.1181919832,0.0
841375092,-1.4238662227\N,-0.1112523041,-0.0235072653,0.0173413534\C,1
.3054959812,-0.0684386068,-1.9275784705\H,-0.5250128598,1.0501698584,-

1.7471419266\O,2.2636369689,-0.2659424489,-1.2097545595\O,1.3556135739
,0.0421832917,-3.2605081494\C,2.665695439,-0.0884190896,-3.8489821764\
H,0.7817874637,-0.2036357959,0.4611124665\C,-1.2481037278,0.1143135332
,0.7319476218\O,-2.3550789652,0.3257799471,0.2661143162\C,-1.058483487
2,0.0036246585,2.262574948\H,-0.7540995607,-0.6856094921,-1.8793567627
\H,2.5127810385,0.0260708601,-4.921634464\H,3.331760262,0.6891309453,-
3.4674456088\H,3.0881774379,-1.0697315663,-3.6203008801\F,-1.889926550
4,-0.915714177,2.7690911045\F,0.2080573428,-0.3483005911,2.598668354\F
,-1.3235167486,1.1829794016,2.8457950573\\Version=Fujitsu-VP-Unix-G94R
evE.2\HF=-770.2166162\MP2=-772.0522848\RMSD=7.381e-09\PG=C01 [X(C5H6F3
N1O3)]\\@

$CF_3CONHCH^{\bullet}CO_2Me$ 5

1\1\GINC-VPP05\SP\ROMP2-FC\6-31G(d)\C5H5F3N1O3(2)\AKC501\31-Mar-1998\0
\\#P ROMP2/6-31G* SCF=DIRECT GUESS=CHECK GEOM=CHECK TEST MAXDISK=20971
520\\CH3O2CCH'NHCOCF3 sp RMP2/6-31G*//B3LYP/6-31G*\\0,2\C,-0.102352627
3,0.,-1.3569836426\N,-0.0842256548,0.,0.0067974199\C,1.1898975766,0.,-
2.0062066926\H,-1.0554562355,0.,-1.8646204514\O,2.2495779074,0.,-1.387
1076531\O,1.0872547885,0.,-3.3518848058\C,2.3375145272,0.,-4.059625881
7\H,0.8390677026,0.,0.4356720212\C,-1.2120204268,0.,0.792973712\O,-2.3
525400784,0.,0.3711063384\C,-0.9271791873,0.,2.3089771847\H,2.07239372
46,0.,-5.1169039161\H,2.9208713526,0.8900860002,-3.8087645456\H,2.9208
713526,-0.8900860002,-3.8087645456\F,0.4032178667,0.,2.5732111592\F,-1
.4625905127,1.0871477471,2.879176664\F,-1.4625905127,-1.0871477471,2.8
79176664\\Version=Fujitsu-VP-Unix-G94RevE.2\State=2-A"\HF=-769.5962938
\MP2=-771.4186474\RMSD=4.485e-09\PG=CS [SG(C5H3F1N1O3),X(H2F2)]\\@

$MeCONHCH(Me)CO_2Me$

1\1\GINC-VPP09\SP\RMP2-FC\6-31G(d)\C6H11N1O3\AKC501\11-Apr-1998\0\\#P
RMP2/6-31G* SCF=DIRECT GUESS=CHECK GEOM=CHECK TEST MAXDISK=8388608\\CH
3CONHCHCH3CO2CH3 sp RMP2/6-31G*//B3LYP/6-31G*\\0,1\C,-0.3667196064,0.0
716605373,-0.3851585219\N,-0.3593680447,0.0963142476,1.0662887614\C,1.
0808071321,-0.0362817008,-0.8478985426\C,-1.0607758274,1.3046628996,-0
.9963952232\O,2.047717929,0.0659179095,-0.1192160876\O,1.1571717024,-0
.2400960536,-2.1728676547\C,2.4886121862,-0.3267202763,-2.7137908888\H
,0.5434545641,0.228654278,1.5041432191\C,-1.4575634565,-0.2628307173,1

.7925221727\O,-2.5283687226,-0.5461233351,1.2645759074\C,-1.2684929532
,-0.2814737137,3.3020748009\H,-0.9069982581,-0.8224565988,-0.719161712
9\H,2.3570402115,-0.4890759774,-3.7834480917\H,3.0372535682,0.60010011
38,-2.5282311505\H,3.0305041193,-1.1605195365,-2.2604873559\H,-2.00231
39405,0.3902365471,3.7578402678\H,-1.4776976635,-1.290486048,3.6711097
592\H,-0.2656671869,0.0155870786,3.6240466441\H,-1.0674609133,1.240711
5494,-2.0882017136\H,-2.0907213239,1.3360728689,-0.6339984271\H,-0.549
1889821,2.2252856527,-0.6956928717\\Version=Fujitsu-VP-Unix-G94RevE.2\
HF=-512.6847518\MP2=-514.148391\RMSD=3.895e-09\PG=C01 [X(C6H11N1O3)]\\
@

MeCONHC•(Me)CO_2Me 93a

1\1\GINC-VPP05\SP\ROMP2-FC\6-31G(d)\C6H10N1O3(2)\AKC501\11-Apr-1998\0\
\#P ROMP2/6-31G* SCF=DIRECT GUESS=CHECK GEOM=CHECK TEST MAXDISK=838860
8\\CH3NHCHCH3CO2CH3 sp RMP2/6-31G*//B3LYP/6-31G*\\0,2\C,-0.2895558464,
-0.0043989742,-0.3447847739\N,-0.261035049,-0.00380632,1.0337444984\C,
1.0459793091,-0.0080072949,-0.9133489793\C,-1.5555484454,-0.0019046287
,-1.1334105164\O,2.0703765082,-0.0099457488,-0.2278632137\O,1.06017805
82,-0.0083980237,-2.2693401626\C,2.3656961084,-0.010978545,-2.86125717
35\H,0.6895533317,-0.0037459104,1.397201705\C,-1.3186104852,0.00137714
21,1.9309312246\O,-2.4906766582,-0.0027993748,1.5852484563\C,-0.899028
5425,0.0366449658,3.3913756635\H,2.1969269553,-0.0113514078,-3.9387266
398\H,2.9284077197,0.8775909206,-2.561443442\H,2.9254200114,-0.9010402
776,-2.560325528\H,-1.1186872703,1.0287940524,3.8018044423\H,-1.503041
5606,-0.6867679405,3.9454182319\H,0.1612567473,-0.1801581586,3.5520032
749\H,-1.3199753637,-0.0000957147,-2.1980861497\H,-2.1732518732,-0.876
3872315,-0.8994100382\H,-2.171979208,0.8725550952,-0.8960406551\\Versi
on=Fujitsu-VP-Unix-G94RevE.2\HF=-512.0662576\MP2=-513.517739\RMSD=5.39
9e-09\PG=C01 [X(C6H10N1O3)]\\@

MeCONHCH(CF_3)CO_2Me

1\1\GINC-VPP12\SP\RMP2-FC\6-31G(d)\C6H8F3N1O3\AKC501\11-Apr-1998\0\\#P
RMP2/6-31G* SCF=DIRECT GUESS=CHECK GEOM=CHECK TEST MAXDISK=8388608\\C
H3CONHCHCF3CO2CH3 sp RMP2/6-31G*//B3LYP/6-31G*\\0,1\C,-0.1237425494,-0
.220071209,-0.0947540658\N,-0.1678951773,-0.1391120853,1.3405000115\C,
1.3343927845,-0.3751654247,-0.5438232934\C,-0.7617972929,1.0234156882,

-0.7420080402\O,2.2792494259,-0.2152826768,0.1979739981\O,1.4189674152
,-0.7002848818,-1.8363420798\C,2.7563475787,-0.8303420316,-2.361706975
9\H,0.668114359,0.2132730801,1.7887705984\C,-1.0942468297,-0.862503460
3,2.0590453619\O,-1.9792366336,-1.5065889996,1.515873719\C,-0.95425750
46,-0.7672556418,3.5678287658\H,-0.7198738183,-1.0805731516,-0.4145561
034\H,2.6284470039,-1.0822901815,-3.4137805414\H,3.299081165,0.1112655
97,-2.2508224597\H,3.2933125382,-1.6225617573,-1.8346980929\H,-1.75591
80721,-0.1301637226,3.9569721291\H,-1.0872485868,-1.7637958509,3.99620
06613\H,0.0059086436,-0.3547992117,3.8923278459\F,-0.911577914,0.86290
11352,-2.0692934724\F,-1.9694376606,1.2697230111,-0.2136022226\F,0.008
9516,2.1176219355,-0.5428209418\\Version=Fujitsu-VP-Unix-G94RevE.2\HF=
-809.2618018\MP2=-811.2302294\RMSD=3.870e-09\PG=C01 [X(C6H8F3N1O3)]\\@

MeCONHC$^{\bullet}$(CF$_3$)CO$_2$Me 94a

1\1\GINC-RSCQC8\SP\ROMP2-FC\6-31G(d)\C6H7F3N1O3(2)\ANNA\12-Apr-1998\0\
\#P ROMP2/6-31G* SCF=DIRECT GUESS=CHECK GEOM=CHECK TEST MAXDISK=104857
6000\\CH3NHCHCF3CO2CH3 sp RMP2/6-31G*//B3LYP/6-31G*\\0,2\C,0.160722190
5,0.0684243528,-0.0353213098\N,0.1799096045,0.11754959,1.336227542\C,1
.5127571483,0.0569882134,-0.6042871416\C,-1.1341264452,0.0967216506,-0
.8087105972\O,2.5018381029,0.1552174293,0.1180458296\O,1.5736052814,-0
.0843922088,-1.9361278716\C,2.9010999862,-0.1064013438,-2.4887703515\H
,1.1300954198,0.2536042645,1.6806307261\C,-0.8178013572,-0.1890432513,
2.2757772795\O,-1.917907999,-0.5926556395,1.961795361\C,-0.3757300626,
0.0540299032,3.707287534\H,2.7610646082,-0.228101642,-3.5626002588\H,3
.4222748581,0.829100819,-2.2699130732\H,3.4742219857,-0.9405120556,-2.
0757846214\H,-0.3233451303,1.1305599346,3.9098208729\H,-1.1098174719,-
0.3952417788,4.3769043043\H,0.612821927,-0.373394036,3.9105257879\F,-0
.9346821418,0.4930644569,-2.07973342\F,-1.7296974294,-1.1105689115,-0.
8572678478\F,-1.99878657,0.9721115178,-0.2573026838\\Version=IBM-RS600
0-G94RevE.1\HF=-808.6289105\MP2=-810.585426\RMSD=8.969e-09\PG=C01 [X(C
6H7F3N1O3)]\\@

MeCO$_2$CH$_2$CO$_2$Me

1\1\GINC-SC44\FOpt\RB3LYP\6-31G(d)\C5H8O4\ROOT\17-Sep-2001\0\\#N B3LYP
/6-31G(D) TEST SCF=DIRECT OPT MAXDISK=39321600\\MeCOOCH2CO2Mea B3LYP /
6-31G(d) geom opt\\0,1\O,-0.531850066,1.2845400629,0.4893611915\C,0.8

655752707,1.0989626135,0.2689654703\H,1.2222236987,2.0343831126,-0.169
6911946\C,1.2237407859,-0.0410062727,-0.6772034314\O,2.3682879664,-0.3
952471144,-0.8484844422\O,0.1569910934,-0.5572953073,-1.3067605013\C,0
.4459024276,-1.645542808,-2.2033926879\H,1.1310951109,-1.3200256342,-2
.9901484186\H,-0.5156527331,-1.938028192,-2.6252489211\H,0.8969602374,
-2.4774008651,-1.6568095095\H,1.391789632,0.9202512132,1.2095173447\C,
-1.1197468039,0.3600805199,1.2982178931\O,-0.5099054113,-0.5406982049,
1.8267544711\C,-2.5993741682,0.6238756935,1.4191782056\H,-3.0286683774
,-0.0482077913,2.1628114187\H,-3.0799848044,0.4546037872,0.4493923608\
H,-2.782536496,1.6658104018,1.6986184688\\Version=DEC-AXP-OSF/1-G98Rev
A.9\HF=-496.2589404\RMSD=6.904e-09\RMSF=1.683e-05\Dipole=-0.9201494,0.
407298,-0.5141795\PG=C01 [X(C5H8O4)]\\@

$MeCO_2CH^{\bullet}CO_2Me$ 95a

1\1\GINC-SC41\FOpt\UB3LYP\6-31G(d)\C5H7O4(2)\ROOT\17-Sep-2001\0\\#N UB
3LYP/6-31G(D) TEST SCF=DIRECT OPT=TIGHT MAXDISK=26214400\\MeCOOCHrCO2M
ea radical UB3LYP / 6-31G(d) geom opt\\0,2\C,-0.2985462021,0.328157662
2,0.\O,1.0534639998,0.3305853874,0.\H,-0.8181134824,1.2764770602,0.\C,
-0.9389103119,-0.9686989061,0.\O,-0.370718501,-2.0482280327,0.\O,-2.29
18543944,-0.8131804208,0.\C,-3.0373484912,-2.0375084901,0.\C,1.7068103
702,1.5565842794,0.\O,1.1202216789,2.6076064653,0.\C,3.1935758461,1.33
73507187,0.\H,3.7015062607,2.3019464507,0.\H,-4.0868036303,-1.74110783
13,0.\H,-2.8062978043,-2.6312379767,0.8891753265\H,-2.8062978043,-2.63
12379767,-0.8891753265\H,3.4868084637,0.7577907476,0.8815433654\H,3.48
68084637,0.7577907476,-0.8815433654\\Version=DEC-AXP-OSF/1-G98RevA.9\S
tate=2-A"\HF=-495.6075722\S2=0.755538\S2-1=0.\S2A=0.75002\RMSD=9.194e-
09\RMSF=3.470e-07\Dipole=0.1415052,0.067908,0.\PG=CS [SG(C5H3O4),X(H4)
]\\@

$MeCOCH_2CH_2CO_2Me$

1\1\GINC-SC96\FOpt\RB3LYP\6-31G(d)\C6H10O3\DJH501\23-May-2004\0\\#N B3
LYP/6-31G* SCF=TIGHT OPT=(CALCFC,TIGHT) MAXDISK=52428800 IOP(1/8=10)\\
CH3COCH2CH2CO2CH3a 13ca B3LYP / 6-31G(d) geom opt\\0,1\C,3.6321484646,
0.6981733691,0.2275881664\C,2.4204952759,-0.1788373626,-0.0361723216\O
,2.5337908231,-1.3364621536,-0.3946512347\C,1.0583636668,0.4737252076,
0.1639709107\C,-0.0980047143,-0.5201722652,0.1084335268\C,-1.438366730

3,0.1646377588,-0.0600943786\O,-1.6072270577,1.3012036122,-0.449860943
4\O,-2.4513168367,-0.671044728,0.258055378\C,-3.7724152167,-0.13421719
86,0.0798188746\H,0.9268155816,1.2378517209,-0.6147231126\H,1.05970141
31,1.0332369834,1.10913642\H,0.0460199103,-1.2042843854,-0.7373025847\
H,-0.128120738,-1.1598476993,0.9961362162\H,4.5392738833,0.1863525471,
-0.0998657167\H,3.5405408573,1.6635067597,-0.2844436206\H,3.7086529427
,0.9128325875,1.3015217947\H,-4.4543344262,-0.9309091028,0.3784884678\
H,-3.9158580843,0.7500500553,0.7065159956\H,-3.9379912452,0.1417796345
,-0.9650781281\\Version=DEC-AXP-OSF/1-G03RevB.05\State=1-A\HF=-460.343
545\RMSD=7.749e-09\RMSF=1.067e-06\Dipole=-0.2453664,0.3987818,0.487740
7\PG=C01 [X(C6H10O3)]\\@

$MeCOCH_2CH^{\bullet}CO_2Me$ 96a

1\1\GINC-SC11\FOpt\UB3LYP\6-31G(d)\C6H9O3(2)\DJH501\23-May-2004\0\\#N
UB3LYP/6-31G* SCF=TIGHT OPT=TIGHT MAXDISK=52428800\\CH3COCH2CH2CO2CH3
13rca B3LYP / 6-31G(d) geom opt\\0,2\C,-2.7838975987,-1.9515241804,0.5
239385787\O,-1.4295145402,-1.8863040137,0.0572721255\C,-0.7150279411,-
0.8211096847,0.5028146774\O,-1.1776574164,0.0338686358,1.2510966874\C,
0.6388467983,-0.8237474417,-0.0163362345\C,1.6071797374,0.2351740311,0
.3640823116\C,1.5905182143,1.3686841116,-0.7071370704\O,2.3399494382,1
.3276892805,-1.6577968777\C,0.5896581274,2.480700869,-0.4789664966\H,1
.3383591385,0.6535603529,1.3392369834\H,2.6266614269,-0.161389256,0.38
31932042\H,0.9114922388,-1.5719668552,-0.7530502092\H,0.4774220601,3.0
772802593,-1.3867160722\H,-0.3727996689,2.0793604417,-0.1462042965\H,0
.9569867647,3.1269912852,0.3298203481\H,-3.2023009876,-2.8566612726,0.
0826100989\H,-2.8147734815,-2.0069750942,1.6158582293\H,-3.3469313695,
-1.0712973117,0.2003016347\\Version=DEC-AXP-OSF/1-G03RevB.05\State=2-A
\HF=-459.6876358\S2=0.757059\S2-1=0.\S2A=0.750036\RMSD=6.167e-09\RMSF=
1.674e-06\Dipole=-0.50824,-0.3482817,0.3809873\PG=C01 [X(C6H9O3)]\\@

MeC(O)OMe

1\1\GINC-SC96\Freq\RB3LYP\6-31G(d)\C3H6O2\DJH501\02-Jun-2004\0\\#N B3L
YP/6-31G(D) SCF=TIGHT FREQ MAXDISK=39321600\\CH3COOCH3 B3LYP / 6-31G(d
) freq\\0,1\C,0.10972725,-0.48146575,0.\O,1.32078725,-0.48146575,0.\O,
-0.63684275,0.64837425,0.\C,-0.77329275,-1.70751575,0.\C,0.10939725,1.
87582425,0.\H,-0.15076275,-2.60274575,0.\H,-1.42212275,-1.70493575,0.8

8201\H,-1.42212275,-1.70493575,-0.88201\H,-0.63593275,2.67188425,0.\H,
0.74219725,1.94220425,0.88921\H,0.74219725,1.94220425,-0.88921\\Versio
n=DEC-AXP-OSF/1-G03RevB.05\State=1-A'\HF=-268.3884834\RMSD=2.988e-09\R
MSF=1.274e-05\Dipole=-0.6573154,0.2410275,0.\ PG=CS [SG(C3H2O2),X(H4)]\\@

$^{\bullet}CH_2C(O)OMe$

1\1\GINC-SC4\Freq\UB3LYP\6-31G(d)\C3H5O2(2)\DJH501\02-Jun-2004\0\\#N U
B3LYP/6-31G(D) SCF=TIGHT FREQ MAXDISK=39321600\\CH2COOCH3 radical UB3L
YP / 6-31G(d) freq\\0,2\C,-1.8444723077,0.3638041026,0.\C,-0.397112307
7,0.3638041026,0.\O,0.2999776923,1.3688341026,0.\O,0.1098676923,-0.899
2058974,0.\C,1.5411676923,-0.9759058974,0.\H,1.7782376923,-2.040405897
4,0.\H,1.9549376923,-0.4906458974,0.88885\H,1.9549376923,-0.4906458974
,-0.88885\H,-2.4065523077,-0.5622958974,0.\H,-2.3578223077,1.316754102
6,0.\\Version=DEC-AXP-OSF/1-G03RevB.05\State=2-A"\HF=-267.7237418\S2=0
.757593\S2-1=0.\S2A=0.750034\RMSD=3.339e-09\RMSF=7.239e-06\Dipole=-0.2
479394,-0.64155,0.\ PG=CS [SG(C3H3O2),X(H2)]\\@

MeCONHMe

1\1\GINC-SC43\FOpt\RB3LYP\6-31G(d)\C3H7N1O1\ROOT\20-Sep-2001\0\\#N B3L
YP/6-31G(D) TEST SCF=DIRECT OPT=TIGHT MAXDISK=26214400\\CH3NHCOMe B3LY
P / 6-31G(d) geom opt\\0,1\C,-0.4911143789,0.,0.1435553401\O,-0.490897
4537,0.,1.3681980287\N,0.6563870228,0.,-0.6032282476\C,-1.7865417781,0
.,-0.6569472348\C,1.9780335208,0.,-0.0042464693\H,-1.6406727833,0.,-1.
7420994326\H,-2.3722417196,0.8813078343,-0.3780784065\H,-2.3722417196,
-0.8813078343,-0.3780784065\H,0.5808145651,0.,-1.6094047741\H,1.839859
9538,0.,1.0779424945\H,2.5473439954,-0.8916373005,-0.2937188935\H,2.54
73439954,0.8916373005,-0.2937188935\\Version=DEC-AXP-OSF/1-G98RevA.9\S
tate=1-A'\HF=-248.5235535\RMSD=2.929e-09\RMSF=2.663e-06\Dipole=0.35188
42,0.,-1.3878438\PG=CS [SG(C3H3N1O1),X(H4)]\\@

$MeCONHCH_2^{\bullet}$

1\1\GINC-SC25\FOpt\UB3LYP\6-31G(d)\C3H6N1O1(2)\ROOT\16-Sep-2001\0\\#N
UB3LYP/6-31G(D) TEST SCF=DIRECT OPT=TIGHT MAXDISK=26214400\\CH2NHCOMe
radical UB3LYP / 6-31G(d) geom opt\\0,2\H,0.8992551135,0.,2.1248188299
\C,-0.169356388,0.,1.9820748476\H,-0.885991519,0.,2.7887828732\N,-0.63
66319189,0.,0.6871411159\C,0.1856851684,0.,-0.4287718583\C,-0.53200691

61,0.,-1.7670129332\H,-1.6240933518,0.,-1.6859919957\H,-0.2218958577,-0.8811374829,-2.3382023159\H,-0.2218958577,0.8811374829,-2.3382023159\O,1.4052110298,0.,-0.3271660408\H,-1.6365745186,0.,0.5383951023\\Version=DEC-AXP-OSF/1-G98RevA.9\State=2-A"\HF=-247.8643843\S2=0.755475\S2-1=0.\S2A=0.75002\RMSD=4.548e-09\RMSF=1.733e-06\Dipole=-1.4887988,0.,0.0253888\PG=CS [SG(C3H4N1O1),X(H2)]\\@

$MeC(O)OCH_2^{\bullet}$

1\1\GINC-SC32\Freq\UB3LYP\6-31G(d)\C3H5O2(2)\DJH501\02-Jun-2004\0\\#N UB3LYP/6-31G(D) SCF=TIGHT FREQ MAXDISK=39321600\\CH2OCOCH3 radical UB3LYP / 6-31G(d) freq\\0,2\C,-0.4200299744,0.1907298974,-0.0007649744\O,-0.2798839744,1.3898188974,0.0011880256\C,-1.7241709744,-0.5636521026,-0.0043469744\O,0.6370080256,-0.6896661026,0.0023290256\H,-2.5510979744,0.1461678974,-0.0390649744\H,-1.7724419744,-1.2362481026,-0.8670329744\H,-1.8040909744,-1.1818961026,0.8962970256\C,1.9051850256,-0.1765011026,0.0370180256\H,2.6728930256,-0.9208401026,-0.1130409744\H,2.0318410256,0.8881338974,-0.0967309744\\Version=DEC-AXP-OSF/1-G03RevB.05\State=2-A\HF=-267.7202621\S2=0.753529\S2-1=0.\S2A=0.750008\RMSD=3.140e-09\RMSF=1.396e-06\Dipole=-0.1060752,-0.7138068,-0.0901543\DipoleDeriv=1.6246121,-0.040066,0.0026134,-0.6828393,1.4438289,-0.0120791,-0.0091086,-0.0047168,0.2702013,-0.5950633,-0.1507957,0.0023889,0.3642111,-1.0383593,0.0074905,0.0030671,-0.001846,-0.3202474,-0.1628473,-0.1317167,0.0028502,-0.1881938,-0.0645748,-0.0002903,0.0135376,0.0073938,0.0521004,-1.4361288,0.1825215,0.0030218,0.3545264,-0.7117499,0.00606,-0.0089353,-0.0089288,-0.1352076,-0.0264519,0.0393555,-0.0027206,0.0723847,0.0050751,0.0035102,-0.0054167,0.0018439,0.0824871,0.0283609,-0.0035234,0.0214789,-0.0102244,0.0365568,-0.0754609,-0.0094937,-0.0811002,-0.0059572,0.0259485,-0.0093759,-0.0195979,-0.0138837,0.0460211,0.0717512,0.0096113,0.0750908,-0.0144199,0.537631,0.0339634,-0.0144478,0.1033607,0.2780924,0.0014251,-0.1174661,0.0207404,-0.2572525,-0.0184204,0.0237018,0.0039482,0.0360592,-0.005506,-0.0075971,0.073109,-0.0354463,0.1611462,0.0223593,0.0559355,0.000465,-0.0354009,0.0106156,0.0051904,0.0510952,0.0269693,0.1671496\Polar=49.8419568,-1.167835,37.5790404,-0.151483,-0.1005587,22.879088\PG=C01 [X(C3H5O2)]\

Table E2. Calculated Total Energies (0 K, Hartrees)[a]

	RMP2/6-311+G(2df,p)[b]	RMP2/G3large[b]
CH_4	–40.35356796	–40.36015706
$^{\bullet}CH_3$	–39.69644468	–39.70159948
$MeCONHCH_2CO_2Me$ (**1**)	–772.7824639	–475.4107229
$MeCONHCH^{\bullet}CO_2Me$ (**2**)	–772.1521235	–474.7822748
$CF_3CONHCH_2CO_2ME$ (**4**)	–772.7824639	–772.8079849
$MeCONHCH^{\bullet}CO_2Me$ (**5**)	–772.1521235	–772.1760476
$MeCONHCH(Me)CO_2Me$	–514.5569434	–514.5835432
$MeCONHC^{\bullet}(Me)CO_2Me$ (**93a**)	–513.9299441	–513.9550152
$MeCONHCH(CF_3)CO_2Me$	–811.981203	–812.010342
$MeCONHC^{\bullet}(CF_3)CO_2Me$ (**94a**)	–811.3396918	–811.3669765
$MeCO_2CH_2CO_2Me$	–495.233293	–495.2548591
$MeCO_2CH^{\bullet}CO_2Me$ (**95a**)	–494.593209	–494.6132193
$MeCOCH_2CH_2CO_2Me$	–459.2973161	–459.321037
$MeCOCH_2CH^{\bullet}CO_2Me$ (**96a**)	–458.6536539	–458.675758
$MeCO_2Me$	–267.79156	–267.8057895
$^{\bullet}CH_2C(O)OMe$	–267.75086	–267.1549448
MeCONHMe	–247.9188892	–247.9345014
$MeCONHCH_2^{\bullet}$	–247.2775387	–247.2916712
$MeC(O)OCH_2^{\bullet}$	–267.74996	–40.36015706
$MeCH=CHCH_2CO_2Me$	–384.1571633	–384.1792338
$MeCH=CHCH^{\bullet}CO_2Me$	–383.5383467	–383.5588545

[a]Electronic energies have been corrected with scaled (by 0.9806) B3-LYP/6-31G(d) zero-point vibrational energies. [b]Calculated on B3-LYP/6-31G(d) optimized geometries.

Table E3. Calculated Radical Stabilisation Energies (0 K, kJ mol^{-1})[a]

radical	RMP2/6-311+G(2df,p)	RMP2/G3large
2	79.6	79.1
5	70.3	69.9
93a	79.1	78.8
94a	41.0	39.9
95a	44.7	44.4
96a	35.3	34.9
$^{\bullet}CH_2C(O)OMe$	20.6	20.2
$MeCONHCH_2^{\bullet}$	41.4	41.3
$MeC(O)OCH_2^{\bullet}$	17.1	17.1
17	100.6	100.2

[a]Radical stabilization energies (RSEs) were calculated from the total energies in Table E2 as the energy changes in the isodesmic reactions $R^{\bullet} + CH_4 \rightarrow RH + {}^{\bullet}CH_3$. The RSEs correspond to the differences between the bond dissociation energies (BDEs) of methane and RH, and reflect the stability of $R^{\bullet}$ compared with $^{\bullet}CH_3$, relative to the corresponding closed-shell systems. Our reported RSEs correspond to values at 0 K.

Bromination Reactions

Treatment of *N*-benzoylglycine methyl ester 61 with *N*-bromosuccinimide.

N-Bromosuccinimide (16.6 mg, 0.09 mmol) was added to a solution of *N*-benzoylglycine methyl ester **61** (20 mg, 0.10 mmol) in carbon tetrachloride (5 mL), under nitrogen, and the mixture was heated at reflux for 30 min whilst being irradiated with a sunlamp. The mixture was then cooled and filtered. The filtrate was concentrated

under reduced pressure, to give *N*-benzoyl-α-bromoglycine methyl ester **90** as an off-white solid, with physical and spectroscopic properties consistent with those previously reported.[98] **^{1}H NMR** (300 MHz, $CDCl_3$): δ 3.92 (s, 3H), 6.68 (d, J = 9.0 Hz, 1H), 7.45.7.58 (m, 4H), 7.82.7.85 (m, 2H).

Treatment of methyl *O*$^{\alpha}$-benzoylglycolate 59 with *N*-bromosuccinimide

Treatment of methyl *O*-benzoylglycolate **59** with *N*-bromosuccinimide, as described above for reaction of the benzamide **61**, gave only unreacted starting materials, even after extended reaction times and when an excess of the succinimide was used.

Relative rates of reaction of 61 and 59 with *N*-bromosuccinimide

The relative rates of reaction of **61** and **59** with *N*-bromosuccinimide were determined in competitive experiments using mixtures of **61** and **59**. After treatment with a slight excess of the brominating agent, all of **61** was consumed after a reaction time of 30 min, but there was no evidence for any reaction of **59**, even after extended reaction times, within the limits of detection using ^{1}H NMR spectroscopy. On this basis the relative rates of reaction of **61** and **59** were determined to be 1.0 and <0.005 respectively.

Assay Procedures, Representative Data Sets and HPLC Traces

Interactions of 15, 64, 70, 72, 76, 79, 85, and 98a,b with PAM

Assays for PAM inhibition were performed with 3 mM ascorbic acid, 2 μM copper sulfate, 100 μg/mL bovine liver catalase, 0.01% Tween 20, 1% ethanol and 0.1 mM substrate [(*R*)-Tyr-(*S*)-Val-Gly], and varying concentrations of inhibitors in 100 mM MES buffer at pH 6.6. Assays were initiated by the addition of the appropriate amount of enzyme to give a final volume of 60 μL, then the mixtures were incubated at 37 °C for 1 h. The assays were quenched by the addition of 30 μL of 1 M NaOH, then the mixtures were neutralized with 30 μL of 1 M HCl. Two 20 μL aliquots were then taken and diluted to 110 μL with water. The duplicate diluted solutions were then analyzed directly using HPLC, and the ratio of substrate [(*R*)-Tyr-(*S*)-Val-Gly] to product [(*R*)-Tyr-(*S*)-Val-NH_2] determined by integration, to give the amount processed.

Assays for the binding strength of *N*-benzoyl-(*S*)-valylglycine **72** with PAM were performed with 3 mM ascorbic acid, 2 μM copper sulfate, 100 μg/mL bovine liver catalase, 0.01% Tween 20 and 1% ethanol, with varying concentrations of *N*-benzoyl-(*S*)-valylglycine **72** in 100 mM MES buffer at pH 6.6. Assays were initiated by the addition of the appropriate amount of enzyme to give a final volume of 20 μL, then the mixtures were incubated at 37 °C for 1 h. The assays were quenched by the addition of 10 μL of 1 M NaOH, then the mixtures were neutralized with 10 μL of 1 M HCl. Two 20 μL aliquots were then taken and diluted to 110 μL with water. The duplicate diluted solutions were then analyzed directly using HPLC, and the ratio of substrate [*N*-Bz-(*S*)-Val-Gly] to product [*N*-Bz-(*S*)-Val-NH_2] determined by integration, to give the amount processed.

The following figures E1, E2, E3, E4 and E5 are representative HPLC traces of assays of **64** at concentrations of 0, 2.0, 4.0, 8.0, 16.0 μM respectively. The first peak observed in the trace is that of the processed substrate whilst the second peak is starting material.

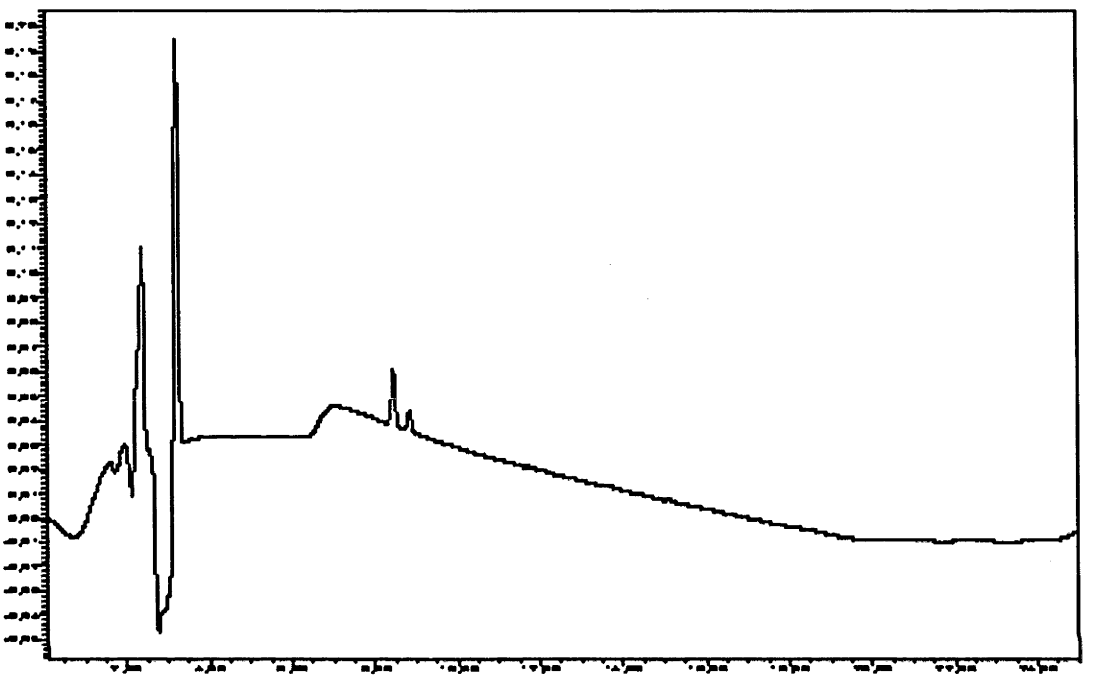

Figure E1. HPLC trace of an assay of **64** at an inhibitor concentration of 0 μM

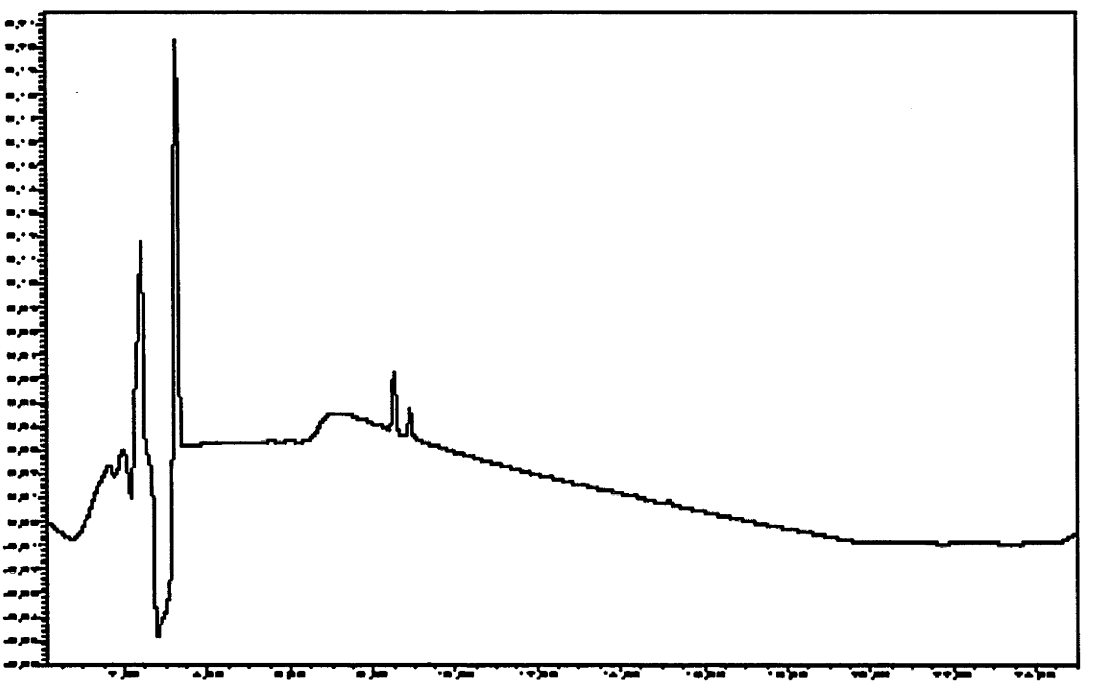

Figure E2. HPLC trace of an assay of **64** at an inhibitor concentration of 2.0 μM

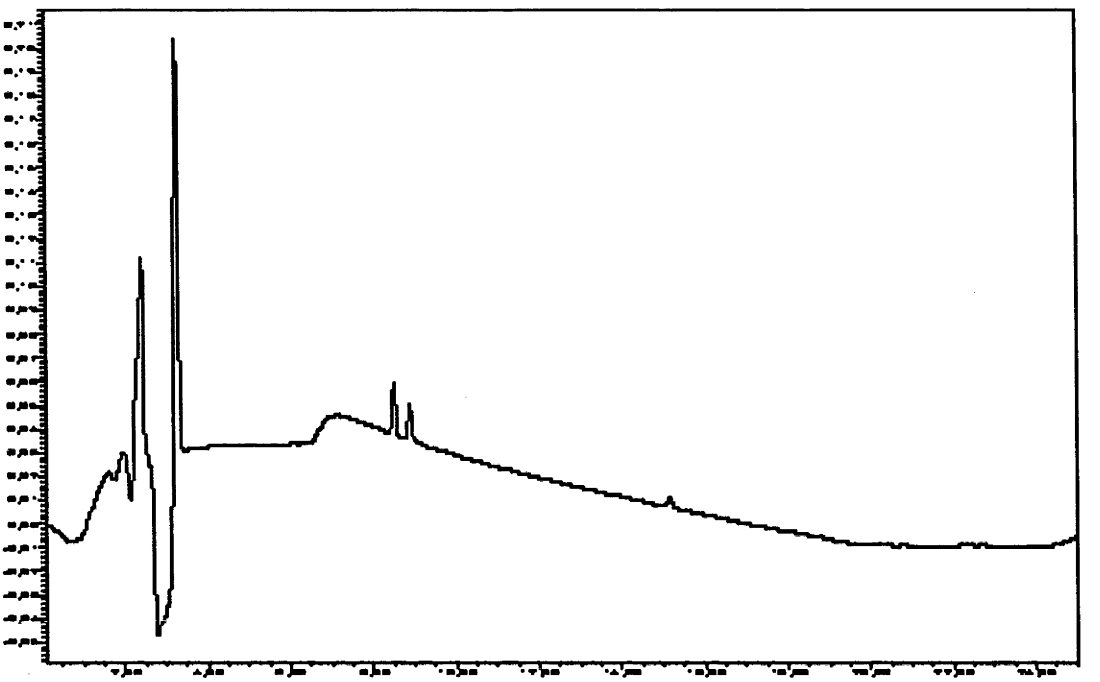

Figure E3. HPLC trace of an assay of **64** at an inhibitor concentration of 4.0 μM

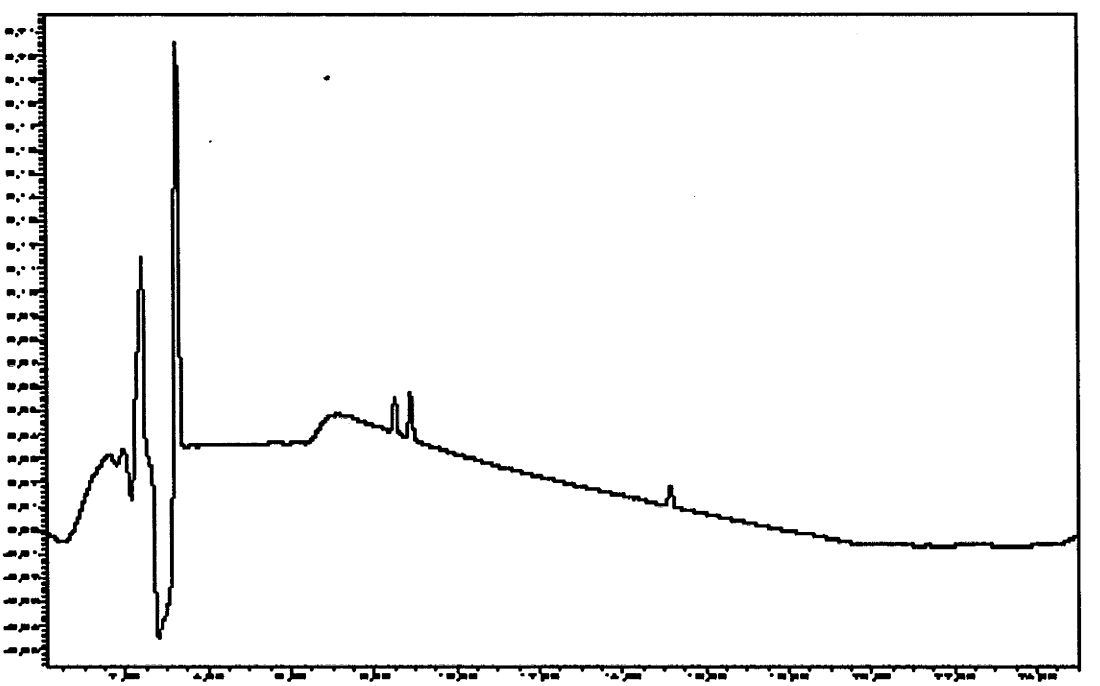

Figure E4. HPLC trace of an assay of **64** at an inhibitor concentration of 8.0 μM

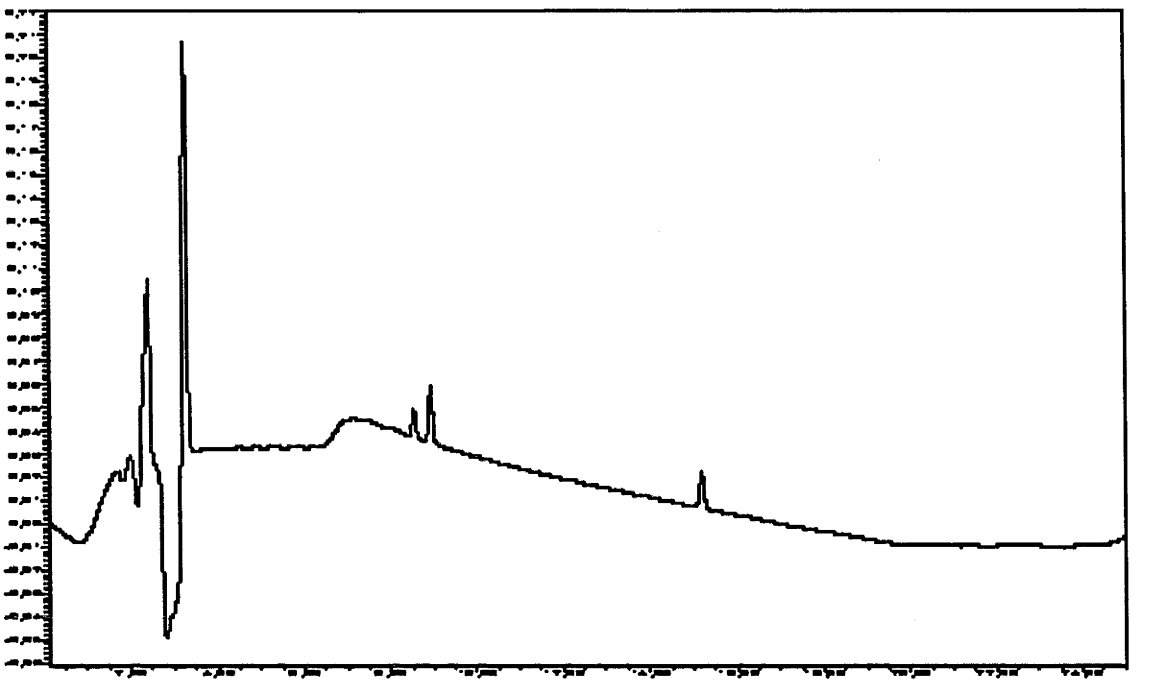

Figure E5. HPLC trace of an assay of **64** at an inhibitor concentration of 16.0 μM

Peak integrations were then used to determine the percentage turnover for each assay. The following table E4 is a representative data set for assays performed with **64** against PAM.

Table E4. Representative data set for assays performed with **64** against PAM.

(I)	Turnover 1	Turnover 2	Average	Sdev	Sdev (%)
0.00	0.91	0.87	0.89	0.0304	3.4221
2.00	0.91	0.86	0.88	0.0304	3.4376
4.00	0.88	0.82	0.85	0.0445	5.2378
8.00	0.81	0.79	0.80	0.0127	1.5850
16.00	0.81	0.78	0.79	0.0191	2.4121
32.00	0.72	0.60	0.66	0.0806	12.1952

The first column lists inhibitor concentration. As assays were performed in duplicate, the second and third columns list substrate turnover. The fourth column lists substrate turnover as an average of the values given in columns 2 and 3.

The inverse of the average rate of substrate turnover were then plotted against inhibitor concentration to produce a Dixon plot. A representative Dixon plot for the assay of **64** against PAM is provided below in Figure E6.

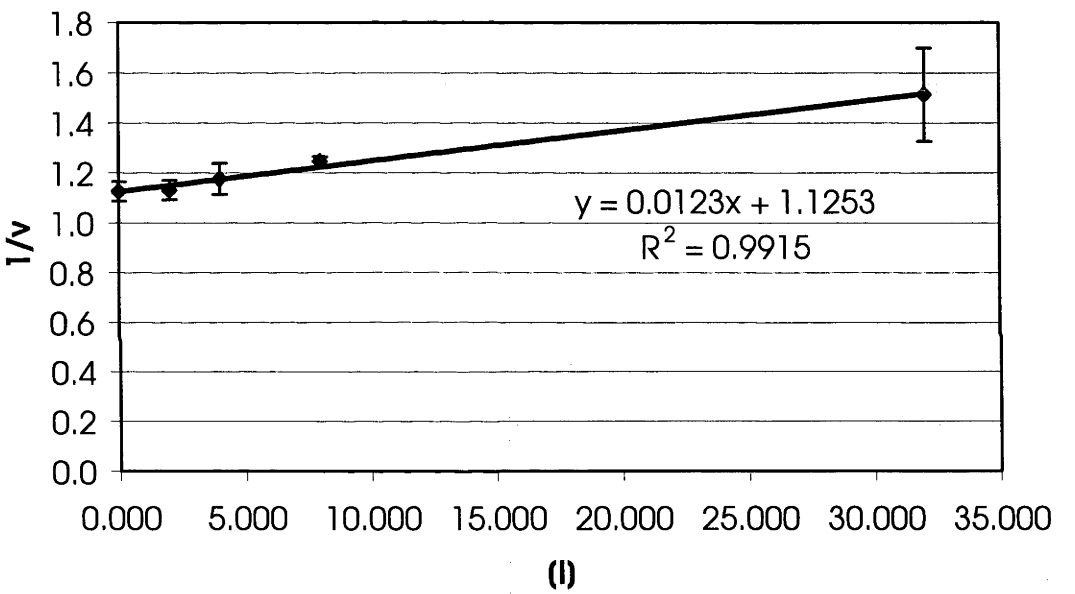

Figure E6. Representative Dixon plot for the assay of **64** against PAM.

The IC_{50} value of **64** was then obtained as the value of –x when y = 0 from the equation obtained for the line of best fit illustrated in Figure E6.

Synthetic Procedures

Methyl *O*-benzoylglycolate 59

Methyl bromoacetate (60 μL, 0.63 mmol) and potassium carbonate (100 mg, 0.73 mmol) were added to a solution of benzoic acid (50 mg, 0.41 mmol) in acetone (30 mL) and the mixture was heated at reflux overnight, then it was cooled and concentrated under reduced pressure. Chromatography of the residue gave the title compound (40 mg, 50%) as a clear oil. **^{1}H NMR** (300 MHz, $CDCl_3$): δ 3.80 (s, 3H), 4.87 (s, 2H), 7.44-7.62 (m, 3H), 8.08-8.12 (m, 2H). **^{13}C NMR** (75 MHz, $CDCl_3$): δ 168.4, 166.1, 133.7, 130.1, 129.3, 128.7, 61.2, 52.5. **HRMS (EI)** calcd. For $C_{10}H_{10}O_4$ [$M^{+\cdot}$]: *m/z* 194.0579, found 194.0579. **Anal.** Calcd. for $C_{10}H_{10}O_4$: C, 61.85, H, 5.19. Found: C, 61.84, H, 5.22%.

Benzyl *O*$^{\alpha}$-(*N*-Acetyl-(*S*)-phenylalanyl-(*S*)-phenylalanyl)glycolate 63

Benzyl bromoacetate (0.46 mL, 2.9 mmol) was added to a suspension of *N*–acetyl-(*S*)-phenylalanyl-(*S*)-phenyalanine **62** (0.50 g, 1.0 mmol) and potassium carbonate (0.14 g, 1.0 mmol) in acetone (100 mL). The mixture was stirred and heated at reflux for 24 h, then it was cooled and filtered. The filtrate was concentrated under reduced pressure to give a colorless solid which was recrystallized from ethyl acetate/hexanes to give the title compound (0.60 g, 84%) as a colorless powder. **Mp** 169 °C. **[α_D]** –27.12° (*c* 0.001, ethanol). **^{1}H NMR** (300 MHz, CD_3OD): δ 1.82 (s, 3H), 2.75 (dd, *J* = 14.1, 9.3 Hz, 1H), 2.94 (dd, *J* = 14.1, 9.3 Hz, 1H), 3.05 (dd, *J* = 14.1, 5.7 Hz, 1H), 3.22 (dd, *J* = 14.1, 5.1 Hz, 1H), 4.60 (dd, *J* = 9.3, 5.7 Hz, 1H), 4.68 (d, *J* = 15.9 Hz, 1H), 4.75 (d, *J* = 15.9 Hz, 1H), 4.76 (dd, *J* = 9.3, 5.1 Hz, 1H), 5.20 (s, 2H), 7.15–7.38 (m, 15H). **^{13}C NMR** (75 MHz, CD_3OD): δ 174.4, 173.8, 172.9, 169.9, 139.3, 138.9, 137.7, 131.2, 131.1, 130.5, 130.4, 130.3, 130.2, 128.7, 125.5, 68.9, 63.2, 56.5, 55.6, 39.6, 39.1, 23.2. **MS (ESI)**

(+ve): *m/z* 503.2 [M+H$^+$], 525.1 [M+Na$^+$], 541.1 [M+K$^+$]. **HRMS (EI)** calcd. for $C_{29}H_{30}N_2O_6$ [M$^{+\bullet}$] 502.2104, found 502.2103. **Anal.** Calcd. for $C_{29}H_{30}N_2O_6$: C, 69.31; H, 6.02; N, 5.57. Found: C, 69.24; H, 6.43; N, 5.49%.

O$^{\alpha}$-(*N*-Acetyl-(*S*)-phenylalanyl-(*S*)-phenylalanyl)glycolic Acid 64

Benzyl *O*$^{\alpha}$-(*N*-acetyl-(*S*)-phenylalanyl-(*S*)-phenylalanyl)glycolate **63** (0.30 g, 0.60 mmol) was added to a suspension of activated palladium on carbon (10%, 30 mg) in tetrahydrofuran (50 mL) under a hydrogen atmosphere and the mixture was stirred overnight at room temperature, then it was filtered through celite. The filtrate was concentrated under reduced pressure to give a colorless solid which was recrystallized from ethanol/hexanes to give the title compound (203 mg, 82%) as colorless crystals. A portion of this material was purified by HPLC eluting with mixtures of acetonitrile and 0.1% acetic acid in water. **Mp** 152 °C. **[α_D]** –23.8° (*c* 0.001, ethanol). **^{1}H NMR** (300 MHz, CD_3OD): δ 1.82 (s, 3H), 2.77 (dd, *J* = 14.1, 9.3 Hz, 1H), 2.99 (dd, *J* = 14.1, 9.0 Hz, 1H), 3.07 (dd, *J* = 14.1, 5.4 Hz. 1H), 3.27 (dd, *J* = 14.1, 4.8 Hz, 1H), 4.60 (d, *J* = 15.9 Hz, 1H), 4.59–4.64 (m, 1H), 4.64 (d, *J* = 15.9 Hz, 1H), 4.74–4.82 (m, 1H), 7.14–7.28 (m, 10H). **^{13}C NMR** (75 MHz, CD_3OD): δ 172.3, 171.8, 170.9, 137.3, 136.9, 129.3, 129.1, 128.3, 128.2, 126.7, 126.5, 61.0, 54.5, 53.7, 37.6, 37.1, 21.2. **MS (ESI)** (+ve): *m/z* 435.1 [M+Na$^+$], 451.1 [M+K$^+$]. **Anal.** Calcd. for $C_{22}H_{24}N_2O_6.1/4H_2O$: C, 63.37; H, 5.92; N, 6.72. Found : C, 63.45; H, 5.95; N, 6.72%.

N-Benzoyl-(*S*)-valine Methyl Ester 67

S-Valine (1.0 g 8.5 mmol) was added to methanol (100 mL), which had been pretreated with thionyl chloride (1.2 g 10.3 mmol), and allowed to stir overnight. The solution was evaporated under reduced pressure to yield a white powder, which was redissolved in methanol and evaporated under reduced pressure twice to remove excess hydrochloric acid. The resultant colourless hydrochloride salt was dissolved in dichloromethane (50 mL) by the addition of triethylamine (1.7 g 17.1 mmol), and benzoyl chloride (1.2 g, 8.5 mmol) was added dropwise with stirring. A precipitate formed and the mixture was stirred overnight. The mixture was washed with 2M hydrochloric acid (2 x 50 mL) and then saturated sodium bicarbonate solution (2 x 50 mL). The organic layer was then dried, filtered and evaporated under reduced pressure to obtain the crude product which was then recrystallised from ethyl acetate/hexane to give the title compound as colourless needles (1.05 g, 53%). **Mp** 86 °C (lit.,[66] 86 °C). **^{1}H NMR** (300 MHz, $CDCl_3$): δ 0.96 (t, *J* = 6.3 Hz, 6H), 2.20-2.27 (m, 1H), 3.72 (s, 3H), 4.74 (dd, *J* = 5.1, 8.7 Hz, 1H), 6.75 (d, *J* = 8.4 Hz, 1H), 7.38-7.49 (m, 3H), 7.76-7.79 (m, 2H). **^{13}C NMR** (75 MHz, $CDCl_3$): δ 172.8, 167.5, 134.3, 131.9, 128.7, 127.3, 57.7, 52.4, 31.7, 19.2, 18.2.

N-Benzoyl-(*S*)-valine 68

N-Benzoyl-(*S*)-valine Methyl Ester **67** (5.53 g, 23.5 mmol) was dissolved in tetrahydrofuran (200 mL) and 2M sodium hydroxide (200 mL) and allowed to stir for three hours. The solution was subjected to rotary evaporation to remove the tetrahydrofuran and the aqueous layer was acidified to pH 3.0 with 5M hydrochloric acid. The solution was then washed with ethyl acetate (3 x 50 mL) and the combined

organics were dried, filtered and concentrated under reduced pressure to give a crude white solid. The crude was then recrystallised from hot ethanol to give the title compound (3.17 g, 61%). **Mp** 129 °C (lit.,[99] 127 °C). **^{1}H NMR** (300 MHz, $CDCl_3$): δ 1.04 (d, *J* = 6.9 Hz, 6H), 2.28 (m, 1H), 4.51 (d, *J* = 6.6 Hz, 1H), 7.41-7.52 (m, 3H), 7.82-7.85 (d, 2H). **^{13}C NMR** (75 MHz, $CDCl_3$): δ 173.9, 169.5, 134.3, 131.7, 128.4, 127.4, 58.7, 30.6, 17.8.

Benzyl *O*$^{\alpha}$-(*N*-Benzoyl-(*S*)-valyl)glycolate 69

N-Benzoyl-(*S*)-valine **68** (0.36 g, 1.62 mmol) was dissolved in acetone (100 mL) to which potassium carbonate (134 mg, 1.62 mmol) and benzyl bromoacetate (0.25 mL, 1.62 mmol) were then added. The resulting suspension was heated at reflux overnight, then it was allowed to cool and was filtered. The filtrate was concentrated under reduced pressure and the residual colorless solid was recrystallized from ethyl acetate to afford the title compound (0.54 g, 90%) as a colorless solid. **Mp** 92 °C. **$[\alpha]_D$** –22.9 °C (*c* 0.001, ethanol). **^{1}H NMR** (300 MHz, $CDCl_3$): δ 1.04 (d, *J* = 6.9 Hz, 3H), 1.07 (d, *J* = 6.9 Hz, 3H), 2.34–2.45 (m, 1H), 4.64 (d, *J*= 15.9 Hz, 1H), 4.86 (d, *J* = 15.9 Hz, 1H), 4.91 (dd, *J* = 8.7, 3.9 Hz, 1H), 5.21 (s, 2H), 6.60 (d, *J* = 8.7 Hz, 1H), 7.33–7.55 (m, 8H), 7.79–7.82 (m, 2H). **^{13}C NMR** (75 MHz, $CDCl_3$): δ 171.8, 167.6, 167.4, 135.1, 134.3, 132.0, 128.9, 128.7, 127.3, 67.5, 61.4, 57.4, 31.7, 19.3, 17.8. **HRMS (EI)** calcd. for $C_{21}H_{23}NO_5$ [$M^{+\bullet}$] 369.1576, found 369.1574. **Anal.** Calcd. for $C_{21}H_{23}NO_5$: C, 68.28; H, 6.28; N, 3.79. Found: C, 68.38; H, 6.60; N, 3.67%.

O$^{\alpha}$-(*N*-Benzoyl-(*S*)-valyl)glycolic Acid 70

Benzyl O^{α}-(*N*-benzoyl-(*S*)-valyl)glycolate **69** (0.5 g, 1.35 mmol) was dissolved in tetrahydrofuran (100 mL) to which activated palladium on carbon (20%, 100 mg) was then added. The reaction vessel was purged with hydrogen and evacuated, three times, and the solution was then stirred under a hydrogen atmosphere for 12 h at room temperature. The suspension was then filtered through celite and the filtrate was concentrated under reduced pressure to give the title compound (358 mg, 95%) as a colorless solid. A portion of this material was purified by HPLC eluting with mixtures of acetonitrile and 0.1% acetic acid in water. **Mp** 100 °C. **[α_D]** –12.5° (*c* 0.001, ethanol). **^{1}H NMR** (300 MHz, CD_3OD): δ 1.05 (d, *J* = 5.7 Hz, 3H), 1.07 (d, *J* = 6.0 Hz, 3H), 2.32–2.38 (m, 1H), 4.36 (d, *J* = 15.0 Hz, 1H), 4.63 (d, *J* = 6.6 Hz, 1H), 4.64 (d, *J* = 15.0 Hz, 1H), 7.43–7.56 (m, 3H), 7.85–7.88 (m, 2H). **^{13}C NMR** (75 MHz, CD_3OD): 171.4, 169.8, 169.6, 134.2, 131.6, 128.3, 127.4, 60.9, 58.6, 30.6, 18.5, 17.7. **HRMS (EI)** calcd. for $C_{14}H_{17}NO_5$ [$M^{+\bullet}$] 279.1107, found 279.1105. **Anal.** Calcd. for $C_{14}H_{17}NO_5$: C, 60.21; H, 6.13; N, 5.02. Found: C, 59.92; H, 6.27; N, 4.84%.

N-Benzoyl-(*S*)-valylglycine *tert*-butyl ester 71

Glycine hydrochloride *tert*-butyl ester (0.49 g, 2.3 mmol), BOP (1.3 g, 2.9 mmol) and diisopropylethylamine (1.0 mL, 4.52 mmol) were added to a solution of *N*-benzoyl-(*S*)-valine **68** (0.64 g, 2.9 mmol) in dichloromethane (100 mL). The solution was allowed to stir overnight at room temperature before it was concentrated under reduced pressure. The residue was taken up in ethyl acetate (50 mL) and the solution was washed with saturated aqueous sodium bicarbonate (3 × 50 mL) and aqueous

hydrochloric acid (1 M, 50 mL), then it was dried and concentrated under reduced pressure. The solid residue was recrystallized from ethyl acetate/hexanes to give the title compound (0.67 g, 89%). **Mp** 172 °C. $[\alpha]_D$ –1.3° (*c* 0.001, ethanol). **^{1}H NMR** (300 MHz, $CDCl_3$): δ 1.02 (d, *J* = 5.8 Hz, 3H), 1.04 (d, *J* = 6.1 Hz, 3H), 1.46 (s, 9H), 2.24 (m, 1H), 3.85 (dd, *J* = 18.2, 4.8 Hz, 1H), 4.04 (dd, *J* = 18.2, 5.5 Hz, 1H), 4.55 (dd, *J* = 8.7, 6.7 Hz, 1H), 6.65 (broad, 1H), 6.89 (d, *J* = 8.7 Hz, 1H), 7.39 (m, 3H), 7.81 (m, 2H). **^{13}C NMR** (75 MHz, $CDCl_3$): δ 171.5, 168.7, 167.6, 134.3, 132.0, 128.8, 127.3, 82.6, 58.9, 42.3, 31.7, 28.3, 19.5, 18.5. **HRMS (EI)** calcd. for $C_{18}H_{26}N_2O_4$ [$M^{+\bullet}$] *m/z* 334.1892, found 334.1892. **Anal.** Calcd. for $C_{18}H_{26}N_2O_4$: C, 64.65; H, 7.84; N, 8.38. Found: C, 64.48; H, 8.02; N, 8.22%.

N-Benzoyl-(*S*)-valylglycine 72

N-Benzoyl-(*S*)-valylglycine *tert*-butyl ester **71** (29 mg, 0.086 mmol) was dissolved in dichloromethane (20 mL), to which triethylsilane (45 μL) and trifluoroacetic acid (0.85 mL) were then added. The mixture was stirred overnight at room temperature before it was concentrated under reduced pressure. The residue was recrystallized from ethyl acetate/hexanes to give the title compound (25 mg, 88%) as a colorless solid. **Mp** 180 °C. $[\alpha]_D$ –32.2° (*c* 0.001, ethanol). **^{1}H NMR** (300 MHz, CD_3OD): δ 1.04 (d, *J* = 6.6 Hz, 3H), 1.06 (d, *J* = 6.6 Hz, 3H), 2.19–2.26 (m, 1H), 3.88 (d, *J* = 18.0 Hz, 1H), 4.02 (d, *J* = 18.0 Hz, 1H), 4.45 (d, *J* = 7.8 Hz, 1H), 7.43–7.56 (m, 3H), 7.82–7.85 (m, 2H). **^{13}C NMR** (75 MHz, CD_3OD): δ 173.1, 171.5, 169.1, 134.2, 131.7, 128.4, 127.3, 59.6, 40.6, 30.9, 18.7, 17.9. **MS (ESI)** (+ve): *m/z* 278.9 [$M+H^+$], 301.3 [$M+Na^+$]. **Anal.** Calcd. for

$C_{14}H_{18}N_2O_4$: C, 60.42; H, 6.52; N, 10.07. Found: C, 60.34; H, 6.69; N, 9.95%.

N-Benzoyl-(*S*)-valinamide 73

N-Benzoyl-(*S*)-valine methyl ester **67** (0.2 g, 0.85 mmol) was dissolved in methanol (5 mL) and cooled in dry ice. To this cooled solution, ammonia was added and the mixture was placed in a sealed pressurised vessel and stirred overnight. The solution was then concentrated under reduced pressure and the crude white solid taken up in ethyl acetate and filtered to wash away any of the remaining starting material. Recrystallisation of the product from hot ethanol then gave the title compound as a white solid (0.1 g, 52%). **Mp**. 221-223 °C (lit.,[100] 220-221 °C). **^{1}H NMR** (300 MHz, CD_3OD): δ 1.02 (t, J = 6.3 Hz, 6H), 2.14-2.12 (m, 1H), 4.40 (d, J = 7.5 Hz, 1H), 7.44-7.55 (m, 3H), 7.83-7.85 (m, 2H). **MS (ESI)** (+ve): *m/z* 221.1 [M+H$^+$], 243.1 [M+Na$^+$].

Benzyl *O*$^\alpha$-decanoylglycolate 75

Decanoic acid **74** (0.20 g, 1.2 mmol) was dissolved in acetone (50 mL) to which potassium carbonate (0.16 g, 1.2 mmol) and benzyl bromoacetate (0.14 mL, 1.2 mmol) were added. The mixture was heated at reflux for 12 h, then it was filtered. The filtrate was concentrated under reduced pressure and the residual oil was subjected to column chromatography (ethyl acetate/hexanes) to give the title compound (196 mg, 52%) as a colorless oil. **^{1}H NMR** (300 MHz, $CDCl_3$): δ 0.90 (t, J = 6.9 Hz, 3H), 1.28 (m, 12H), 1.65 (m, 2H), 2.42 (t, J = 7.5 Hz, 2H), 4.65 (s, 2H), 5.19 (s, 2H), 7.35 (m, 5H). **^{13}C NMR** (75 MHz, $CDCl_3$): δ 173.3, 168.0, 135.3, 128.9, 128.8, 128.6, 67.4, 60.9, 34.2,

32.3, 29.8, 29.7, 29.5, 25.2, 23.1, 14.6. **HRMS (EI)** calcd. for $C_{19}H_{28}O_4$ [$M^{+\bullet}$] 320.1988, found 320.1989.

O$^{\alpha}$-Decanoylglycolic acid 76

Benzyl *O*$^{\alpha}$-decanoylglycolate **75** (0.78 g, 2.4 mmol) was dissolved in methanol (50 mL), to which activated palladium on carbon (10%, 156 mg) was added. The mixture was placed under an atmosphere of hydrogen and stirred overnight at room temperature. The suspension was then filtered through celite, and the filtrate was concentrated under reduced pressure, to give a colorless solid, which was recrystallized from ethyl acetate/hexanes to give the title compound (0.45 g, 80%) as a colorless solid. Mp 54 °C. **^{1}H NMR** (300 MHz, $CDCl_3$): δ 0.90 (t, *J* = 6.9 Hz, 3H), 1.30 (m, 12H), 1.56–1.67 (m, 2H), 2.41 (t, *J* = 7.5 Hz, 2H), 4.59 (s, 2H). **^{13}C NMR** (75 MHz, CD_3OD): δ 175.5, 172.2, 62.3, 35.4, 33.9, 31.4, 31.3, 31.0, 26.7, 24.6, 15.3. **HRMS (EI)** calcd. for $C_{12}H_{23}O_4$ [M+H^+]: 231.1596, found 231.1599. **Anal.** Calcd. for $C_{12}H_{22}O_4$: C, 62.58; H, 9.63. Found: C, 62.21; H, 9.81%.

Benzyl *O*$^{\alpha}$-benzoylglycolate 78

Benzoic acid **77** (5.4 g, 44 mmol) was added to a suspension of potassium carbonate (6.1 g, 44 mmol) in acetone (100 mL). Benzyl bromoacetate (6.9 mL, 44 mmol) was then added and the resulting suspension was heated at reflux overnight. After cooling, the mixture was filtered and the filtrate was concentrated under reduced pressure to give the title compound (10.8 g, 91%) as a colorless solid. **Mp** 54 °C. **^{1}H NMR** (300 MHz, $CDCl_3$): δ 4.86 (s, 2H), 5.20 (s, 2H), 7.32 (m, 5H), 7.41 (m, 2H), 7.54 (m, 1H),

8.07 (m, 2H). **^{13}C NMR** (75 MHz, $CDCl_3$): δ 167.4, 165.6, 134.9, 133.2, 129.7, 128.9, 128.4, 128.3, 128.2, 128.1, 66.9, 61.0. **MS** (EI): *m/z* 270 ($M^{+\bullet}$, 5%), 211 (12), 163 (12), 148 (65), 120 (20), 105 (100), 91 (85), 77 (60). **HRMS (EI)** calcd. for $C_{16}H_{14}O_4$ [$M^{+\bullet}$] *m/z* 270.0892, found 270.0892. **Anal**. Calcd. for $C_{16}H_{14}O_4$: C, 71.10, H, 5.22. Found: C, 71.05, H, 5.27%.

O$^{\alpha}$-Benzoylglycolic acid 79

Palladium on carbon (10%, 2 g) was placed in a dry flask which was then purged with nitrogen and evacuated, three times, followed by purging with hydrogen and evacuating, three times. The vessel was then kept under an atmosphere of hydrogen. Benzyl *O*$^{\alpha}$-benzoylglycolate **78** (2.0 g, 7.4 mmol) in methanol (60 mL) was added and the resulting suspension was stirred overnight at room temperature. The suspension was then filtered through celite, and the filtrate was concentrated under reduced pressure to give the title compound (1.3 g, 98%) as a colorless solid. A portion (1.1 g) of this material was recrystallised from chloroform to give colorless crystals (0.47 g). **Mp** 110 °C (lit.[13] 111–112 °C). **^{1}H NMR** (300 MHz, CD_3OD) δ 4.83 (s, 2H), 7.48 (m, 2H), 7.60 (m, 1H), 8.07 (m, 2H). **^{13}C NMR** (75 MHz, $CDCl_3$): δ 172.4, 167.4, 134.2, 130.7, 130.5, 129.3, 62.8. **MS (EI)**: *m/z* 180 ($M^{+\bullet}$, 24%), 148 (10), 136 (15), 105 (100), 91 (18), 77 (60). **HRMS (EI)** calcd. for $C_9H_8O_4$ [$M^{+\bullet}$] *m/z* 180.0423, found 180.0424. **Anal**. Calcd. for $C_9H_8O_4$: C, 60.00, H, 4.48. Found C, 59.74 , H, 4.52%.

tert-Butyl (*N*-acetylphenylalanyl)acetate 82

A suspension of *N*-acetylphenylalanine **80** (0.50 g, 2.4 mmol) and 1,1'-carbonyldiimidazole (0.41 g, 2.5 mmol) in tetrahydrofuran (10 mL) was stirred at room temperature under a nitrogen atmosphere for 0.5 h. It was then added dropwise to a solution that had been prepared from tetrahydrofuran (5 mL), diisopropylamine (2 mL, 14 mmol), *n*-butyl lithium (1.6 M in hexanes, 6 mL, 9.4 mmol) and *tert*-butyl acetate (1.3 mL, 9.6 mmol), maintained at –78 °C. The resulting mixture was stirred for 40 min, then aqueous hydrochloric acid (1 M, 25 mL) was added and the solution was allowed to warm to room temperature. It was then extracted with ethyl acetate (3 × 50 mL) and the combined organic extracts were dried and concentrated under reduced pressure to give a colorless oil (0.58 g, 79%). **^{1}H NMR** (300 MHz, $CDCl_3$): δ 1.45 (s, 9H), 1.95 (s, 3H), 3.02 (dd, J = 14.1, 6.5 Hz, 1H), 3.16 (dd, J = 14.1, 6.5 Hz, 1H), 3.35 (d, J = 15.9 Hz, 1H), 3.41 (d, J = 15.9 Hz, 1H), 4.92 (apparent q, J = 6.5 Hz, 1H), 6.10 (d, J = 6.5 Hz, 1H), 7.14 (m, 2H), 7.25 (m, 3H). **^{13}C NMR** (75 MHz, $CDCl_3$): δ 202.1, 170.2, 166.2, 136.3, 129.3, 128.8, 127.2, 82.3, 59.4, 48.4, 36.6, 28.0, 23.0. **HRMS (EI)** calcd. for $C_{17}H_{23}NO_4$ [$M^{+\bullet}$] *m/z* 305.1627, found 305.1633. **Anal.** Calcd. for $C_{17}H_{23}NO_4$: C, 66.86; H, 7.59; N, 4.59. Found C, 67.04; H, 7.20; N, 4.32%.

Benzyl 3-(*N*-acetylphenylalanyl)-3-(*tert*-butoxycarbonyl)propionate 83

A solution of *tert*-butyl (*N*-acetylphenylalanyl)acetate **82** (0.84 g, 2.75 mmol) in tetrahydrofuran (10 mL) was added to a solution of sodium hydride (59 mg, 2.75 mmol) in tetrahydrofuran (20 mL). To this solution, benzyl 2-bromoacetate (0.44 mL, 2.75 mmol) in dichloromethane (5 mL) was added dropwise. The mixture was stirred at room temperature for 24 h, then aqueous hydrochloric acid (1 M, 100 mL) was added. The solution was extracted with ethyl acetate (3 × 70 mL) and the combined organic

extracts were dried and concentrated under reduced pressure. The residue was chromatographed on silica, eluting with a gradient of ethyl acetate/hexanes, to give a 1:1 mixture of diastereomers of the title compound as a colorless oil (0.77 g, 62%). **^{1}H NMR** (300 MHz, $CDCl_3$): δ 1.37 (s, 9H), 1.40 (s, 9H), 1.89 (s, 3H), 1.92 (s, 3H), 2.85–3.06 (m, 6H), 3.18 (dd, *J* = 14.4, 6.5 Hz, 1H), 3.24 (dd, *J* = 14.1, 6.5 Hz, 1H), 4.04 (t, *J* = 6.9 Hz, 1H), 4.22 (t, *J* = 7.2 Hz, 1H), 5.08 (s, 2H), 5.08 (apparent q, *J* = 6.5 Hz, 1H), 5.10 (s, 2H), 5.29 (apparent q, *J* = 6.5 Hz, 1H), 6.23 (d, *J* = 6.5 Hz, 1H), 6.25 (d, *J* = 6.5 Hz, 1H), 7.14–7.35 (m, 10H). **^{13}C NMR** (75 MHz $CDCl_3$): δ 203.3, 202.8, 171.7, 171.2, 170.3, 169.6, 167.0, 166.7, 136.9, 136.3, 135.7, 129.5, 128.8, 128.7, 128.6, 128.5, 128.4, 127.2, 127.0, 83.7, 83.1, 67.0, 66.9, 58.9, 58.8, 52.9, 51.9, 37.3, 35.9, 33.0, 32.2, 27.9, 23.2, 23.1. **HRMS (EI)** calcd. for $C_{26}H_{31}NO_6$ [$M^{+\bullet}$] *m/z* 453.2151, found 453.2147.

Benzyl 3-(*N*-acetylphenylalanyl)propionate 84

A solution of benzyl 3-(*N*-acetylphenylalanyl)-3-(*tert*-butoxycarbonyl)propionate **83** (0.40 g, 0.83 mmol) and trifluoroacetic acid (3 mL) in dichloromethane (30 mL) was heated at reflux for 24 h, then it was cooled and concentrated under reduced pressure. The residual oil was chromatographed on silica, eluting with a gradient of ethyl acetate/hexanes, to give the title compound as a colorless solid (0.19 g, 70%). **Mp** 39 °C. **^{1}H NMR** (300 MHz, $CDCl_3$): δ 1.94 (s, 3H), 2.59–2.64 (m, 2H), 2.73–2.79 (m, 2H), 2.97 (dd, *J* = 14.1, 6.5 Hz, 1H), 3.13 (dd, *J* = 14.1, 6.5 Hz, 1H), 4.87 (apparent q, *J* = 6.5 Hz, 1H), 5.10 (s, 2H), 6.20 (d, *J* = 6.5 Hz, 1H), 7.12–7.37 (m, 10H). **^{13}C NMR** (75 MHz, $CDCl_3$): δ 207.2, 172.5, 170.2, 136.2, 135.9, 129.4, 128.9, 128.8, 128.5, 128.4, 127.3, 66.8, 59.2, 37.3, 35.5, 28.0, 23.2. **HRMS (EI)** calcd. for $C_{21}H_{23}NO_4$ [$M^{+\bullet}$]

m/z 353.1627, found 353.1643. **Anal.** Calcd. for $C_{21}H_{23}NO_4$: C, 71.37; H, 6.56; N, 3.96. Found: C, 70.98; H, 6.43; N, 3.96%.

3-(*N*-Acetylphenylalanyl)propionic Acid 85

A suspension of benzyl 3-(*N*-acetylphenylalanyl)propionate **84** (66 mg, 0.19 mmol) and activated palladium on carbon (12 mg) in tetrahydrofuran (20 mL) was stirred under an atmosphere of hydrogen for 24 h, then it was filtered through celite. The filtrate was concentrated under reduced pressure and the residual oil was recrystallized from chloroform to give the title compound as a colorless solid (30 mg, 61%). **Mp** 53 °C. **^{1}H NMR**, (300 MHz, CD_3COCD_3): δ 1.86 (s, 3H), 2.53 (t, *J* = 6.6 Hz, 2H), 2.74–2.88 (m, 3H), 3.17 (dd, *J* = 14.1, 14.1 Hz, 1H), 4.64–4.72 (m, 1H), 7.18–7.28 (m, 5H), 7.47 (d, *J* = 7.2 Hz, 1H). **^{13}C NMR** (75 MHz, CD_3COCD_3): 207.9, 175.1, 172.0, 137.5, 129.0, 128.3, 126.5, 59.9, 35.9, 34.6, 27.4, 21.0. **HRMS (EI)** calcd. for $C_{14}H_{17}NO_4$ [$M^{+\bullet}$] *m/z* 263.1158, found 263.1158. **Anal.** Calcd. for $C_{14}H_{17}NO_4$: C, 63.87; H, 6.51; N, 5.32. Found: C, 63.58; H, 6.52; N, 5.38%.

Experimental for Chapter 2

Synthetic Procedures

N-Benzoyl-α-acetoxyglycine Methyl Ester 14

N-Benzoylglycine **61** (200 mg, 1.03 mmol) and *N*-bromo succinimide (185 mg, 1.04 mmol) was stirred in carbon tetrachloride (30 mL) under nitrogen at reflux. The refluxing solution was then irradiated with a 300W sun lamp for 10 minutes and

allowed to cool, after which sodium acetate (253 mg, 3.09 mmol) was added. The solution was stirred overnight, filtered and purified by column chromatograph eluting with mixtures of ethyl acetate/hexane to give the title compound as clear oil (153 mg, 60%). **^{1}H NMR** (300 MHz, $CDCl_3$): δ 2.77 (s, 3H), 3.81 (s, 3H), 6.77 (d, J = 8.4 Hz, 1H), 7.41-7.55 (m, 4H), 7.79-7.82 (m, 2H). **^{13}C NMR** (75 MHz, $CDCl_3$): δ 175.9, 167.1, 166.7, 132.8, 132.7, 128.9, 127.7, 55.6, 54.0 28.4. **MS (ESI)** (+ve): *m/z* 274.3 $[M+Na]^+$.

N-Benzoyl-α-methoxyglycine Methyl Ester 17

N-Benzoylglycine methyl ester **61** (400 mg, 2.06 mmol) and *N*-bromo-succinimide (370 mg, 2.06 mmol) was stirred in carbon tetrachloride (100 mL) at reflux under irradiation with a 300W sun lamp for ten minutes after which irradiation was ceased. The refluxing mixture was allowed to cool and a solution of methanol (1 ml, 62 mmol) and diisopropylethylamine (0.09 mL, 2.06 mmol) in carbon tetrachloride (25 mL) was added and allowed to stir overnight. The solution was then filtered and reduced by rotary evaporation and purified by column chromatography using a gradient of ethylacetate/hexane to give the title compound as a colourless solid (330 mg, 72%). **Mp**. 77 °C (lit.,[44] 77.5-78.5). **^{1}H NMR** (300 MHz, $CDCl_3$): δ 3.50 (s, 3H), 3.81 (s, 3H), 5.76 (d, J = 9 Hz, 1H), 7.31-7.56 (m, 4H), 7.78-7.86 (m, 2H). **^{13}C NMR** (75 MHz, $CDCl_3$): δ 168.8, 167.8, 133.2, 132.5, 128.9, 127.5, 78.8, 57.0, 53.2.

N-Benzoyl-α-ethoxyglycine Methyl Ester 19

N-Benzoylglycine methyl ester **61** (400 mg, 2.06 mmol) and *N*-bromo-succinimide (370 mg, 2.06 mmol) was stirred in carbon tetrachloride (100 mL) at reflux under irradiation with a 300W sun lamp for ten minutes after which irradiation was ceased. The refluxing mixture was allowed to cool and a solution of ethanol (1 mL, 62 mmol), diisopropylethylamine (0.09 mL, 2.06 mmol) in carbon tetrachloride (25 mL) was added and allowed to stir overnight. The solution was then filtered, reduced by rotary evaporation and purified by column chromatography using a gradient of ethylacetate/hexane to give the title compound as a colourless solid (330 mg, 67%) in 67% yield. **Mp**. 73°C (lit.,[101] 65-66 °C). **^{1}H NMR** (300 MHz, $CDCl_3$): δ 1.25 (t, J = 8.1 Hz, 3H), 3.73-3.82 (m, 2H), 5.85 (d, J = 9 Hz, 1H), 7.18 (d, J = 8.7 Hz, 1H), 7.43-7.57 (m, 3H), 7.58-7.86 (m, 2H). **^{13}C NMR** (75 MHz, $CDCl_3$): δ 169.0, 167.6, 133.3, 132.5, 128.9, 127.5, 77.5, 65.6, 53.3, 15.3. **HRMS (ESI)** (+ve): *m/z* calcd. for $C_{12}H_{15}NO_4Na$ $[M+Na]^+$ 260.0898, found $[M+Na]^+$ 260.0889.

N-Benzoyl-α-phenoxyglycine Methyl Ester 21

N-Benzoylglycine **61** (100 mg, 0.51 mmol) and *N*-bromo succinimide (92 mg, 0.52 mmol) was stirred in carbon tetrachloride (30 mL) under nitrogen at reflux. The refluxing solution was then irradiated with a sun lamp for 10 minutes, allowed to cool, after which phenol (200 mg, 2.12 mmol) and diisopropylethylamine (0.1 mL, 5.7 mmol) in carbon tetrachloride (10 mL) was added. The solution was stirred overnight, filtered, concentrated under reduced pressure and purified by high performance liquid chromatography eluting with a gradient of acetonitrile/water to give the title compound (48 mg, 32%). **Mp** 116 °C. **^{1}H NMR** (300 MHz, CD_3OD): δ 3.85 (s, 3H), 6.44 (s, 1H), 6.99-7.53 (m, 8H), 7.81-7.85 (m, 2H). **^{13}C NMR** (75 MHz, CD_3OD): δ 168.4, 156.6,

133.2, 132.3, 129.5, 128.5, 127.5, 127.4, 122.6, 116.6, 77.1, 52.3. **HRMS (ESI)** (+ve): *m/z* calcd. for $C_{16}H_{15}NO_4$ $[M+H]^+$ 286.1079, $[M+Na]^+$ 308.0898, found 286.1081 $[M+H]^+$, 308.0902 $[M+Na]^+$.

N-Benzoyl-α-succinimidoglycine Methyl Ester 22

N-Benzoylglycine **61** (100 mg, 0.51 mmol) and *N*-bromo succinimide (92 mg, 0.52 mmol) was stirred in carbon tetrachloride (30 mL) under nitrogen at reflux. The refluxing solution was then irradiated with a 300W sun lamp for 10 minutes, allowed to cool. To this cooled mixture a solution of succinimide (500 mg, 5.0 mmol) and diisopropylethylamine (0.18 mL, 10.3 mmol) in acetonitrile (15 mL) was added and allowed to stir overnight. The stirred solution was then filtered and the crude solid purified by column chromatography with a gradient of ethyl acetate/hexane and recrystallised from ethyl acetate/hexane to give the title compound as a white solid (30mg, 19.6%). **Mp**. 97 °C. **^{1}H NMR** (300MHz, $CDCl_3$): δ 2.78 (s, 4H), 3.01 (s, 3H), 6.77 (d, *J* = 8.4 Hz), 7.41-7.63 (m, 4H), 7.80-7.82 (m, 2H). **^{13}C NMR** (75 MHz, $CDCl_3$): δ 175.8, 167.0, 166.6, 132.8, 132.7, 128.9, 127.6, 55.6, 54.1, 28.3. **HRMS (ESI)** (+ve): *m/z* calcd. for $C_{14}H_{14}N_2O_5$ 291.0980 $[M+H]^+$, found 291.0978 $[M+H]^+$.

Experimental for Chapter 3

Synthetic Procedures

Diethyl 2-(Acetamido)-2-[(2-nitrophenyl)methyl)]malonate 116

Sodium metal (360 mg) was dissolved with stirring in ethanol (22 mL) and diethyl acetamidomalonate (3.32 g, 15.3 mmol) was added to the still warm solution. This was allowed to stir for 10 minutes, then 2-nitrobenzyl bromide (3.25 g, 15.0 mmol) dissolved in benzene (9 mL) was added dropwise over 10 minutes. The resulting mixture was stirred for 4 hours at room temperature before being cooled to 0 °C. The mixture was then filtered and the filtrate collected. The solvent was then removed under reduced pressure to give the title compound as colourless crystals (4.22 g, 80%). **Mp**. 104-105.5 (lit.,[102] 103-105 °C). **^{1}H NMR** (300 MHz, $(CD_3)_2SO/CDCl_3$): δ 1.16 (t, J = 7 Hz, 6H), 1.87 (s, 3H), 2.85 (s, 2H), 4.12 (q, J = 7 Hz, 4H), 7.25 (d, J = 8 Hz, 1H), 7.54 (t, J = 8 Hz, 1H), 7.66 (t, J = 8 Hz, 1H), 7.90 (d, J = 8 Hz, 1H).

2-Nitrophenylalanine Hydrochloride 117

Diethyl 2-(acetamido)-2-[(2-nitrophenyl)methyl)]malonate **116** (1.35 g, 3.83 mmol) was heated at reflux in concentrated hydrochloric acid (15 mL) for 6 hours. After being allowed to cool to room temperature, the resulting mixture was filtered. The residue was then recrystallised from hot ethanol to give the title compound as yellow crystals (600 mg, 74%). **Mp** 208 °C (dec.) (lit.,[102] 206-208 °C). **^{1}H NMR** (300 MHz, CD_3OD): δ 3.42 (dd, J = 7.5, 14.0, 1H), 3.67 (dd, J = 7.5, 14.0 Hz, 1H), 4.354 (t, J = 7.5 Hz, 1H), 7.56-7.61 (m, 2H), 7.69-7.72 (m, 1H), 8.09-8.12 (m, 1H). **^{13}C NMR** (75 MHz, CD_3OD): δ 169.8, 149.5, 133.9, 133.4, 130.2, 129.2, 125.4, 53.2, 33.8.

2-Nitrophenylalanine Methyl Ester Hydrochloride 118

2-Nitrophenylalanine hydrochloride **117** (50 mg, 0.24 mmol) was stirred in methanol (20 mL) which had been pretreated with thionyl chloride (4 mL). The solution was allowed to stir overnight and was then evaporated under reduced pressure to give a white powder, which was redissolved in methanol and evaporated under reduced pressure twice to remove excess hydrochloric acid. The crude product was then recrystallised from hot ethanol to give the title compound as a white solid (52 mg, 85%). **Mp**. 198 °C. **^{1}H NMR** (300 MHz, CD_3OD): δ 3.47 (dd, *J* = 7.2, 13.5 Hz, 1H), 3.61 (dd, *J* = 7.8, 13.5 Hz), 3.71 (s, 3H), 4.42 (t, *J* = 7.5 Hz, 1H), 7.54-7.62 (m, 2H), 7.70-7.76 (m, 1H), 8.09-8.12 (m, 1H). **^{13}C NMR** (75 MHz, CD_3OD): δ 169.0, 149.5, 134.0, 133.3, 129.9, 129.3, 125.4, 53.3, 52.5, 33.8. **HRMS (ESI)** (+ve) calcd for $C_{10}H_{12}N_2O_4$ *m/z* 225.0875 $[M]^+$, found *m/z* 225.0869 $[M]^+$. **Anal**. Calcd. for $C_{10}H_{13}N_2O_4Cl$: C, 46.08; H, 5.03; N, 10.75. Found: C, 46.02; H, 4.82; N, 10.62%.

Preparation of the Diastereomers of *N*-Benzoylvalyl-2-nitrophenylalanine Methyl Ester 119

N-Benzoylvaline **68** (170 mg, 0.77 mmol) was stirred in dichloromethane (20 mL) along with BOP (681 mg, 1.44 mmol) and diisopropylethylamine (0.26 mL, 1.44 mmol) for 20 minutes. To this solution, 2-nitrophenylalanine methyl ester **118** (200 mg, 0.77 mmol) was added and the mixture was stirred overnight. The solution was concentrated under reduced pressure, dissolved in ethyl acetate (30 mL) and washed with sodium bicarbonate (3 x 50 mL), 5N citric acid (3 x 50 mL) and brine (3 x 50 mL). The organic layer was then dried, filtered and concentrated under reduced pressure and the crude solid recrystallised from ethyl acetate/hexane to give the title compound (200

mg, 61%) as a 1:5 mixture of diastereomers as determined by ^{1}H NMR spectroscopy. **Mp** 169 °C. **^{1}H NMR** (300 MHz, $CDCl_3$): δ 0.81 (d, *J* = 6.9 Hz, 3H), 0.86 (d, *J* = 6.9 Hz, 3H), 0.95 (d, *J* = 2.5 Hz, 3H), 0.98 (d, *J* = 2.5 Hz, 3H), 2.04 - 2.18 (m, 2H), 3.22 (dd, *J* = 9.6, 14.0, 1H), 3.28 (dd, *J* = 9.3, 13.8 Hz, 1H), 3.53 (dd, *J* = 5.4, 13.8 Hz, 1H), 3.57 (dd, *J* = 4.2, 14.0 Hz, 1H), 3.70 (s, 3H), 3.76 (s, 3H), 4.43 (dd, *J* = 6.6, 8.7 Hz, 1H), 4.47 (dd, *J* = 6, 8.4 Hz, 1H), 4.91-5.01 (m, 2H), 6.63 (d, *J* = 9.3 Hz, 1H), 6.69 (d, *J* = 8.4 Hz, 1H), 6.84 (d, *J* = 7.5 Hz, 1H), 6.93 (d, *J* = 8.4 Hz, 1H), 7.33-7.55 (m, 12H), 7.75-7.78 (m, 4H), 7.89-7.92 (m, 2H). **^{13}C NMR** (75 MHz, $CDCl_3$): δ 171.3, 171.3, 169.4, 169. 3, 167.7, 167.6, 147.4, 147.3, 134.6, 134.4, 134.1, 134.1, 133.1, 132.9, 132.2, 132.0, 129.9, 128.8, 128.7, 127.3, 125.9, 58.7, 58.4, 55.3, 55.0, 53.4, 53.3, 32.1, 31.8, 19.3, 18.5. **HRMS (ESI)** (+ve) calcd. for $C_{21}H_{23}N_3O_6$ *m/z* 450.1641 $[M+Na]^+$, found *m/z* 450.1643 $[M+Na]^+$. **Anal.** Calcd. for $C_{22}H_{25}N_3O_6$: C, 61.82; H, 5.89; N, 9.83. Found: C, 61.54; H, 5.90; N, 9.70%. **HPLC** (analytical) rt = 5.7 min, column: Waters Symmetry C_{18} 3.5 μm column (4.6 x 75 mm); gradient 9:1 water/acetonitrile to 1:9 water/acetonitrile over 10 minutes; flow rate: 1.0 mL min^{-1}.

N-Benzoyl-2-nitrophenylalanine Methyl Ester 120

2-Nitrophenylalanine methyl ester **118** (90 mg, 0.40 mmol) was dissolved with stirring in ethyl acetate (20 mL) to which triethylamine (0.9 mL, 6.74 mmol) and benzoyl chloride (0.03 mL, 0.45 mmol) was added. The solution was refluxed with stirring overnight after which water (50 mL) was added and refluxing was continued for a further 3 hours. The solution was then allowed to cool and the organic layer separated from the aqueous layer. The organic layer was then washed with 2M hydrochloric acid (3 x 50 mL) and saturated sodium bicarbonate (3 x 50 mL) followed by brine (2 x 50

mL). The organic layer was then dried, filtered and evaporated under reduced pressure and the crude solid was recrystallised from ethanol/hexane to give the title compound (100 mg, 75%) as an off white solid. **Mp** 119 °C. **^{1}H NMR** (300 MHz, $CDCl_3$): δ 3.46 (dd, *J* = 8.4, 13.5 Hz, 1H), 3.58 (dd, *J* = 6.0, 13.5, Hz, 1H), 3.76 (s, 3H), 5.10 (m, 1H), 7.04 (d, *J* = 6.6 Hz, 1H), 7.48 (m, 6H), 7.71 (m, 2H), 7.92 (m, 1H). **^{13}C NMR** (75 MHz, $CDCl_3$): δ 171.9, 167.2, 149.9, 133.6, 133.5, 132.9, 132.1, 131.8, 128.8, 128.5, 127.2, 125.2, 53.8, 53.0, 34.8. **Anal**. Calcd. for $C_{17}H_{16}N_2O_5$: C, 62.19; H, 4.91; N, 8.53. Found: C, 62.14; H, 4.81; N, 8.39%. **HRMS (ESI)** (+ve): Calcd. for $C_{17}H_{16}N_2O_5$ *m/z* 329.1137 $[M+H]^+$, *m/z* 351.0956 $[M+Na]^+$, found *m/z* 329.1137 $[M+H^+]$, 351.0957 $[M+Na^+]$.

N-Benzoyl-2-nitrophenylalanine 121

N-Benzoyl-2-nitrophenylalanine methyl ester **120** (40 mg, 0.12 mmol) was added to a solution of tetrahydrofuran (5 mL) and 1M sodium hydroxide (5 mL) and stirred overnight. The solution was then acidified to pH 3 with 1M hydrochloric acid, extracted with ethyl acetate (3 x 20 mL). The combined organic layers were dried, filtered and evaporated under reduced pressure to give a crude solid which was recrystallised from hot ethanol/hexane to give the title compound (30 mg, 85%) as a white solid. **Mp**. 183 °C. **^{1}H NMR** (300 MHz, CD_3OD): δ 3.28 (dd, *J* = 10.5, 13.8 Hz, 1H), 3.79 (dd, *J* = 4.8, 13.8 Hz, 1H), 5.06 (m, 1H), 7.38-7.57 (m, 6H), 7.67-7.70 (m, 2H), 7.96-7.99 (m, 1H), 8.67 (d, *J* = 8.4 Hz, 1H). **^{13}C NMR** (75 MHz, CD_3OD): δ 173.1, 168.9, 149.8, 133.9, 133.1, 132.9, 132.7, 131.6, 128.3, 128.1, 127.1, 124.8, 52.9, 34.5. **Anal**. Calcd. for $C_{16}H_{14}N_2O_5$: C, 61.14; H, 4.49; N, 8.91. Found: C, 60.95; H,

4.57; N, 8.74%. **HRMS (FAB)** (+ve): calcd. for $C_{16}H_{14}N_2O_5$ *m/z* 315.0980 $[M+H]^+$, found *m/z* 315.0987 $[M+H]^+$.

Preparation of the Diastereomers of *N*-Benzoyl-2-nitrophenylalanylalanine Methyl Ester 122

N-Benzoyl-2-nitrophenylalanine **121** (80 mg, 0.25 mmol) was stirred in dichloromethane (20 mL) along with diisoproylethylamine (0.08 mL, 0.5 mmol) and BOP (112 mg, 0.25 mmol) for 30 minutes after which alanine methyl ester hydrochloride (35.5 mg, 0.25 mmol) was added. The solution was allowed to stir overnight then evaporated under reduced pressure and the crude brown oil taken up in ethyl acetate (30 mL). The solution was then washed with 5N citric acid (3 x 50 mL), saturated sodium bicarbonate (3 x 50 mL) and brine (3 x 50 mL) and the organic layer dried, filtered and evaporated under reduced pressure. The crude product was then recrystallised from ethanol to give the title compound as a mixture of diastereomers (40 mg, 40%). **Mp.** 173 °C. **^{1}H NMR** (300 MHz, $CDCl_3$): δ 1.31 (d, *J* = 7.5 Hz, 3H), 1.39 (d, *J* = 7.5 Hz, 3H), 3.30-3.38 (m, 2H), 3.60-3.68 (m, 2H), 3.689 (s, 3H), 3.70 (s, 3H), 4.36-4.45 (m, 2H), 5.03-5.10 (m, 2H), 7.40-7.50 (m, 12H), 7.74-7.76 (m, 6H), 7.90-8.00 (m, 2H). **^{13}C NMR** (125 MHz, CD_3OD) (major diastereoisomer): δ 174.1, 171.8, 167.9, 151.4, 135.7, 134.4, 134.2, 132.8, 131.2, 129.7, 129.5, 128.7, 126.1, 54.7, 52.9, 49.5, 35.9, 18.3. **Anal.** Calcd. for $C_{16}H_{14}N_2O_5.½CH_3OH$: C, 59.27; H, 5.58; N, 10.12. Found: C, 58.92; H, 5.34; N, 9.81%. **HRMS (ESI)** (+ve): calcd. for $C_{20}H_{21}N_3O_6$ *m/z* 422.1328 $[M+Na]^+$, found *m/z* 422.1337 $[M+Na]^+$. **HPLC** (analytical) rt = 5.4 min, column: Waters Symmetry C_{18} 3.5 μm column (4.6 x 75 mm); gradient 9:1 water/acetonitrile to 1:9 water/acetonitrile over 10 minutes; flow rate: 1.0 mL min^{-1}.

Preparation of the Diastereomers of *N*-Benzoylvalyl-2-nitrophenylalanine 123

N-Benzoylvalyl-2-nitrophenylalanine methyl ester **119** (80 mg, 0.189 mmol) was stirred in tetrahydrofuran (10 mL) and 2M NaOH (10 mL) overnight. The solution was then acidified to pH 3.0 using 2M hydrochloric acid and extracted with ethyl acetate (3 x 30 mL). The combined organics were then dried, filtered and concentrated under reduced pressure. The resultant white solid was recrystallised from hot ethanol to give the title compound (52 mg, 64%). **Mp** 240 °C. **^{1}H NMR** (300 MHz, CD_3OD): δ 0.86 (d, *J* = 6.9 Hz, 6H), 0.98 (d, *J* = 6.6 Hz, 3H), 0.99 (d, *J* = 6.6 Hz, 3H), 2.089 (m, 2H), 3.08 (dd, *J* = 10.5, 13.8 Hz, 1H), 3.21 (dd, *J* = 10.5, 13.8 Hz, 1H), 3.74 (m, 2H), 4.37 (dd, *J* = 13.2, 7.5 Hz, 2H), 4.86 (m, 2H), 7.39 (m, 12H), 7.86 (m, 6H). **^{13}C NMR** (75 MHz, CD_3OD): δ 174.8, 174.5, 170.6, 151.7, 151.6, 136.2, 135.4, 135.3, 135.2, 135.0, 134.3, 133.7, 130.4, 130.2, 130.0, 129.3, 126.8, 126.7, 61.7, 61.4, 54.5, 54.0, 37.0, 36.3, 32.8, 20.6, 20.0, 19.5. **Anal.** Calcd. for $C_{21}H_{23}N_3O_6$: C, 61.01; H, 5.61; N, 10.16. Found: C, 60.73; H, 5.61; N, 9.95%. **HRMS (ESI)** (+ve): Calcd. for $C_{21}H_{23}N_3O_6$ *m/z* 414.1665 $[M+H]^+$, found *m/z* 414.1681 $[M+H^+]$.

N-Acetylphenethylamine 125

Phenethylamine **124** (10 g, 10.32 mL, 82.5 mmol) was stirred in acetic anhydride (30 mL) and triethylamine (8.35 g, 11.5 mL, 82.5 mmol) overnight. Water (50 mL) was then added and the solution allowed to stir for a further 30 minutes after which it was

extracted with ethyl acetate (3 x 50 mL). The organic layer was dried, filtered and evaporated under reduced pressure and the crude product recrystallised from ethyl acetate/hexane to give the title compound (10 g, 75%) as a white solid. **Mp**. 68 °C **^{1}H NMR** (300 MHz, $CDCl_3$): δ 1.93 (s, 3H), 2.80 (t, *J* = 7.0 Hz, 2H), 3.50 (q, *J* = 7.0, 12.9 Hz, 2H), 5.73 (s, broad, 1H), 7.17-7.33 (m, 5H). **^{13}C NMR** (75 MHz, $CDCl_3$): δ 170.5, 139.1, 128.9, 128.8, 126.8, 41.0, 35.8, 23.5. **HRMS** (FAB) (+ve): calcd. for $C_{10}H_{13}NO$ *m/z* 136.0997 $[M]^+$, found *m/z* 163.0996 $[M]^+$.

N-acetyl-2-(2-nitrophenyl)ethylamine 126

N-Acetylphenethylamine **125** (10 g, 61.8 mmol) was stirred in nitric acid (50 mL) and sulphuric acid (50 mL) at 0°C for 1 hour after which it was poured into ice water. The solution was then extracted with ethyl acetate (3 x 50 mL) and the combined organics were dried, filtered and evaporated to dryness under reduced pressure to give a mixture of *N*-acetyl-2-nitrophenyethylamine and *N*-acetyl-4-nitrophenylethylamine. The ortho isomer was isolated from a portion of this mixture by high performance liquid chromatography to give the title compound[103] as a yellow oil. **^{1}H NMR** (300 MHz, $CDCl_3$): δ 1.97 (s, 3H), 3.22 (t, *J* = 6.6 Hz, 2H), 3.62 (q, *J* = 6.6, 13.2 Hz, 2H), 5.80 (s, broad, 1H), 7.67 (m, 2H), 8.40 (d, *J* = 6 Hz, 1H), 8.78 (s, 1H). **^{13}C NMR** (75 MHz, CD_3OD): δ 170.8, 147.3, 133.5, 132.7, 129.8, 127.9, 123.9, 40.3, 32.9, 23.3. **HRMS (EI)** (+ve): Calcd for $C_{10}H_{12}N_2O_3$ *m/z* 208.0848 $[M^{+\cdot}]$, found 208.0846.

2-Nitrophenethylamine Hydrochloride 127

N-Acetyl-2-nitrophenethylamine **126** (200 mg, 0.96 mmol) was stirred in concentrated hydrochloric acid (20 mL) at reflux for 3 hours. The solution was allowed to cool and the evaporated to dryness under reduced pressure. The crude solid was then recrystallised from hot ethanol to give the title compound[104] (95 mg, 47 %) as a yellow solid. **Mp**. 205 °C. **^{1}H NMR** (300 MHz, CD_3OD): δ 3.30 (m, 2H), 3.37 (m, partially obscured, 2H), 7.88 (m, 2H), 8.52 (m, 1H), 8.85 (s, 1H). **^{13}C NMR** (75 MHz, CD_3OD): δ 153.5, 151.5, 142.6, 138.2, 131.6, 124.3, 50.9, 34.7. **HRMS (ESI)** (+ve): Calcd. for $C_8H_{10}N_2O_2$ *m/z* 167.0820 $[M+H]^+$, found *m/z* 167.0817 $[M+H]^+$.

N-(2-Nitrophenylethyl)-*N*$^{\alpha}$-benzoylvalinamide 128

N-Benzoylvaline **68** (50 mg, 0.23 mmol) was stirred in dichloromethane (20 mL) along with BOP (101 mg, 0.23 mmol) and diisopropylethylamine (0.08 mL, 0.46 mmol) for 30 minutes. 2-Nitrophenethylamine hydrochloride **127** (47 mg, 0.23 mmol) in dichloromethane (5 mL) was then added and the solution allowed to stir overnight. The solution was then evaporated to dryness under reduced pressure and the crude oil taken up in ethyl acetate and washed with 5N citric acid (3 x 20 mL), saturated sodium bicarbonate (3 x 20 mL) and brine (2 x 20 mL). The organic layer was then dried, filtered and evaporated to dryness under reduced pressure to give the title compound[105] as a white solid (55 mg, 68 %). **Mp** 163 °C. **^{1}H NMR** (300 MHz, $CDCl_3$): δ 0.80 (d, *J* = 6 Hz, 3H), 0.85 (d, *J* = 6.6 Hz, 3H), 2.10 (m, 1H), 3.27 (dd, *J* = 9.6, 13.8 Hz, 1H), 3.53 (dd, *J* = 5.7, 13.8 Hz, 1H), 4.46 (m, 2H), 4.95 (dd, *J* = 5.7, 9.6 Hz, 1H), 6.69 (d, *J* = 7.2 Hz, 1H), 6.95 (d, *J* = 6.6 Hz, 1H), 7.32-7.52 (m, 6H), 7.75-7.78 (m, 2H), 7.89-7.92 (m, 1H). **^{13}C NMR** (75 MHz, CD_3OD): δ 171.5, 167.6, 149.8, 134.0, 133.5, 133.0, 132.1, 131.8, 128.9, 128.6, 127.3, 125.3, 58.7, 53.1, 34.9, 31.3, 19.5. **LRMS**

(ESI) (+ve): calcd. for $C_{20}H_{23}N_3O_4$ *m/z* 369.17, found 370.2 $[M+H]^+$, 392.1 $[M+Na]^+$, 418.2 $[M+K]^+$. **HRMS (ESI)** (+ve): Calcd. for $C_{20}H_{23}N_3O_4$ *m/z* 369.1689 $[M+H]^+$, found *m/z* 369.1690 $[M+H]^+$. **HPLC** (analytical) rt = 5.6 min, column: Waters Symmetry C_{18} 3.5 μm column (4.6 x 75 mm); gradient 9:1 water/acetonitrile to 1:9 water/acetonitrile over 10 minutes; flow rate: 1.0 mL min^{-1}.

Preparation of the Diastereomers of *N*-Benzoylvalyl-2-nitrophenylalanylalanine Methyl Ester 129

N-Benzoylvalyl-2-nitrophenylalanine **123** (21.5 mg, 0.05 mmol) was stirred in dichloromethane (30 mL) along with diisoproylethylamine (0.01 mL, 0.05 mmol) and BOP (23 mg, 0.05 mmol) for 30 minutes after which alanine methyl ester hydrochloride (7.5 mg, 0.05 mmol) was added. The solution was allowed to stir overnight then evaporated under reduced pressure and the crude brown oil taken up in ethyl acetate (30 mL). The solution was then washed with 5N citric acid (3 x 50 mL), saturated sodium bicarbonate (3 x 50 mL) and brine (3 x 50 mL) and the organic layer dried, filtered and evaporated under reduced pressure. The crude product was purified by HPLC eluting with a gradient of acetonitrile/0.01% trifluoroacetic acid in water to give the title compound (15 mg, 60 %) as a white solid. **Mp.** 247 °C (dec.). **^{1}H NMR** (300 MHz, CD_3OD): δ 0.88-0.95 (m, 24H), 1.32-1.48 (m, 12H), 1.95-2.10 (m, 4H), 3.059-3.30 (m, 4H), 3.47-3.65 (m, 4H), 3.585 (s, 3H), 3.66 (s, 3H), 3.70 (s, 3H), 3.71 (s, 3H), 3.99-4.07 (m, 4H), 4.23-4.30 (m, 4H), 4.33-4.48 (m, 4H), 7.27-7.34 (m, 4H), 7.43-7.56 (m, 24H), 7.78-7.83 (m, 8H), 7.90-7.96 (m, 4H). **HRMS (ESI)** (+ve): Calcd. for $C_{25}H_{30}N_4O_7$ *m/z* 499.2193 $[M+H]^+$, found *m/z* 499.2186 $[M+H]^+$. **HPLC** (analytical) rt = 5.4 min,

column: Waters Symmetry C_{18} 3.5 μm column (4.6 x 75 mm); gradient 9:1 water/acetonitrile to 1:9 water/acetonitrile over 10 minutes; flow rate: 1.0 mL min^{-1}.

Diethyl 2-(Acetamido)-2-[(2-nitro-4,5-dimethoxyphenyl)methyl)]malonate 130

Sodium metal (360 mg) was dissolved with stirring in ethanol (22 mL) and diethyl acetamidomalonate (3.32 g, 15.3 mmol) was added to the still warm solution. This was allowed to stir for 10 minutes, then 2-nitrobenzyl bromide (3.25 g, 15.0 mmol) dissolved in benzene (9 mL) was added dropwise over 10 minutes. The resulting mixture was stirred for 4 hours at room temperature before being cooled to 0 °C. The mixture was then filtered and the filtrate collected. The solvent was then removed under reduced pressure to give the title compound as colourless crystals (4.22 g, 80%). **Mp.** 175 °C **^{1}H NMR** (300 MHz, $CD_3OD/(CD_3)_2SO$): δ 1.27 (t, J = 7.2 Hz, 6H), 1.98 (s, 3H), 3.92 (s, 3H), 3.93 (s, 3H), 4.01 (s, 2H), 4.15-4.28 (m, 4H), 6.76 (s, 1H), 7.57 (s, 1H). **^{13}C NMR** (75 MHz, $CD_3OD/(CD_3)_2SO$): δ 171.0, 167.6, 152.5, 148.4, 143.3, 124.2, 115.2, 108.6, 67.1, 62.6, 56.0, 34.2, 21.8, 13.6. **Anal.** Calcd. for $C_{18}H_{24}N_2O_9$: C, 52.42; H, 5.87; N, 6.79. Found: C, 52.43; H, 5.62; N, 6.71%. **HRMS (FAB)** (+ve): Calcd. for $C_{18}H_{24}N_2O_9$ *m/z* 412.1482 $[M+H]^+$, found *m/z* 412.1487 $[M+H]^+$.

2-Nitro-4,5-dimethoxyphenylalanine Hydrochloride 131

Diethyl 2-(acetamido)-2-[(2-nitro-4,5dimethoxyphenyl)methyl)]malonate **130** (3 g, 7.28 mmol) was heated at reflux in concentrated hydrochloric acid (30 mL) for 6 hours.

After being allowed to cool to room temperature, the resulting mixture was filtered. The crude solid was then washed through the filter paper with ethanol to remove the 2-nitro-4,5-dimethoxyphenylalanine from an unknown white solid. The filtrate was then evaporated to dryness under reduced pressure to give the title compound as yellow crystals (1.2 g, 53 %). **Mp**. 200 °C (dec.). **^{1}H NMR** (300 MHz, CD_3OD): δ 3.39 (dd, *J* = 8.1, 13.8 Hz, 1H), 3.72 (dd, *J* = 6.6, 13.8 Hz, 1H), 3.91 (s, 3H), 3.97 (s, 3H), 4.34 (q, *J* = 6.6, 8.1 Hz, 1H), 7.07 (s, 1H), 7.74 (s, 1H). **^{13}C NMR** (75 MHz, CD_3OD): δ 170.0, 153.9, 148.8, 141.6, 124.9, 115.1, 108.7, 56.1, 55.7, 53.3, 34.3. **HRMS (FAB)** (+ve): Calcd. for $C_{11}H_{14}N_2O_6$ *m/z* 271.0930 $[M+H]^+$, found *m/z* 271.0935 $[M+H]^+$.

2-Nitro-4,5-dimethoxyphenylalanine Methyl Ester Hydrochloride 132

2-Nitro-4,5-dimethoxyphenylalanine hydrochloride **131** (50 mg, 0.16 mmol) was stirred in methanol (20 mL) which had been pretreated with thionyl chloride (4 mL). The solution was allowed to stir overnight and was then evaporated under reduced pressure to give a yellow powder, which was redissolved in methanol and evaporated under reduced pressure twice to remove excess hydrochloric acid. The crude product was then taken up in ethanol and filtered and the filtrate was collected and evaporated under reduced pressure to give a yellow solid (20 mg, 40 %). **Mp**. 160 °C (dec.) **^{1}H NMR** (300 MHz, CD_3OD):δ 3.42 (dd, *J* = 7.5, 13.8 Hz, 1H), 3.73 (dd, obscured, 1H), 3.76 (s, 3H), 3.91 (s, 3H), 3.98 (s, 3H), 4.42 (t, *J* = 7.5 Hz, 1H), 7.12 (s, 1H), 7.72 (s, 1H). **^{13}C NMR** (75 MHz, CD_3OD): δ 169.1, 153.9, 148.9, 141.5, 124.6, 114.9, 108.6, 54.1, 53.2, 52.6, 34.1. **HRMS (FAB)** (+ve): Calcd. for $C_{10}H_{12}N_2O_4$ *m/z* 225.0875 $[M+H+]^+$, found *m/z* 225.0877 $[M+H+]^+$.

Preparation of Diastereomers of *N*-Benzoylvalyl-2-nitro-4,5-dimethoxyphenylalanine Methyl Ester 133

N-Benzoylvaline **68** (35 mg, 0.15 mmol) was stirred in dichloromethane (10 mL) along with BOP (69 mg, 0.15 mmol) and diisopropylethylamine (0.05 mL, 0.3 mmol) for 30 minutes. 2-Nitro-4,5-dimethoxyphenylalanine methyl ester hydrochloride **123** (40 mg, 0.14 mmol) was then added and the solution allowed to stir overnight. The solution was then evaporated to dryness under reduced pressure and the crude oil taken up in ethyl acetate and washed with 5N citric acid (3 x 20 mL), saturated sodium bicarbonate (3 x 20 mL) and brine (2 x 20 mL). The organic layer was then dried, filtered and evaporated to dryness under reduced pressure to give the title compound as a white solid (22 mg, 32%). **Mp**. 198 °C. **^{1}H NMR** (300 MHz, $CDCl_3$): δ 0.84 (d, *J* = 6.6 Hz, 3H), 0.88 (d, *J* = 6.9 Hz, 3H), 0.99 (d, *J* = 6.6 Hz, 6H), 2.14 (m, 4H), 3.30 (dd, *J* = 9.0, 13.8 Hz, 1H), 3.31 (dd, *J* = 9.0, 13.2 Hz, 1H), 3.51 (dd, *J* = 9.0, 13.2), 3.54 (dd, *J* = 9.0, 13.8 Hz) 3.71 (s, 3H), 3.76 (s, 3H), 3.83 (s, 3H), 3.89 (s, 3H), 3.91 (s, 3H), 3.95 (s, 3H), 4.44 (dd, *J* = 9.0, 16.5 Hz, 1H), 4.46 (dd, *J* = 9.0, 14.4 Hz), 4.93 (m, 2H), 6.65 (d, *J* = 6Hz, 1H), 6.72 (s, 1H), 6.78 (s, 1H), 6.96 (d, *J* = 9 Hz, 1H), 7.40 - 7.54 (m, 10H), 7.72 - 7.78 (m, 2H). **^{13}C NMR** (300 MHz, $CDCl_3$) (major diastereoisomer): δ 178.1, 167.6, 161.8, 143.1, 132.9, 131.2, 132.9, 131.3, 128.8, 128.1, 128.0, 127.3, 126.5, 121.0, 63.1, 57.7, 52.8, 31.7, 31.4, 19.0. (minor diastereoisomer) δ 173.8, 172.8, 167.7, 134.3, 133.3, 131.7, 128.9, 128.0, 127.9, 127.3, 124.2, 58.6, 53.4, 31.3. **Anal**. Calcd. for $C_{24}H_{29}N_3O_8$: C, 58.06; H, 6.09; N, 8.46. Found: C, 57.82; H, 6.05; N, 8.20%. **HRMS (EI)**. Calcd. for $C_{24}H_{29}N_3O_8$ *m/z* 487.1955 [M^+], found *m/z* 487.1948 [M^+]. **HPLC** (analytical) rt = 5.5 min, column: Waters Symmetry C_{18} 3.5 μm column (4.6 x 75 mm);

gradient 9:1 water/acetonitrile to 1:9 water/acetonitrile over 10 minutes; flow rate: 1.0 mL min^{-1}.

Preparation of 2-nitrophenylalanylprolylglycine extended oxytocin 160

N-FMOC-2-nitrophenylalanine **162** was incorporated into polypeptide **160** by automated peptide synthesis.[91]

N-FMOC-2-Nitrophenylalanine 162

To a solution of 2-nitrophenylalanine hydrochloride **117** (1.5 g, 6.09 mmol) in dioxane (10 mL) and 10% sodium bicarbonate (20 mL) was added slowly with stirring and ice bath cooling a solution of 9-fluorenylmethyl chloroformate (1.9 g, 7.3 mmol) in dioxane (10 mL). The mixture was stirred at 0 °C for 4 hrs and at room temperature for 12 hrs, poured into water (450 mL) and extracted with ether (3 x 50 mL). The aqueous layer was cooled in an ice bath, acidified to pH 3.0 with concentrated hydrochloric acid and extracted with ethyl acetate. The organic layer was dried, filtered and evaporated under reduced pressure to give the title compound as a clear oil (2.1 g, 80%). **^{1}H NMR** (300 MHz, CD_3OD): δ 3.10 (dd, *J* = 10.5, 13.8 Hz, 1H), 3.67 (dd, *J* = 4.8, 13.8 Hz, 1H), 4.06 (t, *J* = 6.9 Hz, 1H), 4.18 (d, *J* = 3 Hz, 2H), 4.62 (m, 1H), 7.25-7.59 (m, 6H), 7.74-7.77 (m, 2H), 7.93-7.96 (m, 1H). **^{13}C NMR** (75 MHz, CD_3OD): δ 173.4, 157.2, 149.7, 144.0, 141.3, 133.3, 132.9, 132.5, 128.0, 127.6, 127.0, 125.1, 124.7, 119.7, 66.8, 54.3, 54.2, 34.9. **HRMS (ESI)** (+ve): Calcd. for $C_{24}H_{20}N_2O_6$ *m/z* 455.1219 $[M+Na]^+$, found 455.1231 $[M+Na]^+$.

References

(1) Prigge, S. T., Mains, R. E., Eipper, B. A., Amzel, L. M. *Cellular and Molecular Life Sciences* **2000**, *57*, 1236-1259.

(2) Prigge, S. T., Mains, R.E., Eipper, B. A., Kolhekar, A. S., Amzel, L. M. *Science* **1997**, *278*, 1300-1305.

(3) Bolkenius, F. N., Ganzhorn, A. J., *General Pharmacology* **1998**, *31*, 655-659.

(4) Wilcox, B. J., Ritenour-Rodgers, K. J., Asser, A. S., Baumgart, L. E., Baumgart, M. A., Boger, D. L., DeBlassio, J. L., deLong, M. A., Glufke, U., Henz, M. E., King, L., Merkler, K. A., Patterson, J. E., Robleski, J. J., Vederas, J. C., Merkler, D. J. *Biochemistry* **1999**, *38*, 3235-3245.

(5) Merkler, D. J. *Enzyme and Microbial Technology* **1994**, *16*, 450-456.

(6) Salido, M., Vilches, J., Lopez, A., Roomans, G. M. *Cancer* **2002**, *94*, 368-377.

(7) DeVane, L. *Pharmacotherapy* **2001**, *21*, 1061-1069.

(8) Lundberg, J. M. *Canadian Journal of Physiology and Pharmacology* **1995**, *73*, 908-914.

(9) Sanchez-Margalet, V. *Diabetologia* **1999**, *42*.

(10) Nilsson, C. L., Brinkmalm, A., Minthon, L., Blennow, K., Ekman, R. *Peptides* **2001**, *22*, 2105-2112.

(11) Vrinten, D. H., Kalkman, C. J., Adan, R. A. H., Gispen, W. H. *European Journal of Pharmacology* **2001**, *429*, 61-69.

(12) Bradbury, A. F., Mistry, J., Roos, B. A., Smyth, D. G. *European Journal of Pharmacology* **1990**, *189*, 363-368.

(13) Kaptodis, A. G., May, S. W. *Biochemistry* **1990**, *29*, 4541-4548.

(14) Ogonowski, A. A., May, S. W., Moore, A. B., Barrett, L. T., O'Bryant, C. L., Pollock, S. H. *The Journal of Pharmacological and Experimental Therapeutics* **1997**, *280*, 846-853.

(15) Feng, J., Shi, J., Sirimanne, S. R., Mounier-Lee, C. E., May, S. W. *Biochemical Journal* **2000**, *350*, 521-530.

(16) Andrews, M. D., O'Callaghan, K. A., Vederas, J. C. *Tetrahedron* **1997**, *53*, 8295-8306.

(17) Merkler, D. J., Kulathila, R., Francisco, W. A., Ash, D. E., Bell, J. *FEBS Letters* **1995**, *366*, 165-169.

(18) Merkler, D. J., Kulathila, R., Asd, D. E. *Archives of Biochemistry and Biophysics* **1994**, *317*, 93-102.

(19) Easton, C. J. *Chemical Reviews* **1997**, *97*, 53-82.

(20) Dewar, M. J. S. *Journal of the American Chemical Society* **1952**, *74*, 3353.

(21) Croft, A. K., Easton, C. J., Radom, L. *Journal of the American Chemical Society* **1998**, *125*, 4119-4124.

(22) Goldfinger, P., Adam, J., Gosselain, P. *Nature* **1953**, *171*, 704.

(23) Walling, C., El-Taliawi G. M., Zhao, C. *Journal of the American Chemical Society* **1983**, *105*, 5119-5124.

(24) Croft, A. K. PhD. Thesis, Australian National University, **1998**.

(25) Henry, D. J., Parkinson, C. J., Mayer, P. M., Radom, L. *Journal of Physical Chemistry* **2001**, *105*, 6750 - 6756.

(26) Parkinson, C. J., Mayer, P. M., Radom, L. *Journal of the Chemical Society: Perkin Transactions 2* **1999**, 2305 - 2313.

(27) Croft, A. K., Easton, C. J., Kociuba, K., Radom, L. *Tetrahedron: Asymmetry* **2003**, *14*, 2919-2926.

(28) Stryer, L. *Biochemistry*; W. H. Freeman and Company, 1995.

(29) Snider, M. G., Temple, B. S., Wolfenden, R. *Journal of Physical Organic Chemistry* **2004**, *17*, 586-591.

(30) Landymore-Lim, A. E. N., Bradbury, A. F., Smyth, D. G. *Biochemical and Biophysical Research Communications* **1983**, *117*, 289-293.

(31) Bisswanger, H. *Enzyme Kinetics*; Wiley-VCH, 2002.

(32) Burlingham, B. T., Widlanski, T. S. *Journal of Chemical Education* **2003**, *80*, 214-218.

(33) Cheng, Y.-C., Prusoff, W. H. *Biochemical Pharmacology* **1973**, *22*, 3099-3108.

(34) Loffet, A. *Journal of Peptide Science* **2002**, *8*, 1-7.

(35) Carroll, P. *Best Practice and Research in Clinical Endocrinology and Metabolism* **2001**, *15*, 435-451.

(36) Nauck, M. A. *Acta Diabetolgia* **1998**, *35*, 117-129.

(37) Perry, P., Greig, N. H. *Journal of Alzheimers Disease* **2002**, *4*, 487-496.

(38) Torchilin, V. P., Lukyanov, A. N. *Drug Discovery Today* **2003**, *8*, 259-266.

(39) Brannon-Peppas, L., Blanchette, J. O. *Advanced Drug Delivery Reviews* **2004**, *56*.

(40) Bundgaard, H., Kahns, A. H. *Peptides* **1991**, *12*, 745-748.

(41) Bundgaard, H., Burr, A. *International Journal of Pharmaceutics* **1987**, *37*, 185-194.

(42) Mueller, G. P., Driscoll, W. J., Eipper, B. A. *The Journal of Pharmacological and Experimental Therapeutics* **1999**, *290*, 1331-1336.

(43) Ege, S. *Organic Chemistry - Structure and Reactivity*; Third Edition ed., 1994.

(44) Kawai, M., Hosada, K., Omori, Y., Yamada, K., Hayakawa, S., Yamamura, H., Butsugan, Y. *Synthetic Communications* **1996**, *26*, 1545-1554.

(45) Bochet, C. G. *Perkin Transactions 1* **2002**, 125-142.

(46) Patchornik, A., Amit, B., Woodward, R. B. *Journal of the American Chemical Society* **1970**, *92*, 6333-6335.

(47) Corrie, J. E. T., Barth, A., Munasinghe, V. R. N., Trentham, D. R., Hutter, M. C., *Journal of the American Chemical Society* **2003**, *125*, 8546-8554.

(48) Baldwin, J., Cutting, J., Dupont, W., Kruse, L., Silberman, L., Thomas, R. C. *Chemical Communications* **1976**, 736-738.

(49) Walbert, S., Pfleiderer, W., Steiner, U. E. *Helvetica Chimica Acta* **2001**, *84*, 1601-1611.

(50) Bhushan, K. R., DeLisi, C., Laursen, R. A. *Tetrahedron Letters* **2003**, *44*, 8585-8588.

(51) Henriksen, D. B., Breddam, K., Moller, J., Buchardt, O. *Journal of the American Chemical Society* **1991**, *114*, 1876-1877.

(52) England, P. M., Lester, H. A., Davidson, N., Dougherty, D. *Proceedings of the National Academy of Science* **1997**, *94*, 11025-11030.

(53) Henriksen, D. B., Breddam, K., Buchardt, O. *International Journal of Peptide and Protein Research* **1993**, *41*, 169-180.

(54) Barth, A., Corrie, J. E. T., Gradwell, M. J., Maeda, Y., Mantele, W., Meier, T., Trentham, D. *Journal of the American Chemical Society* **1997**, *119*, 4149-4159.

(55) Walker, J. W., Reid, G. P., McCray, J. A., Trentham, D. R. *Journal of the American Chemical Society* **1988**, *1988*, 7170-7177.

(56) Itsuno, S., Darling, G. D., Stover, H. D. H., Frechet, J. M. J. *Journal of Organic Chemistry* **1987**, *52*, 4645-4646.

(57) Lopez, R. F. V., Lange, N., Guy, R., Bentley, M. V. L. B. *Advanced Drug Delivery Reviews* **2004**, *56*, 77-94.

(58) Saxton, R. E., Paiva, M. B., Lufkin, R. B., Castro, D. J. *Seminars in Surgical Oncology* **1995**, *11*, 283-289.

(59) Dorman, G., Prestwich, G. D. *Trends in Biotechnology* **2000**, *18*, 64-77.

(60) Prigge, S. T., Mains, R.E., Eipper, B. A., Amzel, L. M. *Science* **2004**, *304*, 864-867.

(61) Ping, D., Mounier, C. E., May, S. W. *Journal of Biological Chemistry* **1995**, *270*, 29250-29255.

(62) Tamburini, P. P., Jones, B. N., Consalvo, A. P., Young, S. D., Lovato, S. J., Gilligan, J. P., Wennogle, L. P., Erion, M., Jeng, A. Y. *Archives of Biochemistry and Biophysics* **1988**, *267*, 623-631.

(63) Niemann, C., Applewhite, T. H., Martin, R. B. *Journal of the American Chemical Society* **1958**, *80*, 1457.

(64) *Dictionary of Organic Compounds*; Sixth Edition; Vol. 6.

(65) Carpino, L. A., El-Faham, A. *The Journal of Organic Chemistry* **1994**, *59*, 695-698.

(66) Oh Hashi, J., Harada, K. *Bulletin of the Chemical Society of Japan* **1966**, *39*, 2287.

(67) Barratt, B. J. W., Easton, C. J., Henry, D. J., Li, I. H. W., Radom, L., Simpson, J. S. *Journal of the American Chemical Society* **2004**, *126*, 13306-13311.

(68) Parkinson, C. J., Mayer, P. M., Radom, L. *Theoretical Chemistry Accounts: theory, computation and modelling* **1999**, *102*, 92-96.

(69) These levels of theory have been found to be suitable for the calculation of radical stabilisation energies: see reference 25.

(70) Casara, P., Ganzhorn, A., Phillipo, C., Chanal, M. C., Danzin, C. *Bioorganic and Medicinal Chemistry Letters* **1996**, *6*, 393-396.

(71) Krygowski, T. M., Guilleme, J. *Journal of the Chemical Society. Perkin Transactions 2* **1982**, 531-534.

(72) Rauk, A., Yu, D., Taylor, J., Shustov, G. V., Block, D. A., Armstrong, D. A. *Biochemistry* **1999**, *38*, 9089-9096.

(73) RSE values quoted in the text in addition to those listed in Table 2 were also calculated using RMP2/G3large level of theory.

(74) Welle, F. M., Beckhaus, H. D., Ruchhardt, C. *Journal of Organic Chemistry* **1997**, *62*, 552-558.

(75) Schulze, R., Beckhaus, H. D., Ruchardt, C. *Chemichie Berichte* **1993**, *126*, 1031-1038.

(76) Blaney, F. E., GlaxoSmithKline. Personal Communication.

(77) McMurry, J. *Organic Chemistry*; Fourth ed., 1996.

(78) Deslongchamps, P. *Stereoelectronic Effects in Organic Chemistry*; Pergamon Press, 1983.

(79) *N*-Benzoyl-α-hydroxyglycine **7** was generously donated by Candace Tsai, Research School of Chemistry, Australian National University.

(80) *N*-Benzoyl-α-hydroxyglycine methyl ester **8** was generously donated by Dr. Adam Wright, Research School of Chemistry, Australian National University.

(81) Atkins, P. W. *Physical Chemistry*; Oxford University Press, 1982.

(82) Dougherty, D. A. *Current Opinion in Chemical Biology* **2000**, *4*, 645-652.

(83) Hasan, A., Stengele, K., Giegrich, H., Cornwell, P., Isham, K. R., Sachleben, R. A., Pfleiderer, W., Foote, R. S. *Tetrahedron* **1997**, *53*, 4247-4264.

(84) Cell based assays were organised by Dr Adam Wright of the Australian National University at the Research School of Chemistry.

(85) Testing performed by MDS Pharma.

(86) Testing performed by Atsuko Inoue of Hiroshima University

(87) Testing performed by L'Houcine Ouafik of the University of the Mediteranean.

(88) Samson, W. K. *Endocrine Updates* **1998**, *1*, 257-278.

(89) Ballinger, P., Long, F. A. *Journal of the American Chemical Society* **1959**, *81*, 1050.

(90) Ballinger, P., Long, F. A. *Journal of the American Chemical Society* **1960**, *82*, 795.

(91) Automated peptide synthesis was performed by Kerry McAndrew of the Australian National Univerisity at the John Curtin School of Medicine.

(92) Synthesis performed by Kerry McAndrew of the Australian National University at the John Curtin School of Medicine

(93) Klima, R. F., Gudmundsdottir, A. D., *Journal of Photochemistry and Photobiology, A: Chemistry* **2004**, *162*, 239-247.

(94) McMahon, K., Wagner, P. J., *Canadian Journal of Chemistry* **2003**, *81*, 669-672.

(95) Lalevee, J., Allonas, X., Loueerat, F., Fouassier, J. P., *Journal of Physical Chemistry A* **2002**, *106*, 6702-6709.

(96) Cuppoletti, A., Dinnocenzo, J. P., Goodman, J. L., Gould, I. R. *Journal of Physical Chemistry A* **1999**, *103*, 11253-11256.

(97) Walters, N., Atemnkeng, L. D., Louisiana, L. D., Promise, Y. K., Vottero, B., Banerjee, A. *Organic Letters* **2003**, *5*, 4469-4471.

(98) Easton, C. J., Hutton, C. A., Rositano, G., Tan, E. W. *Journal of Organic Chemistry* **1991**, *56*, 5614-5618.

(99) Randhawa, G. S. *Discov. Innovat.* **1991**, *3*, 43–46.

(100) Badsha, A., Khan, N. H., Kidwai, A. R. *Journal of Organic Chemistry* **1972**, *37*, 2916.

(101) Easton, C. J., Burgess, V., Steele, P. *Australian Journal of Chemistry* **1988**, *41*, 701-710.

(102) Vasil'eva, M. N., Shkondinskaya, E. N., Berlin, A. Y. *Zhurnal Obshchei Khimii* **1961**, *31*, 1027.

(103) Nicholas, H. O., Erickson, J. L. E. *Journal of the American Chemical Society* **1926**, *48*, 2174-2176.

(104) Wu, T. Z., Guo, P., Xie, M. H. *Chinese Chemistry Letters* **2000**, *11*, 857-860.

(105) Johnson, T. B., Guest, H. H. *American Chemical Journal* **1910**, *43*, 310-322.

Appendix: Published Work

J|A|C|S
ARTICLES
Published on Web 09/23/2004

Inhibition of Peptidylglycine α-Amidating Monooxygenase by Exploitation of Factors Affecting the Stability and Ease of Formation of Glycyl Radicals

Brendon J. W. Barratt,† Christopher J. Easton,*,† David J. Henry,† Iris H. W. Li,† Leo Radom,†,‡ and Jamie S. Simpson†

Contribution from the Research School of Chemistry, Australian National University, Canberra, ACT 0200, Australia, and School of Chemistry, University of Sydney, Sydney, NSW 2006, Australia

Received June 27, 2004; E-mail: easton@rsc.anu.edu.au

Abstract: Peptidylglycine α-amidating monooxygenase catalyzes the biosynthesis of peptide hormones through radical cleavage of the *C*-terminal glycine residues of the corresponding prohormones. We have correlated ab initio calculations of radical stabilization energies and studies of free radical brominations with the extent of catalysis displayed by peptidylglycine α-amidating monooxygenase, to identify classes of inhibitors of the enzyme. In particular we find that, in closely related systems, the substitution of glycolate for glycine reduces the calculated radical stabilization energy by 34.7 kJ mol^{-1}, decreases the rate of bromination with *N*-bromosuccinimide at reflux in carbon tetrachloride by a factor of at least 2000, and stops catalysis by the monooxygenase, while maintaining binding to the enzyme.

Introduction

Peptidylglycine α-amidating monooxygenase (PAM) catalyzes the biosynthesis of a wide variety of *C*-terminal peptide amides through oxidative cleavage of the corresponding glycine-extended precursors (Scheme 1). The products include mammalian peptide hormones,[1] as well as physiologically active peptides of other organisms such as insects[2,3] and cnidarians,[4,5] and the *C*-terminal amide moiety is vital to the activity of many of these compounds. Amidated peptide hormones are important in cellular communication, in particular as neuropeptides,[1] and are implicated in a broad range of pathological conditions, including asthma,[6] inflammation,[7] and cancers.[8−10] The biosynthesis of amides from glycine-extended precursors other than peptides, such as fatty acids,[11] bile acids,[12] nicotinic acid,[13] and aspirin,[14] has also been attributed to PAM. Fatty acid amides are known to affect a number of neurochemical communication pathways, including sleep regulation,[15,16] while the amidation of aspirin may be important in its metabolic processing.

Scheme 1

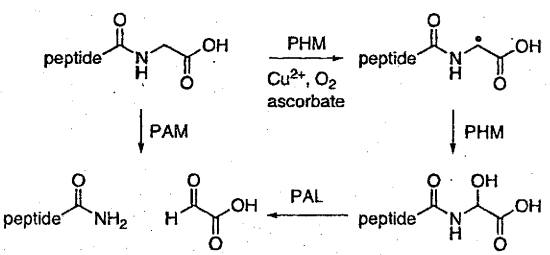

The importance of PAM in pathological conditions has led to interest in its regulation and the development of a number of inhibitors. One of the first was *trans*-4-phenylbut-3-enoic acid,[17] which is effective in vivo in reducing serum PAM activity[18] as well as showing anti-inflammatory and analgesic effects.[19]

† Australian National University.
‡ University of Sydney.

(1) Merkler, D. J. *Enzyme Microb. Technol.* **1994**, *16*, 450−456.
(2) Konopinska, D.; Rosinski, G.; Sobotka, W. *Int. J. Pept. Protein Res.* **1992**, *39*, 1−11.
(3) Schoofs, L.; Veelaert, D.; VandenBroeck, J.; DeLoof, A. *Peptides* **1997**, *18*, 145−156.
(4) Hauser, F.; Williamson, M.; Grimmelikhuijzen, C. J. P. *Biochem. Biophys. Res. Commun.* **1997**, *241*, 509−512.
(5) Williamson, M.; Hauser, F.; Grimmelikhuijzen, C. J. P. *Biochem. Biophys. Res. Commun.* **2000**, *277*, 7−12.
(6) Groneberg, D. A.; Springer, J.; Fischer, A. *Pulm. Pharmacol. Ther.* **2001**, *14*, 391−401.
(7) Wiesenfeld-Hallin, Z.; Xu, X. J. *Eur. J. Pharmacol.* **2001**, *429*, 49−59.
(8) Schally, A. V.; Comaru-Schally, A. M.; Nagy, A.; Kovacs, M.; Szepeshazi, K.; Plonowski, A.; Varga, J. L.; Halmos, G. *Front. Neuroendocrinol.* **2001**, *22*, 248−291.
(9) Du, J. L.; Keegan, B. P.; North, W. G. *Cancer Lett.* **2001**, *165*, 211−218.
(10) Jimenez, N.; Jongsma, J.; Calvo, A.; van der Kwast, T. H.; Treston, A. M.; Cuttitta, F.; Schroder, F. H.; Montuenga, L. M.; van Steenbrugge, G. J. *Int. J. Cancer* **2001**, *94*, 28−34.
(11) Wilcox, B. J.; Ritenour-Rodgers, K. J.; Asser, A. S.; Baumgart, L. E.; Baumgart, M. A.; Boger, D. L.; DeBlassio, J. L.; deLong, M. A.; Glufke, U.; Henz, M. E.; King, L.; Merkler, K. A.; Patterson, J. E.; Robleski, J. J.; Vederas, J. C.; Merkler, D. J. *Biochemistry* **1999**, *38*, 3235−3245.
(12) King, L.; Barnes, S.; Glufke, U.; Henz, M. E.; Kirk, M.; Merkler, K. A.; Vederas, J. C.; Wilcox, B. J.; Merkler, D. J. *Arch. Biochem. Biophys.* **2000**, *374*, 107−117.
(13) Merkler, D. J.; Glufke, U.; Ritenour-Rodgers, K. J.; Baumgart, L. E.; DeBlassio, J. L.; Merkler, K. A.; Vederas, J. C. *J. Am. Chem. Soc.* **1999**, *121*, 4904−4905.
(14) DeBlassio, J. L.; deLong, M. A.; Glufke, U.; Kulathila, R.; Merkler, K. A.; Vederas, J. C.; Merkler, D. J. *Arch. Biochem. Biophys.* **2000**, *383*, 46−55.
(15) Cravatt, B. F.; Lerner, R. A.; Boger, D. L. *J. Am. Chem. Soc.* **1996**, *118*, 580−590.
(16) Cravatt, B. F.; Prosperogarcia, O.; Siuzdak, G.; Gilula, N. B.; Henriksen, S. J.; Boger, D. L.; Lerner, R. A. *Science* **1995**, *268*, 1506−1509.
(17) Bradbury, A. F.; Mistry, J.; Roos, B. A.; Smyth, D. G. *Eur. J. Biochem.* **1990**, *189*, 363−368.
(18) Mueller, G. P.; Driscoll, W. J.; Eipper, B. A. *J. Pharmacol. Exp. Ther.* **1999**, *290*, 1331−1336.

10.1021/ja046204n CCC: $27.50

Others include α,β-unsaturated acids,[20−22] a peptide terminating in α-vinylglycine,[23] and diastereomers of a peptide terminating in an α-styrylglycine.[24] These are all mechanism-based inhibitors in that they show turnover-dependent inactivation of the enzyme. Inhibitors of other types have also been reported, such as inorganic sulfite,[25] benzyl hydrazine,[26] and *N*-formylamides,[27] as well as derivatives of β-mercaptostyrene[28] and homocysteine.[29]

PAM consists of two functional subunits, peptidylglycine α-hydroxylating monooxygenase (PHM, E.C. 1.14.17.3) and peptidylamidoglycolate lyase (PAL, E.C. 4.3.2.5.) (Scheme 1). PHM catalyzes the copper-, molecular oxygen-, and ascorbate-dependent hydroxylation of a *C*-terminal glycine residue of a peptide substrate. The product hydroxyglycine is then hydrolyzed to the corresponding amide and glyoxylate, a process that is catalyzed by PAL at physiological pH. The determination of the crystal structure of PHM in both reduced and oxidized forms,[30−32] and kinetic[33−35] and mutagenesis studies,[36] have resulted in a detailed picture of the mechanism of action of this enzyme. In particular, it has been concluded that, in the first step, a copper-bound superoxide radical abstracts the pro-*S* hydrogen from the glycine residue, to give a glycyl radical.

In the present work we have sought to exploit factors affecting the formation of such radicals in order to design analogues of the substrates of PAM that competitively bind to, but are not processed by, the enzyme and therefore inhibit reaction of the substrates. To this end, we have compared the results of ab initio calculations and studies of relative reaction rates in free radical brominations, which identify factors affecting the stability and ease of formation of glycyl and related radicals,[37,38] with the kinetic parameters defining the interactions of analogous compounds with PAM.

Publication of our results is very timely in the light of a quite recent paper by Prigge et al.,[32] in which crystallography of frozen protein soaked with a slowly reacting substrate was used to identify and characterize the precatalytic complex of PHM with copper, oxygen, and the substrate. That study was the first to delineate the role of copper in the activation of dioxygen in this or any other enzyme system. The authors also drew a correlation between the reactivity of PHM substrates and the stability of the corresponding radical intermediates. They reported that our earlier theoretical studies[37] showed a peptide α-carbon-centered alanyl radical to be 9.1 kJ mol^{-1} less stable than a corresponding glycyl radical and noted that, even so, *N*-acetyl-(*S*)-tryptophanyl-(*R*)-alanine is still processed by the enzyme during X-ray diffraction. They also predicted, on the basis of our calculations with related amino acids, that an α-carbon-centered threonyl radical would be even less stable than an alanyl radical, and accordingly found that a peptide containing (*R*)-threonine instead of (*R*)-alanine at the *C*-terminus was less effectively turned over by the enzyme. Our calculations of glycyl and alanyl radical stability[37] were based on the radicals **3c** and **5d** (Chart 1). Contrary to the above discussion, their relative radical stabilization energies (RSEs), which correspond to the negative of the relative bond dissociation energies of the corresponding closed-shell molecules, actually showed the alanyl radical **5d** to be less stable than the glycyl radical **3c** by only 1.6 kJ mol^{-1}. We have not studied threonine derivatives, but Rauk et al.[39] used two different methods to calculate that an α-carbon-centered threonyl radical is destabilized relative to a glycyl radical by only 7−14 kJ mol^{-1}. Consequently, the destabilization of alanyl and threonyl radicals appears to have been somewhat over-estimated by Prigge et al.,[32] with the result that the relationship between the stabilization energies of radicals and the ease of their formation through PAM catalysis warrants further investigation. We also include in the present study a further comparison with the relative rates of formation of radicals in conventional brominations.

Results

The natural substrates of PAM all have in common an *N*-acylated glycine, and they are therefore comprised of acyl, amido, methylene, and carboxyl groups. Since the carboxyl group of a substrate is known to be important for binding to PAM,[31] we have not examined alternatives to this moiety in the present study. However, the effect of modifying each of the other groups was explored. A range of *N*-acyl substituents was investigated, since these are known to affect the stability and ease of formation of glycyl radicals[38,40] and to be tolerated by PAM. Although derivatives of α-substituted amino acids tend not to bind to PAM, small α-alkyl substituents, such as the methyl group of (*R*)-alanine,[32,41] the vinyl moiety of (*R*)-vinylglycine,[42] and the hydroxyethyl group of (*R*)-threonine,[32] are accommodated. The incorporation of a trifluoromethyl group was therefore studied since β,β,β-trifluoroalanine derivatives are known to be resistant to α-carbon-centered radical formation.[37] The effect of replacing the amido group with an ester or ketone using derivatives of glycolate or γ-keto acids instead of *N*-acylglycines was also explored. Glycolate inhibitors of PAM have been previously reported[22,42] in studies of broad ranges of

(19) Ogonowski, A. A.; May, S. W.; Moore, A. B.; Barrett, L. T.; O'Bryant, C. L.; Pollock, S. H. *J. Pharmacol. Exp. Ther.* **1997**, *280*, 846−853.
(20) Feng, J.; Shi, J.; Sirimanne, S. R.; Mounier-Lee, C. E.; May, S. W. *Biochem. J.* **2000**, *350*, 521−530.
(21) Moore, A. B.; May, S. W. *Biochem. J.* **1999**, *341*, 33−40.
(22) Katopodis, A. G.; May, S. W. *Biochemistry* **1990**, *29*, 4541−4548.
(23) Zabriskie, T. M.; Cheng, H. M.; Vederas, J. C. *J. Am. Chem. Soc.* **1992**, *114*, 2270−2272.
(24) Andrews, M. D.; O'Callaghan, K. A.; Vederas, J. C. *Tetrahedron* **1997**, *53*, 8295−8306.
(25) Merkler, D. J.; Kulathila, R.; Francisco, W. A.; Ash, D. E.; Bell, J. *FEBS Lett.* **1995**, *366*, 165−169.
(26) Merkler, D. J.; Kulathila, R.; Ash, D. E. *Arch. Biochem. Biophys.* **1995**, *317*, 93−102.
(27) Klinge, M.; Cheng, H. M.; Zabriskie, T. M.; Vederas, J. C. *J. Chem. Soc., Chem. Commun.* **1994**, 1379−1380.
(28) Casara, P.; Ganzhorn, A.; Philippo, C.; Chanal, M. C.; Danzin, C. *Bioorg. Med. Chem. Lett.* **1996**, *6*, 393−396.
(29) Erion, M. D.; Tan, J.; Wong, M.; Jeng, A. Y. *J. Med. Chem.* **1994**, *37*, 4430−4437.
(30) Prigge, S. T.; Kolhekar, A. S.; Eipper, B. A.; Mains, R. E.; Amzel, L. M. *Nat. Struct. Biol.* **1999**, *6*, 976−983.
(31) Prigge, S. T.; Kolhekar, A. S.; Eipper, B. A.; Mains, R. E.; Amzel, L. M. *Science* **1997**, *278*, 1300−1305.
(32) Prigge, S. T.; Eipper, B. A.; Mains, R. E.; Amzel, L. M. *Science* **2004**, *304*, 864−867.
(33) Francisco, W. A.; Merkler, D. J.; Blackburn, N. J.; Klinman, J. P. *Biochemistry* **1998**, *37*, 8244−8252.
(34) Francisco, W. A.; Knapp, M. J.; Blackburn, N. J.; Klinman, J. P. *J. Am. Chem. Soc.* **2002**, *124*, 8194−8195.
(35) Francisco, W. A.; Blackburn, N. J.; Klinman, J. P. *Biochemistry* **2003**, *42*, 1813−1819.
(36) Bell, J.; El Meskini, R.; D'Amato, D.; Mains, R. E.; Eipper, B. A. *Biochemistry* **2003**, *42*, 7133−7142.
(37) Croft, A. K.; Easton, C. J.; Radom, L. *J. Am. Chem. Soc.* **2003**, *125*, 4119−4124.
(38) Croft, A. K.; Easton, C. J.; Kociuba, K.; Radom, L. *Tetrahedron: Asymmetry* **2003**, *14*, 2919−2926.
(39) Rauk, A.; Yu, D.; Taylor, J.; Shustov, G. V.; Block, D. A.; Armstrong, D. A. *Biochemistry* **1999**, *38*, 9089−9096.
(40) Easton, C. J. *Chem. Rev.* **1997**, *97*, 53−82.
(41) Landymore-Lim, A. E. N.; Bradbury, A. F.; Smyth, D. G. *Biochem. Biophys. Res. Commun.* **1983**, *117*, 289−293.
(42) Ping, D.; Mounier, C. E.; May, S. W. *J. Biol. Chem.* **1995**, *270*, 29250−29255.

Chart 1

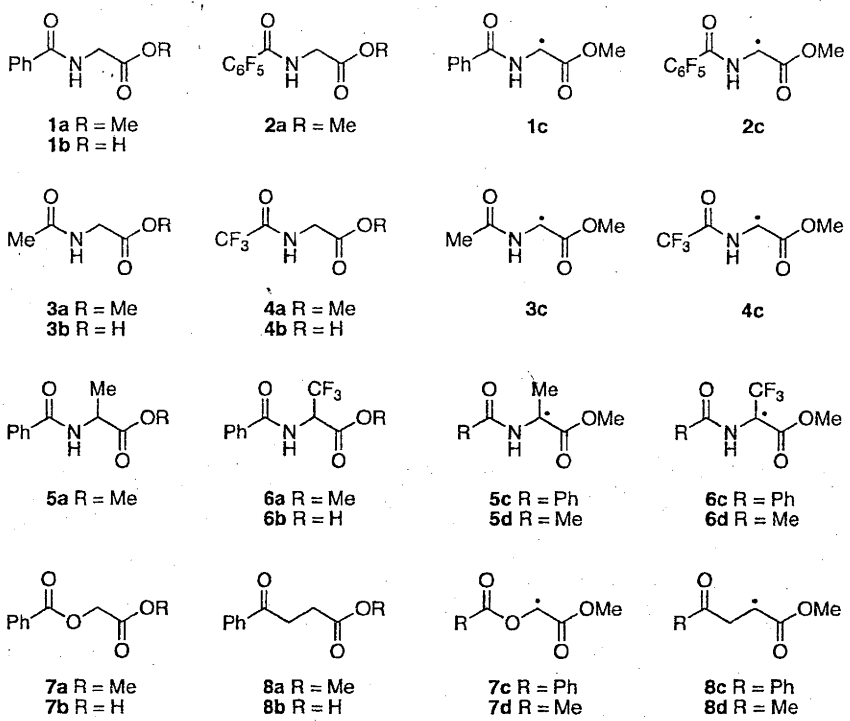

Table 1. Correlation of Studies of Free Radical Brominations and ab Initio Calculations of Radical Stabilization Energies with the Extent of Catalysis Displayed by Peptidylglycine α-Amidating Monooxygenase

	PART A relative rates of reaction of **1a–8a** with *N*-bromosuccinimide to give the corresponding radicals **1c–8c**		PART B radical stabilization energies [0 K, RMP2/G3large] of derivatives of glycyl and related radicals		PART C kinetic parameters for interactions of various substrates and inhibitors with peptidylglycine α-amidating monooxygenase				
						kinetic parameters			
glycine derivative or substitute	compd	relative rate of reaction[a]	radical	RSE[b]	compd	$V_{M,app}$ (μmol min^{-1} mg^{-1})	$K_{M,app}$ (mM)	K_I (mM)	IC_{50}[c] (mM)
N-benzoyl	**1a**	1.0[d]			**1b**	6.5[e]	1.3[e]		
N-pentafluorobenzoyl	**2a**	0.25[f]							
N-acetyl	**3a**	1.2[f]	**3c**	79.1	**3b**	6.4[e]	9.3[e]		
N-trifluoroacetyl	**4a**	0.05[f]	**4c**	69.9	**4b**	1.4[e]	4.1[e]		
other *N*-acyl					**10a**	12.6[e]	0.1[e]		
					11a		0.03		
					12a	3.3[g]	0.0012[g]		
					13a	8.2[e]	0.096[e]		
					14a	5.6[g]	0.0079[g]		
α-methyl	**5a**	0.33[h]	**5d**	78.8					
α-trifluoromethyl	**6a**	<0.0005[i,j]	**6d**	39.9	**9a**	inhibitor			5
					9b	inhibitor			5
glycolate	**7a**	<0.0005[j]	**7d**	44.4	**7b**	inhibitor			0.25
					10b	inhibitor			0.04
					11b	inhibitor			0.5
					12b	inhibitor			0.05
					13b	inhibitor		0.0598[g]	
					14b	inhibitor		0.0452[g]	
γ-keto acid	**8a**	<0.0005[j]	**8d**	34.9	**15**	inhibitor			6
					16	inhibitor			3

[a] From mixtures of substrates, in carbon tetrachloride at reflux. [b] Radical stabilization energies (RSEs) were calculated as the energy change in the isodesmic reaction $R^{\bullet} + CH_4 \rightarrow RH + {}^{\bullet}CH_3$. The RSEs correspond to the differences between the bond dissociation energies (BDEs) of methane and RH,[45] and reflect the stability of $R^{\bullet}$ compared with ${}^{\bullet}CH_3$, relative to the corresponding closed-shell systems. [c] Corresponds to loss of 50% of the catalytic activity of PAM in processing the substrate (*R*)-tyrosyl-(*S*)-valylglycine at a concentration of 0.1 mM, under conditions where $K_{M,app}$ for the substrate is 0.2 mM. Although $K_{M,app}$, K_I, and IC_{50} values are not directly comparable as measures of enzyme binding affinity, they are adequate as used in the present work, mainly to establish that compounds interact with PAM. [d] Assigned as unity. [e] Data from ref 11. [f] Data from ref 38. [g] Data from ref 42. [h] Data from ref 44. [i] Data from ref 37. [j] No detectable bromination.

compounds, but there has been no analysis of, nor explanation for, their behavior. One γ-keto acid has been previously investigated, but it was found not to interact with PAM, either as a substrate or an inhibitor.[43]

Compiled in Table 1 (part A) are the relative rates of reaction of the acylated glycine derivatives **1a**–**4a**, as well as the derivatives of alanine **5a**, trifluoroalanine **6a**, glycolate **7a**, and γ-ketopropionate **8a**, with *N*-bromosuccinimide at reflux in carbon tetrachloride. They were derived by measuring the

(43) Tamburini, P. P.; Jones, B. N.; Consalvo, A. P.; Young, S. D.; Lovato, S. J.; Gilligan, J. P.; Wennogle, L. P.; Erion, M.; Jeng, A. Y. *Arch. Biochem. Biophys.* **1988**, *267*, 623–631.

relative rates of consumption of **1a**–**8a** from mixtures.[37,38,44] Since the reactions involve radical bromination, with hydrogen atom transfer from the carbon adjacent to the ester group of each substrate determining the relative rate at which that compound is brominated, the relative rates of reaction correspond to the relative ease of formation of the radicals **1c**–**8c**.

For comparison with the relative rates of bromination of **1a**–**8a**, and the relative ease of formation of the radicals **1c**–**8c** in those reactions, RSEs for the radicals **3c**, **4c**, and **5d**–**8d** were determined (Table 1, part B). The RSEs relate the stability of the radicals in question to that of methyl radical (relative to the corresponding closed-shell species), with a more stable radical having a more positive RSE.[45] The geometries and zero-point vibrational energies were determined at the B3-LYP/6-31G(d) level, while improved relative energies were obtained by carrying out single-point calculations on these optimized structures at the RMP2 level with the 6-311+G(2df,p) and G3large basis sets.[46] The results quoted in Table 1, part B, correspond to RMP2/G3large//B3-LYP/6-31G(d) RSEs at 0 K. The radicals **1c**, **2c**, and **5c**–**8c** were not studied because their aryl groups would substantially increase the complexity of the calculations. The acetamides **5d**–**8d** were examined instead of the benzamides **5c**–**8c**. The effect of different acyl groups was examined with only **3c** and **4c**, and not **1c** and **2c**. The level of theory used in these calculations is significantly higher than that used in our earlier studies.[37,38] Nevertheless, the results are in good agreement where comparisons are possible. In particular, they show the RSEs of the radicals **3c** and **5d** to differ only slightly (by 0.3 kJ mol^{-1}), consistent with our previous work (which gave a difference of 1.6 kJ mol^{-1}).

Also shown in Table 1 (part C) are kinetic parameters for the interactions of the glycine derivatives **1b**, **3b**, **4b**, and **10a**–**14a**, the trifluoroalanine derivatives **9a** and **9b**, the glycolates **7b** and **10b**–**14b**, and the γ-keto acids **15** and **16** with PAM. The data for the glycine derivatives **1b**, **3b**, and **4b**, and the glycolate **7b**, allow for a direct comparison with the rates of bromination of the analogous esters **1a**, **3a**, **4a**, and **7a**, and the stability and ease of formation of the corresponding radicals **1c**, **3c**, **4c**, and **7c**. The properties of the glycine derivatives **10a**–**14a** and the glycolates **10b**–**14b** allow for further analysis of the relationships between these two classes of compounds. It was not feasible to examine the interaction of either the trifluoroalanine derivative **6b** or the γ-keto acid **8b** with PAM, for comparison with the glycine derivative **1b**, due to their poor enzyme-binding affinities. Instead, the effect of these substitutions was explored using the more tightly binding trifluoroalanine derivatives **9a** and **9b**, and the γ-keto acids **15** and **16**, and relating their behavior to that of the analogous glycinated dipeptide derivatives **13a** and **14a**. The data for **1b**, **3b**, **4b**, **10a**, **12a**–**14a**, **13b**, and **14b** have been previously reported.[11,22,42] The trifluoroalanine derivatives **9a**,**b**, the glycolates **7b** and **10b**–**12b**, the dipeptide **11a**, and the γ-keto acids **15** and **16** were prepared as described in the Supporting Information. Their interactions with PAM were assayed using modified literature procedures.[19,22,28] There was no evidence of enzyme-catalyzed reaction for **7b**, **9a**,**b**, **10b**–**12b**, **15**, or **16**. A double-reciprocal plot of $1/V$ vs 1/[S] was used to determine the $K_{M,app}$ value for **11a**, and Dixon plots of $1/V$ vs [I] were used to determine the IC_{50} values for **7b**, **9a**,**b**, **10b**–**12b**, **15**, and **16**.

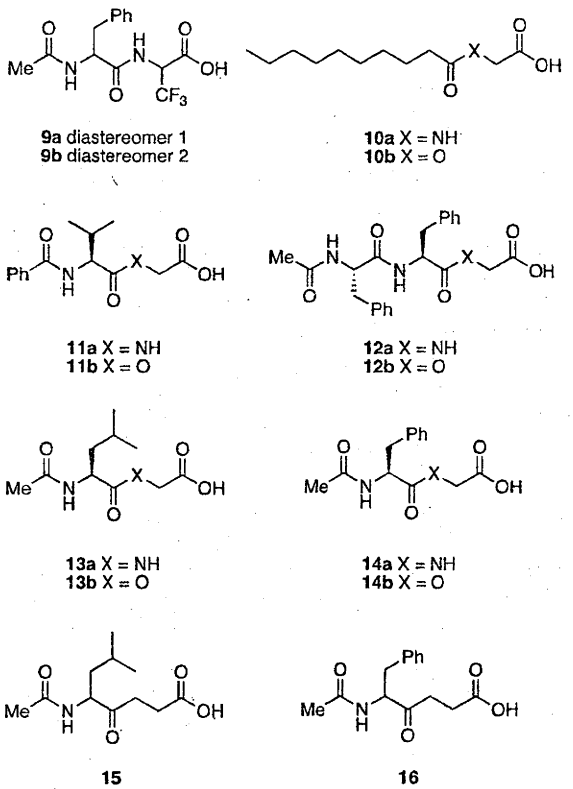

Discussion

N-Benzoyl-, pentafluorobenzoyl-, acetyl-, and trifluoroacetylglycine methyl esters **1a**–**4a** differ only in their *N*-acyl substituents. In their reactions with *N*-bromosuccinimide, the benzamide **1a** is 4 times more reactive than the pentafluorobenzamide **2a**, and the acetamide **3a** is 24 times more reactive than the trifluoroacetamide **4a** (Table 1, part A). These relative reactivities can be attributed to differences between the π-electron-donating abilities of the various amido groups, to stabilize and therefore facilitate formation of the corresponding radicals **1c**–**4c**. The inductively electron-withdrawing fluorines of the pentafluorobenzamide **2a** and the trifluoroacetamide **4a** decrease the extent of resonance stabilization and rates of formation of the radicals **2c** and **4c**, relative to those radicals **1c** and **3c** derived from the non-halogenated precursors **1a** and **3a**, respectively. This effect of the fluorines is reflected in the calculated RSEs in the cases of the radicals **3c** and **4c**, where the trifluoroacetamide **4c** is less stable than the acetamide **3c** by 9.2 kJ mol^{-1} (Table 1, part B). The fluorines also exert an inductive effect that decreases the pK_as of the carboxylic acid analogues of the amido groups, due to stabilization of the corresponding carboxylate anions (the pK_as of benzoic acid, pentafluorobenzoic acid, acetic acid, and trifluoroacetic acid are 4.2, 1.5, 4.8, and 0.6, respectively[47]). As a result, there is a strong correlation between the effect of the fluorines on the relative

(44) Burgess, V. A.; Easton, C. J.; Hay, M. P. *J. Am. Chem. Soc.* **1989**, *111*, 1047–1052.
(45) See, for example: (a) Parkinson, C. J.; Mayer, P. M.; Radom, L. *Theor. Chem. Acc.* **1999**, *102*, 92–96. (b) Parkinson, C. J.; Mayer, P. M.; Radom, L. *J. Chem. Soc., Perkin Trans. 2* **1999**, 2305–2313. (c) Henry, D. J.; Parkinson, C. J.; Mayer, P. M.; Radom, L. *J. Phys. Chem.* **2001**, *105*, 6750–6756.
(46) These levels of theory have been found to be suitable for the calculation of radical stabilization energies: see ref 45c.
(47) Krygowski, T. M.; Guilleme, J. *J. Chem. Soc., Perkin Trans. 2* **1982**, 531–534.

reactivity of the glycine derivatives (**1a**−**4a**), the relative acidity of the acids, and the RSEs of the radicals **3c** and **4c**. The effect of the fluorines on the reactivity of **1a**−**4a** and the acidity of the corresponding carboxylic acids is greatest with the trifluoroacetamide **4a** and trifluoroacetic acid, relative to the acetamide **3a** and acetic acid, respectively.

In analogous systems, the fluorines have a related impact on the interactions of *N*-acetylglycine **3b** and *N*-trifluoroacetylglycine **4b** with PAM. They decrease the overall rate of turnover ($V_{M,app}$) of **4b** relative to **3b**, via the corresponding glycyl radicals, by a factor of 4.5 (Table 1, part C). Consequently, the correlation of the differences between the RSEs of the *N*-acetyl- and trifluoroacetyl-glycyl radicals **3c** and **4c**, the relative rates of bromination of *N*-acetyl- and trifluoroacetyl-glycine methyl esters **3a** and **4a**, and the pK_as of acetic and trifluoroacetic acids extends to the relative rates of the enzyme-catalyzed reactions of *N*-acetyl- and trifluoroacetyl-glycine **3b** and **4b**. The fluorines reduce the RSE of the radical **4c** (by 9.2 kJ mol^{-1}), the rate of bromination of the ester **4a** (by a factor of 24), the pK_a of trifluoroacetic acid (by 4.2 units), and the rate of turnover of the acid **4b** by the enzyme (by a factor of 4.5). By way of comparison, replacing the acetyl substituent of *N*-acetylglycine methyl ester **3a**, *N*-acetylglycine **3b**, and acetic acid with the benzoyl group of *N*-benzoylglycine methyl ester **1a**, *N*-benzoylglycine **1b**, and benzoic acid has relatively little effect on any of these properties. It decreases the rate of bromination of the ester **1a** by a factor of only 1.2, decreases the pK_a of benzoic acid by only 0.6, and changes the rate of the enzyme-catalyzed reaction of the acid **1b** by less than 2%.

The effect of the fluorines, although reducing the rate of turnover, is clearly insufficient to prevent the PAM-catalyzed reaction of *N*-trifluoroacetylglycine **4a**. On the basis of the calculations with the *N*-acetyl- and trifluoroacetyl-glycyl radicals **3c** and **4c**, this indicates that a reduction in the RSE of 9.2 kJ mol^{-1} is not sufficient to stop glycyl radical formation by the enzyme. This is consistent with reductions in the RSEs of alanyl and threonyl radicals relative to those of the corresponding glycyl radicals, of 0.3 and 7−14 kJ mol^{-1}, respectively,[37,39] being too small to block the enzyme-catalyzed reactions of alanine and threonine derivatives.[32] The effect of the trifluoromethyl substituent on the stability of the trifluoroalanyl radical **6d** is much larger, reducing the calculated RSE relative to that of the corresponding glycyl radical **3c** by 39.2 kJ mol^{-1} (Table 1, part B). This substituent also prevents bromination of *N*-benzoyl-*β*,*β*,*β*-trifluoroalanine methyl ester **6a** (Table 1, part A) and the processing of the trifluoroalanine-containing dipeptides **9a**,**b** by PAM (Table 1, part C). *N*-Benzoyl-*β*,*β*,*β*-trifluoroalanine methyl ester **6a** was inert on treatment with *N*-bromosuccinimide, either alone or as a mixture with *N*-benzoylglycine methyl ester **1a**, that nevertheless reacted smoothly to give the corresponding α-bromoglycine derivative. There was no evidence of reaction of either of the trifluoroalanine-containing dipeptides **9a** or **9b** being catalyzed by PAM, even though competitive experiments with (*R*)-tyrosyl-(*S*)-valylglycine established that both **9a** and **9b** bind to the enzyme, albeit with IC_{50} values of around 5 mM (Table 1, part C). It is therefore apparent that the decrease in the RSE brought about by introducing the trifluoromethyl group is sufficient to prevent radical formation by PAM. However, this does not give effective enzyme inhibitors, as the trifluoromethyl substituent prevents tight binding to the enzyme. This is seen from the IC_{50} value of 5 mM for each of the trifluoroalanine derivatives **9a** and **9b**. As an indirect comparison, the $K_{M,app}$ value of the corresponding glycine derivative **14a** is 7.9 μM.

In a manner similar to the effect of introducing the trifluoromethyl group, replacing the glycine moiety with glycolate, which is a simple substitution of the glycine NH by O, reduces the RSE of the glycolyl radical **7d** compared with that of the corresponding glycyl radical **3c** by 34.7 kJ mol^{-1} (Table 1, part B). This can be attributed to the decreased π-electron-donating and increased σ-electron-withdrawing ability of the acetoxy group of **7d** relative to the acetamido substituent of **3c**, as reflected in the RSEs of the radicals $MeCONHCH_2^{\bullet}$ and $MeCO_2CH_2^{\bullet}$ of 41.3 and 17.1 kJ mol^{-1}, respectively.[48] The effect is magnified in the captodatively stabilized[49,50] glycyl and glycolyl radicals **3c** and **7d**, where the extent of the synergy displayed by the acetamido and acetoxy substituents in combination with the carboxyl group corresponds to 17.6 and 7.1 kJ mol^{-1}. These values are based on the differences between the RSEs of $MeCONHCH_2^{\bullet}$ (41.3 kJ mol^{-1}), $^{\bullet}CH_2CO_2Me$ (20.2 kJ mol^{-1}), and **3c** (79.1 kJ mol^{-1}) and $MeCO_2CH_2^{\bullet}$ (17.1 kJ mol^{-1}), $^{\bullet}CH_2CO_2Me$, and **7d** (44.4 kJ mol^{-1}), respectively. The substitution of glycine by glycolate prevents bromination of methyl O^{α}-benzoylglycolate **7a** (Table 1, part A). It also blocks catalysis of the reactions of the glycolates **7b** and **10b**−**14b** by PAM (Table 1, part C). The glycine derivatives **1b** and **10a**−**14a** are all turned over by the enzyme, but there is no evidence of reaction of any of the corresponding glycolates **7b** and **10b**−**14b**. In this case, the substitution does not severely disrupt binding to the enzyme. The IC_{50} and K_I values of the glycolates **7b** and **10b**−**14b** are all in the 0.04−0.5 mM range. The corresponding glycine derivatives **1b** and **10a**−**14a** have $K_{M,app}$ values between 1 μM and 1 mM. Therefore, the glycolates constitute a general class of inhibitors of the enzyme because they do not readily undergo hydrogen atom transfer, yet they bind effectively to PAM.

Replacing the acylglycine with a γ-keto acid or ester, through substitution of the glycine NH by CH_2, has effects similar to the swapping of glycine for glycolate. The RSE of the keto ester radical **8d** is less than that of the analogous glycyl radical **3c** by 44.2 kJ mol^{-1} (Table 1, part B). The γ-keto ester **8a** is inert to bromination (Table 1, part A), and the γ-keto acids **15** and **16** are not processed by PAM (Table 1, part C), even though, unlike the example reported previously,[43] these keto acids **15** and **16** do bind to some extent to the enzyme, with IC_{50} values of 6 and 3 mM, respectively. Again it is apparent that a reduction in the RSE of around 35−45 kJ mol^{-1} is sufficient to stop both the bromination with *N*-bromosuccinimide and the catalysis by the monooxygenase.

From the $K_{M,app}$ values of the glycine derivatives **13a** and **14a**, 96 and 7.9 μM, respectively, the K_I values of the corresponding glycolates **13b** and **14b**, 59.8 and 45.2 μM, and the IC_{50} values of the analogous γ-keto acids **15** and **16**, 6 and 3 mM (Table 1, part C), it appears that the replacement of an acylglycine with a γ-keto acid has a more adverse effect on the

(48) RSE values quoted in the text, in addition to those listed in Table 1, were also calculated using the RMP2/G3large level of theory.
(49) Welle, F. M.; Beckhaus, H.-D.; Rüchardt, C. *J. Org. Chem.* **1997**, *62*, 552−558.
(50) Schulze, R.; Beckhaus, H.-D.; Rüchardt, C. *Chem. Ber.* **1993**, *126*, 1031−1038.

binding to PAM than does the substitution of glycine by glycolate. One explanation for this is that both acylglycines and glycolates can form hydrogen bonds with the enzyme, through NH and the corresponding O, respectively, to facilitate binding, but this is not possible with the methylene of an analogous γ-keto acid. An alternative explanation for the less effective binding of the γ-keto acids relates to their greater conformational freedom in free solution. As a result of conjugation of the amide NH of an acylglycine and the analogous ester O of an acylglycolate, in each case there is easy rotation only around the bonds to the α-carbon. By contrast, with a γ-keto acid there is easy rotation around the bonds to both the α- and β-carbons. Assuming that the acylglycines, glycolates, and keto acids all bind to PAM with similar orientations, and that the planarity of the amide and ester groups of the acylglycine and acylglycolate is maintained, there is therefore a greater degree of conformational constraint and loss of entropy on binding of a γ-keto acid.

In any event, it is clear that introducing an α-trifluoromethyl substituent into the glycine residue of a PAM substrate, or replacing the acylglycine of a substrate with either a glycolate or a γ-keto-acid, stops catalysis by the enzyme, because it reduces by around 35−45 kJ mol^{-1} the RSE of the radical that would be formed. By contrast, swapping the acylglycine for a β,γ-unsaturated acid is likely to increase the RSE of the radical intermediate by around 21.1 kJ mol^{-1}, based on the values calculated for the acetamido and propenyl radicals **3c** and **17**, 79.1 and 100.2 kJ mol^{-1}, respectively. Thus, it is not surprising that, as outlined in the Introduction, β,γ-unsaturated acids are processed by PAM.[17,23,24]

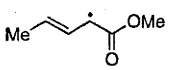

17

Conclusion

In summary, there are strong correlations between calculated radical stabilization energies (RSEs), the ease of formation of glycyl and related radicals in free radical brominations, and the extent of catalysis of the reactions of analogous compounds by peptidylglycine α-amidating monooxygenase (PAM). A decrease in the RSE of around 10 kJ mol^{-1} relative to that of a normal peptide glycyl radical slows but does not stop the rate of radical formation through either bromination or enzyme catalysis. However, reducing the RSE by around 35−45 kJ mol^{-1}, either through introduction of a trifluoromethyl substituent at the α-position or by replacing the acylglycine NH with a glycolate O or a γ-keto acid CH_2, stops both bromination and enzyme processing. Of these changes, only the glycolate substitution does not adversely affect the enzyme binding affinity. Consequently, glycolates are a general class of PAM inhibitors because they do not readily undergo hydrogen atom transfer, yet they bind effectively to the enzyme. We are now beginning to study the associated in vivo effects of this class of compounds, and already we have found that both the glycolates **10b** and **12b** actively reduce the levels of the peptide hormone Substance P produced by rat DRG cells over a 6 h period.[51]

Acknowledgment. We gratefully acknowledge receipt of financial support from the Australian Research Council and generous allocations of computing time from the National Facility of the Australian Partnership for Advanced Computing and the Australian National University Supercomputing Facility.

Supporting Information Available: Details of the procedures and methods used to determine the relative rates of reaction of **1a**−**8a** with *N*-bromosuccinimide, the methods used for the ab initio calculations, the Gaussian archive entries for the UB3-LYP/6-31G(d) optimized structures of derivatives of glycyl and related radicals, calculated RMP2/G3large and RMP2/6-311+G(2df,p) total energies and corresponding RSEs; protocols for the syntheses of **7b**, **9a,b**, **10b**, **11a,b**, **12b**, **15**, and **16** with studies of their interactions with PAM. This material is available free of charge via the Internet at http://pubs.acs.org.

JA046204N

(51) Easton, C. J.; Inoue, A.; Wright, A. Unpublished results.